TECHNICAL REPORT STANDARD TITLE PAGE

1. Report No.	2. Government Accession No.	3. Recipient's Catalog No.
TX-92/1313-1F		

4. Title and Subtitle	5. Report Date
Evaluation and Repair of Fatigue Damage to Midland County Bridges	October, 1992
	6. Performing Organization Code
7. Author(s)	8. Performing Organization Report No.
P. B. Keating and A. R. Crozier	Report 1313-1F
9. Performing Organization Name and Address	10. Work Unit No.
Texas Transportation Institute The Texas A&M University System College Station, Texas 77843-3135	11. Contract or Grant No. Study No. 2-5-91-1313
12. Sponsoring Agency Name and Address	13. Type of Report and Period Covered
Texas Department of Transportation Transportation Planning Division P. O. Box 5051 Austin, Texas 78763	July 1991 Final - March 1992
	14. Sponsoring Agency Code

15. Supplementary Notes

Research performed in cooperation with the Texas Department of Transportation, Bridge Division
Research Study Title: "Bridge Repair of Eastbound and Westbound Structures Midland County"

16. Abstract

The IH-20 Midland County bridge has experienced fatigue related problems due to the unintended interaction between the longitudinal girders and the cross-frame diaphragms. Fatigue cracks developed in unstiffened web gaps at the ends of the diaphragm connection plates and in the diaphragm cross frame members. This study investigated the cause of the fatigue cracking through field strain measurements and finite element analysis, and developed procedures for their repair.

Web gaps fatigue cracks were caused by the distortion of the web gap by the diaphragm member forces. Under a single truck load condition, uneven load distribution between girders resulted in significant diaphragm member forces. The diaphragm member cracking was due to the eccentric connection used in the construction of the bridge. This resulted in bending stresses in the diaphragm members large enough to initiate the fatigue cracks. The effect of diaphragm removal on overall structural behavior of the bridge was studied. Removal of all diaphragms from the bridge was found to result in unacceptable increases in the longitudinal girder bending stresses. A staggered diaphragm pattern was selected that minimized the number of diaphragms needing repair while not significantly changing either the load distribution characteristics of the bridge nor member stresses. At remaining diaphragm locations, repair procedures were developed that included a welded attachment of the connection plates ends and an improved design for the diaphragms.

17. Key Words	18. Distribution Statement
Bridge, Highway, Steel, Fatigue, Diaphragm, Load Distribution.	No restrictions. This document is available to the public through the National Technical Information Service 5285 Port Royal Road Springfield, Virginia 22161

19. Security Classif. (of this report)	20. Security Classif. (of this page)	21. No. of Pages	22. Price
Unclassified	Unclassified	160	

METRIC (SI*) CONVERSION FACTORS

APPROXIMATE CONVERSIONS TO SI UNITS

Symbol	When You Know	Multiply By	To Find	Symbol
LENGTH				
in	inches	2.54	centimetres	cm
ft	feet	0.3048	metres	m
yd	yards	0.914	metres	m
mi	miles	1.61	kilometres	km
AREA				
in^2	square inches	645.2	centimetres squared	cm^2
ft^2	square feet	0.0929	metres squared	m^2
yd^2	square yards	0.836	metres squared	m^2
mi^2	square miles	2.59	kilometres squared	km^2
ac	acres	0.395	hectares	ha
MASS (weight)				
oz	ounces	28.35	grams	g
lb	pounds	0.454	kilograms	kg
T	short tons (2000 lb)	0.907	megagrams	Mg
VOLUME				
fl oz	fluid ounces	29.57	millilitres	mL
gal	gallons	3.785	litres	L
ft^3	cubic feet	0.0328	metres cubed	m^3
yd^3	cubic yards	0.0765	metres cubed	m^3

NOTE: Volumes greater than 1000 L shall be shown in m^3.

TEMPERATURE (exact)

°F	Fahrenheit temperature	5/9 (after subtracting 32)	Celsius temperature	°C

APPROXIMATE CONVERSIONS TO SI UNITS

Symbol	When You Know	Multiply By	To Find	Symbol
LENGTH				
mm	millimetres	0.039	inches	in
m	metres	3.28	feet	ft
m	metres	1.09	yards	yd
km	kilometres	0.621	miles	mi
AREA				
mm^2	millimetres squared	0.0016	square inches	in^2
m^2	metres squared	10.764	square feet	ft^2
km^2	kilometres squared	0.39	square miles	mi^2
ha	hectores (10 000 m^2)	2.53	acres	ac
MASS (weight)				
g	grams	0.0353	ounces	oz
kg	kilograms	2.205	pounds	lb
Mg	megagrams (1 000 kg)	1.103	short tons	T
VOLUME				
mL	millilitres	0.034	fluid ounces	fl oz
L	litres	0.264	gallons	gal
m^3	metres cubed	35.315	cubic feet	ft^3
m^3	metres cubed	1.308	cubic yards	yd^3

TEMPERATURE (exact)

°C	Celsius temperature	9/5 (then add 32)	Fahrenheit temperature	°F

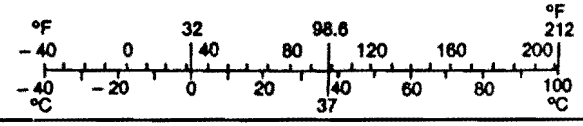

These factors conform to the requirement of FHWA Order 5190.1A.

* SI is the symbol for the International System of Measurements

Evaluation and Repair of Fatigue Damage to Midland County Bridges

06-165-0005-15-201 (IH 20 Westbound)
06-165-0005-15-202 (IH 20 Eastbound)

Final Report

October 1992

Peter B. Keating
Allen R. Crozier

Texas Department of Transportation
Study No. 2-5-91-1313
Texas Transportation Institute
Texas A&M University

SUMMARY

The IH-20 Midland County bridge has experienced fatigue related problems due to the unintended interaction between the longitudinal girders and the cross-frame diaphragms. Fatigue cracks have developed in the web gap at the diaphragm connection plates and in the diaphragm members. This study investigates the cause of the fatigue cracking through field strain measurements and finite element analysis. Effect of diaphragm removal on overall structural behavior of the bridge is studied. Retrofit procedures are developed that include a welded attachment of the connection plates ends, an improved design for the diaphragms, and permanent removal of over half the cross-frame diaphragms. Additional field measurements are to be taken upon completion of the repairs.

IMPLEMENTATION

The results of this study will provide competent recommendations to the Odessa District of the repair of the IH-20 Midland County bridge. Future monitoring of the performance, combined with sound engineering judgement, will result in an acceptable repair procedure for this frequently occurring problem.

DISCLAIMER

The contents of this report reflect the views of the authors who are responsible for the facts and their accuracy of the data presented herein. The contents do not necessarily reflect the official views of the Texas Department of Transportation. This report does not constitute a standard, specification or regulation. It is not intended for construction, bidding of permit purposes.

TABLE OF CONTENTS

LIST OF FIGURES

LIST OF FIGURES (continued)

LIST OF FIGURES (continued)

LIST OF TABLES

1. INTRODUCTION

The Midland County Bridges are used to carry IH 20 traffic over US 80 and the Missouri Pacific Railroad east of the city of Midland, Texas. The bridges were originally constructed in 1966 to carry two lanes of traffic in both the eastbound and westbound directions using twin parallel spans. Each bridge consists of two continuous multiple steel girder spans. The first continuous span (North Structure) is 90'-125'-125'-105' for a total of 445 ft. and the second continuous span (South Structure) is 95'-125'-105' for a total of 325 ft. The original bridge cross section consisted of four 48 in. deep plate girders spaced at 8'- 8" supporting a 33'- 7-3/4" thick concrete deck, as shown in Fig 1-1. All spans have a 60 degree right hand forward skew.

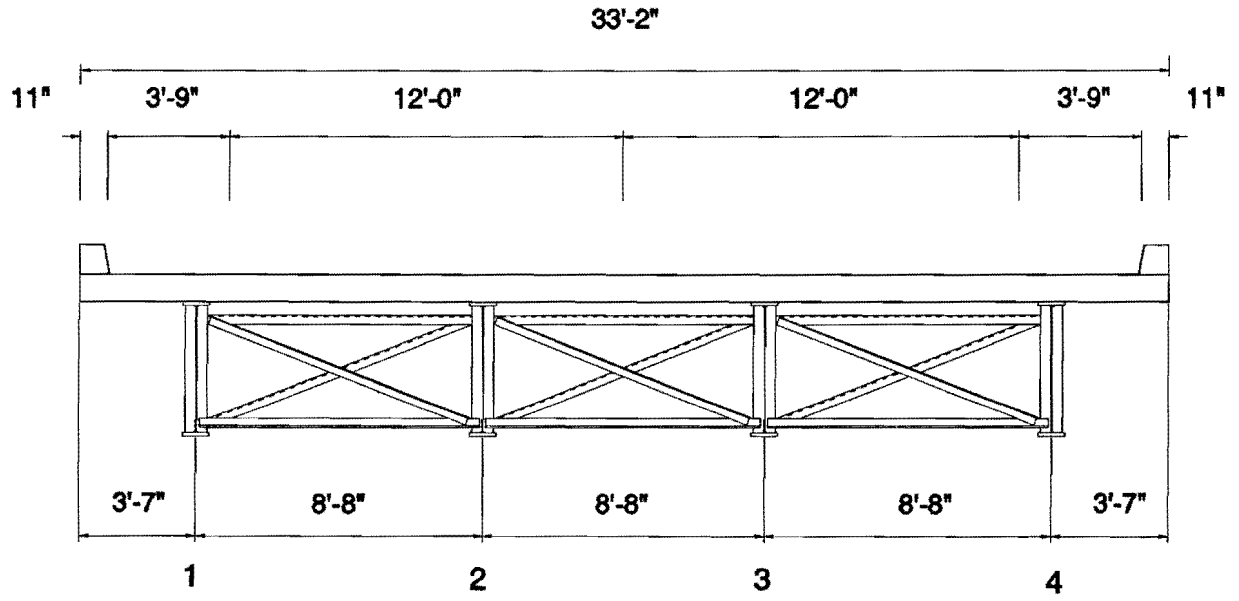

Figure 1-1: Typical bridge cross section prior to shoulder widening.

In 1983 the bridges were widened by the placement of an additional plate girder (Girder 5) on the outside (shoulder side) of the spans (see Fig. 1-2). This allowed the

right shoulder lane to be widened from 3'-9" to 10'-0" and resulted in a shift of the center lane stripe 7 in. towards the outside lane. This resulted in a new overall roadway width of 40'-2". The new girder is of similar construction as the original girders. The concrete slab thickness was increased to 8-3/4 in. While the original concrete deck was constructed using removable plywood forms, stay-in-place metal deck forms were used to cast the deck slab in Bay D.

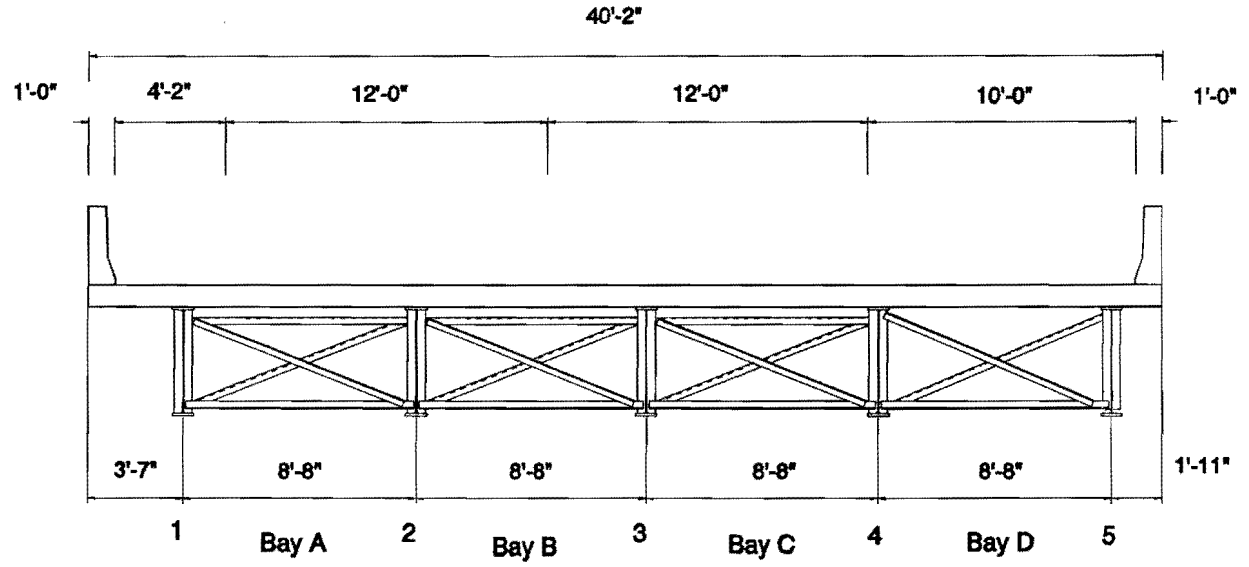

Figure 1-2: Typical bridge cross section after shoulder widening.

Transverse web stiffeners are placed at 5 ft. intervals with cross frame diaphragms at 15 ft. intervals. With the exception of the end supports, all diaphragms are oriented normal to the girder and aligned across the girder bays at each diaphragm line. The framing plans for the North Structures and South Structures are shown in Figs. 1-3 and 1-4, respectively. Lateral wind bracing was placed in the center bay (Bay B) and is attached to the bottom flange by means of a fillet welded gusset plate.

For the original structure, two intermediate cross frame diaphragms were used as shown in Figs. 1-5 and 1-6. The Type C Diaphragm (Fig. 1-6) used a heavier upper strut than the Type B Diaphragm (Fig. 1-5): ST12WF38 (equivalent to a WT12X38) versus

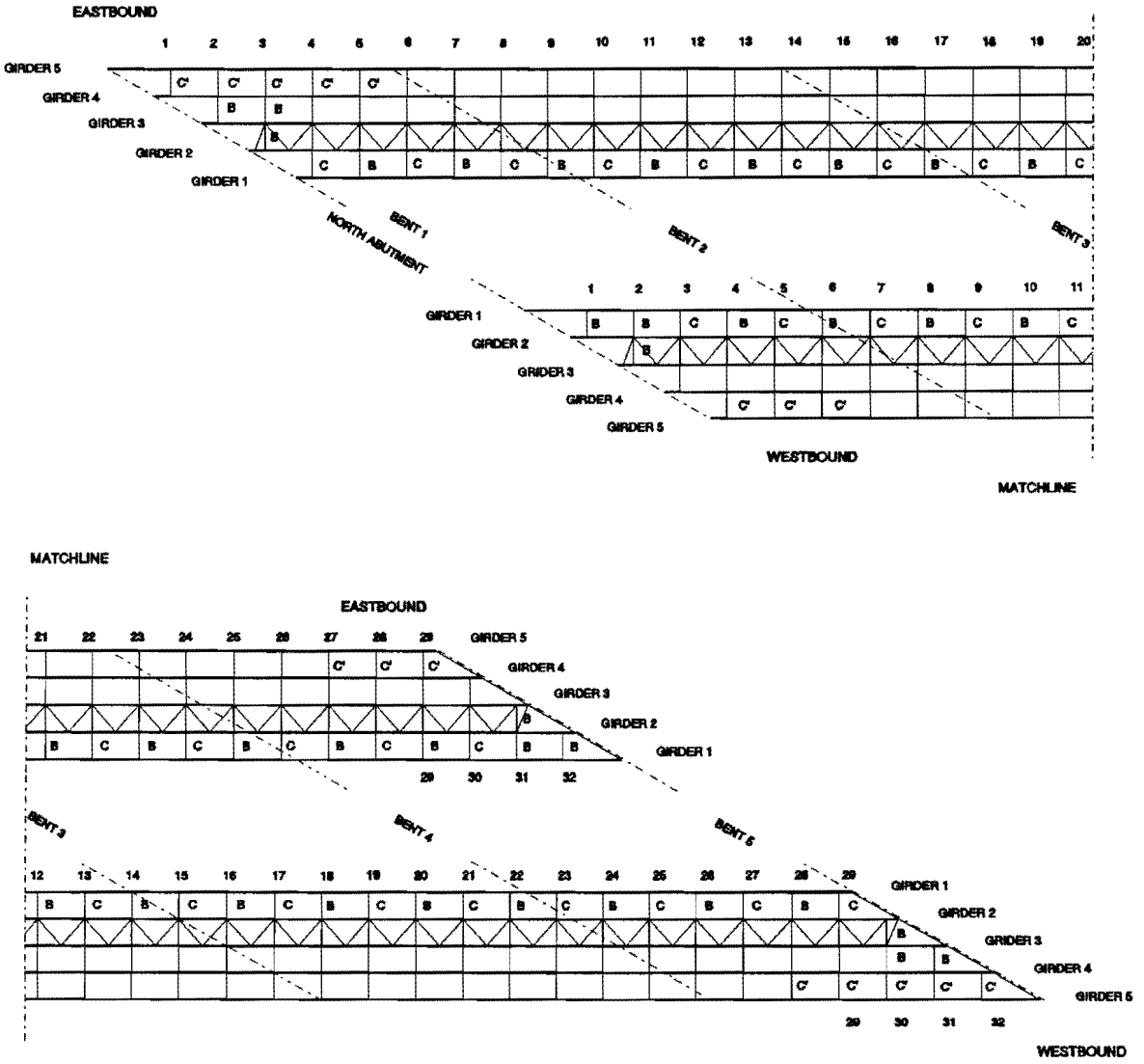

Figure 1-3: Framing plan of 445 ft. structures.

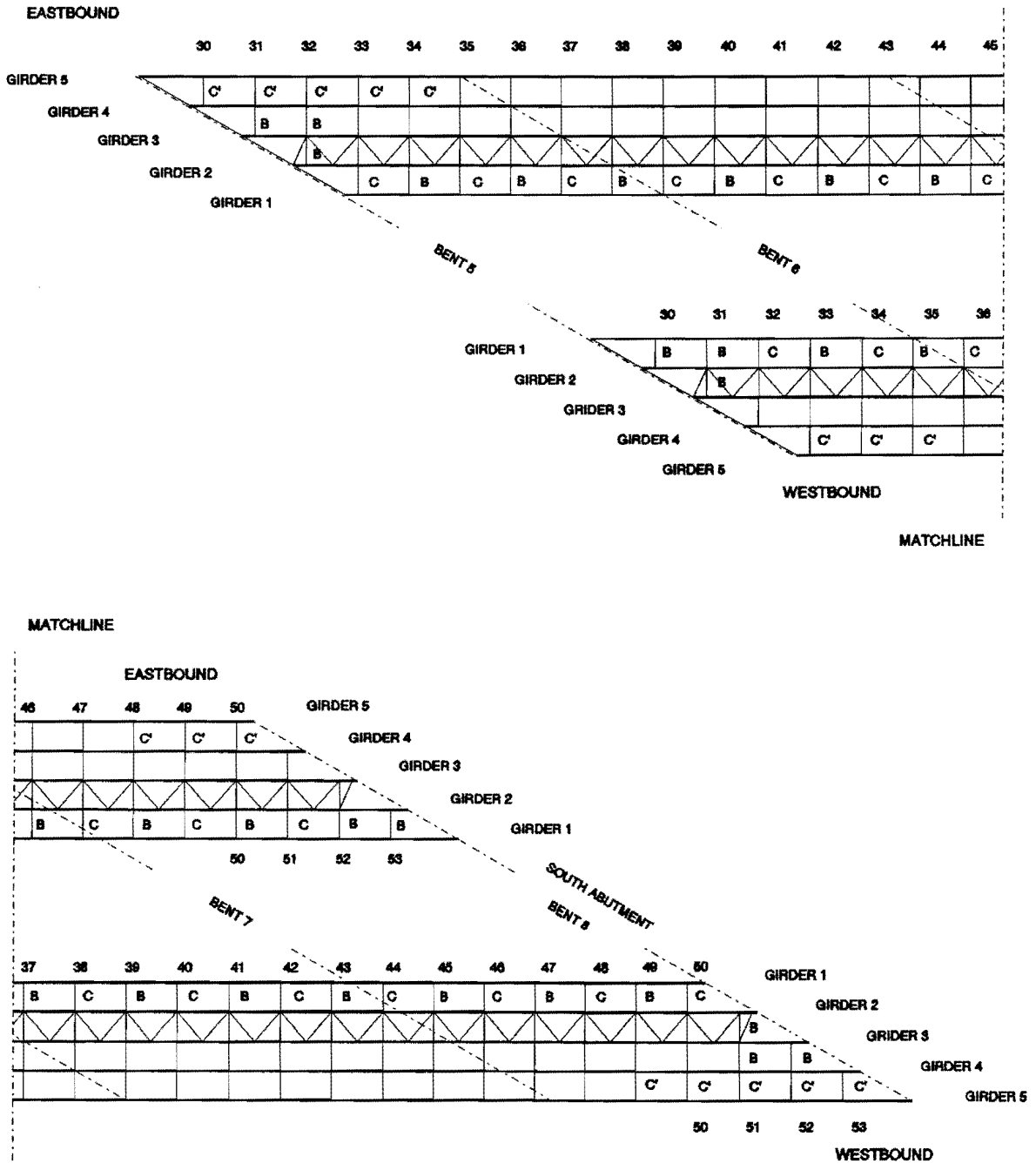

Figure 1-4: Framing plan of 325 ft. structures.

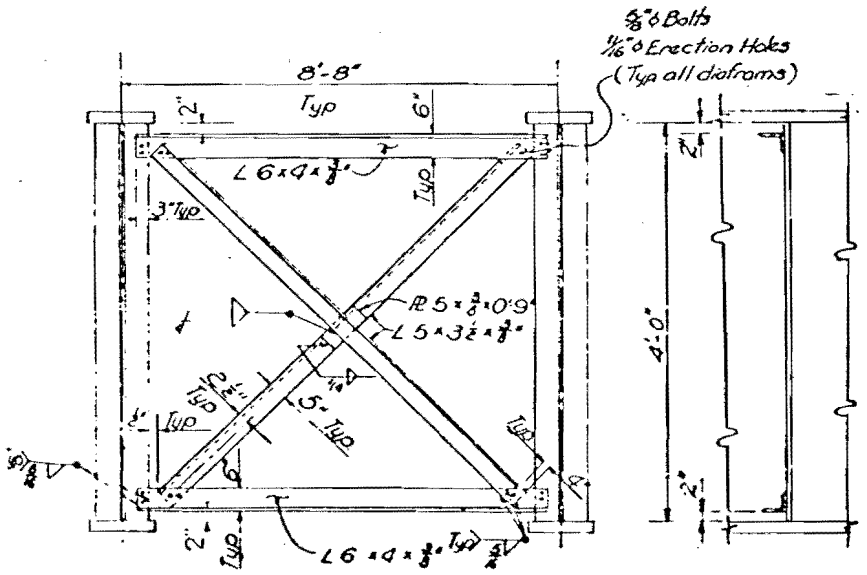

Figure 1-5: Type B diaphragm detail.

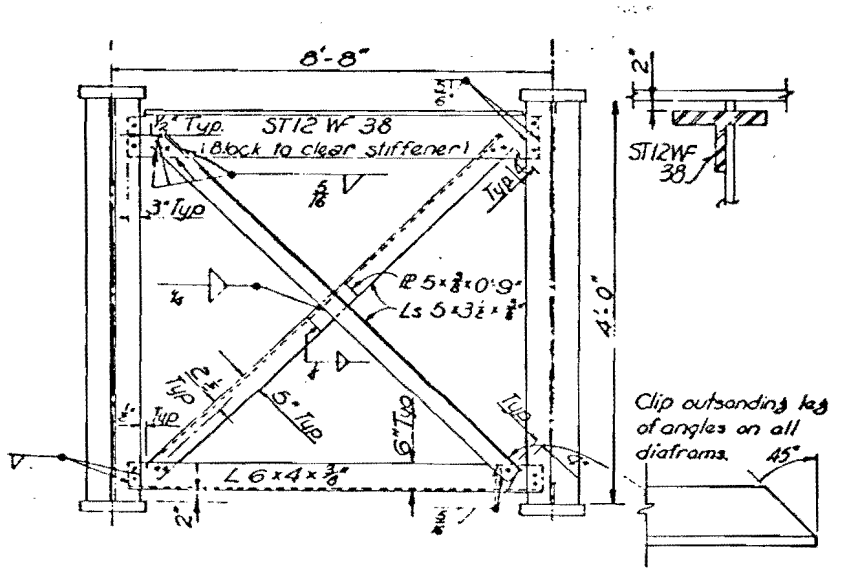

Figure 1-6: Type C diaphragm detail.

L6X4X3/8. The diaphragm type alternates as one moves longitudinally across the bridge except in the vicinity of the end supports where Type B is used. For a given diaphragm line, the same diaphragm type was used in all three of the original girder bays (A-C). The

diaphragm connection plate consists of a 5x5/16 plate.

Examination of Figs. 1-5 and 1-6 show that the ends of the diaphragm diagonal members are welded to either the upper or lower struts. This type of connection provided a convenient means of attaching the diagonals without the use of a gusset plate. However, this resulted in diagonal member forces no longer being concentric and is the primary reason for the growth of fatigue cracks in the diaphragm members.

As was a common practice during the 1960s, the ends of the connection plates were not rigidly attached to the girder tension flanges. Instead, a tight fit detail was called for in the original design drawings and is shown schematically in Fig. 1-7. This provided an unstiffened web gap susceptible to distortion-induced fatigue [3]. The ends of the connection plates were welded to the girder compression flanges.

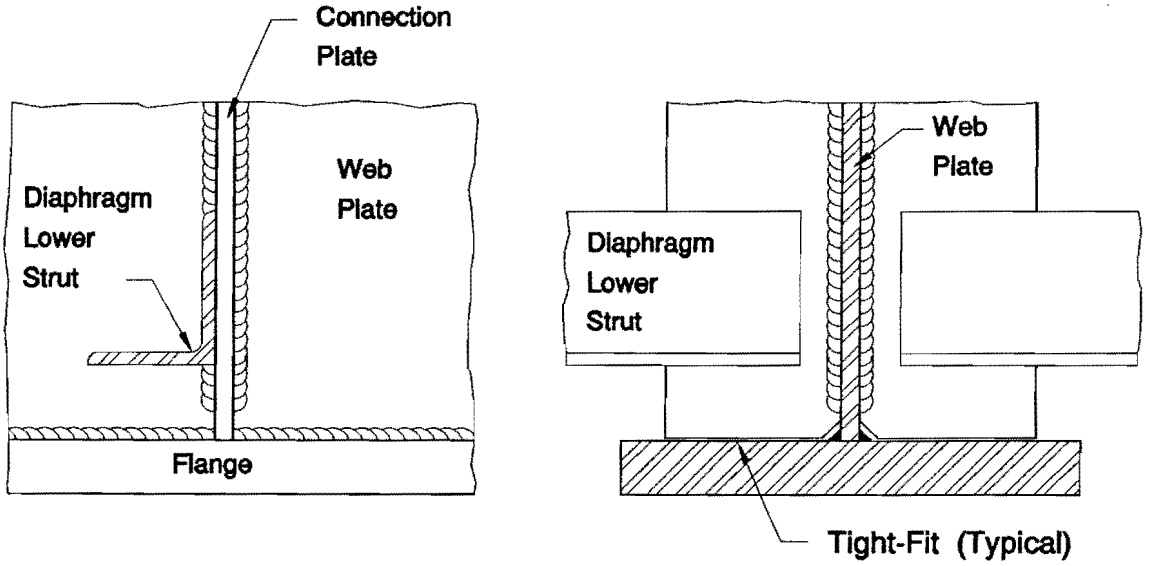

Figure 1-7: Connection plate detail (tight-fit) for original construction.

For the bridge widening in 1983, the Type B diaphragm design was modified by eliminating the upper strut member, as shown in Fig. 1-8. The upper strut in the older diaphragms was used to brace the top flange of the girder during construction, prior to the strengthening of the concrete deck. The 1983 construction incorporated the use of stay-in-place metal deck forms which provided lateral flange support. The top ends of both diagonal members were field welded directly to the transverse connection plates. The construction drawings for bridge widening designated the diaphragm as Type C. For the purposes of identification in this report, this diaphragm type is designated as Type C'.

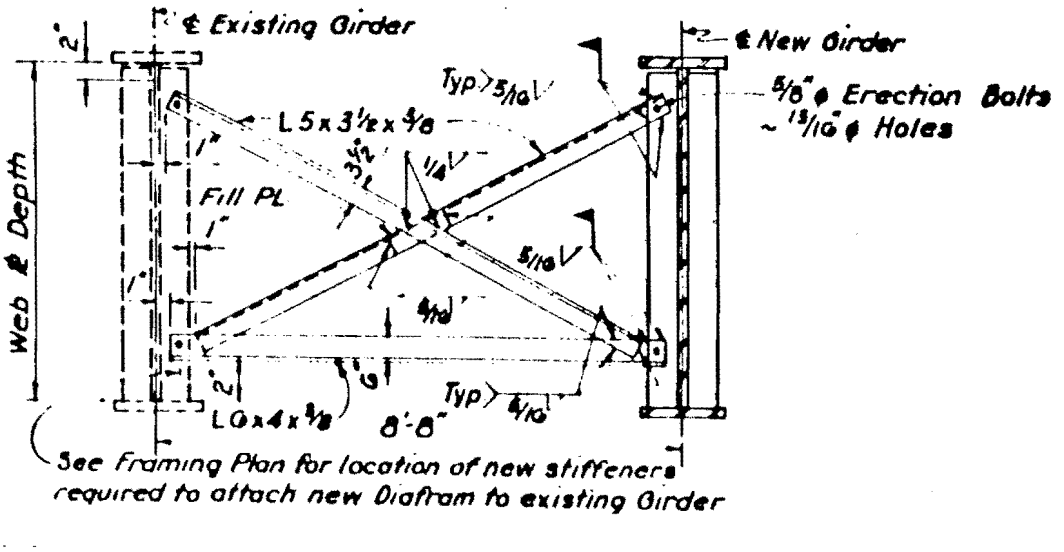

Figure 1-8: Type C' diaphragm detail (modified Type B diaphragm).

Similar to the original design, the ends of the connection plates were not rigidly attached to the tension flanges. However, the new construction utilized a one-inch web gap instead of the tight-fit detail as shown in Fig. 1-9.

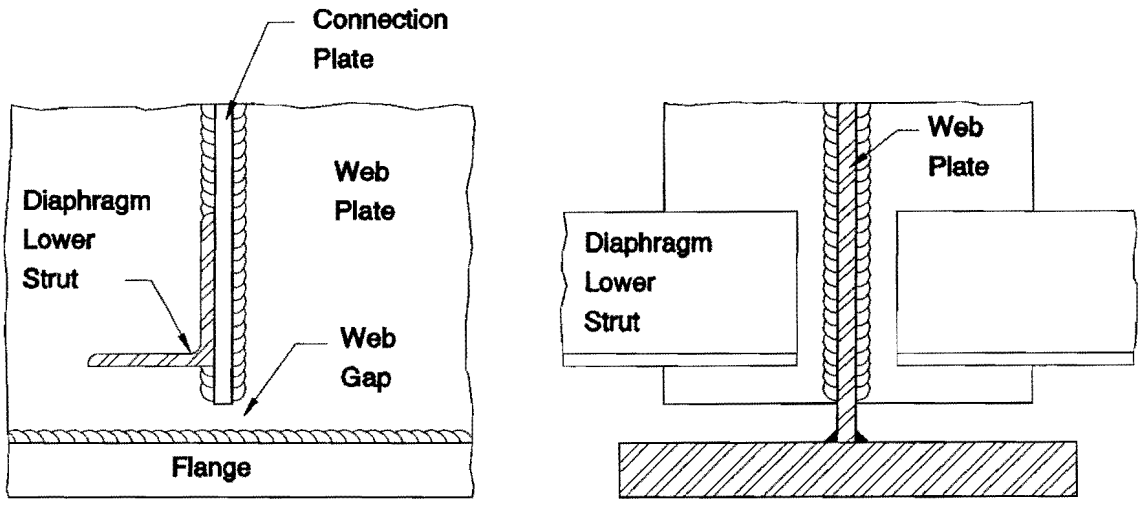

Figure 1-9: Connection plate detail for new construction.

The concrete deck acts compositely with the steel girders in the positive moment regions. The slab anchors consists of three 7/8 in. diameter shear studs spaced at 4.0 ft. intervals. No slab anchors were used in the negative moment region.

A total of 400 diaphragms of Types B, C, and C' are in the bridges. This results in 800 connection plate ends that have not been rigidly attached to the tension flange.

2. BRIDGE CONDITION

The following discussion concerning the type and location of fatigue cracks in the Midland County Bridge is based on an inspection report [1] performed by ARE, Inc., Consulting Engineers July of 1990 (herein referred to as the "Inspection Report") and the Special Report prepared by 1983 by the Texas Division of the Federal Highway Administration (see Appendix D). Additional observations were made during a July 10-11, 1991, site visit. Additional information is provided in Appendix A.

2.1 Type of Fatigue Cracks

The type of fatigue cracking observed in both the eastbound and westbound structures of the Midland County bridges can be classified into two general types:

Type A: Fatigue cracks that developed in the primary members such as in the diaphragm connection plate web gaps and in the girder flanges at the end of the diaphragm connection plate.

Type B: Fatigue cracks that developed in the diaphragm members or at their welded connections.

Both types of fatigue cracks can be attributed to the distortion resulting from the interaction of the diaphragms and the girders. As per the Inspection Report, the two general crack types are subdivided into three additional classifications according to location as outlined in Table 2-1.

The Inspection Report also mentions a Type C fatigue crack which is used to identify locations where cracking may potentially develop in the diaphragm members. It is unclear as to the basis for this category.

Type A1 - This type of cracking is found at or near the web gap in positive moment regions. Therefore, the cracking occurs near the bottom flange as shown in Fig. 2-1. The cracking was found at both the tight-fit stiffener end (diaphragm Type B and C) as well as the one-inch web gap detail (diaphragm Type C'). The more severe cracking

Crack Type	Description of Crack Location
A1	Vertical stiffener, girder web and bottom flange (web gap)
A2	Vertical stiffener, girder web and top flange (web gap)
A3	Weld between vertical stiffener and top girder flange
B1	Weld between lower diaphragm strut and connection plate
B2	Separated lower diaphragm strut
B3	Weld between top diaphragm strut and connection plate

Table 2-1: Crack type classifications and locations.

occurred in the westbound span where the new diaphragms in Bay D were staggered relative to the existing diaphragm line (Diaphragm Nos. 4-11). The location of all detected Type A1 cracks are given in Figs. A-1 and A-2 (see Appendix A).

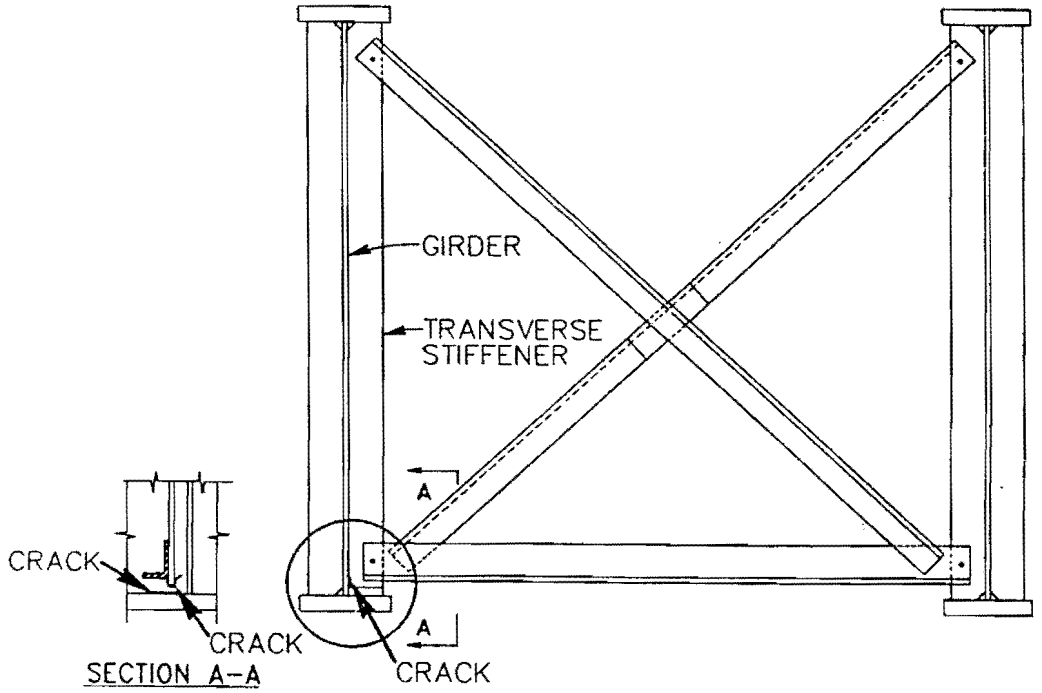

Figure 2-1: Location of Type A1 fatigue cracking.

Illustrative examples of Type A1 cracking are given in Figs. 2-2 and 2-3 for the tight-fit and one-inch web gap detail respectively. Note that the cracking can occur at one or both boundaries of the web gap. A fatigue crack can develop along the web-to-flange fillet weld, running parallel with the primary bending stress. Fatigue cracks also developed vertically along the toe of the fillet weld between the connection plate and the web plate. As this crack increases in length, there is a tendency for it to turn perpendicular to the weld axis.

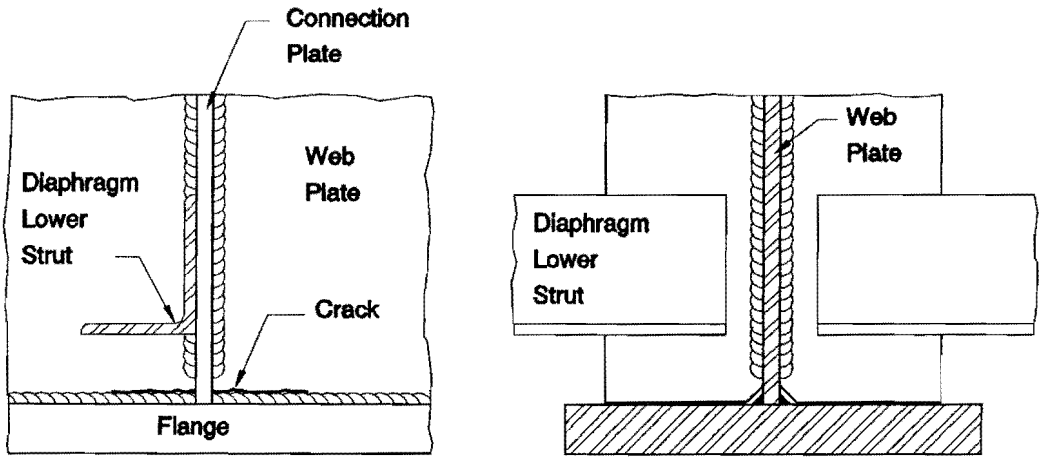

Figure 2-2: Type A1 fatigue cracking in tight-fit detail.

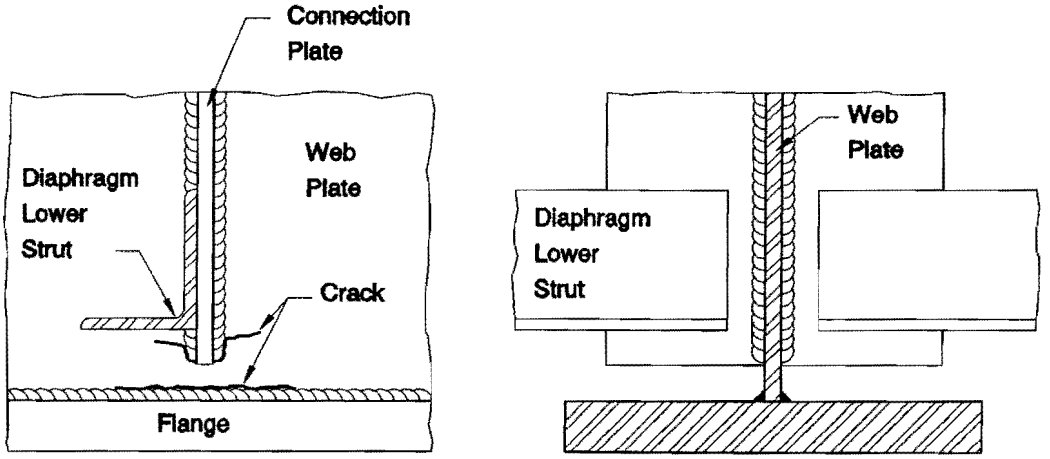

Figure 2-3: Type A1 fatigue cracking, web gap detail.

Type A2 - This type of fatigue cracking is similar to Type A1 but is found in the negative moment region where the tension flange is on the top. The cracking occurred at both the tight-fit and cut short detail and exhibited crack patterns to those shown in Figs. 2-2 and 2-3 for the positive moment region. A schematic view of the fatigue cracking is shown in Fig. 2-4. Only three Type A2 cracks were detected during the 1990 inspection (see Figs. A-3 and A-4).

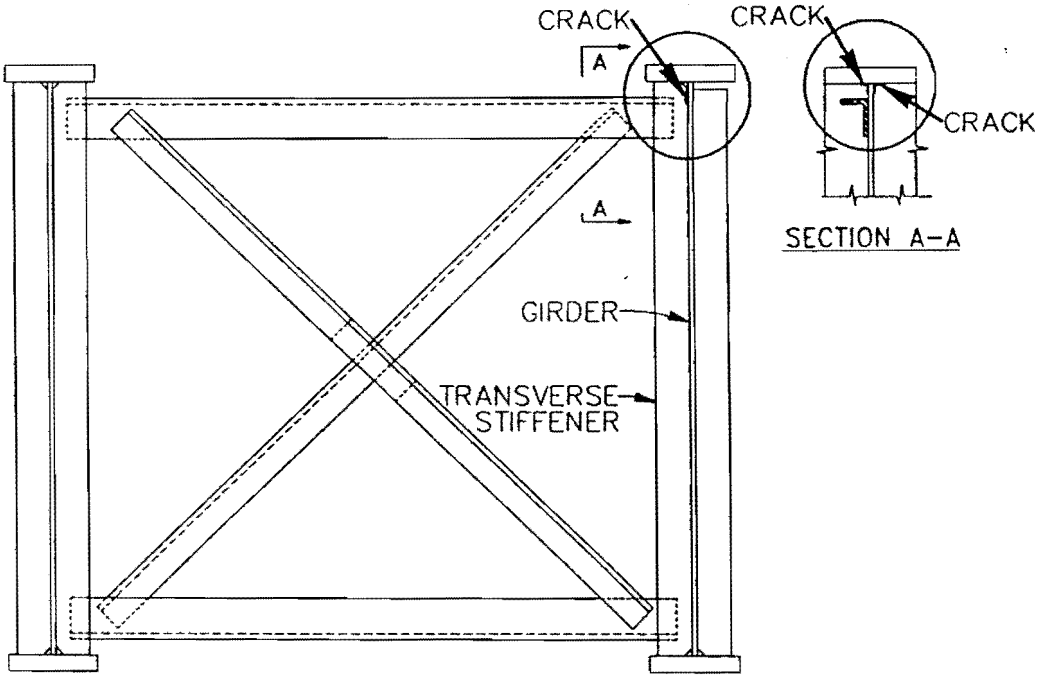

Figure 2-4: Typical location Type A2 fatigue cracking.

Based on information obtained from the contract drawings for the 1983 widening, a retrofit procedure was developed to repair Type A2 cracking. A total of 28 web gap locations were repaired (21 Westbound and 7 Eastbound). All of this type of cracking occurred in the negative moment region, at or near a support bent (see Fig. A-15 and A-16).

Type A3 - This type of fatigue cracking is one of the more perplexing cases of distortion-induced fatigue cracking. Even though a rigid attachment was provided between the end of the connection plate and flange, fatigue cracking still developed, as illustrated in Fig. 2-5. High stress ranges can occur at the connection plate end due to the eccentricity of the diaphragm member forces and, possibly, poor weld quality. This initiates a fatigue crack at the root of the fillet weld that will eventually propagate through the weld throat and into the connection plate or flange plate.

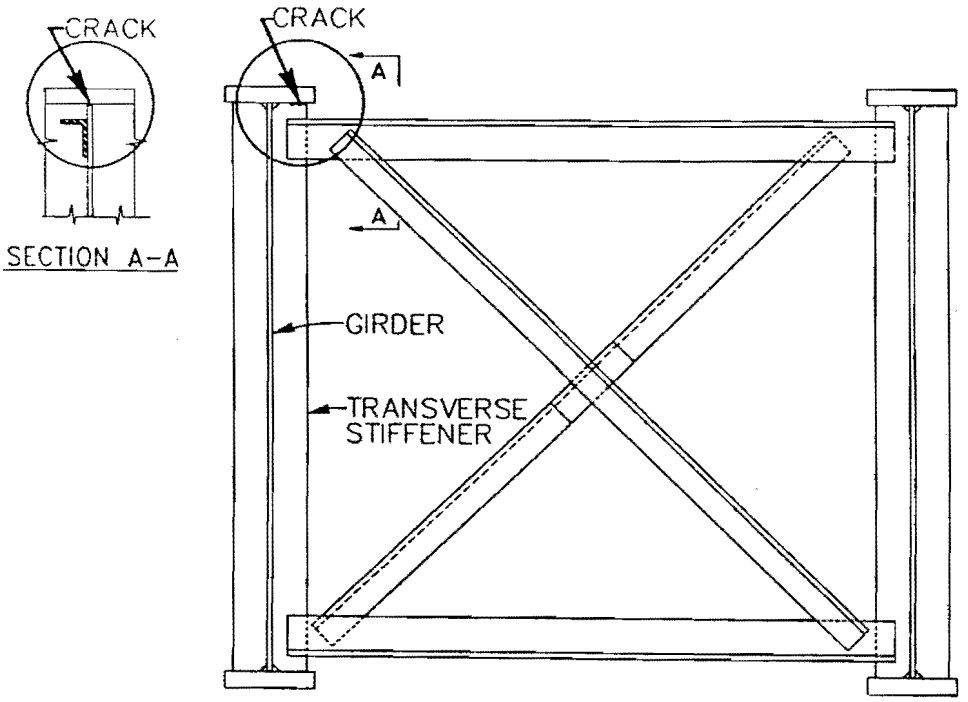

Figure 2-5: Typical location of Type A3 fatigue cracking.

The Type A3 cracking has occurred at all three diaphragm details (B, C, and C') but appears to be confined to the top flange in the positive moment regions of bending where the concrete deck provides a higher degree of restraint against the rotation of the flange.

Table 2-2 summarizes all Type A fatigue cracking with respect to girder location for both westbound and eastbound structures. The numbers shown in parentheses indicate Type A2 cracks repaired during 1983. Note that most of the cracking has been

confined to the two girders below the driving lane (Girder Nos. 3 and 4). This would be expected since most of the truck traffic crossed the bridges in this lane.

Girder	Type A1	Type A2	Type A3
		Westbound	
1	0	0 (2)	0
2	0	0 (1)	1
3	0	0 (9)	6
4	8	0 (9)	5
5	0	2 (-)	0
		Eastbound	
1	0	0 (-)	0
2	0	0 (-)	0
3	0	0 (2)	0
4	0	0 (5)	1
5	3	1 (-)	0

Table 2-2: Summary of Type A fatigue cracking.

Type B1 - This type of fatigue cracking occurs in the weldment between the lower diaphragm strut and the connection plate as shown in Fig. 2-6. This type of fatigue cracking developed due to the eccentric load on the lower strut from the diagonal member. All three diaphragm types exhibited this type of fatigue cracking.

Type B2 - This type of fatigue cracking is similar to Type B1 but is used to identify fatigue cracks that have advanced to the stage where the lower strut has completely separated from the connection plate. This has occurred at approximately 20 locations in both structures.

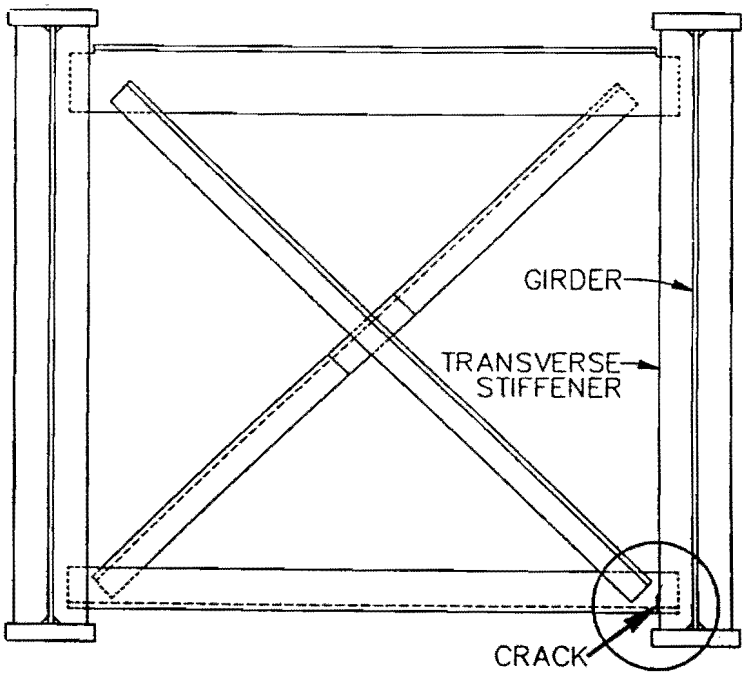

Figure 2-6: Typical location of Type B1 fatigue cracking.

Type B3 - This type of fatigue cracking is confined to the Type C diaphragm detail where the crack developed at the cope where the flange of the WT section was blocked. This type of fatigue crack developed at approximately 13 different locations (Fig. 2-7).

Table 2-3 summarizes all Type B fatigue cracking with respect to diaphragm type and girder bay location. The westbound structures contain 48 damaged diaphragms while the eastbound structures contain 28. This is consistent with the general trend of increased fatigue damage in the westbound structures. No significant trend exists between the diaphragm types with the exception of the Type C' diaphragm. This type does not have the upper strut, eliminating two potential crack sights, and has experience fewer load cycles. Most of the damage occurred in Bays C and D (driving lane) for the westbound structures and Bays A and B (passing lane) for the eastbound structures.

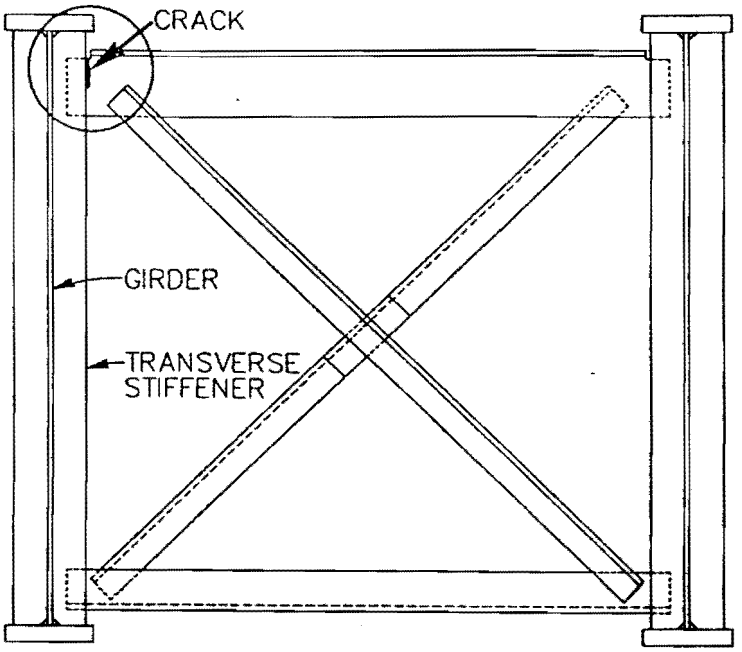

Figure 2-7: Typcial location of Type B3 fatigue cracking.

Bay	Diaphragm Type		
	B	C	C'
	Westbound		
A	1	4	--
B	5	4	--
C	14	18	--
D	--	--	2
SubTotal	20	26	2
	Eastbound		
A	4	4	--
B	3	6	--
C	2	5	--
D	--	--	4
SubTotal	9	15	4
Total	29	41	6

Table 2-3: Summary of diaphragm member fatigue cracking.

2.2 Additional Observations

Additional observations made during the July 10-11, 1991, field tests are summarized as follows:

1) The girder No. 5 line on the westbound structures was improperly aligned during construction. It appears that the entire girder line (773 ft.) is shifted to the west approximately 2 in. This has resulted in an offset or skew of the diaphragms between Girder No. 4 and No. 5, as shown in Fig. 2-8. This may add to the bending stresses in the diaphragm members.

2) The diaphragm connection plates on the first girder shop segment of girder line No. 5 of the westbound structure (from Bent 1 to Dia. No. 12) were improperly laid out during fabrication, as shown in Fig 2-9. The connection plates were offset

Figure 2-8: View of Girder No. 5 offset, Westbound Structures.

approximately 4 in. to the west of the correct position. This would have resulted in a large skew if the diaphragm relative to the web plate of the connection plate was connected as fabricated. This condition was apparently corrected in the field by welding additional connection plates on the outside face of Girder No. 4. As a consequence, the diaphragm connection plates on Girder No. 4 are offset to the existing diaphragm connection plates. The offset between these connection plates has exasperated the distortion at the web gap as indicated by the severity of the cracking reported in the inspection report. This condition resulted in a more flexible web gap since the diaphragm forces are not directly distributed out to adjacent girder bays and diaphragms.

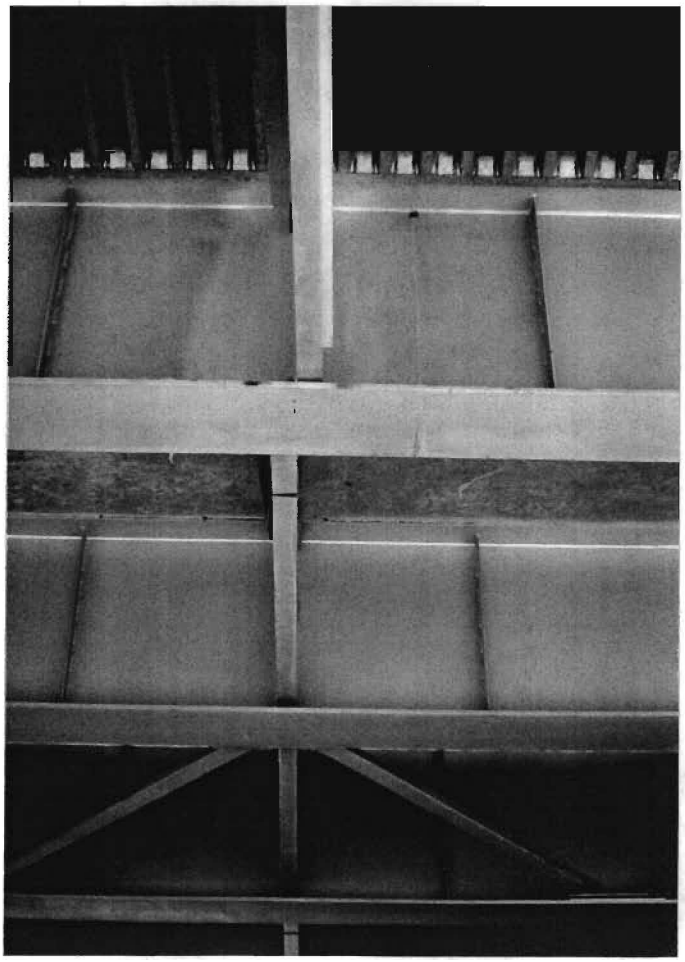

Figure 2-9: View of Girder No. 5 connection plate offset, Westbound Structures.

3) A 30 minute tr ıck traffic count was taken between 1:40pm and 2:10pm on July 11, 1991. As indicated in Table 2-4, the eastbound structures carried 50 percent more truck traffic during the recorded period. However, due to the short duration of the traffic count, it would be difficult to draw any conclusion of the degree of fatigue cracking observed in both structures.

Direction	Number of Trucks
Eastbound	45
Westbound	30

Table 2-4: Truck traffic count for 1:40pm to 2:10pm, July 11, 1991.

4) The Special Report states that:

> "Interstate 20 at this location serves some 10,000 vehicles per day. Approximately 40% of the vehicles are trucks with interstate cargos as well as trucks with loads which support the petroleum and other industries in the area."

The report does not distinguish between the two directions.

5) The orientation of the cross frame diaphragm members was opposite to that shown on the original design drawings (the long leg of the angle was outstanding instead of the short leg).

6) The lateral connection plates are welded directly to the bottom flanges. The type of connection results in a Category E classification and may warrant further investigation and increased inspection.

3. FIELD MEASUREMENTS

In order to assess the severity of the fatigue cracking and aid in the development of retrofit procedures, strain gage measurements were obtained at various locations on the structure. The field testing was conducted during July 11-12, 1991, and involved testing the structure in the as-built condition.

All testing and recording equipment was provided by the Texas Department of Transportation. This included the data acquisition system, strain gages, transducers, and all material necessary to perform the testing. Traffic control was also maintained by the State.

3.1 Test Procedure

The field measurements were recorded on the existing structure prior to any retrofitting in order to provide the following information:

1) Determine magnitude of diaphragm member forces under known load conditions for each diaphragm type.

2) Provide a structural behavior reference with which to investigate effects of modifications to the bridges.

The recording equipment allowed the recording of only eight strain gages per single truck passage. Therefore, six gage groups were used to study the behavior of various diaphragm types and load distributions as summarized in Table 3-1 and shown in Fig. 3-1. The 325 ft. unit of the eastbound structure was chosen for strain gaging since it contained less reported fatigue damage and was easily accessible from the frontage road below. It was desirable to avoid locations of extensive damage since this would not allow for the observation of the as-built condition. The actual location of each gage group was dictated by reasonable access from the ground by a truck mounted bucket and for safety reasons. As shown in Fig. 3-1, diaphragms between Bents 6 and 7 on the

eastbound structure were selected. This location provided diaphragms in both positive and negative regions of bending.

Gage Group Number	Description of Gage Group Location
1	Type C' diaphragm members, Diaphragm Number 40, Bay D, Positive Moment Region.
2	Type B diaphragm members, Diaphragm Number 40, Bay C, Positive Moment Region.
3	Type C diaphragm members, Diaphragm Number 43, Bay C, Negative Moment Region.
4	Type C' diaphragm members, Diaphragm Number 43, Bay D, Negative Moment Region.
5	Bottom flanges and diaphragm lower struts at Diaphragm Line 40
6	Type C diaphragm members, Diaphragm Number 39, Bay C

Table 3-1: Summary of gage group locations.

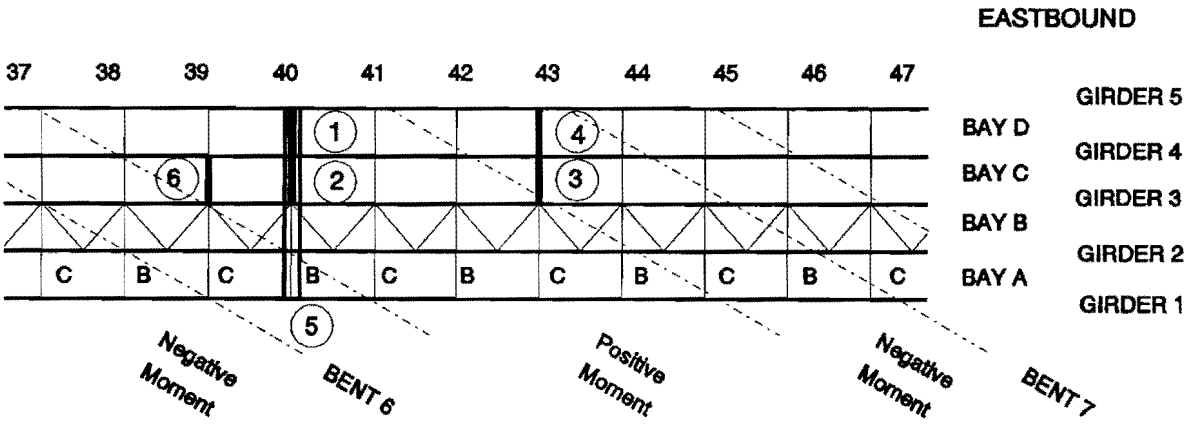

Figure 3-1: Gage group locations on Eastbound structure.

Five of the six gage groups (Gage Groups 1, 2, 3, 4, and 6) involved diaphragm members. For each group, six gages were placed on diaphragm members and two gages were placed on the bottom of each adjacent girder flange. This provided a means of determining the difference in stress levels between the girders which can be related to their relative deflection and the primary source of the distortion in the web gaps.

A sixth gage group (Gage Group 5) was used to study the load distribution between all five girders in a cross section. All five girder bottom flanges were gaged as well as the diaphragm lower struts in Bay B, C, and D.

In order to provide a known load condition, a TxDOT vehicle of known weight was used and is shown in Fig. 3-2. The axial configuration and measured weights are given in Fig. 3-3. The truck driver was instructed to maintain a constant speed of 50 mph while traversing the bridge and to remain in the designated lane position as best as possible. For all measured test truck passages, the truck driver was successful in isolating himself from the normal traffic. Therefore, the measured strains are those produced only from the test truck. No superposition with normal truck traffic occurred during the recorded test truck passages.

In addition to recording the passage of the test truck, strain measurements were obtained for several semi tractor trailers for both Gage Groups 4 and 6. While the weights of this vehicles are unknown, it allowed for the observation of the bridge under normal truck traffic.

Various lane positions were used for the gage groups. The most significant lane position was when the test truck was positioned in the center of the driving lane, as shown in Fig 3-4. This position represents the predominate truck position that the bridge is subject to and is the cause of the distortion problems. The other truck positions were recorded to allow for a better understanding of the bridge behavior and are shown in Figs. B-3 to B-8 of Appendix B.

Figure 3-2: View of TxDOT vehicle used as test truck.

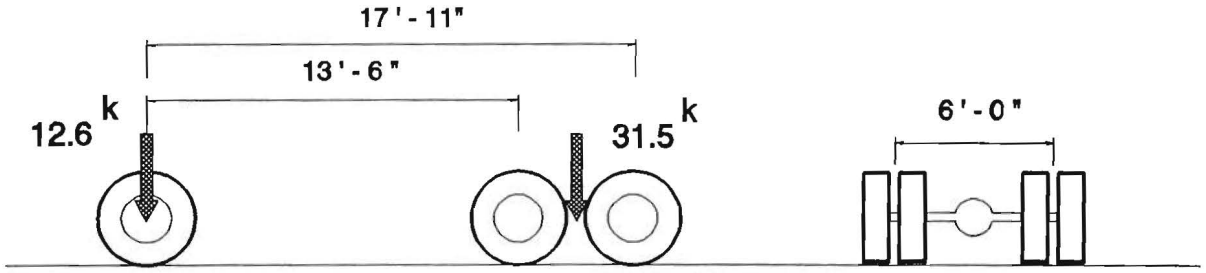

Figure 3-3: Test truck axial weight and configuration.

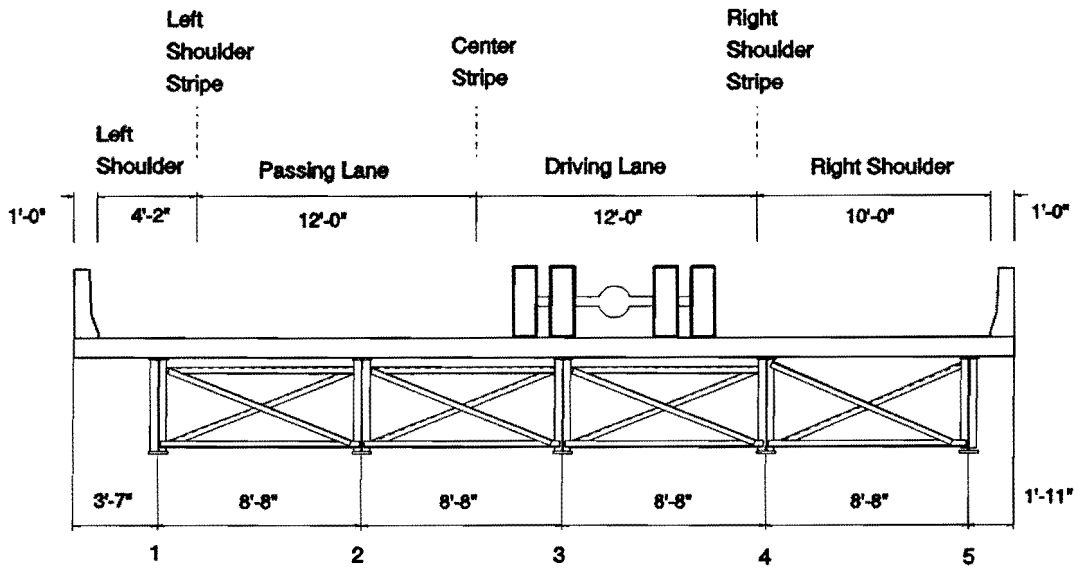

Figure 3-4: Location for test truck positioned in center of driving lane.

3.2 Analysis of Field Test Data

The following discussion is based on a review of the strain data obtained from the July 10-11, 1991, field test. For a complete listing of stress histories for all tested truck positions, see Appendix B.

Gage Group 1 was used to measure the diaphragm member forces in a Type C′ diaphragm located in the positive moment region of bending. The locations of the eight gages are given in Fig. 3-5.

The recorded stress histories of the gages located on the diaphragm members (Gage Nos. 3 through 7) are given in Fig. 3-6 for the test truck positioned on the center of the driving lane. Note that in plotting the stress histories, the recorded values were increased by a positive integer in order to separate the traces and avoid overlaps. Each gage was zeroed without any traffic prior to recording the truck passage. Tensile stress is plotted above the integer baseline and compressive stress below. Of interest are the

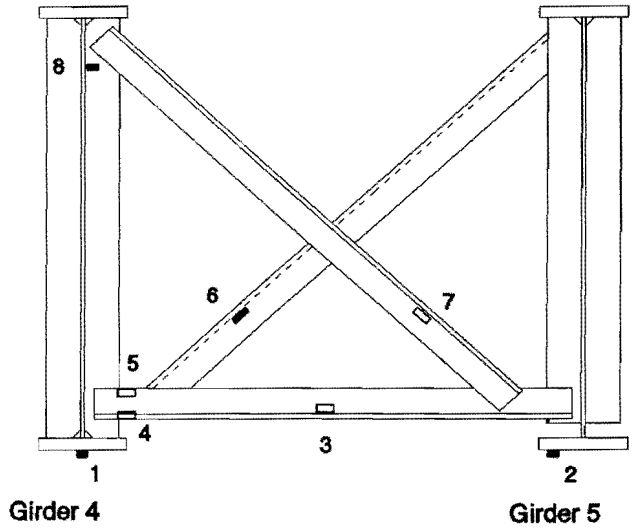

Figure 3-5: Strain gage locations for Gage Group 1.

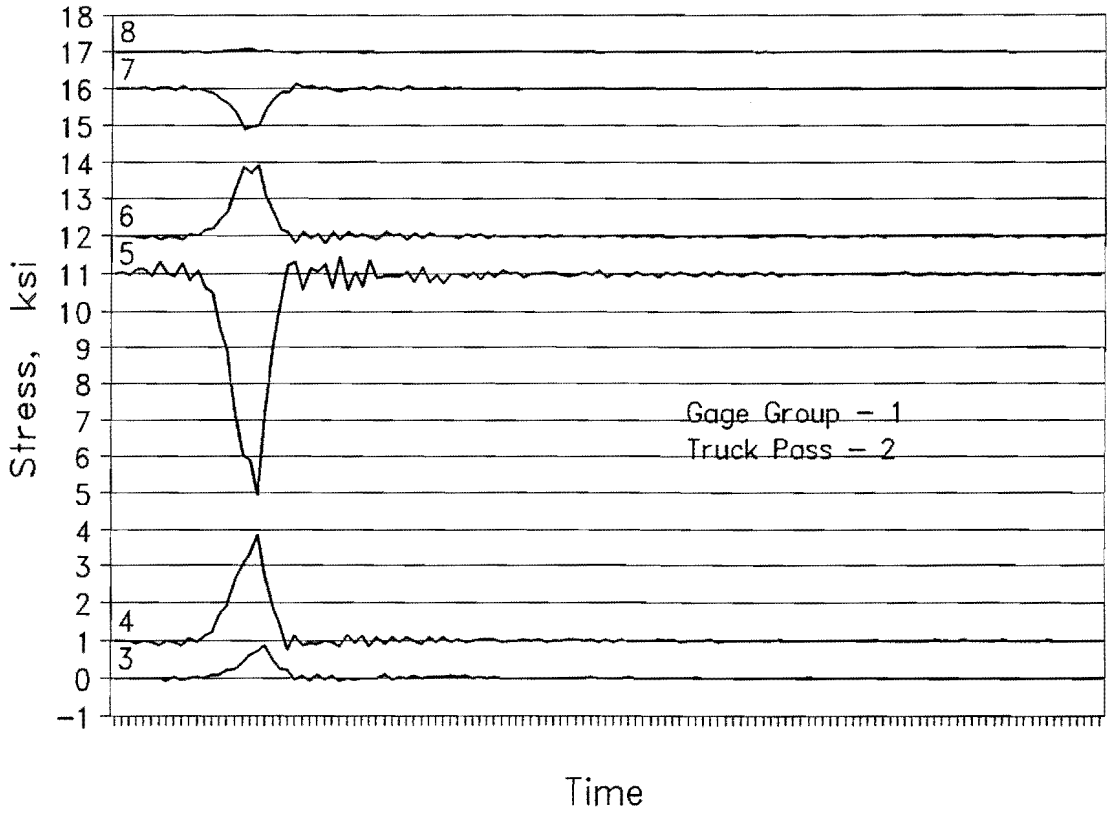

Figure 3-6: Diaphragm D-40 member stress histories for Gage Group 1, Truck Pass 2 (test truck centered in driving lane).

stresses obtained for Gage Nos. 4 and 5 which show the effect of the eccentric connection between the diagonal and lower strut. A measured diagonal force of 6.4 kips resulted in a bending stress range of 6.6 ksi. near the top of the lower strut. The vertical fillet weld that attaches the strut to the connection plate can be classified as an AASHTO Category D detail with a corresponding fatigue limit of 7 ksi. Therefore, any truck weight above that of the test truck (greater than 43 kips) is likely to initiate fatigue crack propagation. A truck loaded to the legal weight limit would result in a stress range approximately double that of the test truck.

The finite element analysis discussed in Sec. 4 and Appendix C shows that higher diaphragm diagonal forces occur at diaphragm locations other than the one gaged. Therefore, this gage group does not necessarily provide the highest stress condition in a Type C′ diaphragm located in the positive moment region of bending. As indicated by the stress histories in Figs. B-9, B-11, and B-12 other test truck positions did not result in as severe stress conditions. Strain gage No. 8 of Gage Group 1 was used to locate the neutral axis of Girder 4. As indicated by the stress history in Fig. 3-6, the gage was located at the neutral axis by chance. The gage was located 5.5 in. from the bottom of the top flange.

Member forces for a Type B diaphragm located in the positive moment region of bending were investigated with Gage Group 2. The strain gage locations for this gage group are given in Fig. 3-7. Typical stress histories with the test truck located in the driving lane are shown in Fig. 3-8. This truck position results in the highest lower strut and diagonal member forces of the three truck positions tested. (See Figs. B-14 and B-15 for the other truck position stress histories.) When the test truck was located in the right shoulder, the resulting stress range in the lower strut was less than 1.0 ksi.

Strain gages were also placed on the upper strut between the diagonal and the connection plate. At this location, a tensile bending stress of only 1.0 ksi was measured due to the eccentric nature of the connection. However, the diaphragm location is not indicative of the highest members forces as given in Table C-8.

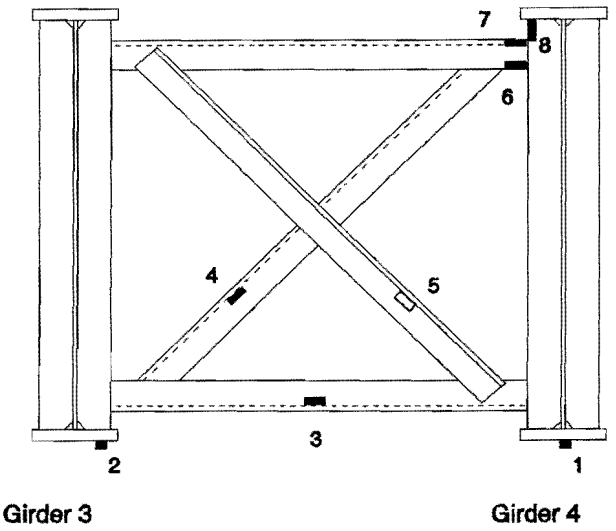

Figure 3-7: Strain Gage locations for Gage Group 2.

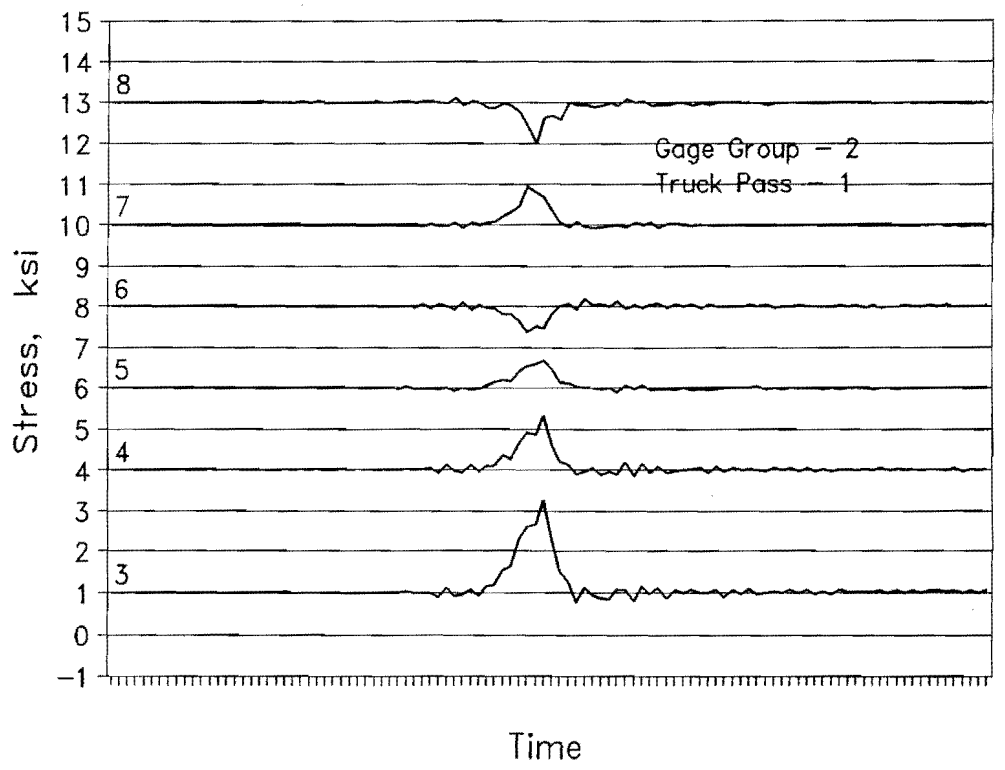

Figure 3-8: Diaphragm C-40 member stress histories for Gage Group 2, Truck Pass 1 (test truck centered in driving lane).

In addition, a strain gage was placed at the outer edge of the connection plate, above the upper strut. When the test truck was located in the right shoulder, a stress range of 2.6 ksi was measured, though the stress cycle was compressive. The driving lane load condition resulted in a compressive stress range of approximately 1.0 ksi. The test truck positioned in the passing lane resulted in a tensile stress range of 1.0 ksi. While the measured stresses at this location are relatively lower, the details that exhibited fatigue cracking at the connection plate end weld were all located in the negative moment region.

No Type B diaphragm was tested in the negative moment region of the bridge.

Gage Group 3 was used to study the behavior of a Type C diaphragm located in the negative moment region of bending. Strain gage locations for this gage group are given in Fig. 3-9.

The stress histories for Gage Nos. 3 - 8 are given in Figs. 3-10 for the test truck centered in the driving lane. Strain gages (Nos. 7 and 8) were placed at the end of the upper strut to measure the bending stress caused by the eccentric diagonal connection. For a tensile axial force of 4.6 kips in the diagonal member, a bending stress range of 4.5 ksi was measured at the cope. Lower stress ranges were measured for other test truck positions (see Figs. B-17 through B-20).

Of significance is the fact that no stress was measured in the main portion of the upper strut (between the diagonal connections). This was found to be true for all truck positions. The absence of load indicates that while the upper strut is needed for girder flange stability during construction, it serves no function other than that of a gusset plate for the diagonals in the as-built condition.

Gage Group 4 consists of strain gages placed on a Type C′ diaphragm located in a negative moment region. Actual strain gage locations are given in Fig. 3-11, and the measured stress histories for the test truck in the driving lane are given in Fig. 3-12.

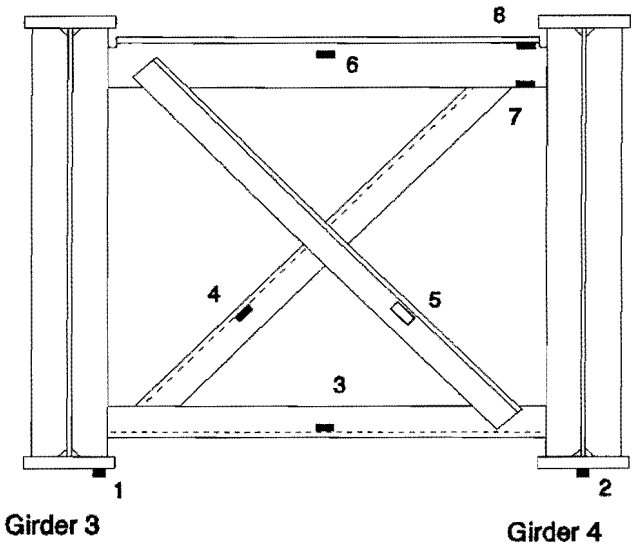

Figure 3-9: Strain gage locations for Gage Group 3.

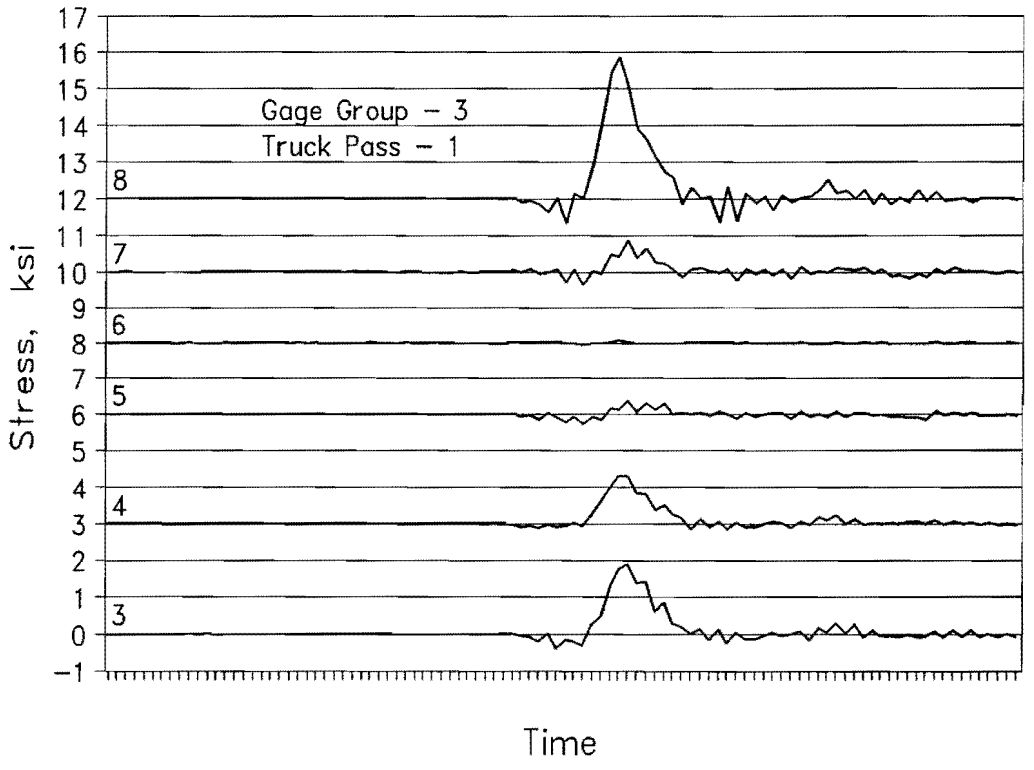

Figure 3-10: Diaphragm C-43 member stress histories for Gage Group 3, Truck Pass 1 (test truck centered in driving lane).

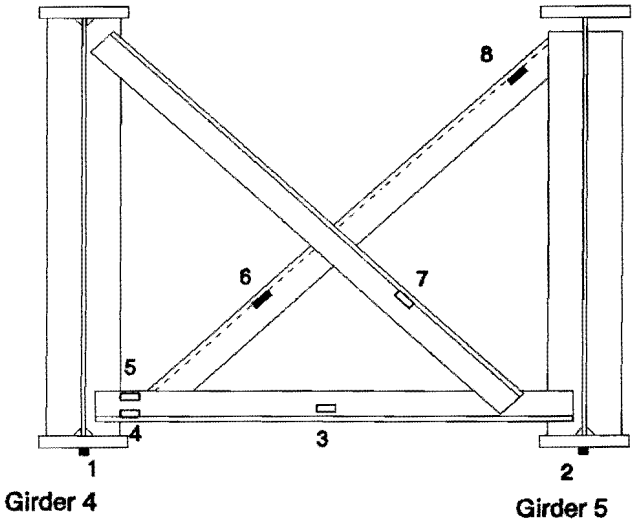

Figure 3-11: Strain gage locations for Gage Group 4.

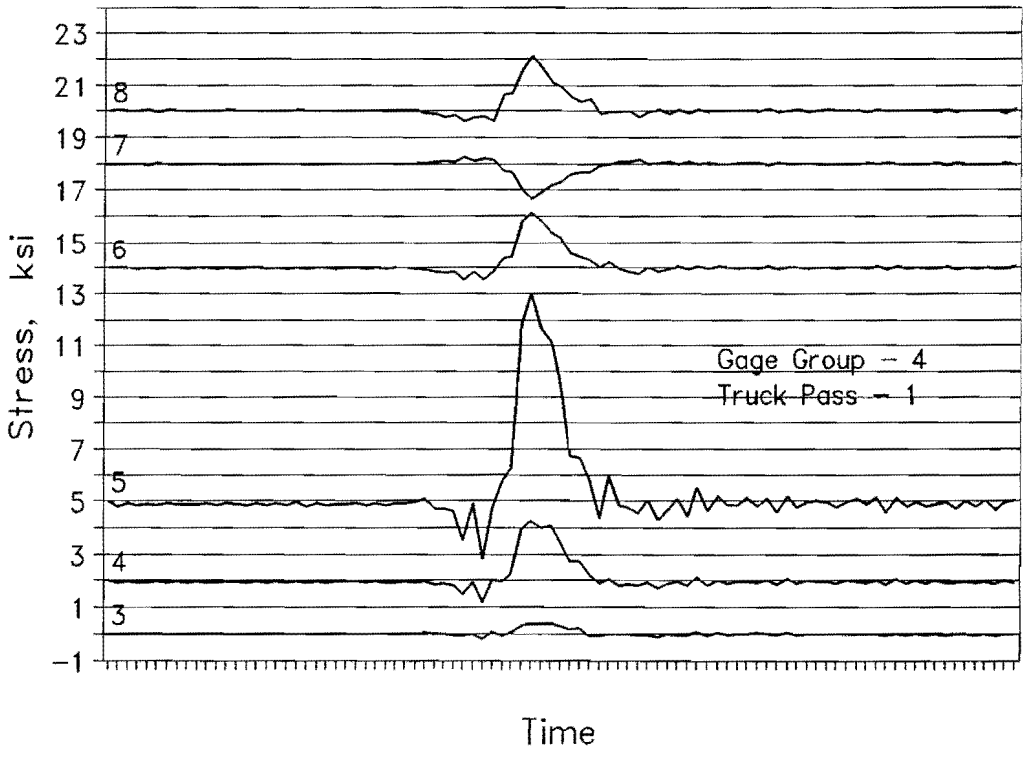

Figure 3-12: Diaphragm D-43 member stress histories for Gage Group 4, Truck Pass 1 (test truck centered in driving lane).

Gage Numbers 4 and 5 of Gage Group 4 were placed on the lower strut between the diagonal and connection plate to measure the bending stress caused by the eccentric diagonal connection. For a 7.9 kip tensile axial force in the diagonal, a maximum bending stress range of 10.2 ksi was measured. as shown in Fig. 3-12. Higher stresses were recorded for other truck positions. For example, when the test truck was positioned in the right shoulder lane, a stress range of 12 ksi was measured. The truck position places the truck directly above the instrumented diaphragm in Bay D. (See Figs. B-23 through B-27 for stress histories of other test truck positions.)

Stress histories were measured for two tractor trailer trucks in the driving lane of unknown weights with this gage group as shown in Fig. 3-13. A maximum stress range of 11.7 ksi was measured for Gage No. 5.

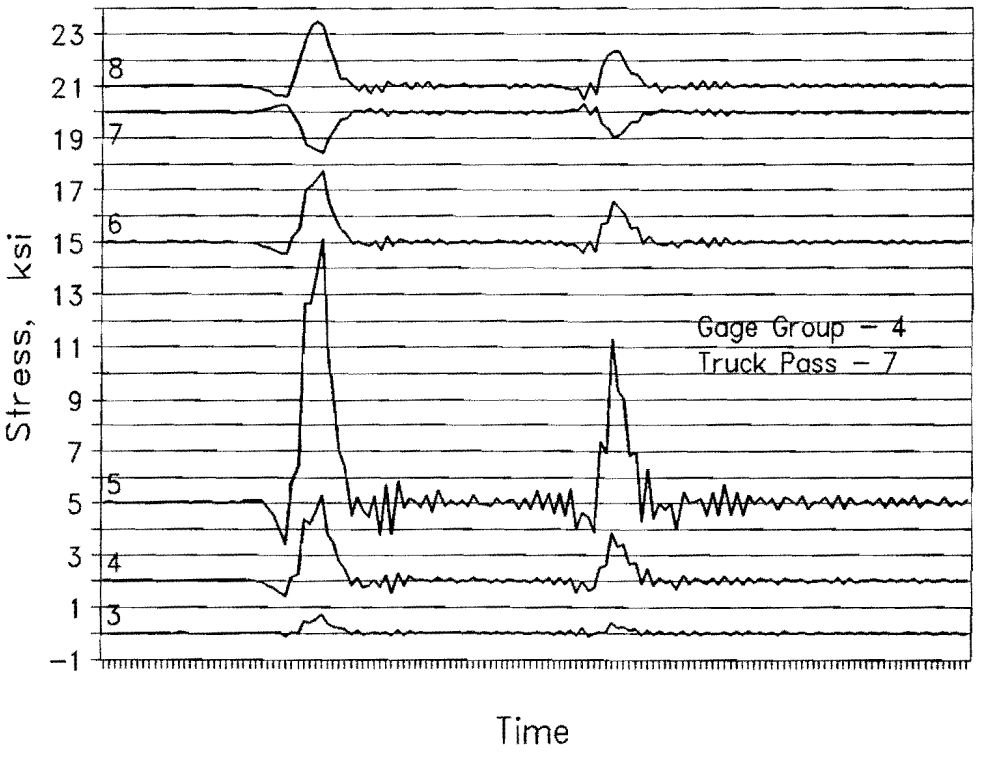

Figure 3-13: Diaphragm D-43 member stress histories for Gage Group 4, Truck Pass 7 (two tractor trailer trucks centered in driving lane).

Gage Group 6 was used to measure the diaphragm member stresses in a Type C diaphragm located in the positive moment region of bending. Strain gage locations are given in Fig. 3-14.

Similar to the Type C diaphragm located in the negative moment region, no stress was recorded in the upper strut (see Fig. 3-15). While the maximum bending stress of the eccentric diagonal connection was relatively low (1.2 ksi), the finite element analysis indicated that higher diaphragm member forces occurred at other diaphragm locations. (See Figs. B-35 through B-39 for other truck positions.)

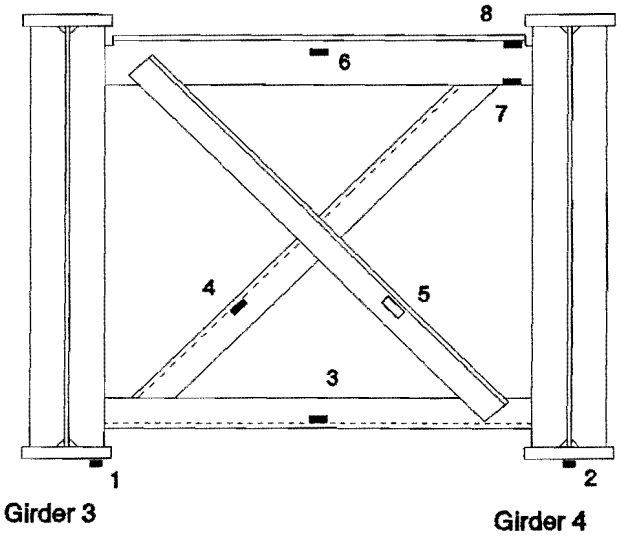

Figure 3-14: Strain gage locations for Gage Group 6.

3.3 Conclusions

The recorded stress ranges indicate that high local bending stresses are induced into both the upper and lower diaphragm struts from the eccentric diagonal connection. The stresses are high enough in magnitude to be the cause of the fatigue cracking observed in the diaphragm members.

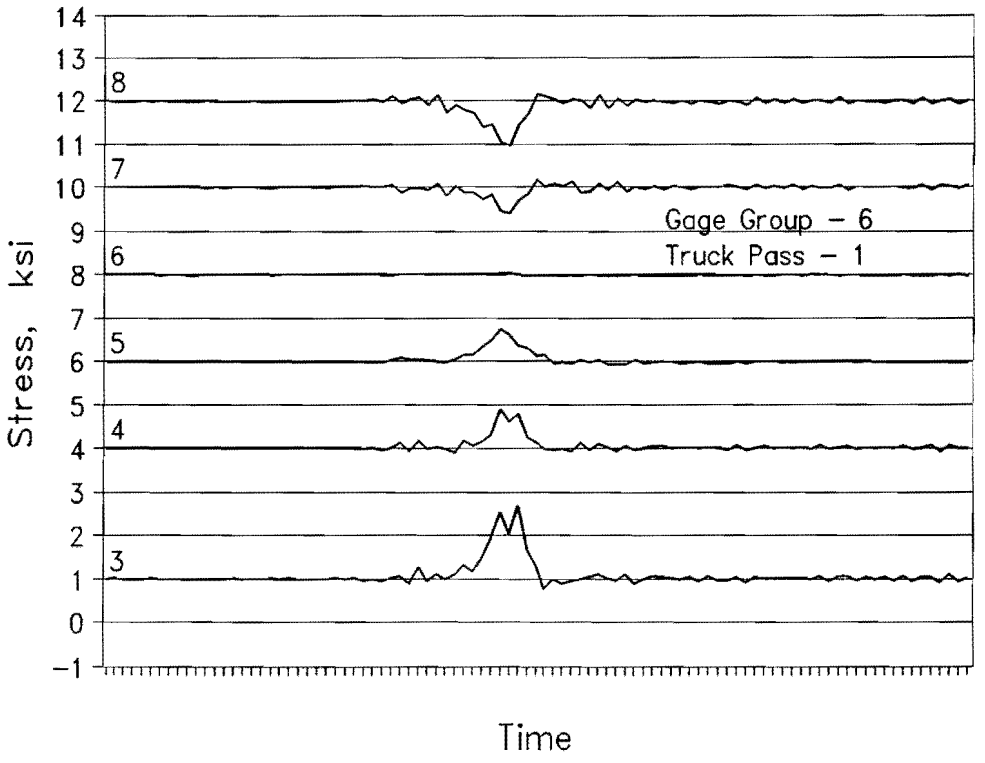

Figure 3-15: Diaphragm C-39 member stress histories for Gage Group 6, Truck Pass 1 (test truck centered in driving lane).

The stress measurements indicate that the upper strut of the Type B and C diaphragms is non-loading under service load conditions. A design to replace the existing diaphragm on the Midland County Bridges need not incorporate an upper strut member.

4. FINITE ELEMENT STUDY

Four finite element models were developed in order to evaluate the effect of selective diaphragm removal on the remaining diaphragm member forces, lateral distribution between girders, and concrete deck stresses. By removing diaphragms from the bridge, the two fatigue problems afflicting the structure, mainly web gap and diaphragm member cracking, can be either reduced or eliminated entirely.

4.1 Finite Element Model Development

The finite element models used for this portion of the study were created using a three-dimensional finite element program called Algor, which uses the Hyper SAP0 algorithm. While the Algor program has dynamic analysis capabilities, only a static analysis of the structure was performed so as to reduced the computational time required for a solution. Also, the main concern with the diaphragm removal is the relative change in stress, not the actual stress magnitudes.

Only the three-span continuous structure on which field measurements were obtained was modeled (the 325 ft. unit of the eastbound structure). It is assumed the behavior of this structure is representative of the other three structures. Four different finite element types were used to model various components of the bridge structure. Beam elements were used to model the top and bottom girder flanges, and plane stress elements were used for the girder web. Truss elements were used to model the diaphragm members and lateral cross-bracing members, while rectangular plate bending elements were used for the concrete deck slab. The web stiffeners were not included in the model.

The finite element model was created with the generation features of an accessory program called Aedit, which is part of the Algor package. No particular attention was given to the numbering sequence of the nodes since Algor incudes a bandwidth

minimization routine. Nodes were placed at 7.5 ft. increments along the entire length of the bridge and element connectivity was established. Finally, the material and section properties were entered for the different elements. The finalized model included 757 nodes with 4,369 degrees of freedom, 710 beam elements, 218 plane stress elements, 284 truss elements, and 262 plate bending elements. The finite element model with ten load cases required approximately 2.5 hours of solution time running on a 386-33MHz personal computer. A plot of the finite element model is given in Fig. 4-1.

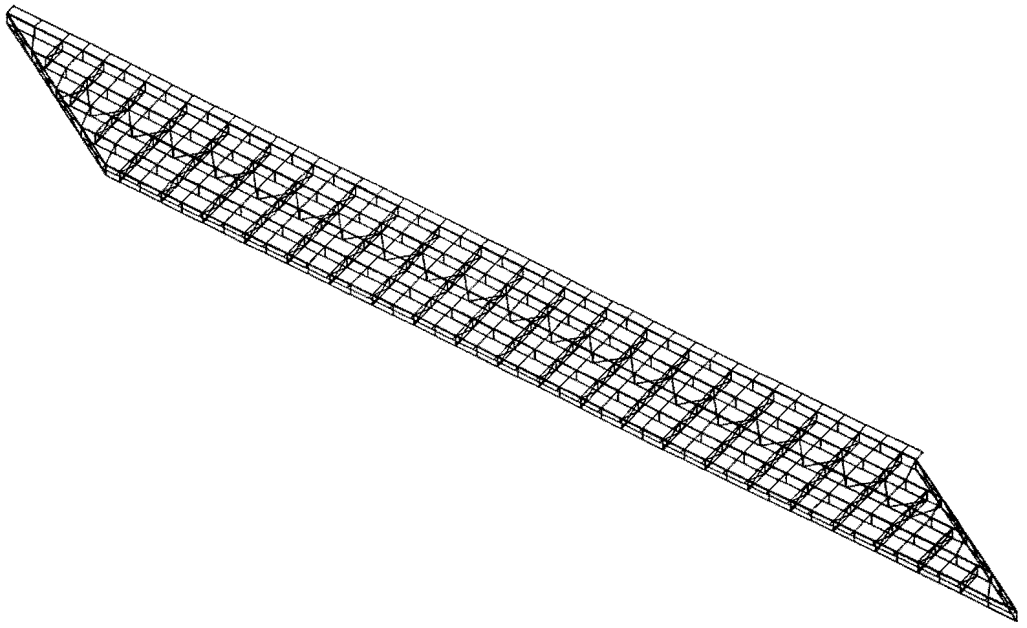

Figure 4-1: Plot of finite element model for as-built structure.

The truss elements were used to model the diaphragm elements since bending stiffness of a single diaphragm member contributes little to the overall stiffness of the diaphragm. During the initial test runs of the model, the diaphragm upper struts were included. However, after investigation of these member stresses produced by Algor and the fact that the stresses measured in the field were very small, these members were removed form the model to reduce computation times and to increase the accuracy of the model's behavior to the actual structure.

4.2 Finite Element Model Calibration

In order to verify that the bridge's structural behavior had been correctly modeled, calibration runs were made with the model which simulated the as-built, uncracked condition. For these runs, the test truck axle loads were discretized into nodal point loads which could be placed on the structure to simulate its passage across the structure. The test truck load was proportioned between Girders 3 and 4 to simulate the truck in the driving lane. To fully test the structure, four computer runs with ten load cases each were performed. This simulated the movement of the test truck across the entire length of the structure.

The stress values obtained from the finite element model were compared with the values obtained from the field at the measured locations. The finite element model values were found to be approximately 25 percent below the stress values measured in the field. For example, the finite element analysis yielded a maximum bottom flange stress of 1.4 ksi at Diaphragm Line 40 of Girder 4. Correspondingly, a maximum stress of 1.7 ksi was measured at the same location by Gage Group 5. This discrepancy was found to be acceptable since the finite element solution did not include dynamic effects (test truck was run at 50 mph) and finite element solutions are inherently more stiff than the actual structure, thus reducing element stresses. In addition, the tabulated values for the field measures are maximum stress range values, including all vibratory effects.

4.3 Finite Element Models for Evaluation

In addition to the as-built finite element model previously discussed, three other models were developed in order to evaluate the effect of diaphragm removal on the behavior of the bridge. Therefore, all four models used in this study were similar with the exception of the diaphragms. A summary of the four finite element models is given as follows:

Model 0 - This finite element model was of the as-built structure with all

diaphragms in place. In addition to being used for calibration, the results for this model were used as a reference in comparing results from the other three models.

Model 1 - This finite element model was similar to Model 0 but with all Type B diaphragms removed from the structure. This allowed for the investigation of the change in load distribution characteristics of the structure with only approximately one-half the original number of diaphragms remaining in the structure. A plot of the finite element model and the framing plan for Model 1 are shown in Figs. 4-2 and 4-3, respectively.

Model 2 - In this model, all the diaphragms were removed from the structure. This represents the ideal repair procedure since it eliminates both the source of out-of-plane distortion at the web gap and the need to repair any fatigue damaged diaphragm members.

Model 3 - Diaphragms were selectively removed in the model in an attempt to maintain the original load distribution characteristics of the structure while reducing necessary repairs to a minimum. Examination of the results from Models 1 and 2 indicated that the largest deviation in stresses occurred in the positive moment region. Therefore, a staggered diaphragm pattern was used that provided more diaphragms in the positive moment region of bending than in the negative moment region. A plot of the finite element model and the framing plan for Model 3 is shown in Figs. 4-4 and 4-5, respectively.

For all four finite element models evaluated, a unit axle loading of 10 kips was passed over the structure in the driving lane and influence lines developed. A single unit axle load was used instead of some given truck load and axle configuration since the concern in this study was the relative change in behavior, not actual stress magnitudes. The study was confined to axle loads in the driving lane since most of the truck traffic is in this lane and causes most of the fatigue damage.

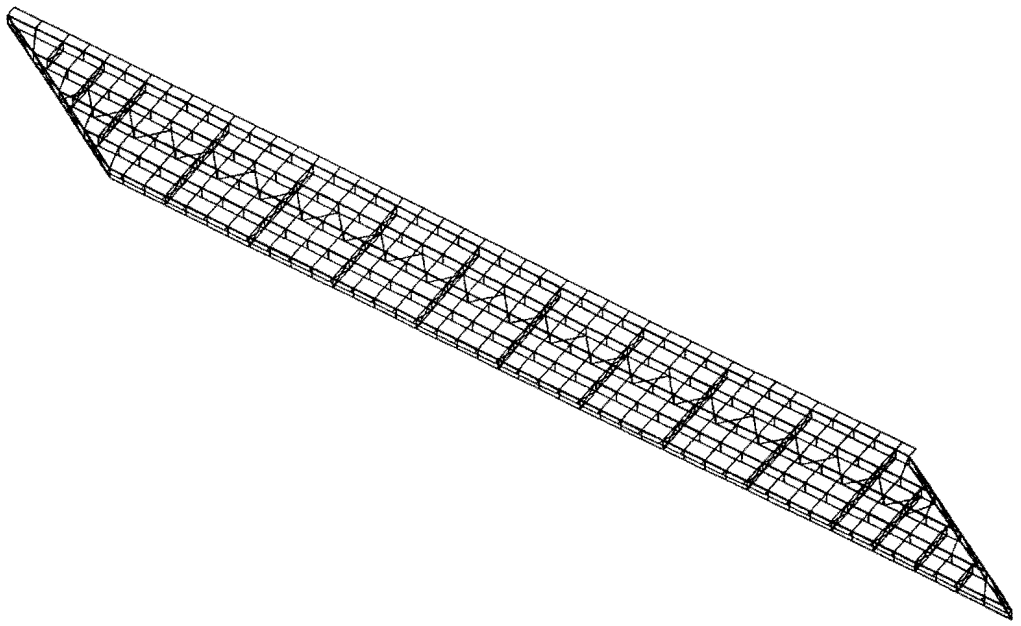

Figure 4-2: Plot of finite element model with Type B diaphragms removed.

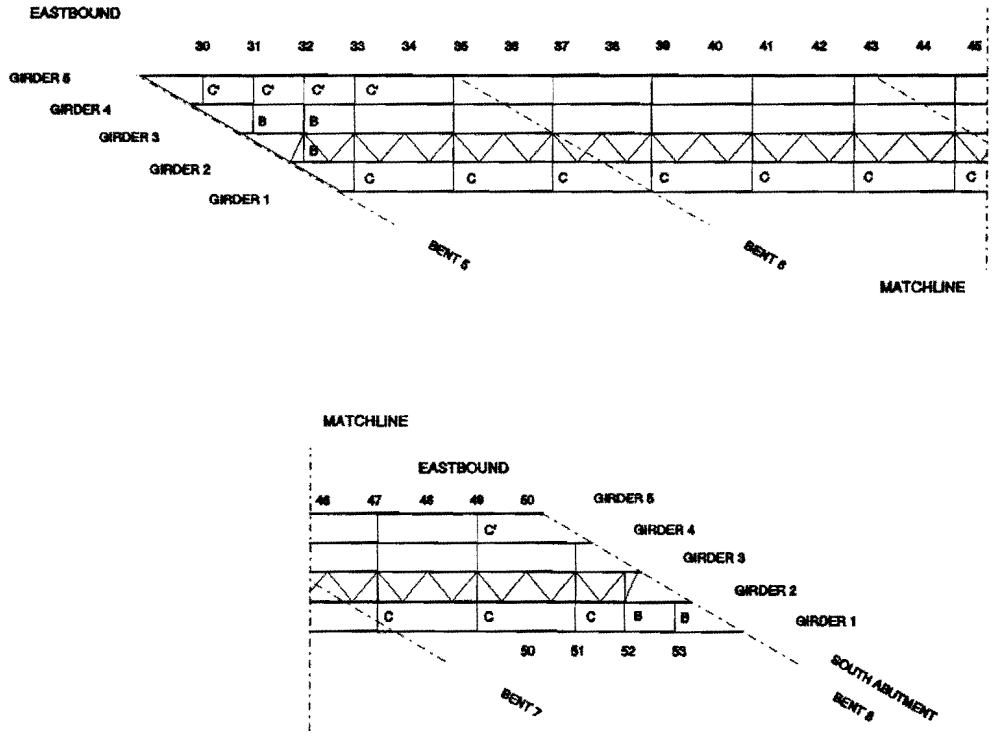

Figure 4-3: Framing plan for finite element Model 1.

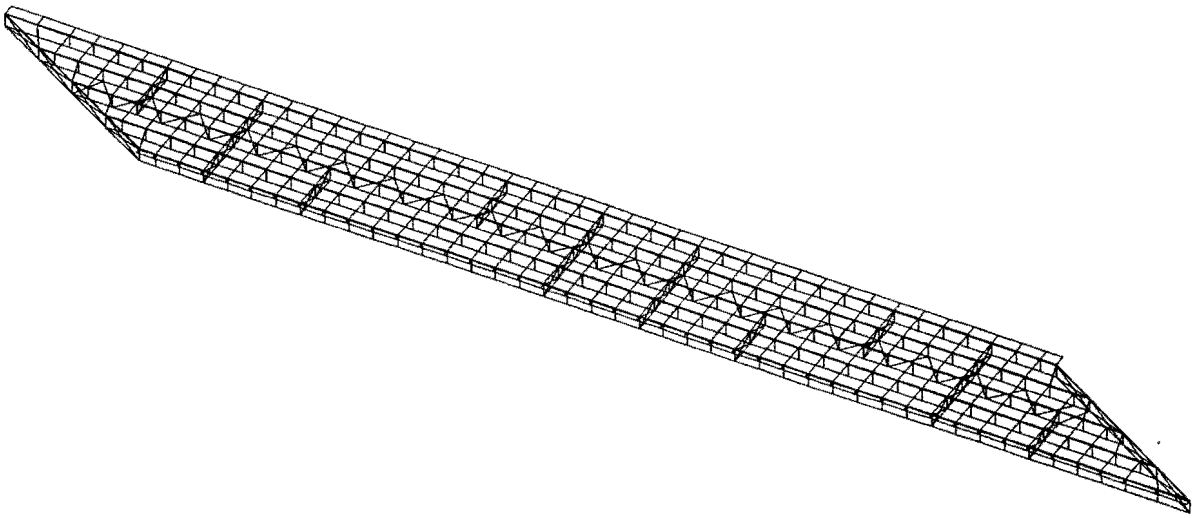

Figure 4-4: Plot of finite element model with staggered diaphragms.

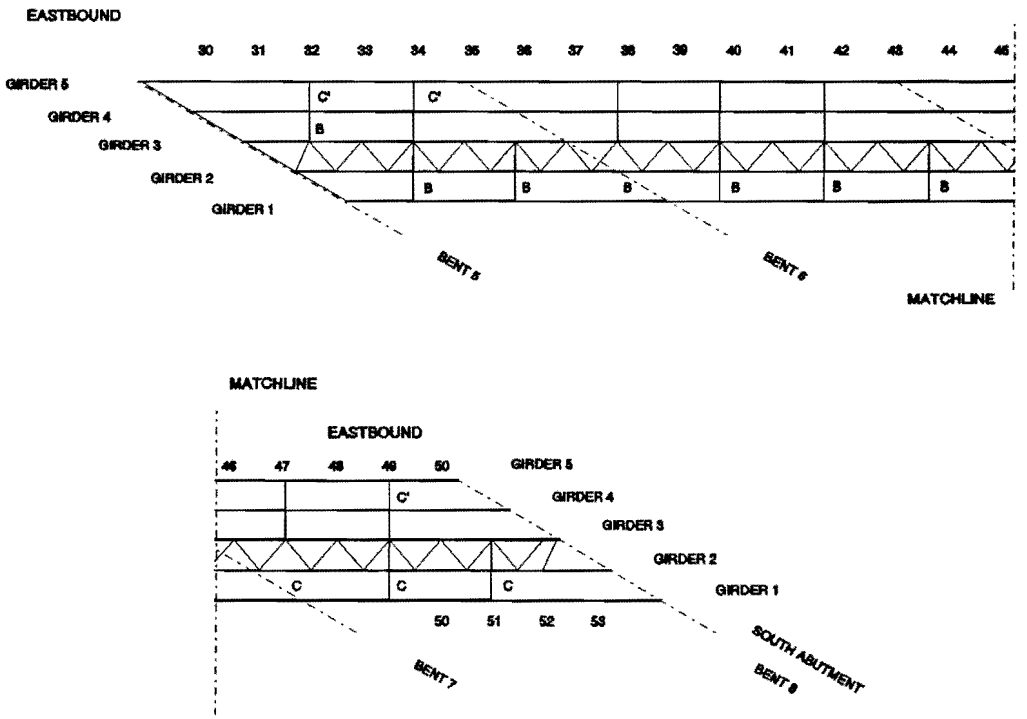

Figure 4-5: Framing plan for finite element Model 3.

4.4 Results of the Finite Element Analysis

The maximum bottom flange stresses for Girders 3 and 4 are plotted in Figs. 4-6 and 4-7, respectively, for all four finite element models. These plots, as well as other plots referred to in this discussion, were obtained by determining the maximum stress level for any longitudinal load position on the structure for a given model node position. Table C-1 provides the relation between each model node number and the corresponding diaphragm or bent number. Note that the model node numbering increases in the direction of the eastbound traffic, but is opposite to the diaphragm or bent numbering sequence.

As shown in Figs. 4-6 and 4-7, the largest deviation in the overall behavior was when all diaphragms were removed from the structure. The largest changes occurred in the positive moment region of bending and in Girder 3 more than Girder 4. Girder 3 carries 65 percent of the 10 kip unit axle load as compared to 30 percent for Girder 4 when the truck was positioned in the center of the driving lane (Girder 2 carries 4 percent). The bottom flange stresses increased an average of 25 percent in the positive moment region of Girder 3 between the as-built condition (Model 0) and no diaphragms (Model 2). The other models did not result in stress values as high as those given by Model 2.

Figures 4-8 and 4-9 are similar to the plots given in Figs. 4-6 and 4-7 but show the top flange stresses for both Girder 3 and Girder 4. The deviation in stress between the different models is less than that given for the bottom flange stresses.

As shown in Figs. 4-6 through 4-9, the largest deviation in flange stress occurs when all the diaphragms are removed form the structure. Both the Type B diaphragm removal and the staggered diaphragm pattern result in less deviation of stress and are therefore acceptable solutions to the fatigue problems experienced by the bridge.

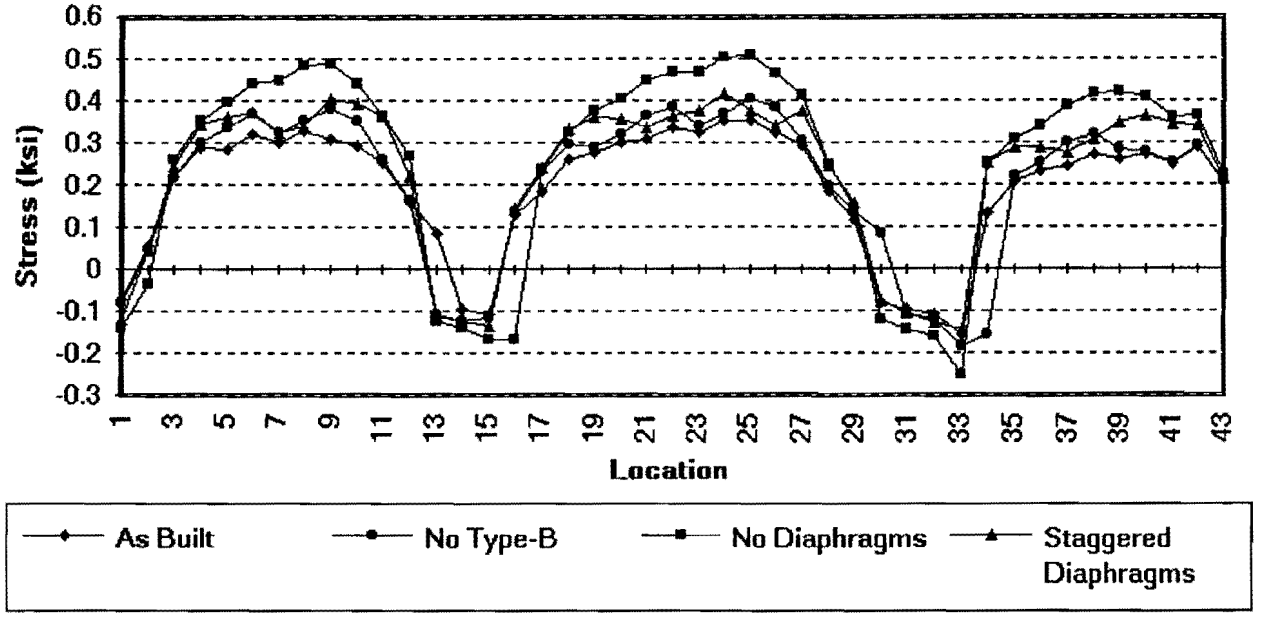

Figure 4-6: Comparison of maximum bottom flange stresses for all models, Girder 3, 10 kip unit axle load.

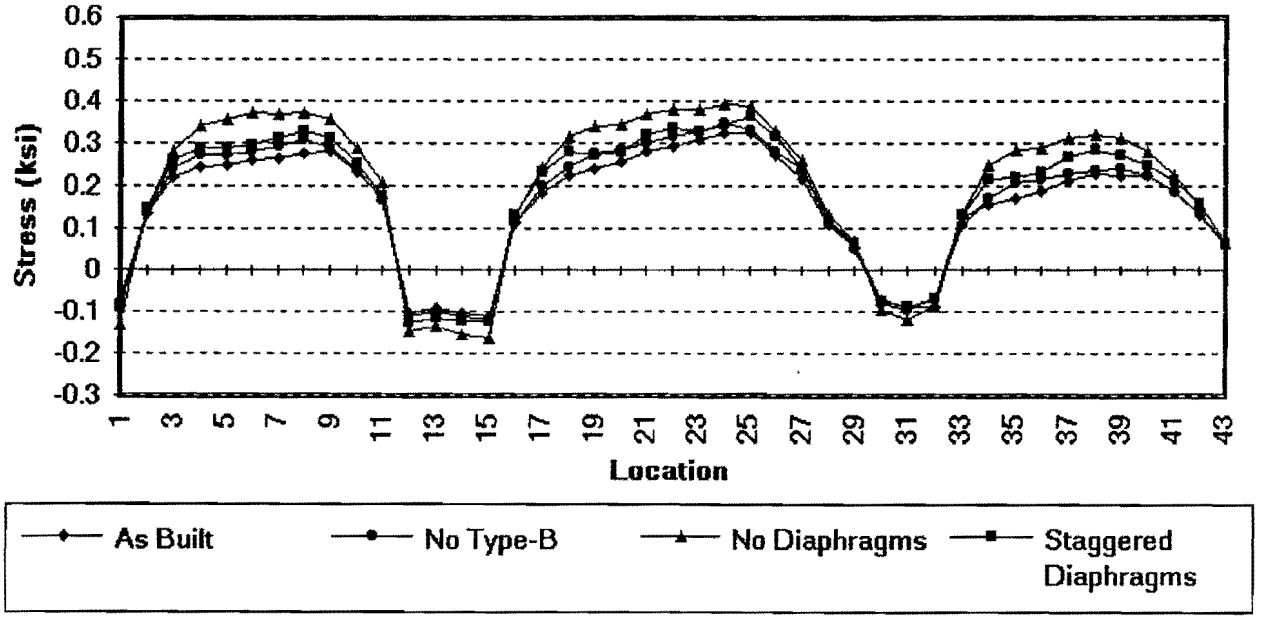

Figure 4-7: Comparison of maximum bottom flange stresses for all models, Girder 4, 10 kip unit axle load.

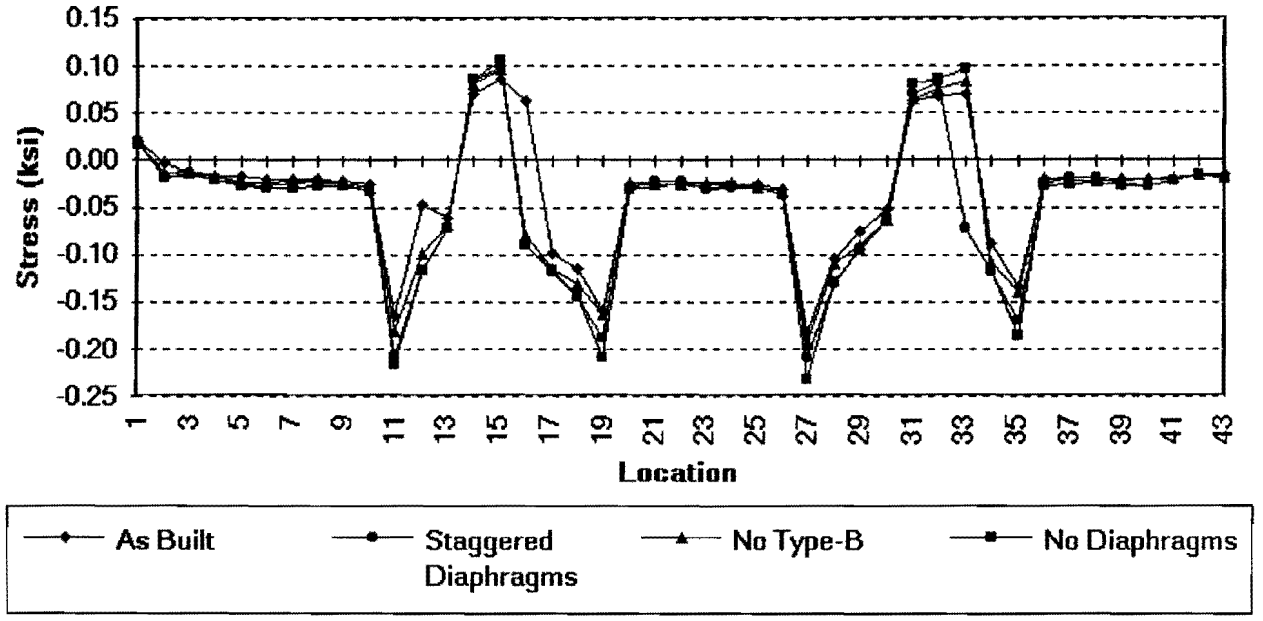

Figure 4-8: Comparison of maximum top flange stresses for all models, Girder 3, 10 kip unit axle load.

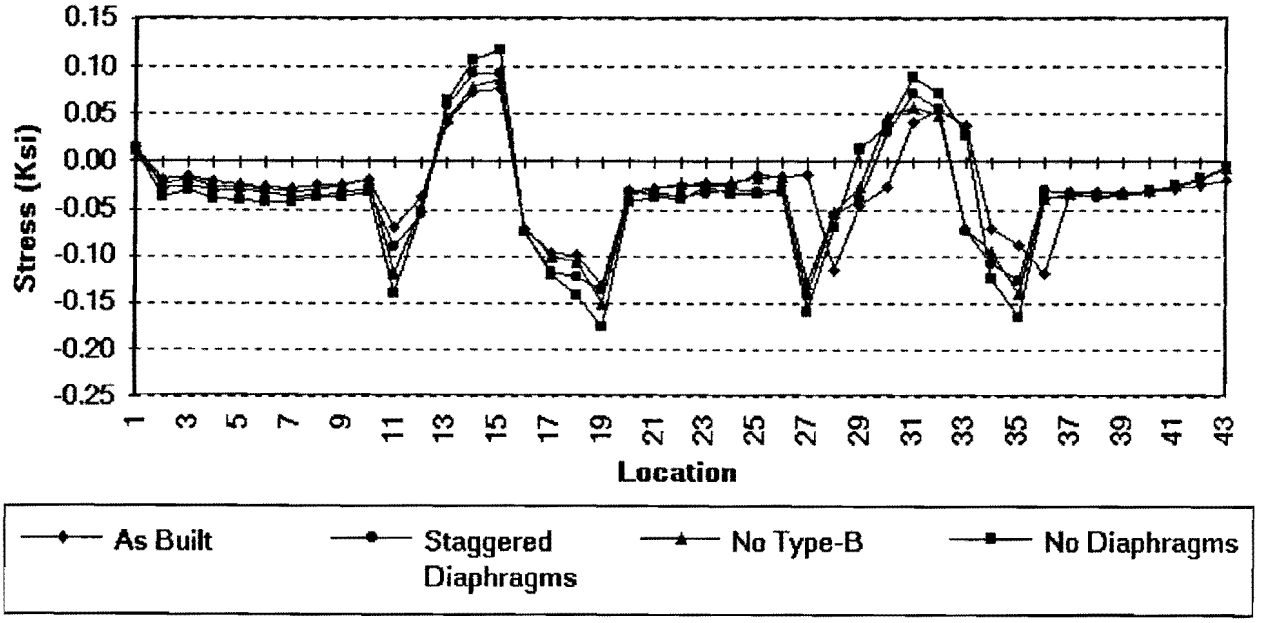

Figure 4-9: Comparison of maximum top flange stresses for all models, Girder 4, 10 kip unit axle load.

In Figs. 4-10 and 4-11, the maximum bottom flange stresses are plotted for both Girders 3 and 4 for the as-built condition and the staggered diaphragm pattern. As indicated by the plots, a maximum increase in stress in the bottom flange in Girder 3 is given as 15 ksi. This increase occurs in the positive moment region of bending. In the negative moment region, no significant increase in bending stress is indicated.

Figures 4-12 and 4-13 plot the maximum top flange bending stress in Girders 3 and 4, respectively, for both the as-built condition and staggered diaphragm pattern. As indicated by the stress plots, the change in stress at various locations along the girders between the two models is not significant.

Figures 4-14 and 4-15 plot the bottom flange stresses for the as-built condition and the staggered diaphragm pattern for all five girders. As indicated by the plots, there is a slight increase in the flexibility of the structure. Plots for the top flange bending stresses are given in Fig. 4-16 and 4-17, and similar conclusions can be drawn.

If diaphragms are to be removed, the stiffness of the structure is reduced. Consequently, the axial forces in the diaphragm members that remain will increase. Any diaphragm replacement design must take the increase into account. Tables C-6 through C-9 provide diaphragm member forces for both the as-built condition and the staggered diaphragm pattern.

The slab bending stresses in the transverse direction (across the lanes of traffic) were investigated, along the entire length of the structure, to determine the relative increase caused by the removal of diaphragms. All slab stresses were taken from Bay C (between Girders 3 and 4) and were the result of a single 10 kip axle load passing over the structure in the driving lane. This location was used since these two girders carry the majority of the load when truck traffic is in the driving lane.

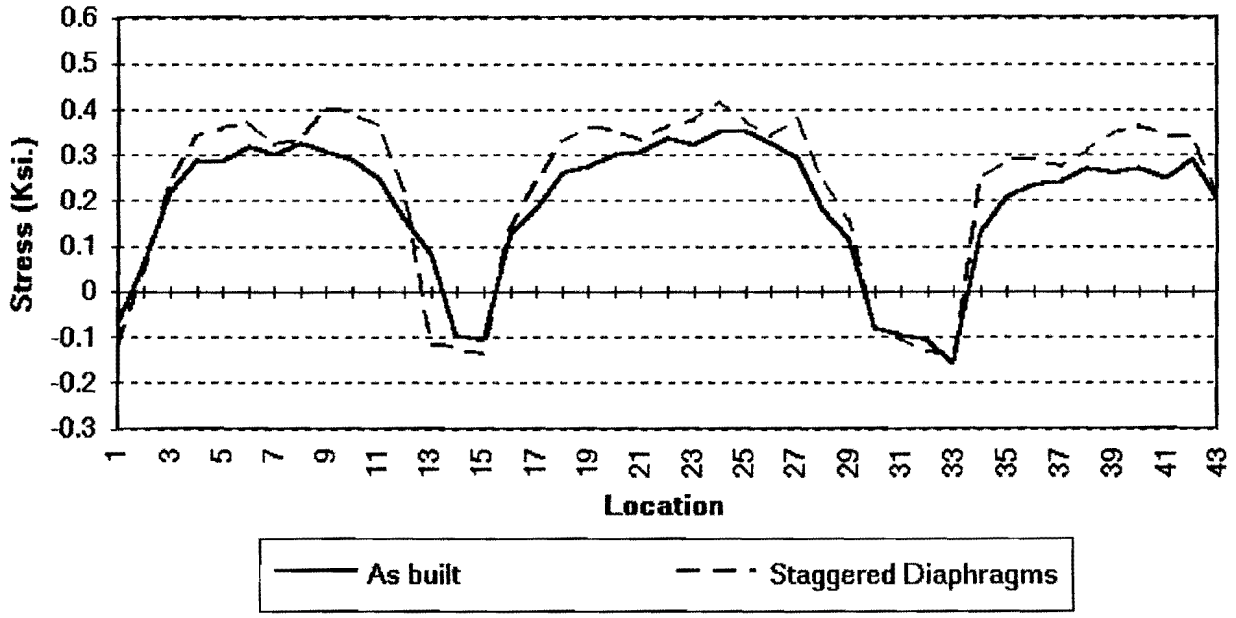

Figure 4-10: Comparison of maximum bottom flange stresses for as-built (Model 0) and staggered diaphragms (Model 3), Girder 3, 10 kip unit axle load.

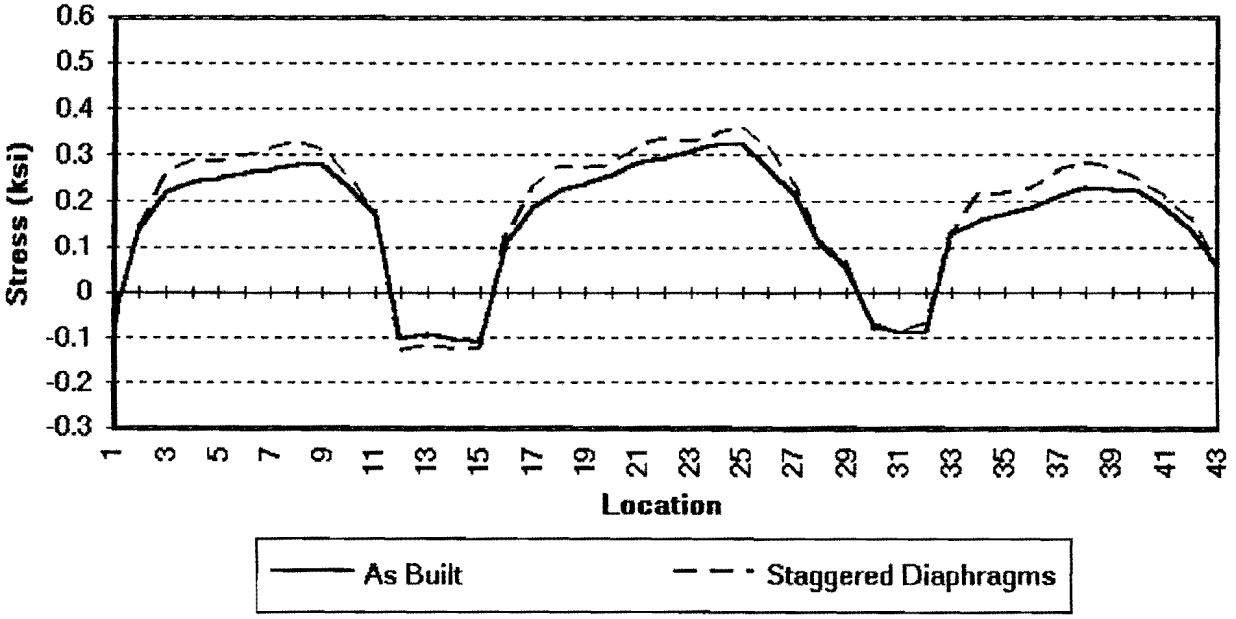

Figure 4-11: Comparison of maximum bottom flange stresses for as-built (Model 0) and staggered diaphragms (Model 3), Girder 4, 10 kip unit axle load.

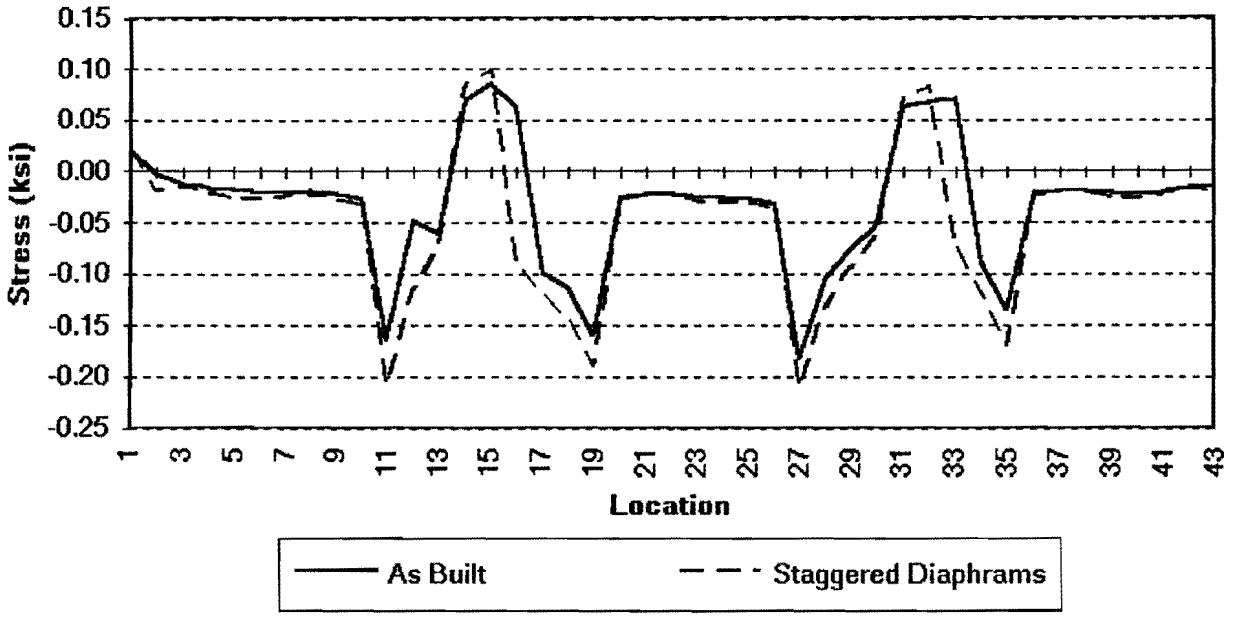

Figure 4-12: Comparison of maximum top flange stresses for as-built (Model 0) and staggered diaphragms (Model 3), Girder 3, 10 kip unit axle load.

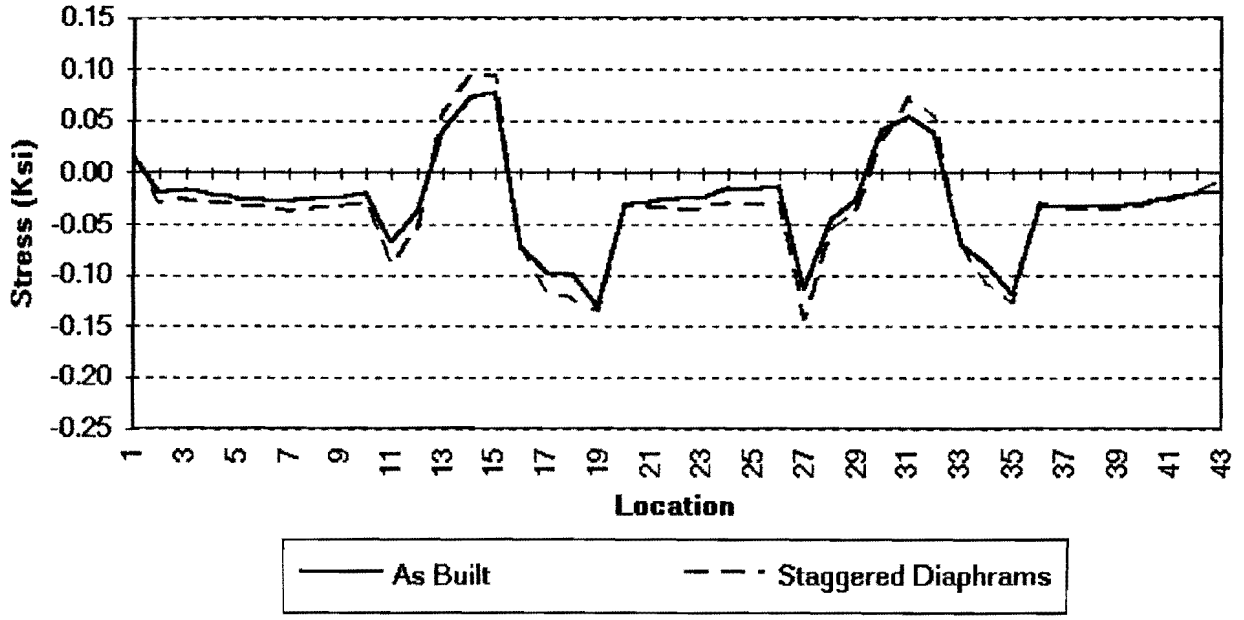

Figure 4-13: Comparison of maximum top flange stresses for as-built (Model 0) and staggered diaphragms (Model 3), Girder 4, 10 kip unit axle load.

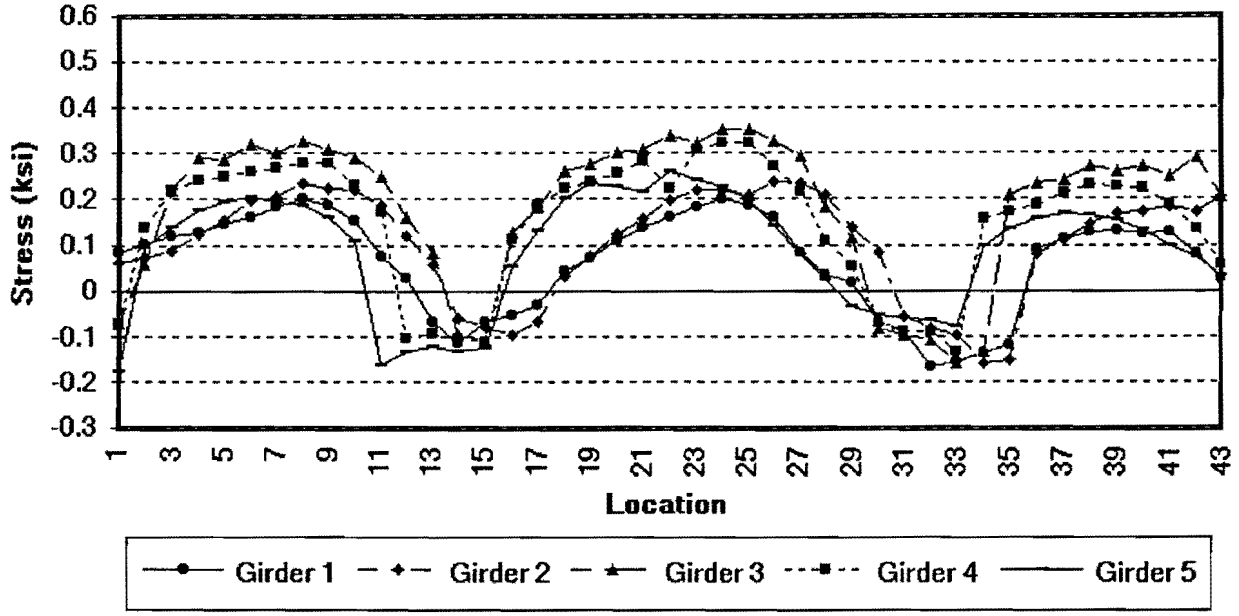

Figure 4-14: Comparison of maximum bottom flange stresses for as-built (Model 0), all girders, 10 kip unit axle load.

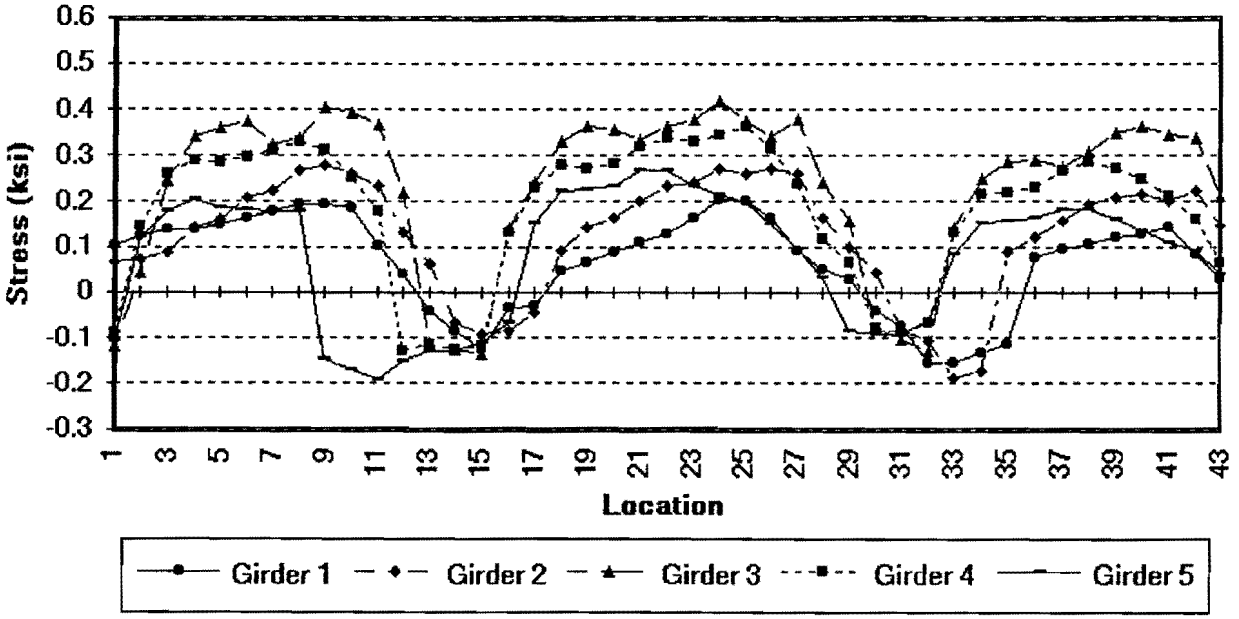

Figure 4-15: Comparison of maximum bottom flange stresses for staggered diaphragms (Model 3), all girders, 10 kip unit axle load.

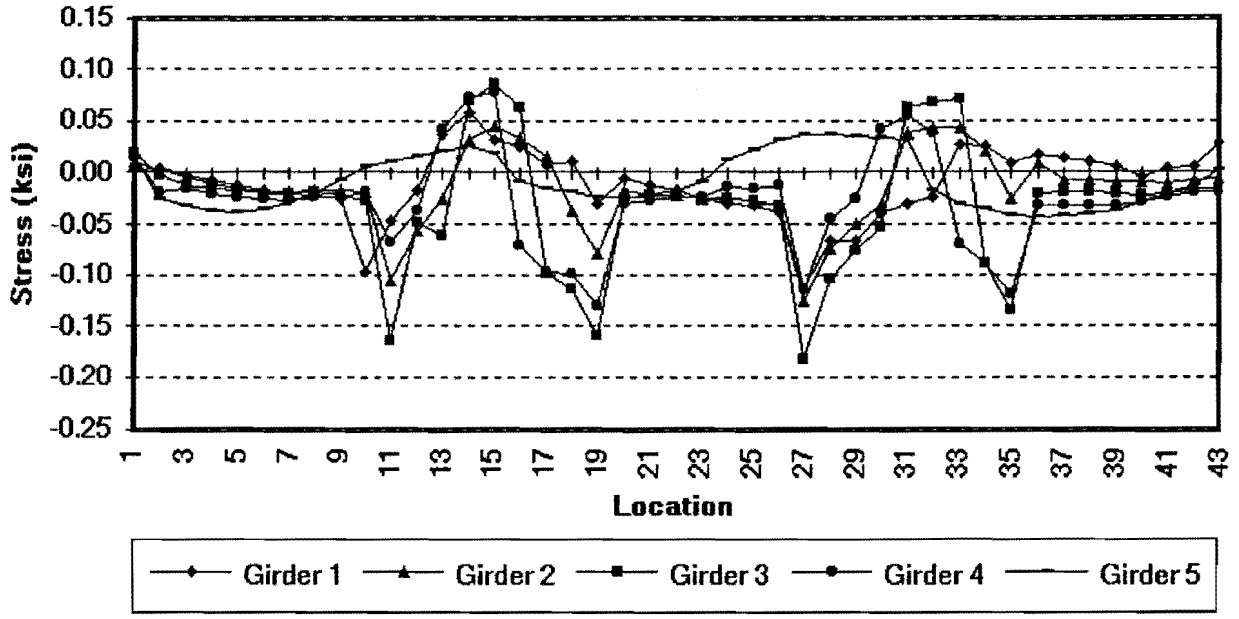

Figure 4-16: Comparsion of maximum bottom flange stresses for as-built (Model 0), all girders, 10 kip unit axle load.

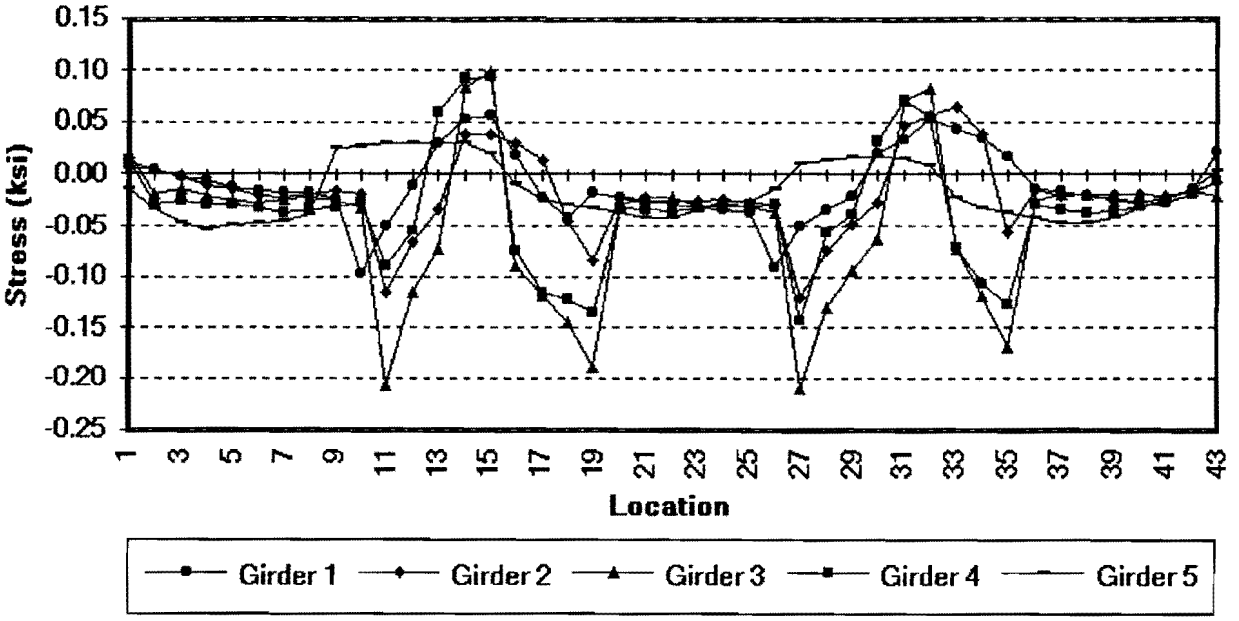

Figure 4-17: Comparison of maximum bottom flange stresses for staggered diaphragms (Model 3), all girders, 10 kip unit axle load.

As would be expected, the slab bending stresses in the transverse direction increase as diaphragms are removed from the structure, as shown in Fig. 4-18. The stresses shown have been multiplied by eight to provide an approximate maximum value of the slab stresses under a single AASHTO HS-20 truck loading. The average increase in slab stresses in the staggered diaphragm model (model 3) were approximately 40 percent. The stresses increased 80 percent at Location 9. Although this increase appears large, the values of the stresses were very small. For example, the slab stress at Location 35 (midspan) was calculated as 0.11 ksi for the as-built condition and .15 ksi for the staggered diaphragm pattern. The average maximum increase in the slab stresses for Model 2 (no diaphragms) is approximately 120 percent. Again, the percent change is great, but the actual stress values are low. Therefore, diaphragm removal should not have a deleterious effect on the serviceability of the concrete deck. For a complete listing of the slab bending stresses in the transverse direction in Bay C, see Table C-10.

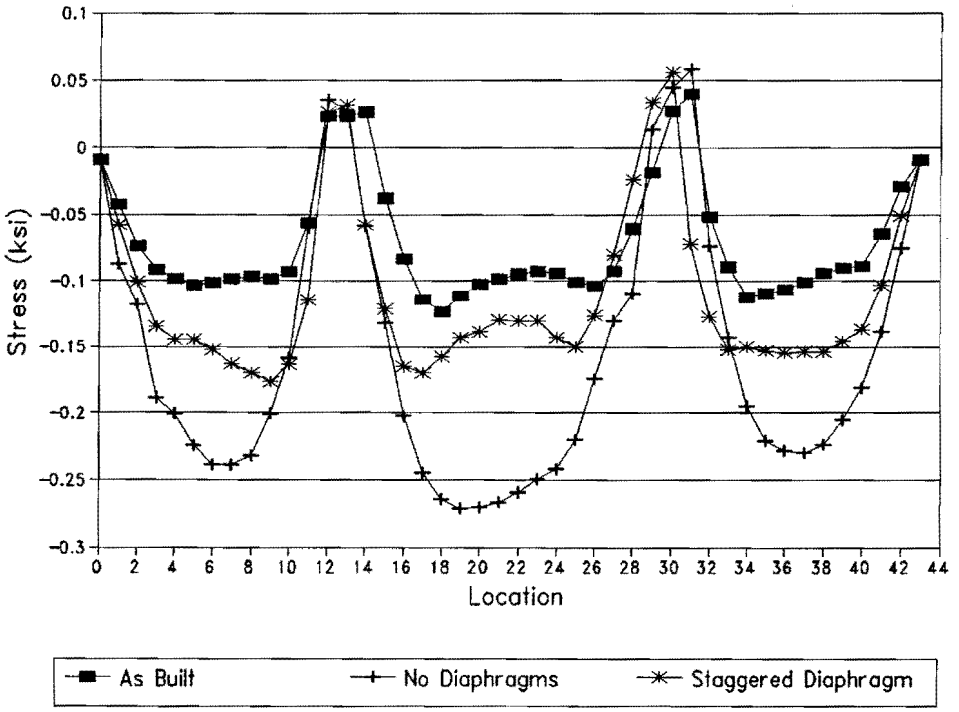

Figure 4-18: Comparison of maximum transverse slab bending stresses in Bay C for three diaphragm conditions: as-built, no diaphragms, and staggered.

5. RECOMMENDATIONS

Based on the condition of the bridge as reported in the Inspection Report, additional field observations, the measured strain behavior of the bridge, and the finite element study, recommendations for the repair of the Midland County bridge are given in the following sections.

5.1 Repair Options

Basically, three types of repair methods must be performed: crack arresting, elimination of web gap distortion, and repair or replacement of diaphragm members. Due to extensive fatigue damage throughout the bridge structures, several repair options are provided so that the chosen option is consistent with the needs and capability of the Texas Department of Transportation. The following repair options are recommended:

Option 1: Existing web gap fatigue cracks caused by the out-of-plane diaphragm forces should be arrested by holes drilled at the crack tips. At locations where the fatigue damage is not extensive, no further repair action is required. However, retrofitted web gaps should be periodically monitored for crack reinitiation. At locations where a high degree of fatigue damage has occurred, a rigid attachment of the connection plate to the flange is required. All fatigue damaged diaphragms should be replaced by a new diaphragm detail as discussed in Sec. 5.6.

This option recognizes the fact that since fatigue crack growth histories and inspection records are unavailable, some of the crack growth may have self-arrested. As the fatigue crack(s) propagates through the web plate, the flexibility of the web gap increases. Depending on the stiffness of the bridge (this being an unknown), the driving stresses behind the crack growth may decrease. However, without knowing how long the fatigue cracks have been present, the severity of the fatigue damage cannot be adequately determined. Therefore, monitoring the retrofitted locations through periodic

inspections will be required.

To provide greater flexibility in the cracked web gap, a saw cut can be made between the drilled holes, along the crack path. This releases the shear lock condition that often exists with this type of cracking. The shear lock forms due to the fatigue crack actually being two cracks that initiated on either side of the web plate and grew together on different planes.

Replacement of the entire diaphragm recognizes the fact that the existing design is inherently prone to fatigue damage due to the eccentric loading between the diagonal and horizontal strut members. Rewelding the connection will not change the stress condition that is causing the development of the fatigue cracks. There is not enough length in the diaphragm member connection to allow a slip-critical bolted connection.

This option reduces the need for extensive repair and retrofitting of the bridge structures, thus reducing the initial repair costs. However, an inspection program would be required to detect continued cracking at retrofitted locations and any new fatigue damage that might develop in the future.

Option 2: All cracked web gap details would be retrofitted by providing a rigid attachment (either welded or bolted) between the end of the connection plate and flange. Diaphragms in which members have sustained fatigue damage would be replaced by a new diaphragm design.

This option assumes that the level of distortion that occurs in the web gaps cannot be sufficiently reduced to prevent further crack propagation. Providing a rigid attachment of the connection plate to the flange, as is now required by the AASHTO Specifications, would eliminate the drive force behind the fatigue cracking. This option does not however preclude the possibility of fatigue cracking at other locations in the future.

In addition to the rigid attachment, holes must be drilled at all crack tips to prevent continued propagation from the primary bending stresses even, though the distortion will have been eliminated.

Option 3: Selective diaphragm removal would be performed. At connection plates where the diaphragm has been removed, holes would be drilled at the tips of all existing fatigue cracks. All remaining diaphragms would be replaced by a new diaphragm design. Connection plates for the remaining diaphragms would require a rigid attachment.

By permanently removing diaphragms from the bridge structures, both the problems of fatigue cracking in the diaphragm members as well as the web gap fatigue cracking are eliminated. The finite element analysis has shown that a staggered diaphragm pattern in the positive moment region of bending (Model 3) does not significantly change the load distribution characteristics of the structure. Removing every other diaphragm (Model 1) results in even less change in behavior but requires a greater number of remaining diaphragms to be replaced and connection plates to be rigidly attached to the flanges.

5.2 Arresting of Fatigue Cracks

As mentioned in the various repair options, regardless of the method used to prevent further fatigue damage in the structure, all existing cracks must be arrested to prevent continued propagation. If not, these cracks could propagate to failure due to the primary or in-plane bending stresses, even though the distortion or secondary stresses may have been eliminated.

It is recommended that holes be drilled at the tips or fronts of all fatigue cracks. The hole, with a diameter between 3/4-in. and 1.0-in. reduces the crack tip acuity, thereby reducing the crack tip stress concentration. Research has indicated that crack reinitiation from the hole is prevented by satisfying the following relationship [2,4]:

$$\frac{\Delta K}{\sqrt{\rho}} < 4\sqrt{F_y} \quad (5\text{-}1)$$

where

ρ = radius of the hole drilled, in.

F_y = yield stress of the web plate (or plate containing crack), ksi.

and ΔK is the stress intensity range for the in-plane bending stress and is given as

$$S_r\sqrt{\pi a_r} \quad (5\text{-}2)$$

in which

S_r = in-plane bending stress range, ksi.

a_r = one-half the crack length, in.

Equation (5-1) can be put into a more usable form by letting L be equal to the total length of the retrofitted crack or 2a and letting ϕ be equal to the hole diameter or 2ρ. By making the proper substitutions and rearranging to solve for the required hole diameter:

$$\phi \geq \frac{S_r^2 L}{5F_y} \quad (5\text{-}3)$$

Strain measurements of in-service bridges have indicated that the stress range seldom exceeds 6.0 ksi. Therefore, for plates having yield stress of 36 ksi, a diameter between 3/4-in. and 1.0-in. is usually sufficient. It may be more practical to specify hole diameters of 13/16-in. and 1-1/16-in. since drill bits of these sizes are used for high-strength bolts and are commonly on hand. Larger diameter holes should be avoided to minimize the web cross section loss. A typical drilled hole pattern is given in Fig. 5-1 for

cracked web gap details. Note that the diaphragm may require its removal in order to gain proper clearance for the drill.

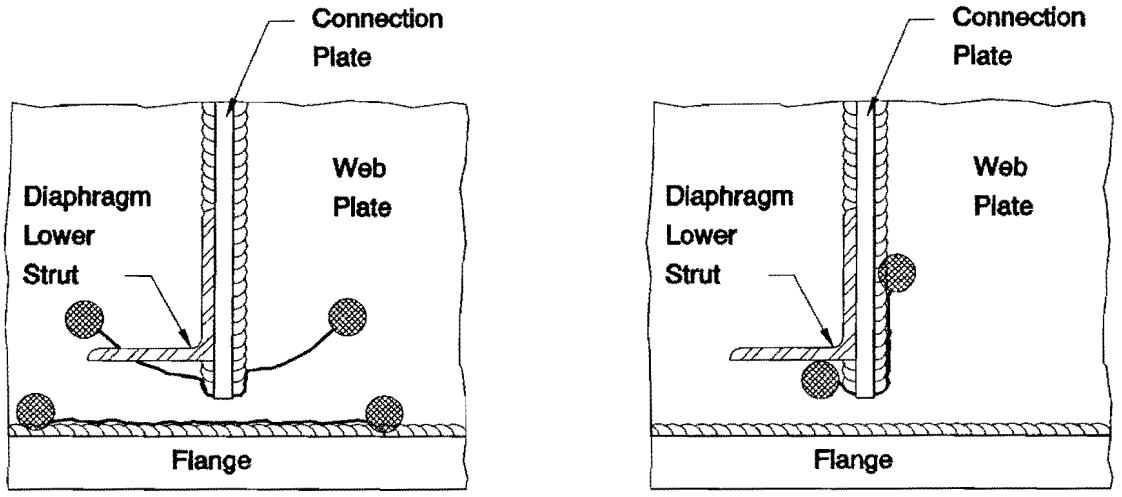

Figure 5-1: Typical drilled hole pattern for web gap cracking.

A factor not considered in the development of Eq. 5-1 was the method of hole preparation and degree of finish given to the hole. This is more important than simply satisfying the equation. If burrs or rough edges remain after the drilling operation, crack initiation may occur due to the stress risers. All drilled holes should be ground and surfaced to a polished finish. Dye penetrant inspection should be performed upon completion to insure that the hole circumference is free of defects and that the crack tip has been properly located.

Proper location of the crack tip is essential. If the crack is not properly located and the hole is drilled behind the crack tip, an additional stress concentration is provided by the hole, increasing its propagation rate. It has been suggested that the crack tip be located on the inside circumference of the hole to ensure that the crack intersects the hole as shown schematically in Fig. 5-2. However, it is recommended that the center of the hole be positioned at the crack tip to reduce the overall length of the finished crack and minimize the web section loss. Normally, the crack tip can be adequately located visually due to the high degree of corrosion emanating from the working crack or through

the use of dye penetrant. The concern with properly locating the crack tip was derived from a laboratory setting where fatigue cracks propagate in the absence of any corrosion, making it more difficult to detect.

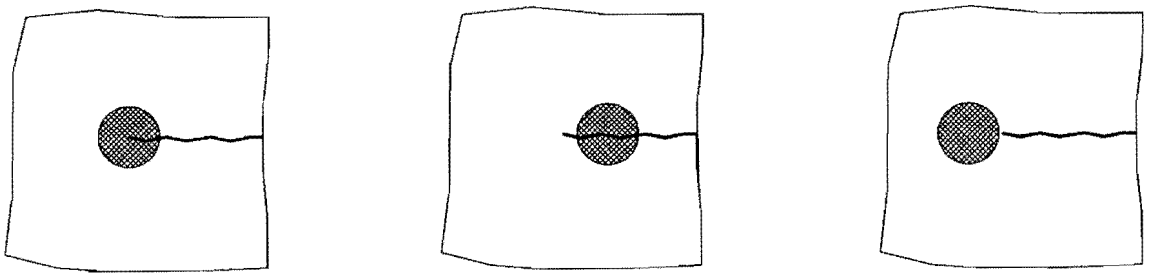

Figure 5-2: Possible drilled hole locations relative to crack tip.

5.3 Fatigue Crack Gouging and Rewelding

It is strongly recommended that the fatigue cracks not be arc-gouged and rewelded. This method of weld repair is difficult to perform in the field and can often result in a defect more severe than the original condition [4]. In addition, this type of repair does not solve or remove the source causing the crack propagation. Crack reintiation will occur if the out-of-plane distortion is not eliminated through the use of a rigid attachment. An existing fatigue crack is adequately stabilized by holes drilled at the crack tip and if the distortion is eliminated to prevent reinitiation.

5.4 Repair of Web Gap Fatigue Cracking

The method of repair for web gap fatigue cracking is based on whether a diaphragm has been removed. At connection plates where the diaphragm has been

removed, it is not necessary to provide a rigid attachment between the end of the connection plate and the flange. Existing fatigue cracks need only be arrested by holes drilled at the crack tips.

At locations where the diaphragm is to remain or be replaced, a rigid attachment between the end of the connection plate and the flange must be provided either by welding or bolting.

A bolted attachment is commonly the preferred detail due to the difficulty in obtaining quality field welds. Possible bolted retrofit details for the connection plate end are shown schematically in Fig. 5-3 and 5-4. However, use of a bolted detail is difficult in the negative moment region where the rigid attachment is required on the top (tension) flange. Installation of the high-strength bolts requires removal of a portion of the concrete deck, thus complicating the repair procedure. Tapping the flange is precluded due to its relative thinness. In addition, the clearance between the flange and the diaphragm strut is typically 2.0 in. for all diaphragm types (see Figs. 1-5, 1-6, and 1-8). This makes for a difficult bolted attachment between the connection plate and the vertical component of the angle of tee as given in Fig. 5-3 and 5-4.

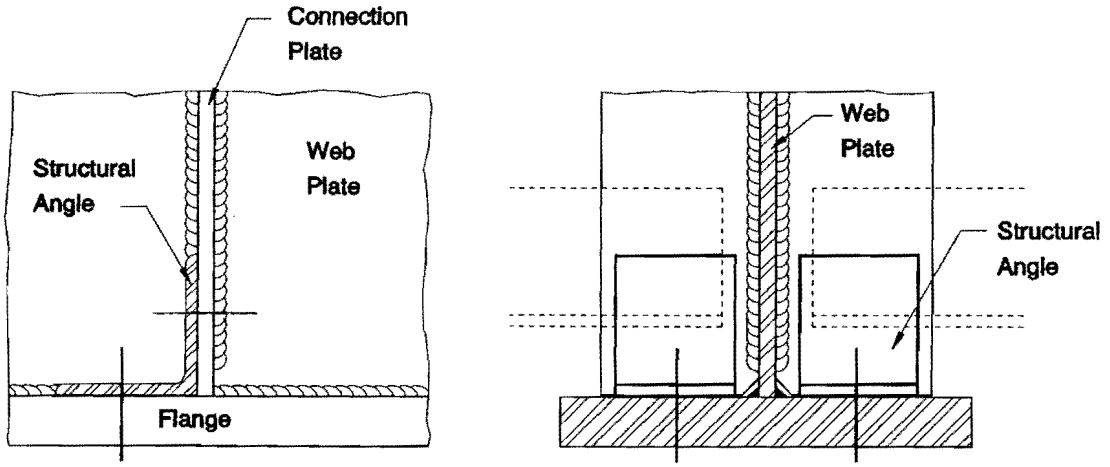

Figure 5-3: Typical bolted retrofit for tight-fit connection detail.

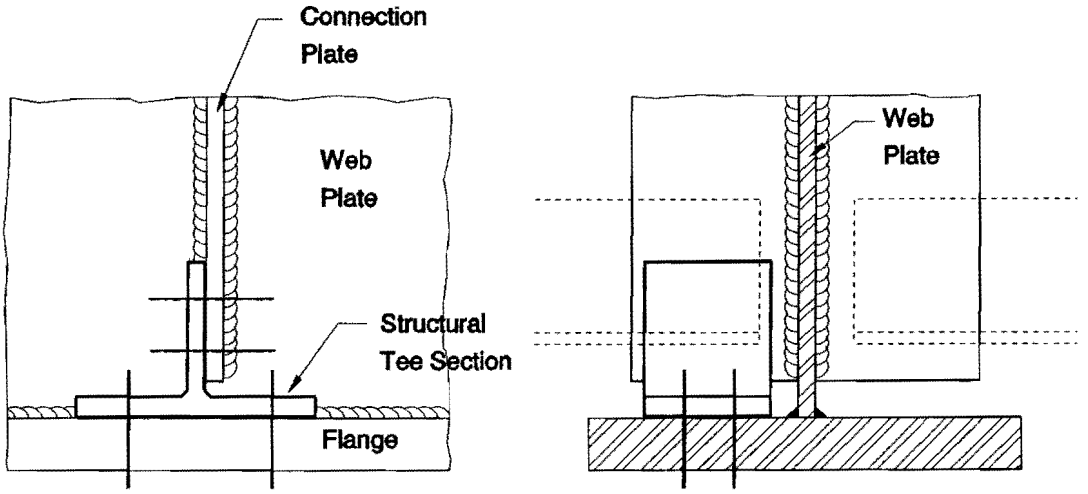

Figure 5-4: Typical bolted retrofit for cut-short connection detail.

Given the acceptance of field welding by TxDOT, it is recommended that welded attachments be used at the ends of connection plates provided that weld quality can be assured.

At locations where the tight-fit connection plate detail was used (at original Type B and C diaphragms), a 5/16 in. fillet weld should be used as shown in Fig. 5-5. Prior to placement of the weld, the end of the connection plate and flange should be free of all foreign material, including paint. Welding must be performed in the absence of traffic on the bridge.

Where a gap exists between the end of the connection plate and the flange, a filler block is required. The thickness of the block in the longitudinal direction of the bridge should be kept as short as possible (approximately 1.0 in, thick) so as to minimize the stress concentration at the weld toes. A fillet weld size of 5/16 in. should be used as shown in Fig. 5-6. It should be noted that this is the same detail that was used to provide rigid attachments at fatigue cracked web gaps repaired during the 1983 bridge widening.

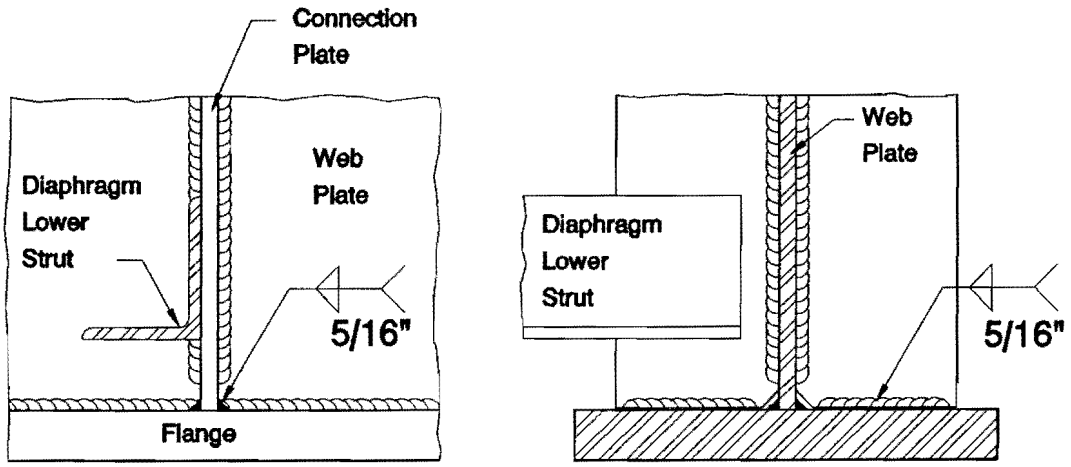

Figure 5-5: Recommended welded attachment for tight-fit connection detail.

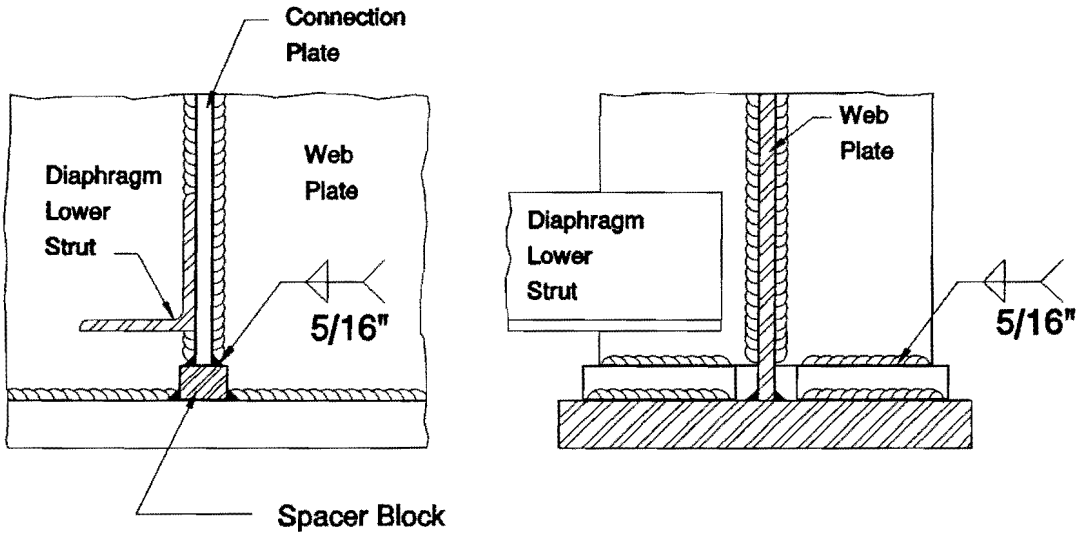

Figure 5-6: Recommended welded attachment for cut-short connection detail.

The placement of a transverse fillet weld on the flange results in an AASHTO fatigue Category C classification. The severity of the detail changes little due to the Category C classification for the vertical weld termination at the end of the connection plate of the original detail.

The transverse fillet welds should be terminated short of plate edges to avoid weld wrap-a-rounds. A 1/4 in. tolerance is recommended. In addition, the end of the transverse fillet weld should be kept approximately 1.0 in. from the longitudinal fillet weld between the web and flange plate.

The fatigue strength of the transverse fillet weld can be improved by grinding the weld and/or peening the weld toe.

5.5 Repair of Connection End Plate Fatigue Cracking

This type of distortion-induced fatigue cracking is one of the more difficult types to repair. Fortunately, this type of cracking has occurred where welded attachments between the connection and compression flange were used. If the diaphragm is removed or replaced, the driving force behind the crack propagation is removed and no further action is required. The existing fatigue crack will not propagate under the compressive bending stress in the flange plate.

5.6 Repair of Diaphragm Member Fatigue Cracking

As discussed in Section Three, the fatigue cracks that have developed in the diaphragm members can be attributed to the inherently poor design detail used for the diaphragms. The primary force that causes the fatigue cracking is due to the overall distortion of the bridge and cannot be prevented. Repairing the fatigue cracks by either rewelding or hole drilling will most certainly lead to crack reinitiation. Therefore, two viable options exist, either remove or replace the damaged diaphragms.

Complete removal of a fatigue damaged diaphragm obviously precludes the need for repair. In addition, the removal of a diaphragm also eliminates the driving force behind the web gap fatigue cracking. The diaphragm connection plate then behaves as an intermediate transverse stiffener.

As indicated by the finite element analysis, the overall load distribution of the structure is not significantly affected by the removal of every other diaphragm line or by the staggered diaphragm pattern shown in Figs 5-7 and 5-8. Diaphragm removal cannot be used to remove only those diaphragms that are fatigue cracked or those that are the cause of cracking in the web gap. To remove the diaphragms in a random fashion would lead to an aggravated situation at the remaining diaphragm locations.

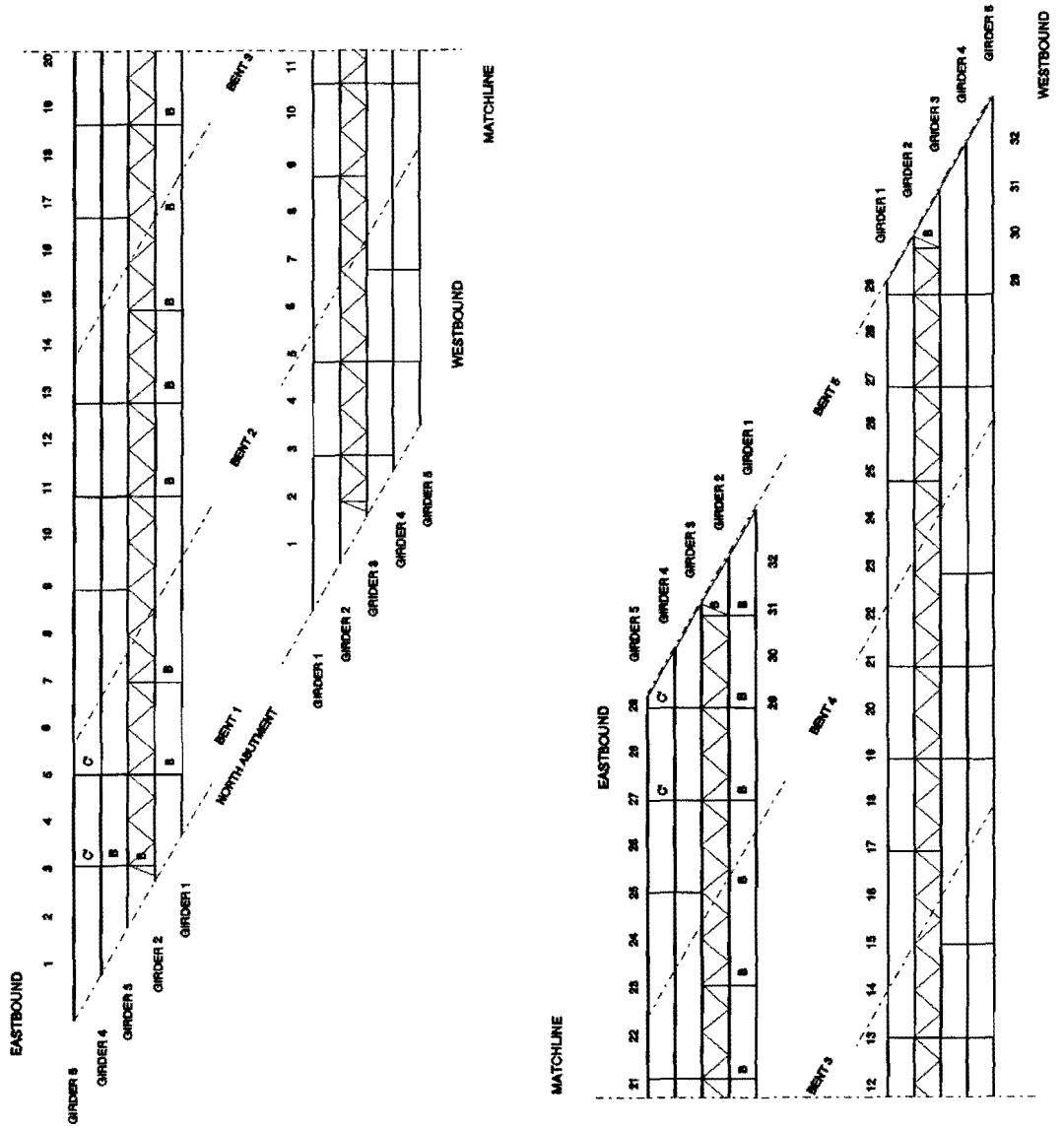

Figure 5-7: Recommended staggered diaphragm pattern for North Structures.

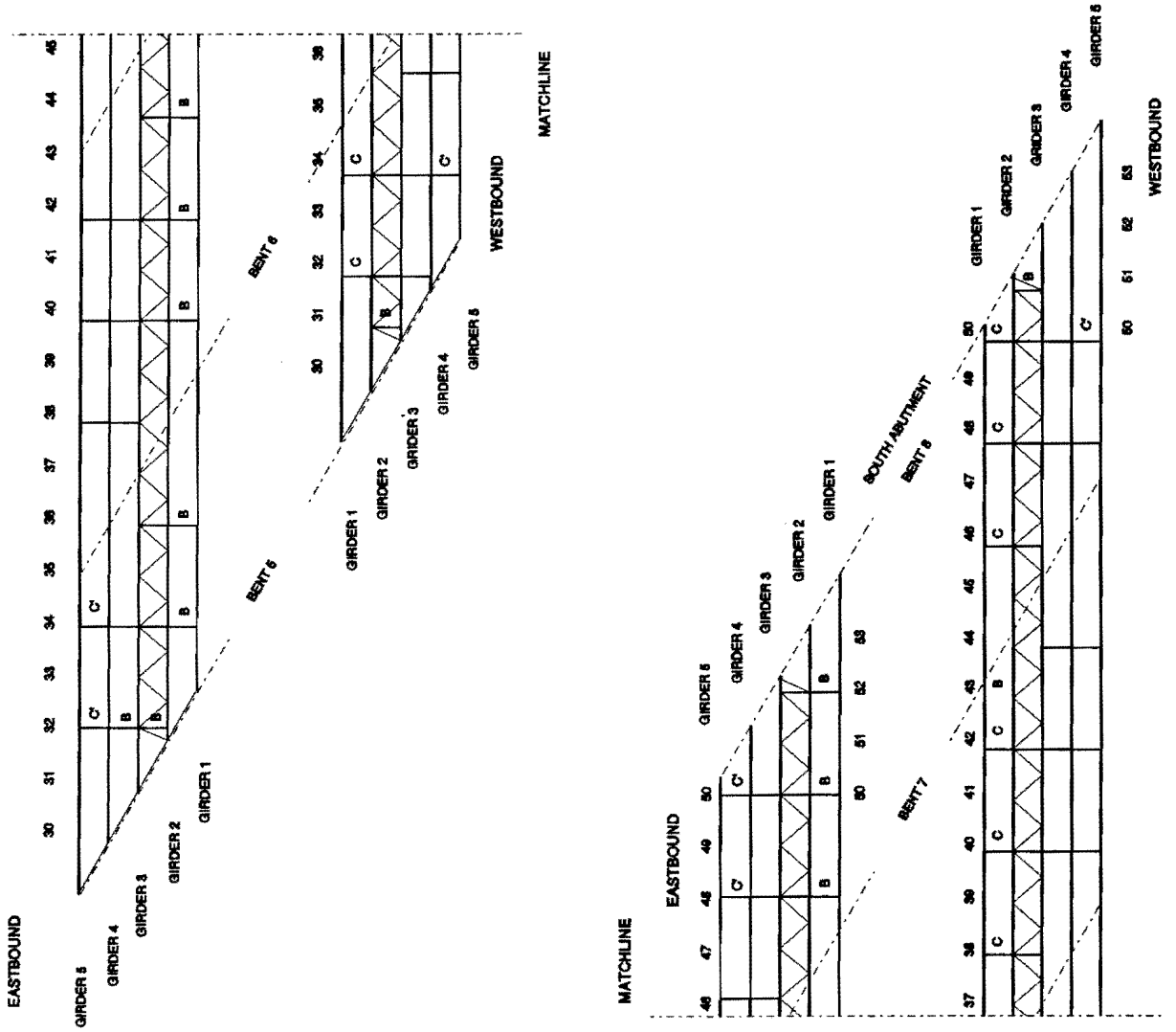

Figure 5-8: Recommended staggered diaphragm pattern for South Structures.

Possible replacement diaphragm designs are given in Figs. 5-9 to 5-11. The three details shown are taken from design standards used by other states. These can be fabricated in-shop and then brought to the bridge site as sub-assemblies. This simplifies the erection process. Two of these designs (Figs. 5-9 and 5-10) incorporate gusset

plates to aid in the connection of the diaphragm members to the connection plate. The diaphragm members are welded to the gusset plate, and the gusset plate is then bolted to the connection plate. The third detail (Fig. 5-11) has the diaphragm members bolted directly to the connection plate with a gusset plate. A bolted connection at the connection plate is recommended due to the high level of forces occurring in the diaphragm members. A welded connection between the gusset plate and connection plate would be susceptible to fatigue cracking similar to that experienced by the original design.

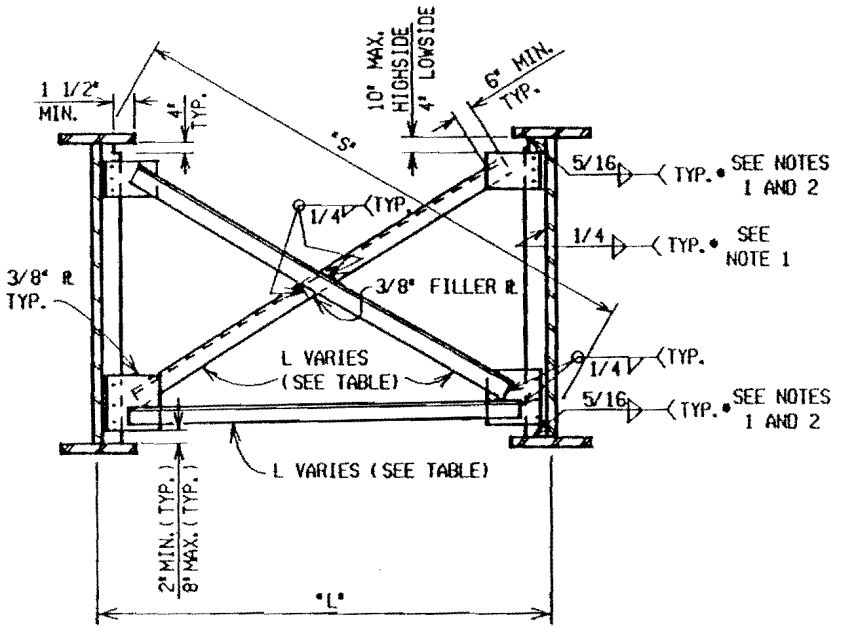

PIER AND INTERMEDIATE CROSS FRAMES

NOTE 1: STOP WELD 1/4" SHORT OF CORNER CLIPS
NOTE 2: WRAP WELD AROUND OUTSIDE EDGE

STRAIGHT GIRDERS	
"L" OR "S"	MIN. ANGLE SIZE
LESS THAN 6'-9"	3" X 3" X 5/16"
6'-9" TO 9'-3"	4" X 4" X 5/16"
9'-3" TO 11'-6"	5" X 5" X 3/8"
11'-6" TO 13'-9"	6" X 6" X 3/8"
13'-9" TO 18'-6"	8" X 8" X 1/2"
CURVED GIRDERS	
LESS THAN 5'-9"	3" X 3" X 5/16"
5'-9" TO 7'-9"	4" X 4" X 5/16"
7'-9" TO 9'-9"	5" X 5" X 3/8"
9'-9" TO 11'-9"	6" X 6" X 1/2"
11'-9" TO 15'-9"	8" X 8" X 5/8"

NOTES:

USE FULL DEPTH STIFFENERS OR 1/2" CONNECTION PLATE.

FOR ANGLES OF CROSSING >70°, SET CONNECTION PLATE AND BEARING STIFFENER TO ANGLE OF CROSSING. FOR ANGLE OF CROSSING <70°, SET CONNECTION PLATE AND BEARING STIFFENER NORMAL TO WEB. USE BENT GUSSET PLATES ON PIER CROSSFRAMES.

CLIP ALL CORNERS PER GUIDE 8.06.02.

USE DETAIL A, GUIDE 8.06.02 IF CONNECTION PLATE EXTENDS BEYOND FLANGE

INTERMEDIATE CROSS FRAMES TO BE IN LINE.

ANGLE SIZE BASED ON L/R RATIO. STRESSES MAY REQUIRE USE OF LARGER ANGLES.

USE DIAPHRAGMS FOR WEB DEPTHS <48". (30" DIAPHRAGM FOR 42" WEB DEPTH.) SEE GUIDE 8.11.03 FOR DETAILS.

• WELD TOP AND BOTTOM UNLESS FATIGUE LIMITATIONS CONTROL. CONNECTION PLATE WELDING SHOWN HERE. SEE GUIDE 8.06.02 FOR STIFFENER WELDING DETAILS. SEE GUIDE 8.11.08 FOR CONNECTION PLATE DETAILS IF FATIGUE LIMITATIONS CONTROL.

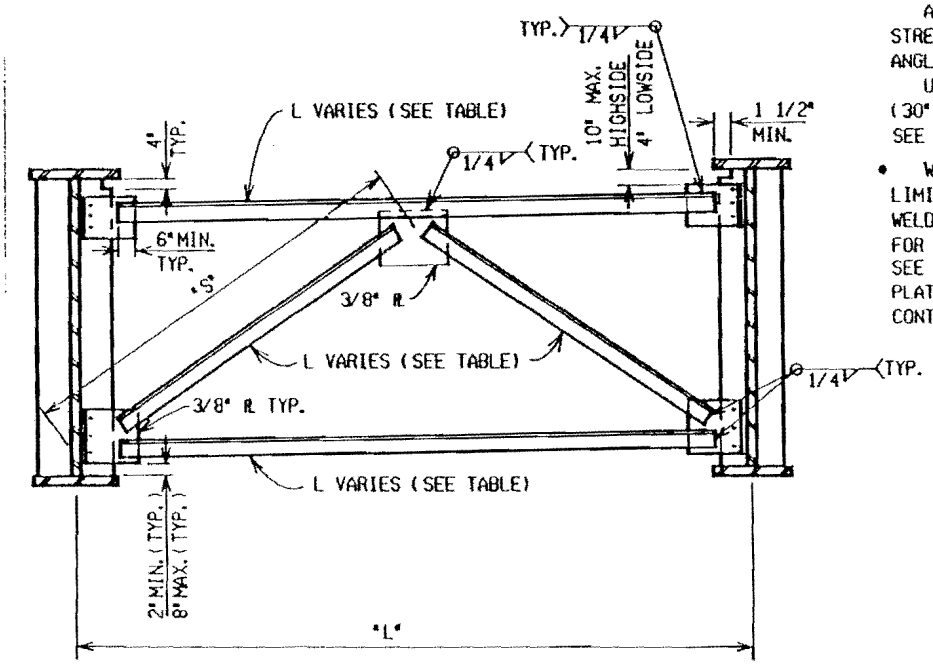

PIER CROSS FRAMES

BEAM SPACING > 12'-6"

Figure 5-9: Standard intermediate and pier cross frame diaphragm detail used by the Michigan Department of Transportation - Bureau of Highways.

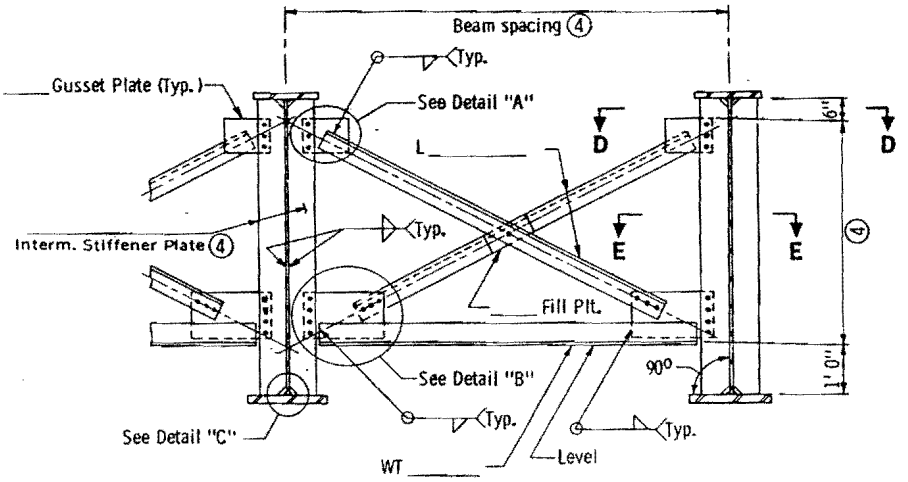

ELEVATION

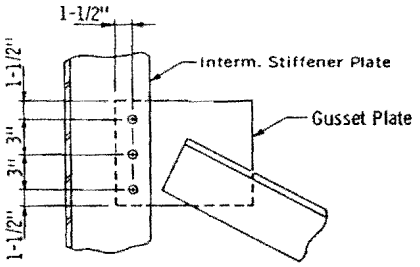

DETAIL "A"
(Typical Bolt Hole Spacing Shown)

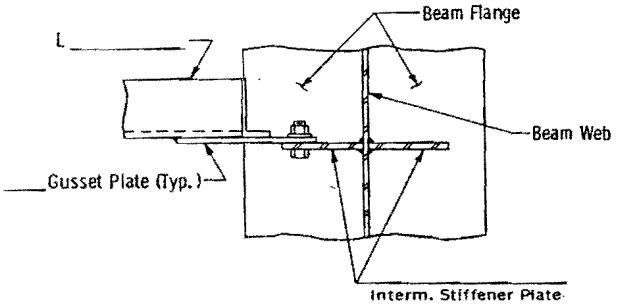

SECTION D-D

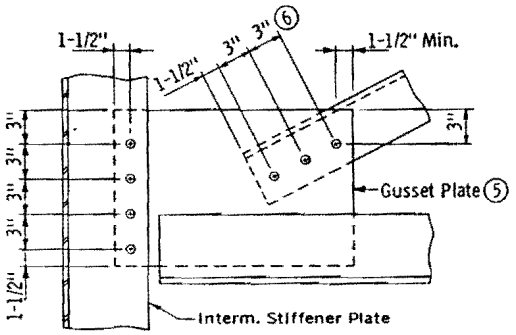

DETAIL "B"
(Typical Bolt Hole Spacing Shown)

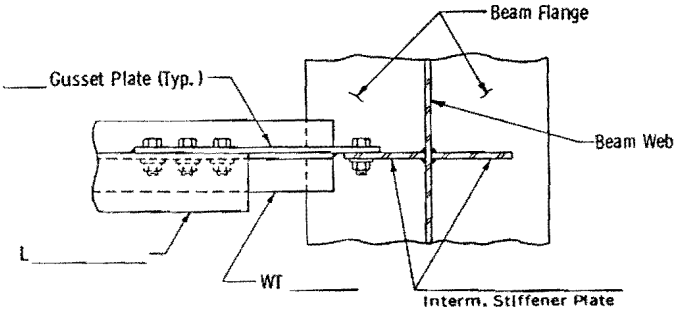

SECTION E-E

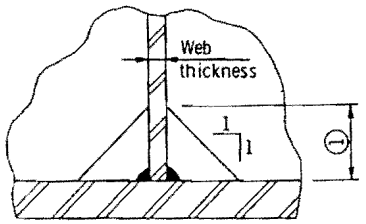

(1) Distance = 4 x web thickness or 2" min.

DETAIL "C"

NOTES:

(1) Field connections shall be made with 7/8" high strength bolts or 7/8" pin bolts.

(2) All steel shall conform to Spec. 3309 unless otherwise noted.

(3) Construct as per Spec. 2402 unless otherwise noted.

(4) See Bridge Superstructure Sheets for additional information.

(5) Bolt holes in gusset plate may be field drilled.

(6) Welding may be used in lieu of bolts shown.

(7) High strength fasteners shall meet the requirements of ASTM A325, Type 3, and shall be in accordance with Spec. 3391.

Figure 5-10: Standard intermediate cross frame diaphragm detail used by the Minnesota Department of Transportation.

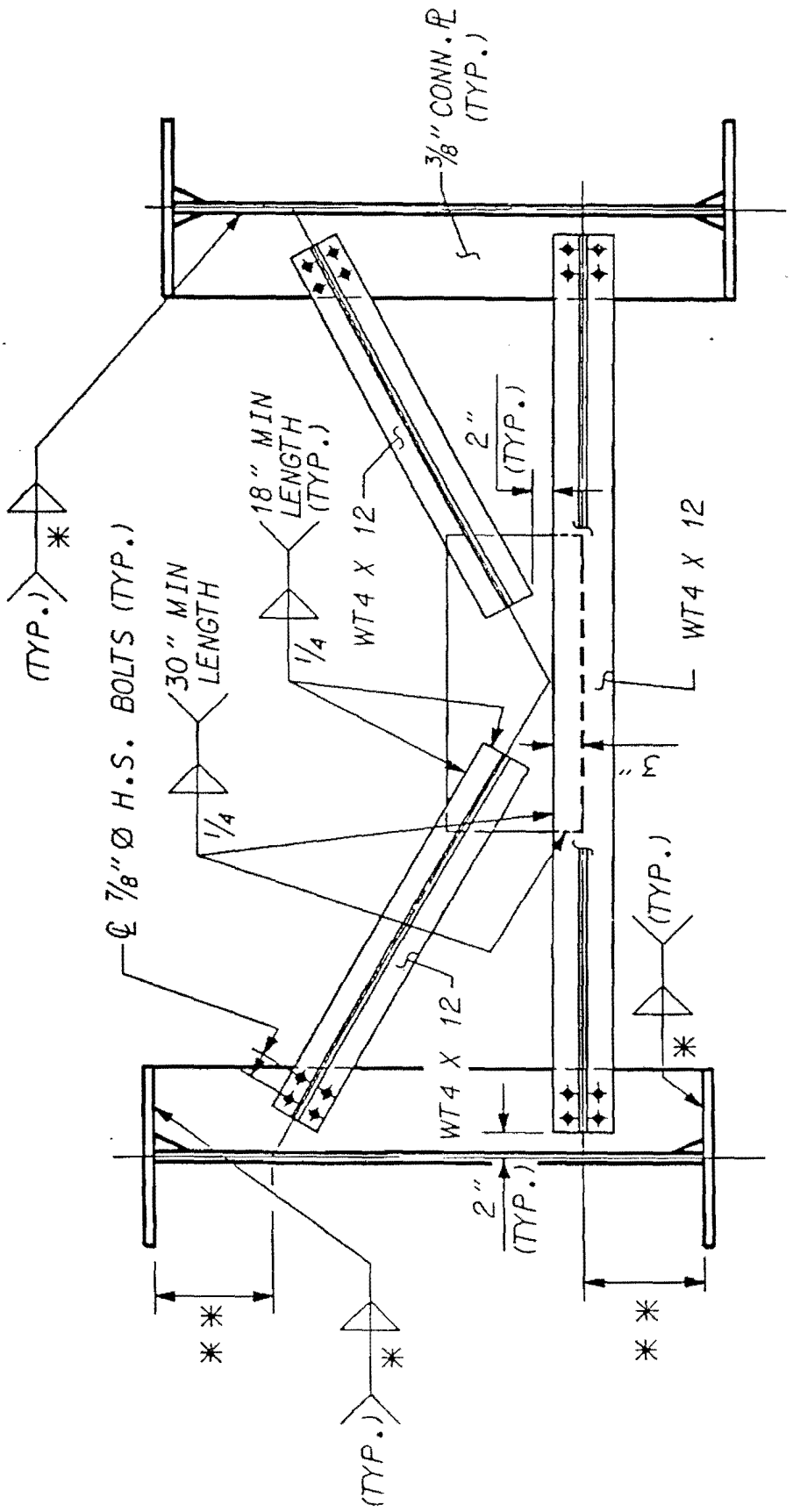

Figure 5-11: Standard intermediate pier cross frame diaphragam detail used by the North Carolina Department of Transportation.

REFERENCES

1. Diaz, M. and Andrews; "Detailed Structural Condition Report for Bridge 06-165-0005-15-201 (IH 20 WestBound) and 06-165-0005-15-202 (HI 20 WestBound)"; ARE, Inc., Engineering Consultants; July 9-17, 1990.

2. Fisher, J.W., Nussbauner, A., Keating, P.B., and Yen, B.T.; "Resistance of Welded Details Under Variable Amplitude Long Life Fatigue Loading; ATLSS Report No. 92-04 (FInal Report, NCHRP Project 12-15(5)), Lehigh University, April, 1992.

3. Fisher, J.W, Jian, J., Wagner, D.C., and Yen B.T.; "Distortion-Induced Fatigue Cracking in Steel Bridges"; NCHRP Report 336; National Cooperative Highway Research Program, December, 1990.

4. Fisher, J.W., Hausammann, H., Sullivan, M.D., and Pense, A.W.; "Detection and Repair of Fatigue Damage in Welded Highway Bridges"; NCHRP 206; National Cooperative Highway Research Program; 1979.

Appendix A

Summary of Fatigue Crack Locations

List of Figures

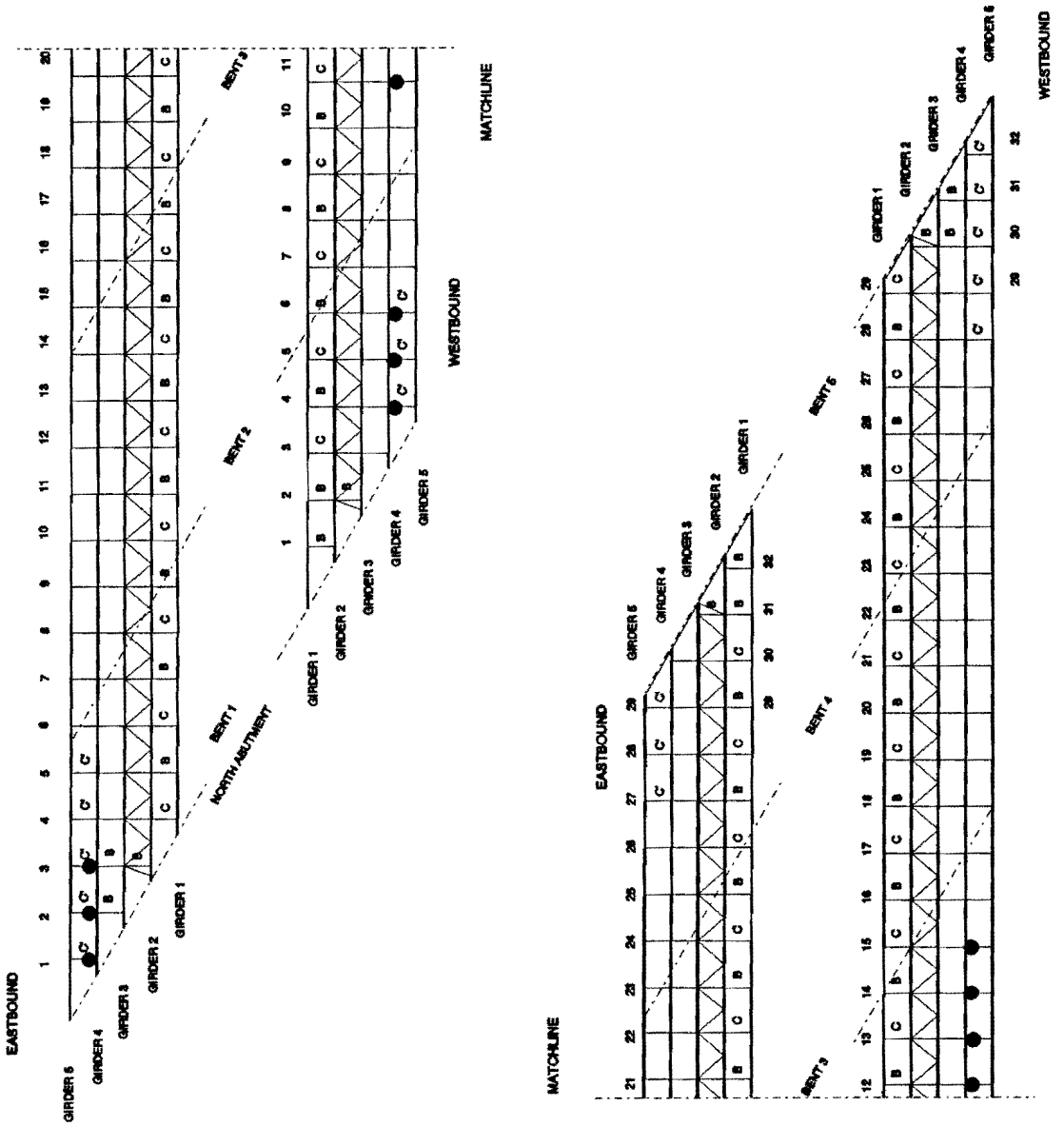

Figure A-1: Type A1 crack locations in North Structures.

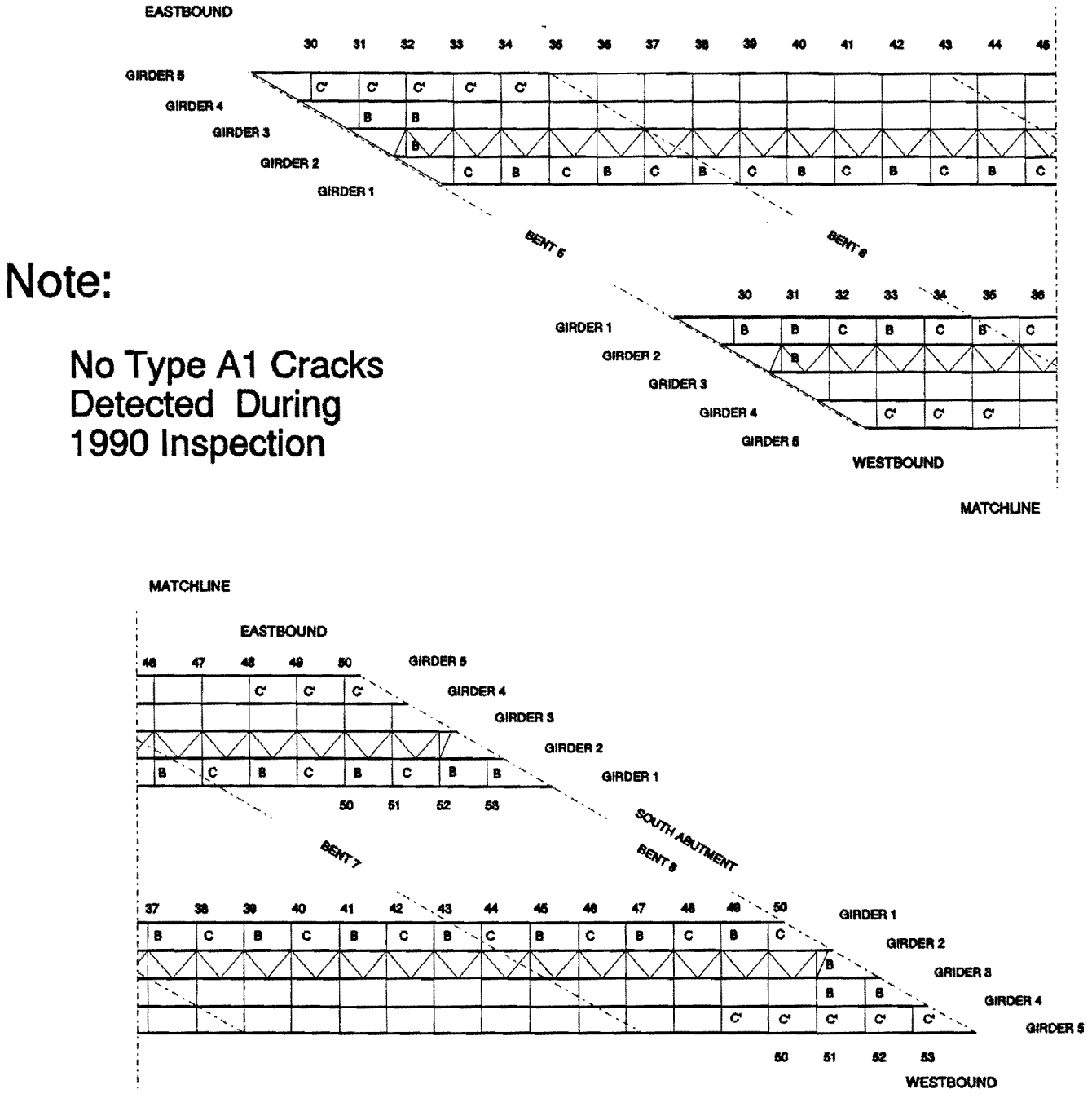

Figure A-2: Type A1 crack locations in South Structures.

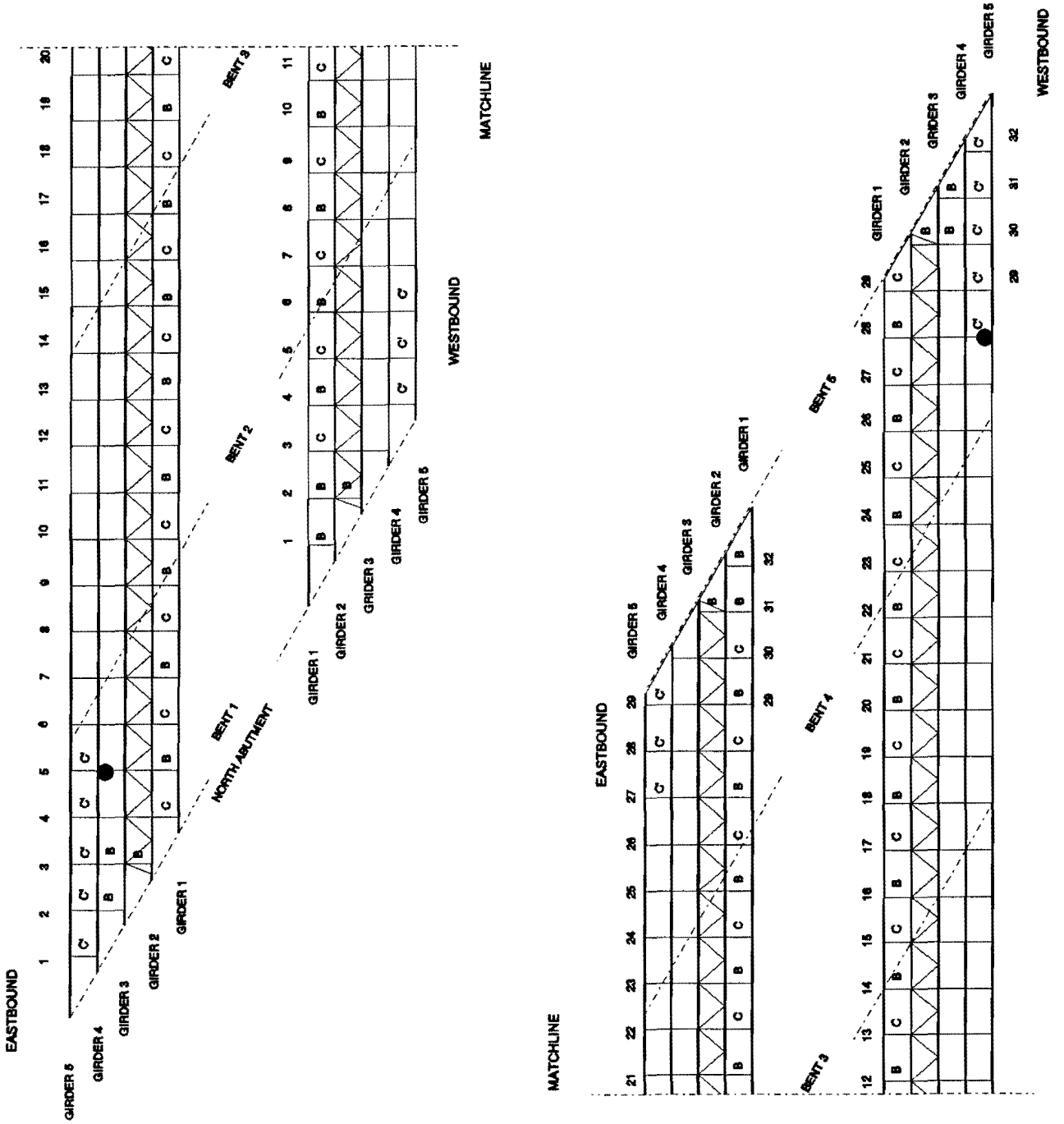

Figure A-3: Type A2 crack locations in North Structures.

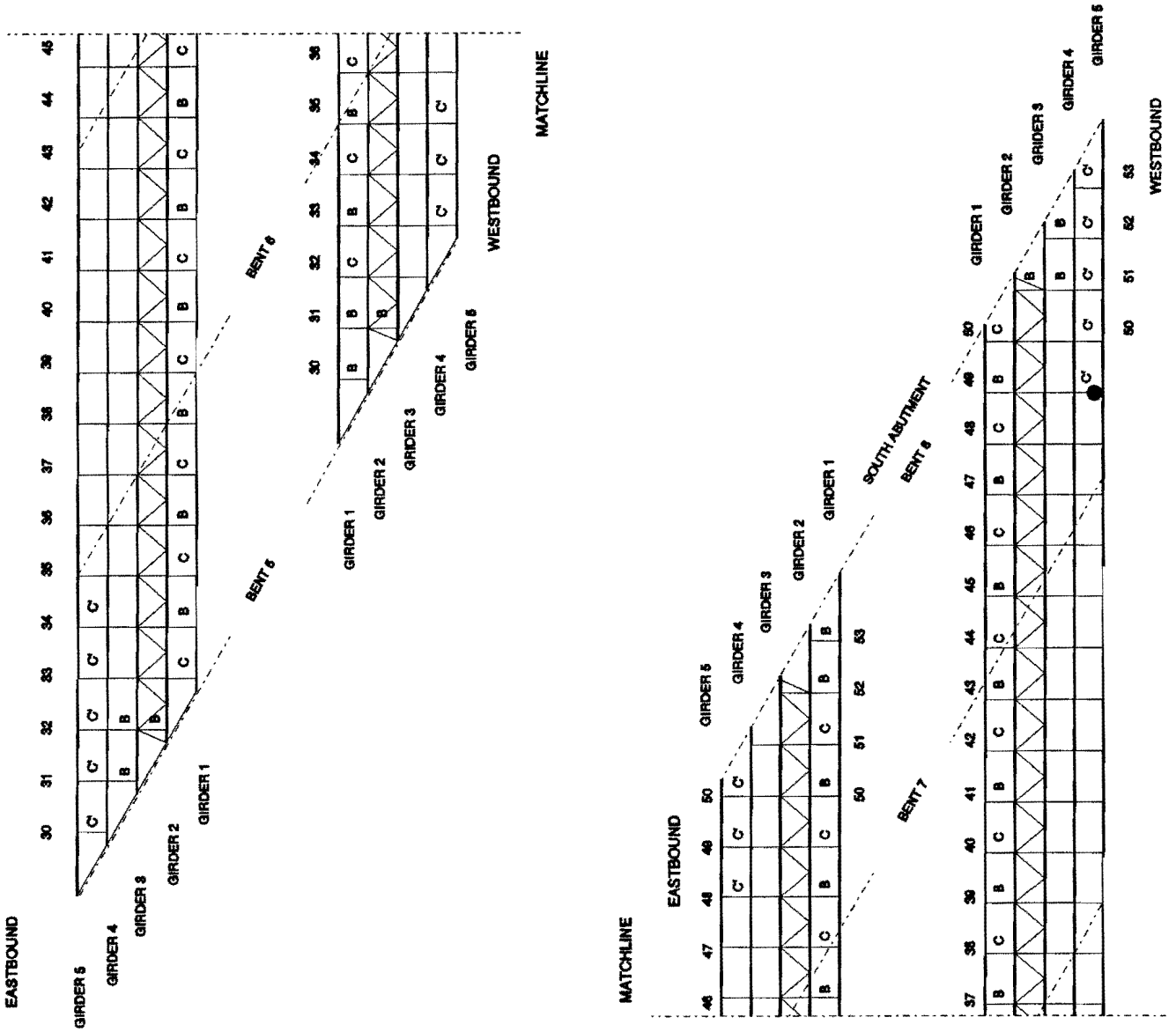

Figure A-4: Type A2 cracking, South Structures.

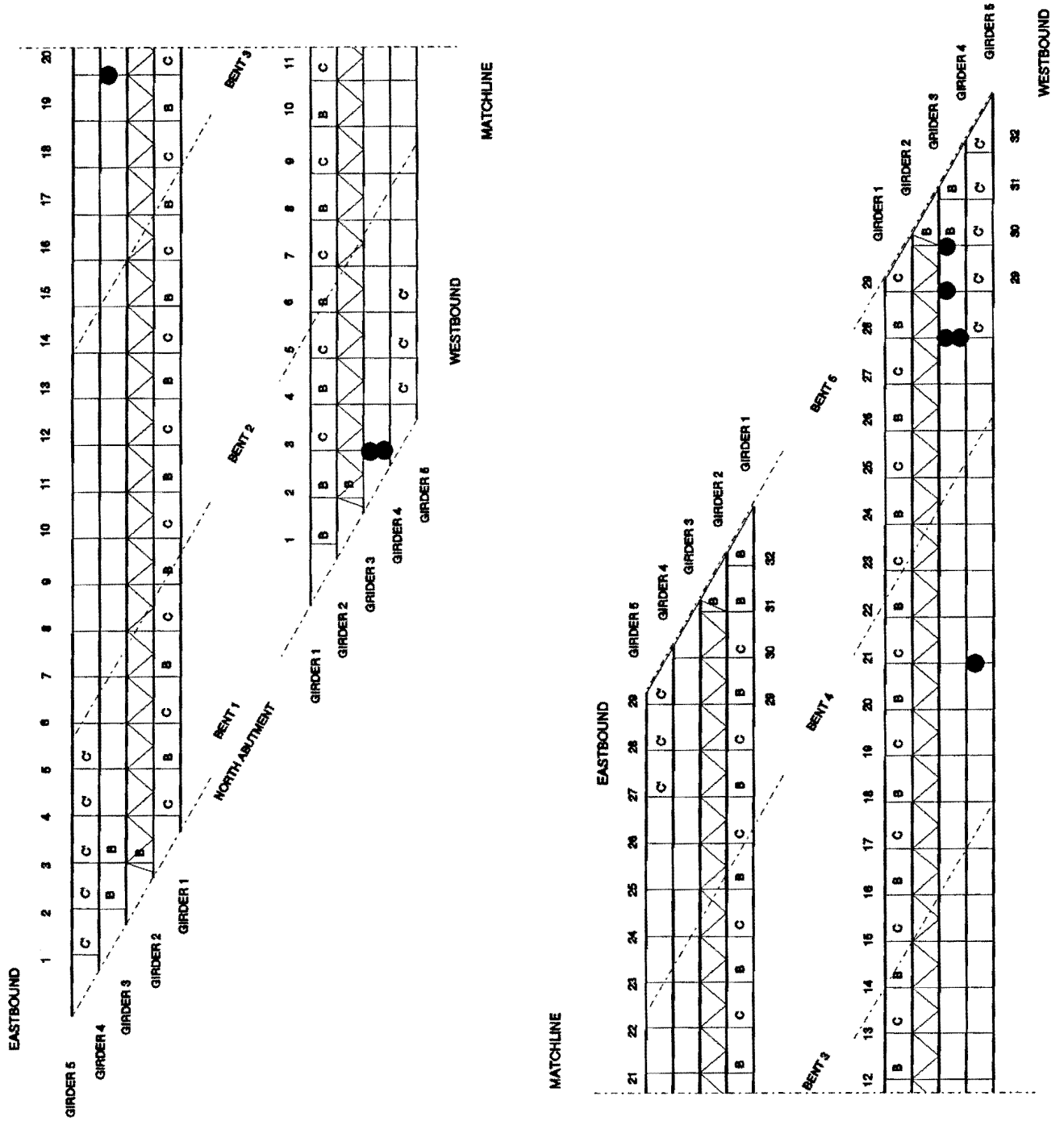

Figure A-5: Type A3 cracking, North Structures.

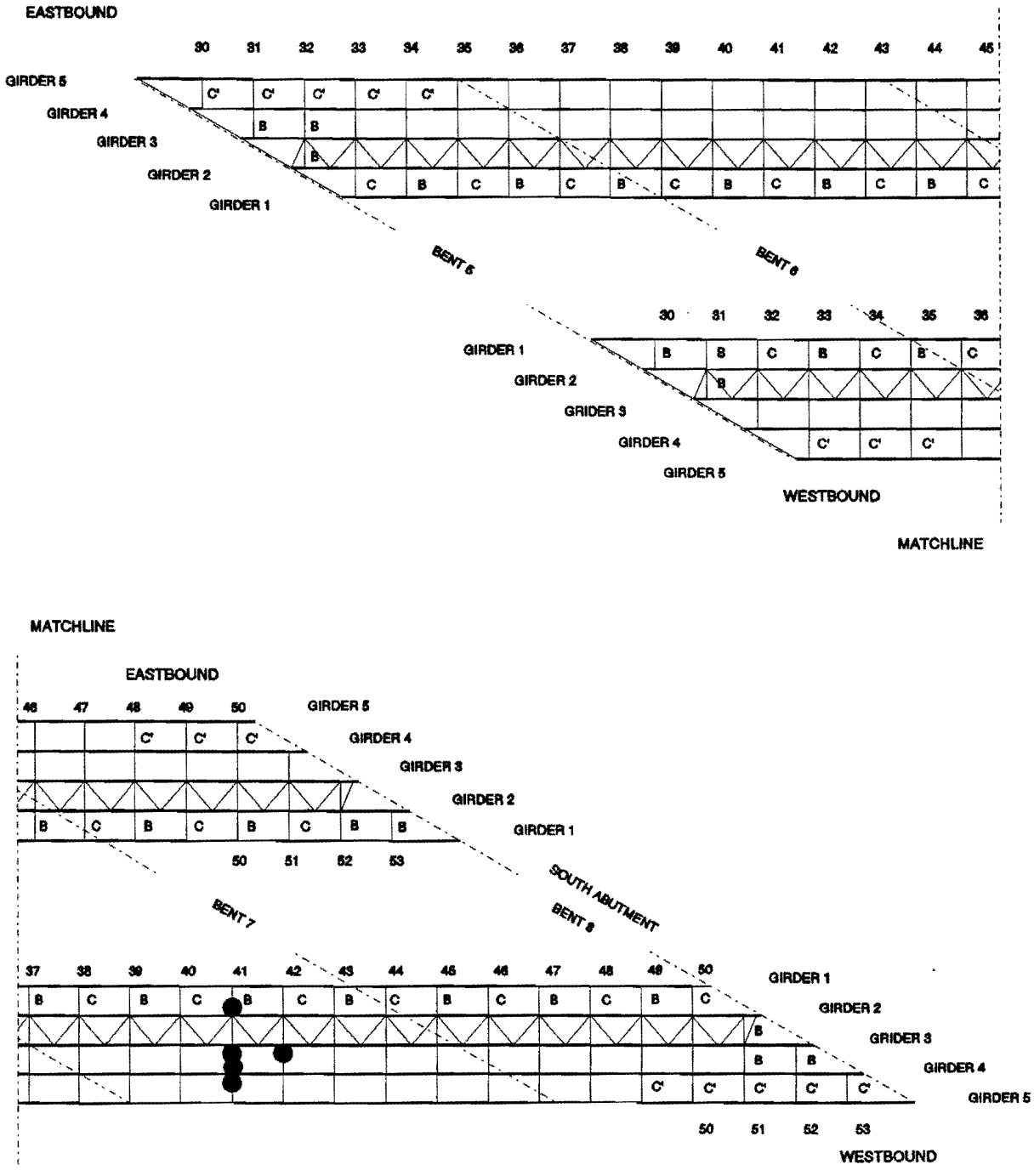

Figure A-6: Type A3 cracking, South Structures.

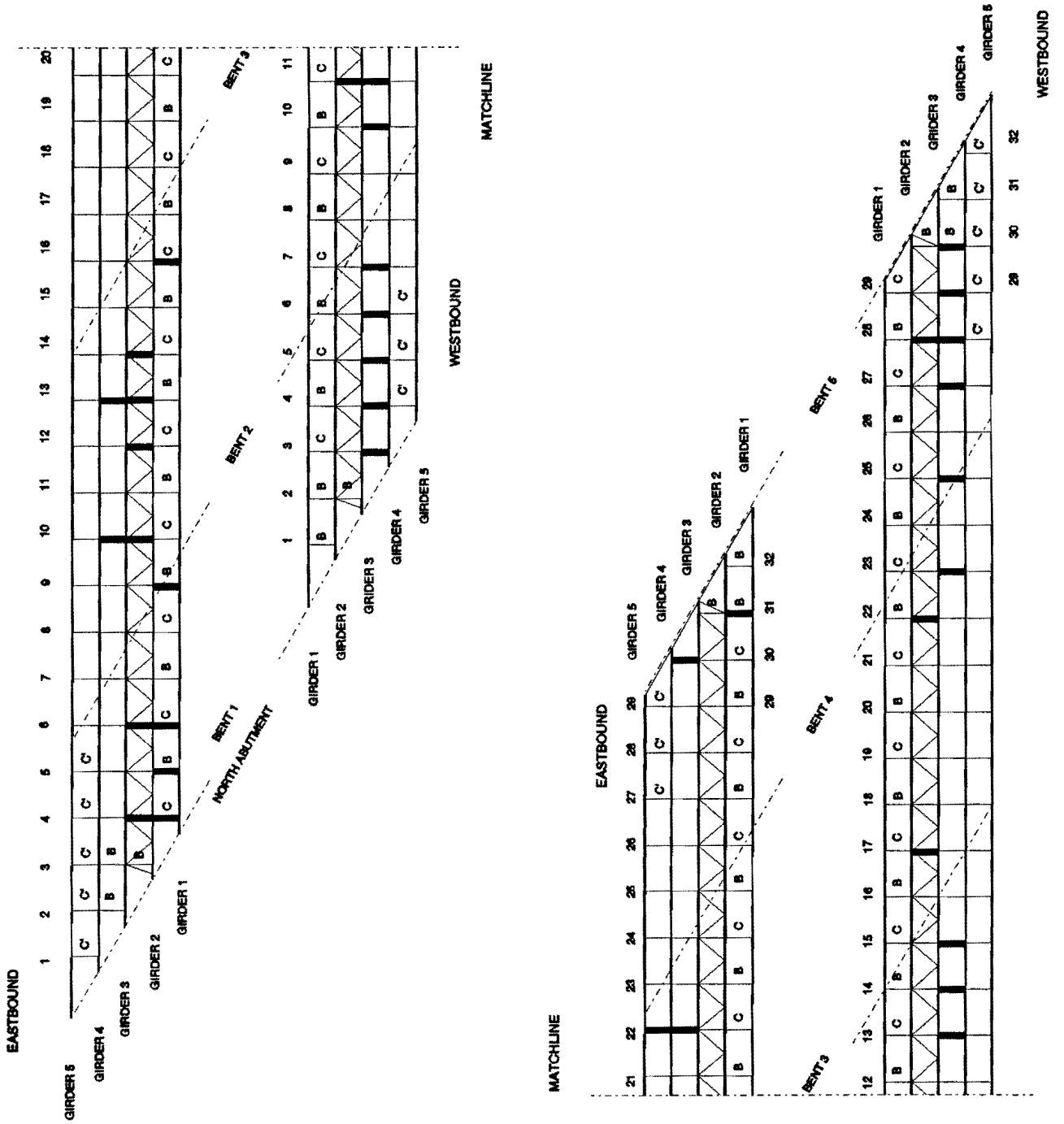

Figure A-7: Type B cracking, North Structures.

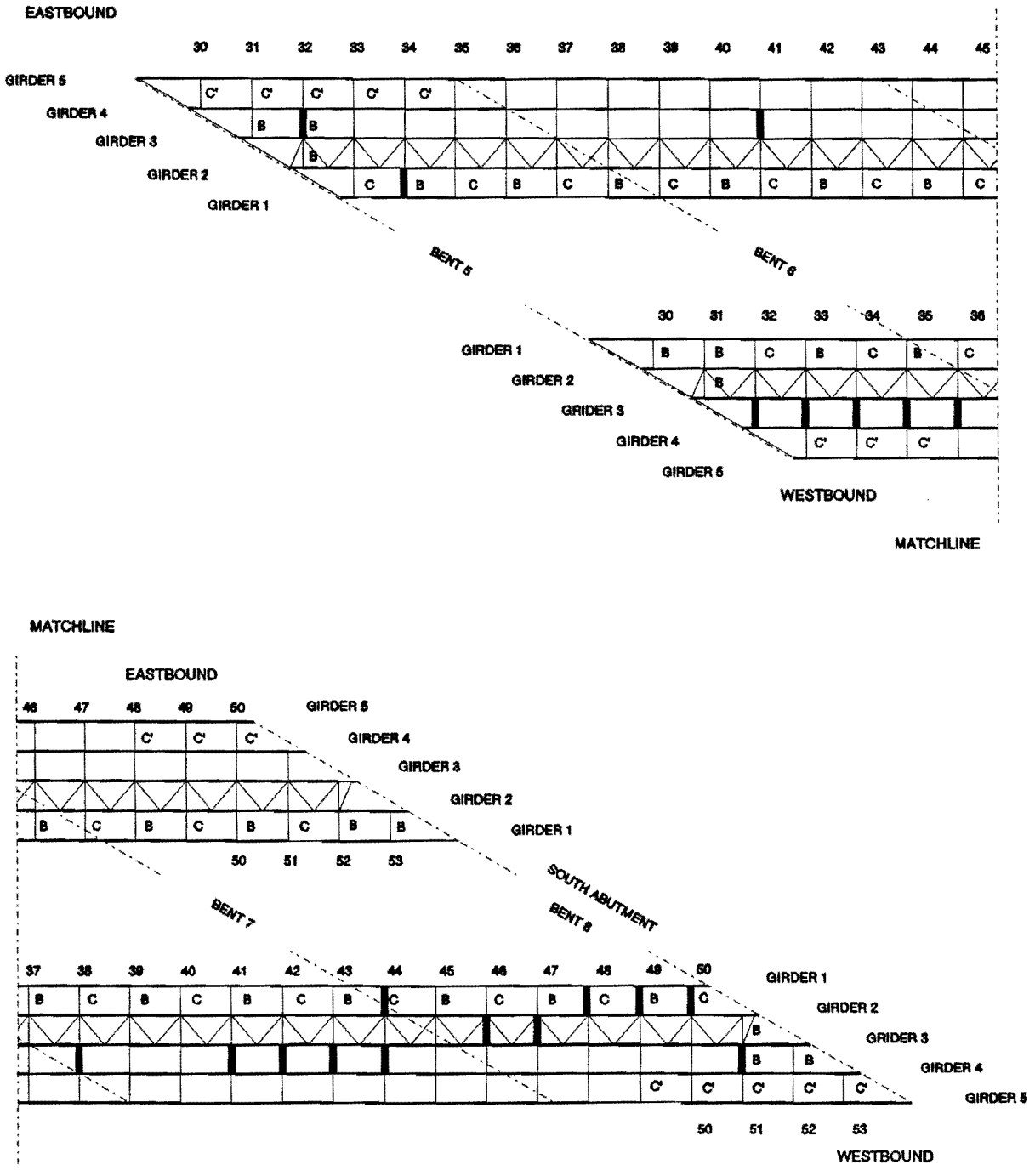

Figure A-8: Type B cracking, South Structures.

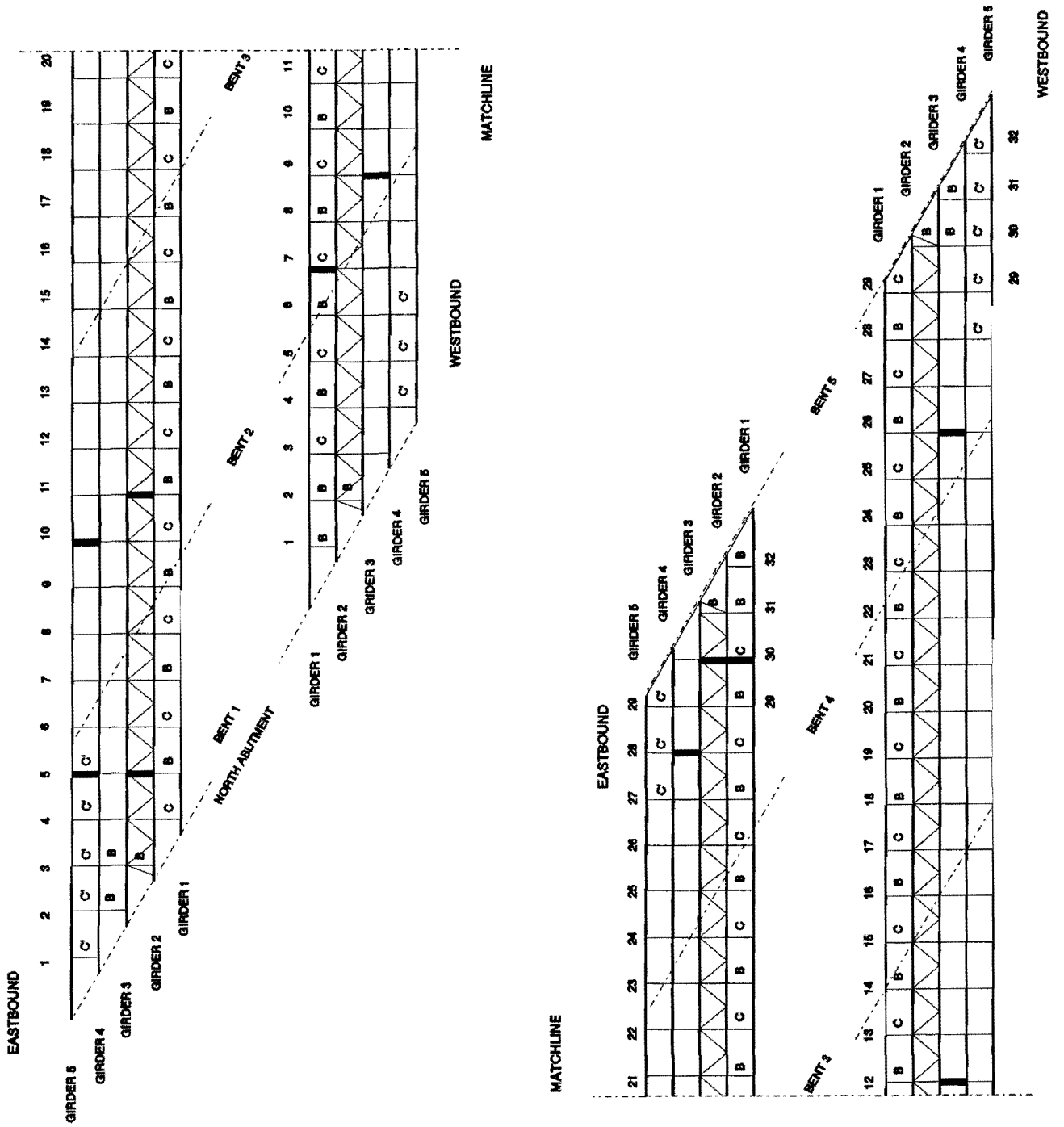

Figure A-9: Type C cracking, North Structures.

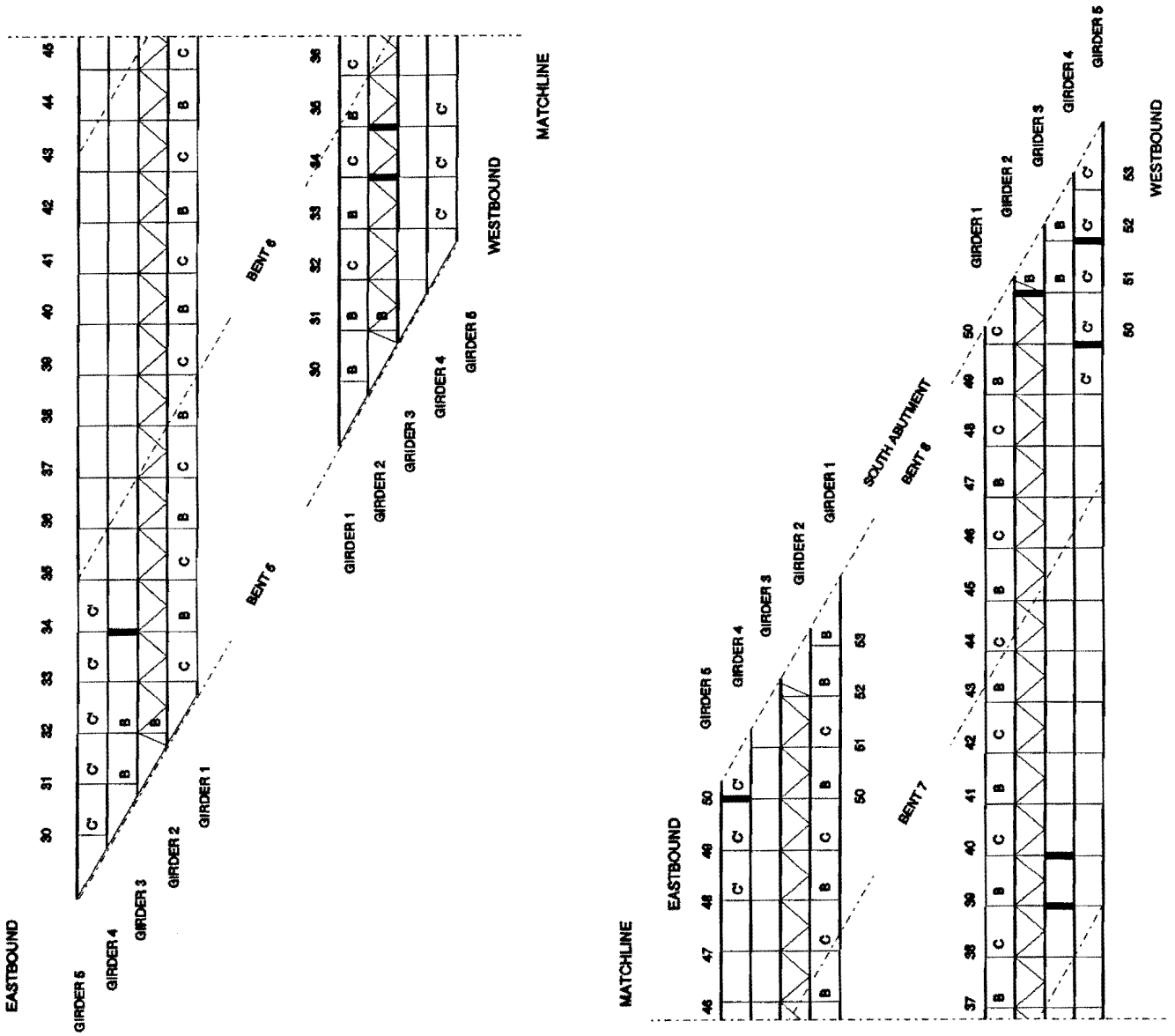

Figure A-10: Type C cracking, South Structures.

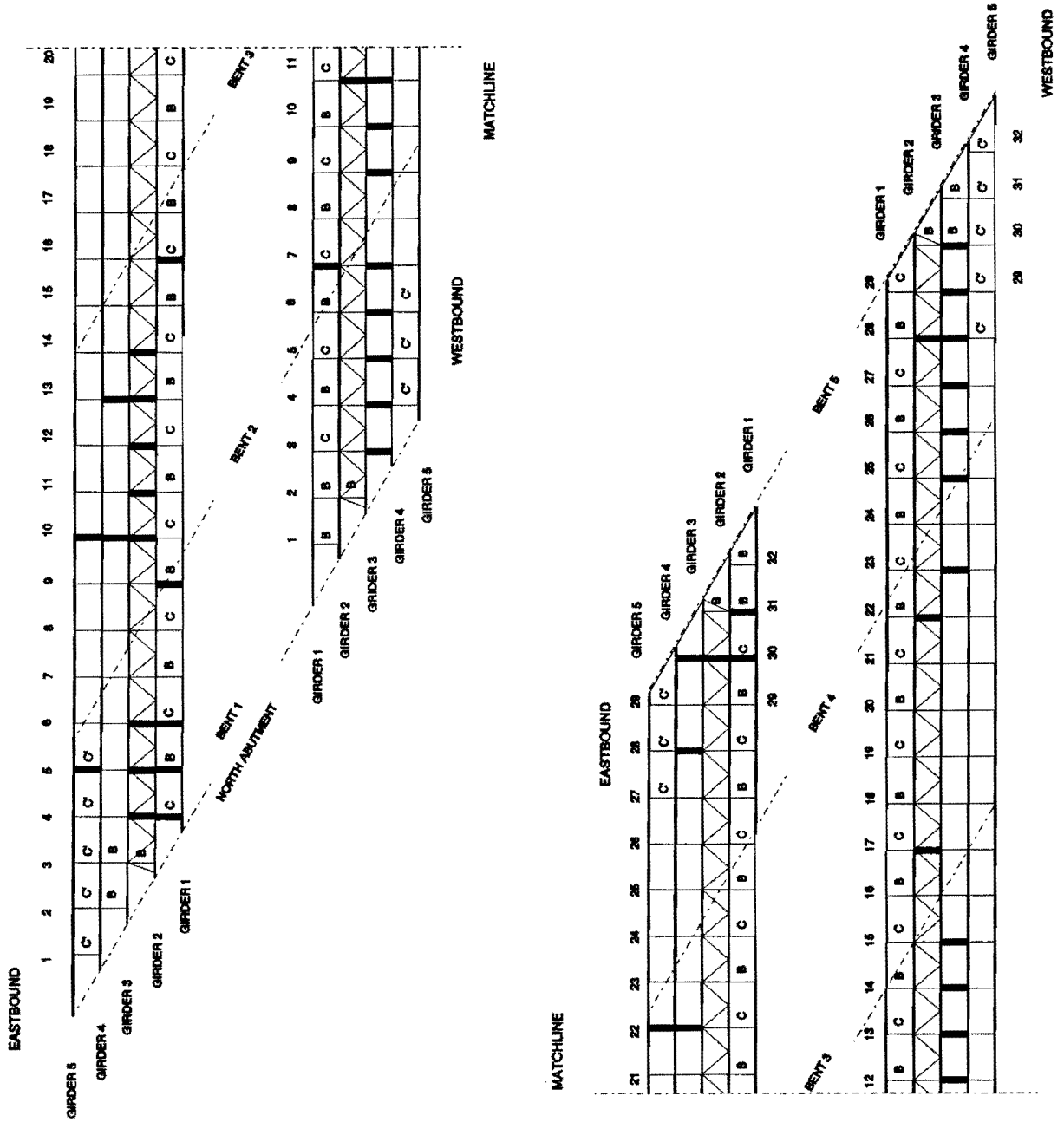

Figure A-11: All diaphragm member cracking, North Structures.

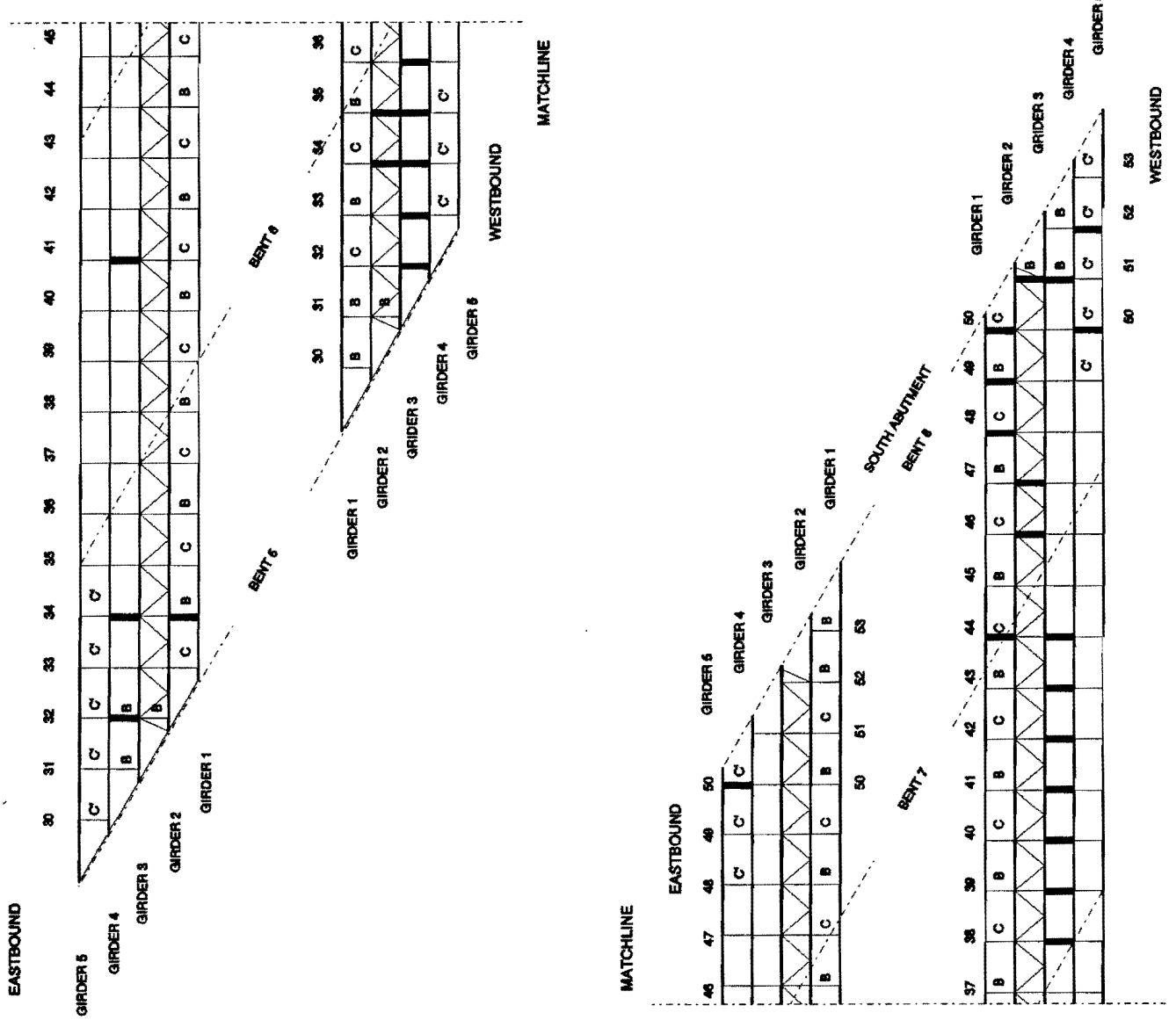

Figure A-12: All diaphragm member cracking, South Structures.

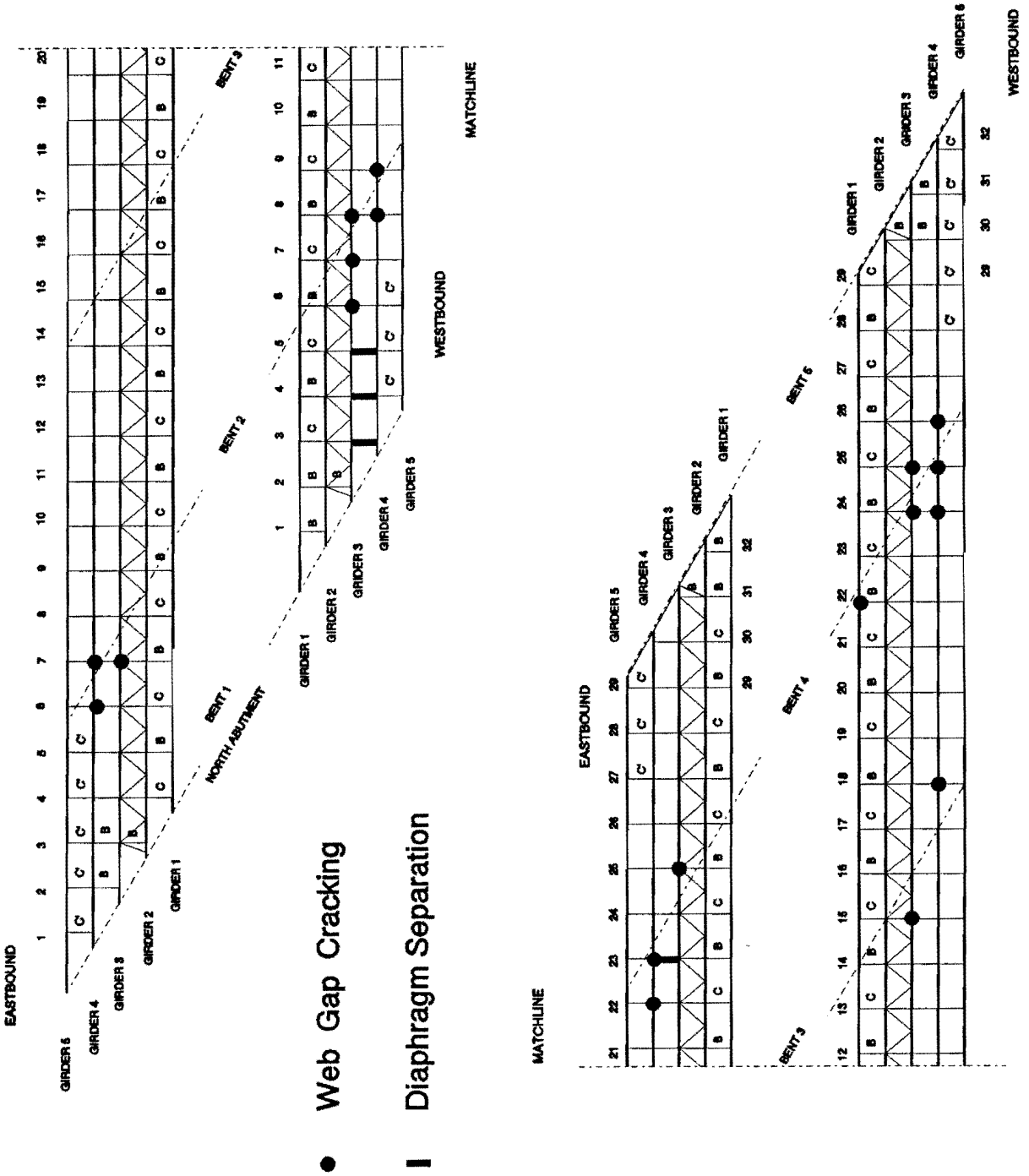

Figure A-13: 1983 repair locations, North Structures.

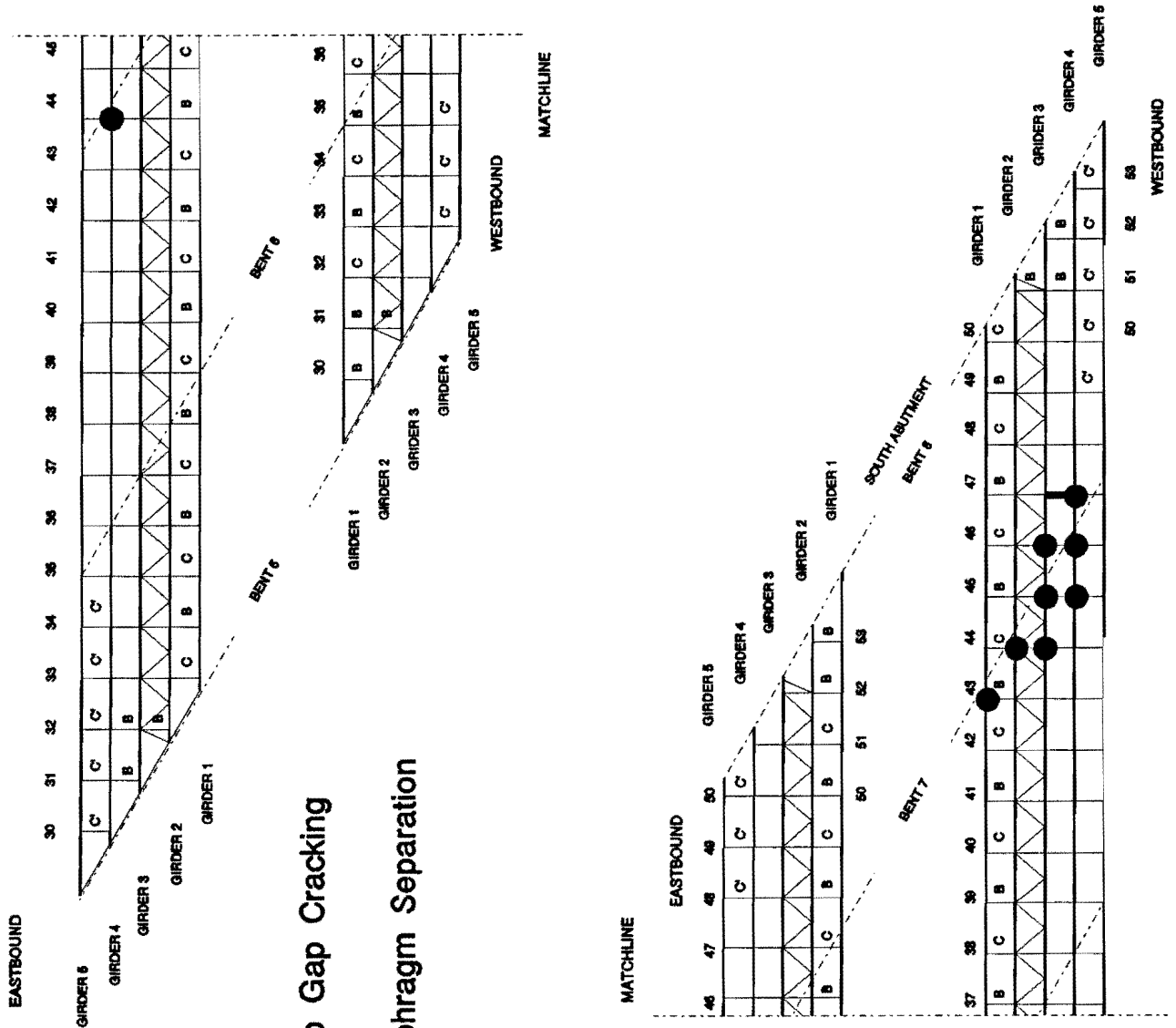

Figure A-14: 1983 repair locations, South Structures.

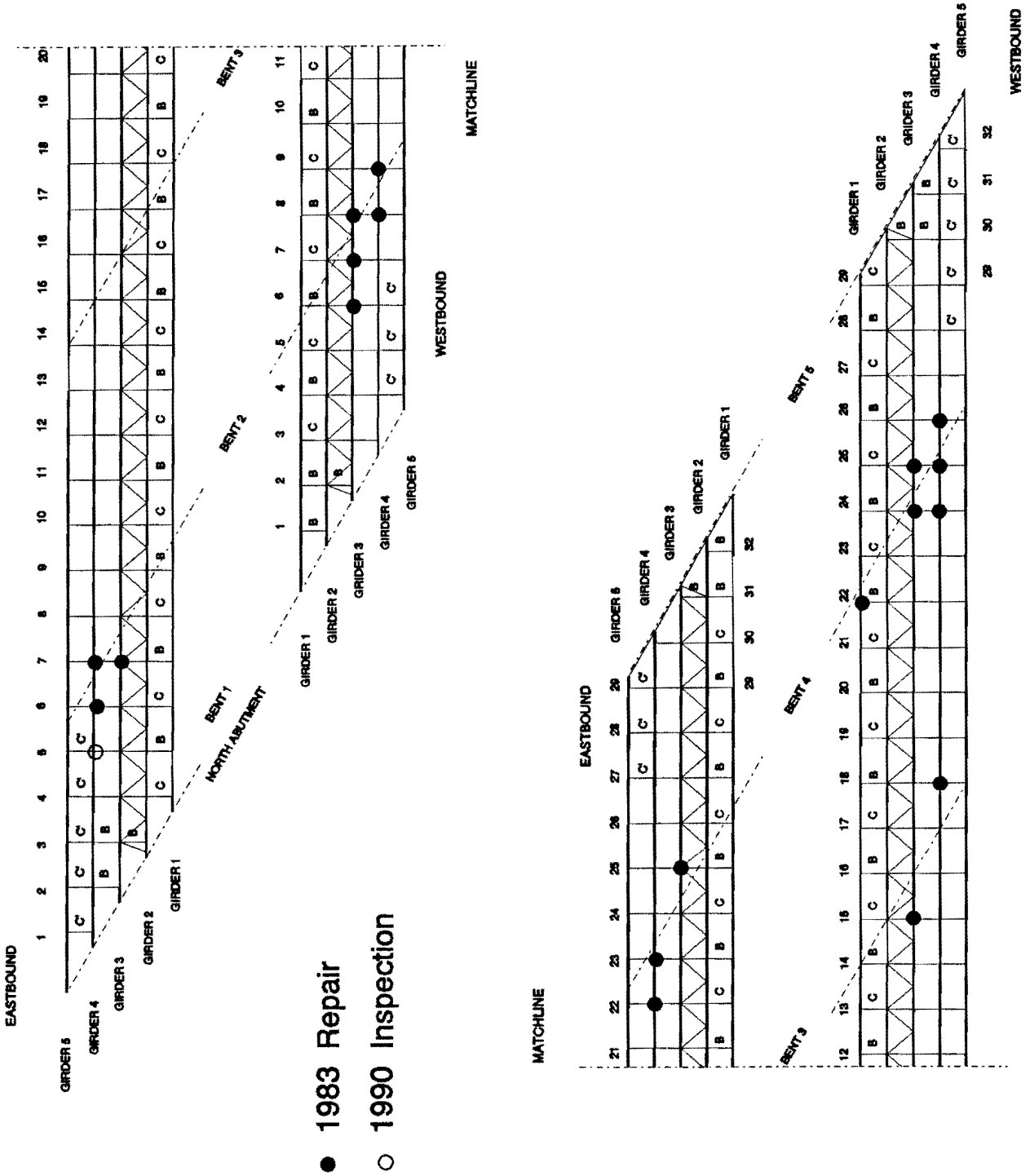

Figure A-15: All Type A2 cracking, North Structures.

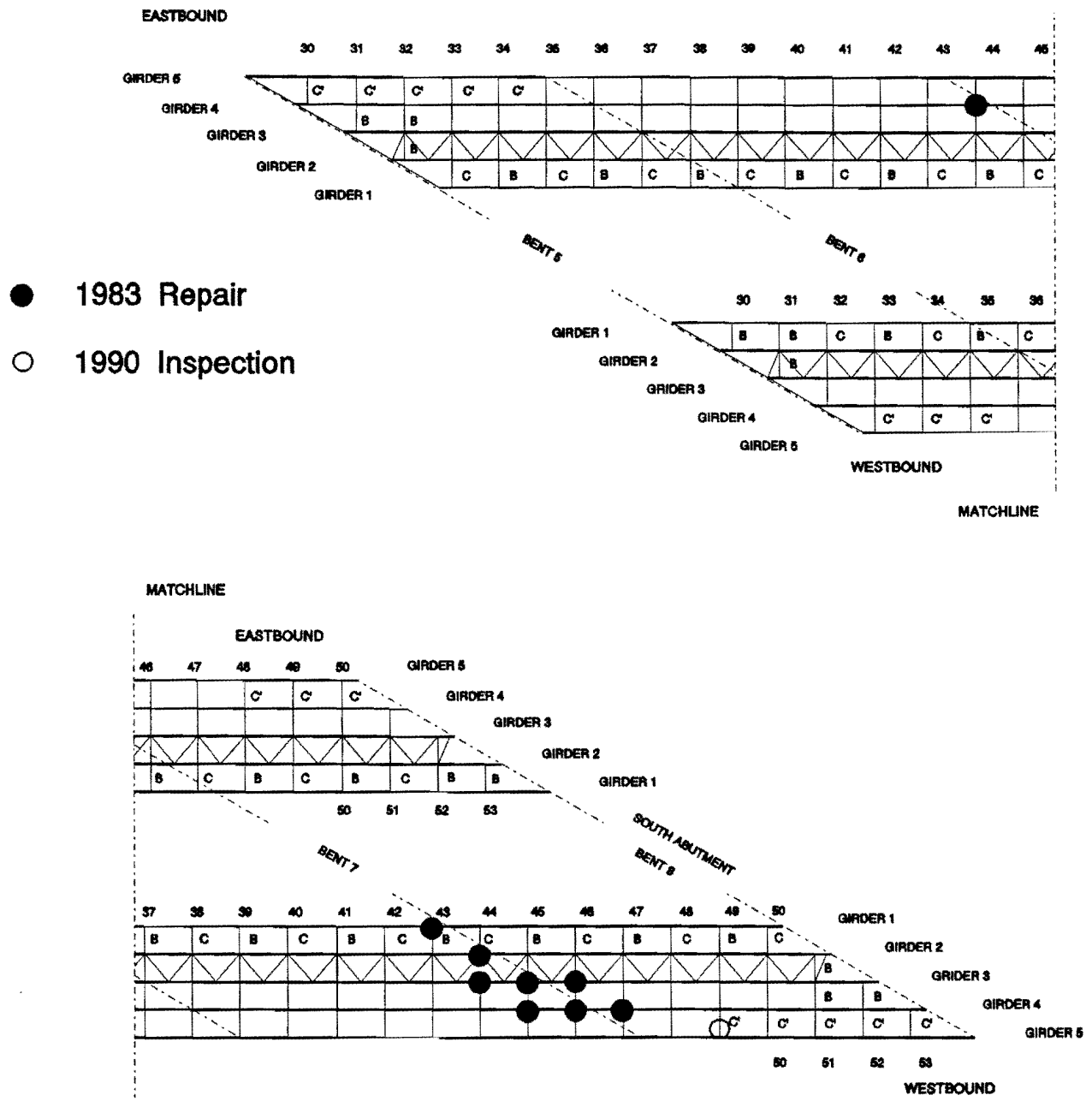

Figure A-16: All Type A2 cracking, South Structures.

Appendix B

Field Measurements

Filename	Gage Group	Truck Pass	Truck Position	Number of Scans
GRP1PS1	1	1	Truck straddled center strip	255
GRP1PS2	1	2	Truck centered in driving lane	133
GRP1PS3	1	3	Truck centered in right shoulder	92
GRP1PS4	1	4	Truck centered in passing lane	96
GRP2PS1	2	1	Truck centered in driving lane	108
GRP2PS2	2	2	Truck centered in right shoulder	102
GRP2PS3	2	3	Truck centered in passing lane	108
GRP3PS1	3	1	Truck centered in driving lane	116
GRP3PS2	3	2	Truck centered in right shoulder	96
GPR3PS3	3	3	Truck centered in passing lane	90
GRP3PS4	3	4	Right wheel on right shoulder stripe	100
GPR3PS5	3	5	Left wheel on center stripe	97
GPP4PS1	4	1	Truck centered in driving lane	93
GPR4PS2	4	2	Truck centered in right shoulder	97
GRP4PS3	4	3	Truck straddled right shoulder stripe	99
GRP4PS4	4	4	Same as Pass No. 3	98
GRP4PS5	4	5	Truck straddled center stripe	101
GRP4PS6	4	6	Truck centered in passing lane	144
GRP4PS7	4	7	18 wheeler centered in driving lane	148

Table B-1: Summary of recorded test truck passages.

Filename	Gage Group	Truck Pass	Truck Position	Number of Scans
GRP5PS1	5	1	Truck centered in driving lane	111
GRP5PS2	5	2	Truck centered in right shoulder	99
GRP5PS3	5	3	Truck centered in passing lane	108
GRP5PS4	5	4	Truck centered in left shoulder	104
GRP5PS5	5	5	Truck straddled center stripe	101
GRP6PS1	6	1	Truck centered in driving lane	95
GPR6PS2	6	2	Truck centered in right shoulder	105
GRP6PS3	6	3	Truck straddled right shoulder stripe	98
GRP6PS4	6	4	Truck straddled center stripe	123
GRP6PS5	6	5	Truck centered in passing lane	93
GRP6PS6	6	6	Two 18 wheelers in driving lane	103
GPR6PS7	6	7	Data logger failure, no data obtained	144
GRP6PS8	6	8	Tandem centered in right lane	70

Table B-1: Cont.

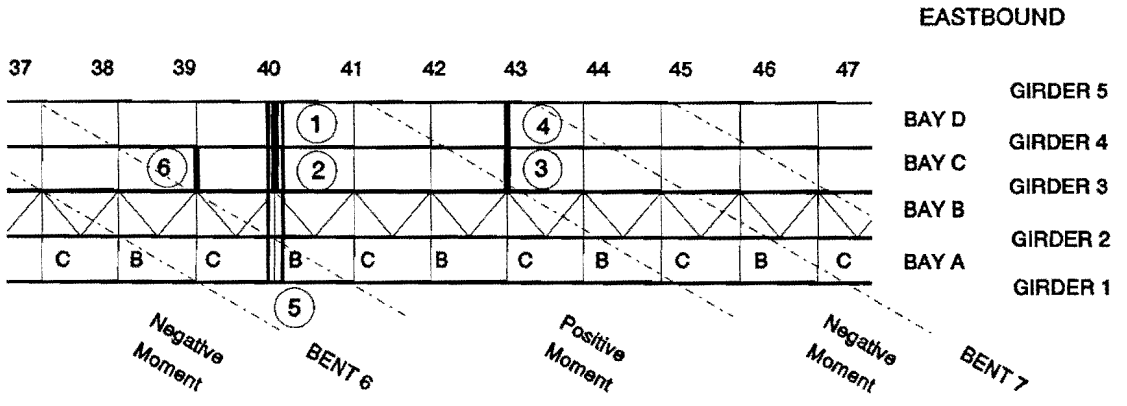

Figure B-1 Gage group locations on Eastbound structure.

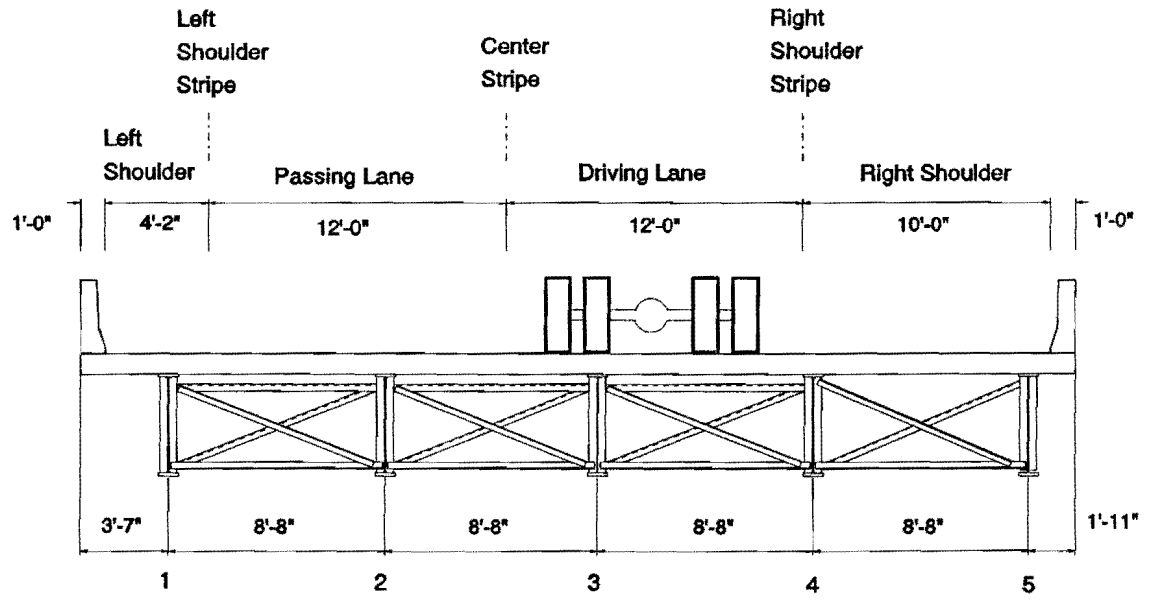

Figure B-2: Location for test truck positioned in center of driving lane.

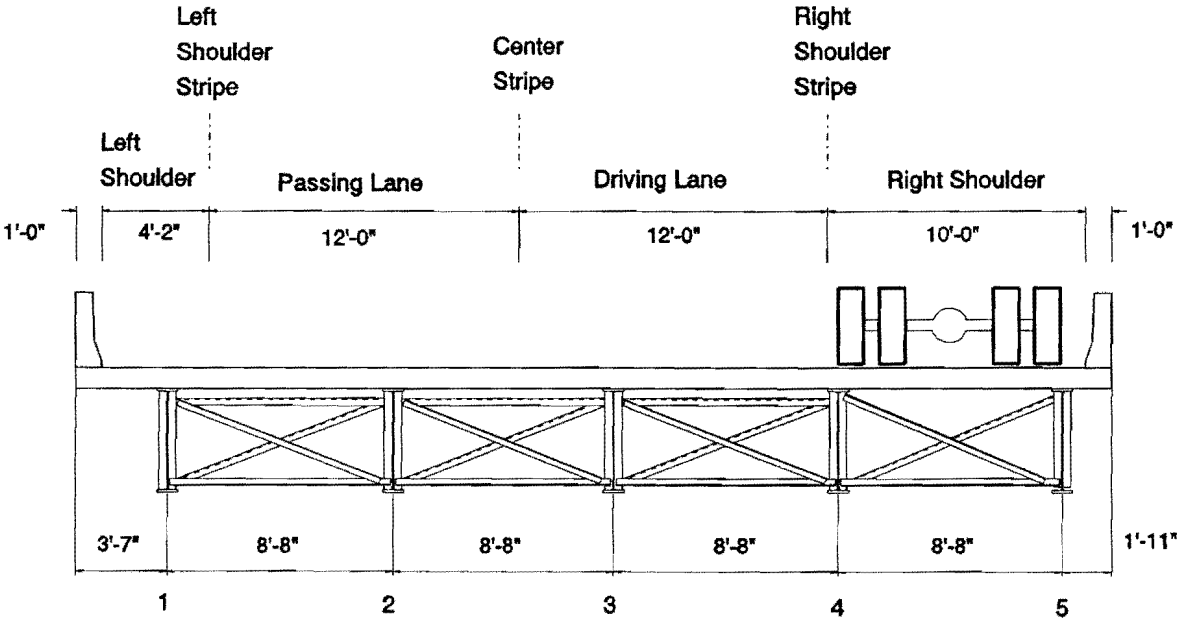

Figure B-3: Location for test truck positioned in center of right shoulder lane.

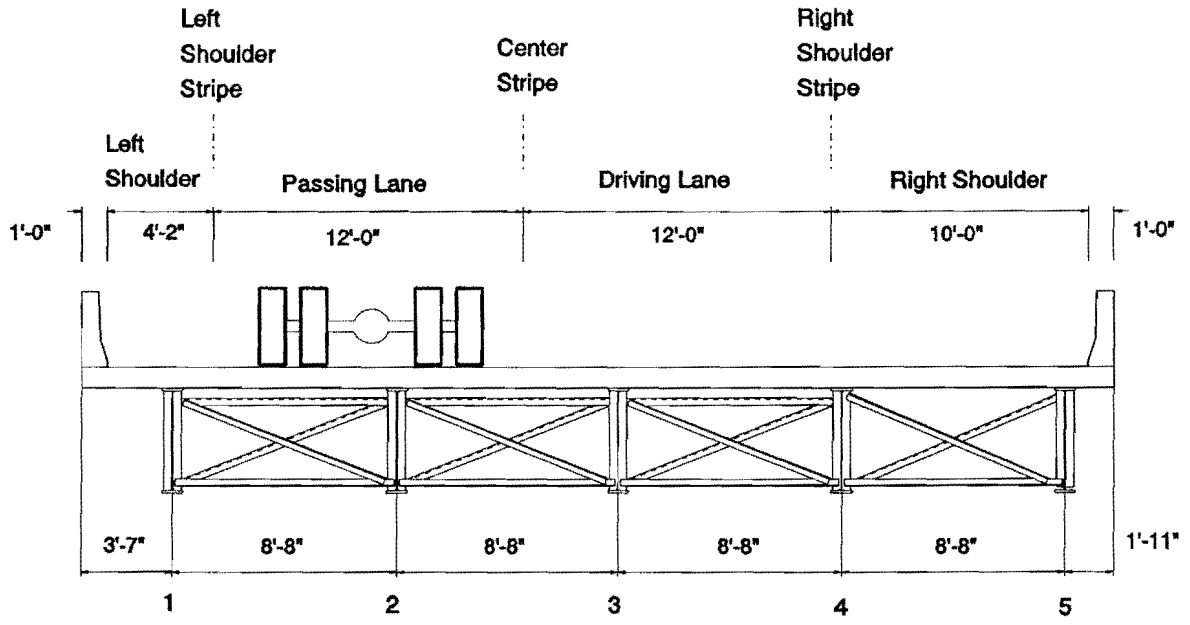

Figure B-4: Location for test truck positioned in center of passing lane.

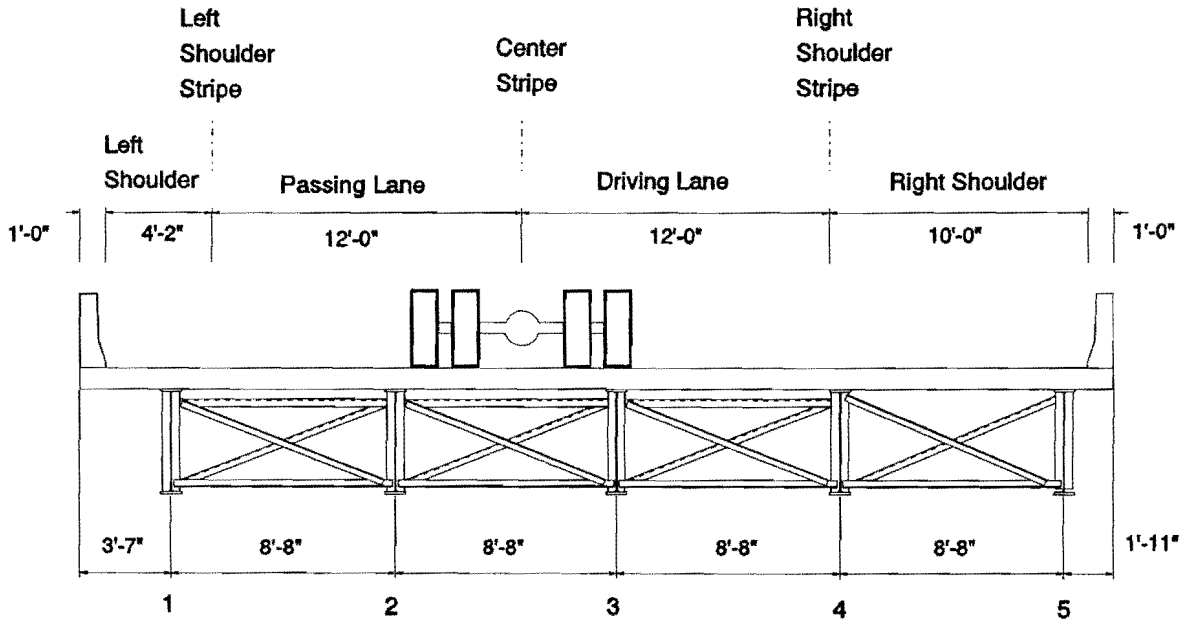

Figure B-5: Location for test truck positioned straddling center stripe.

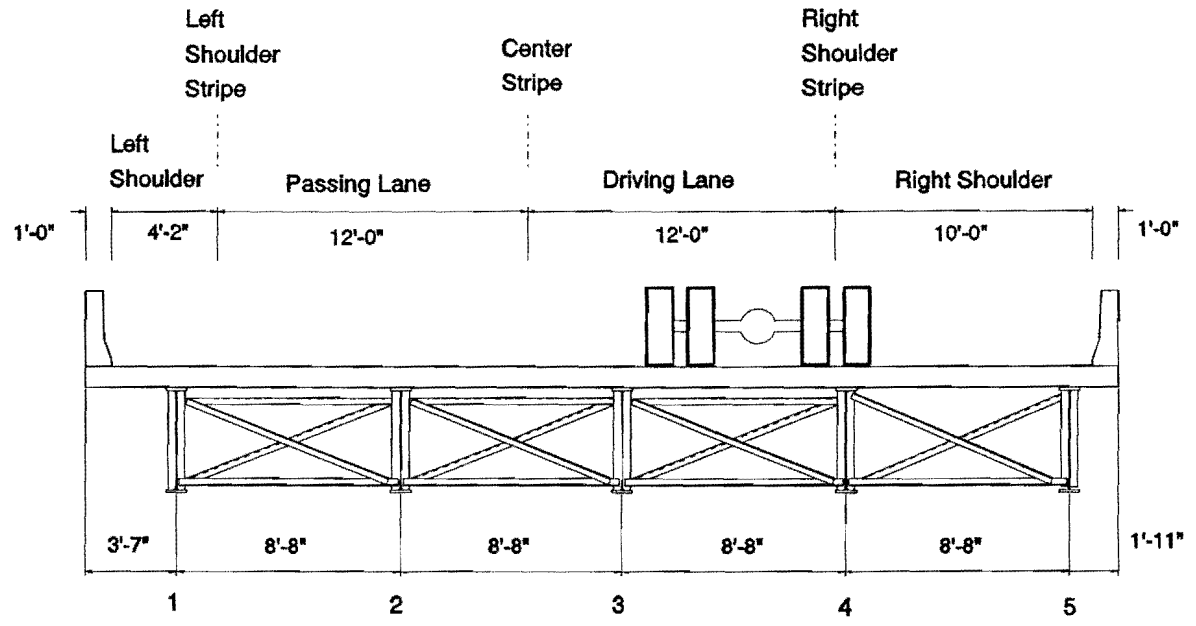

Figure B-6: Location for test truck positioned with right wheel on right shoulder stripe.

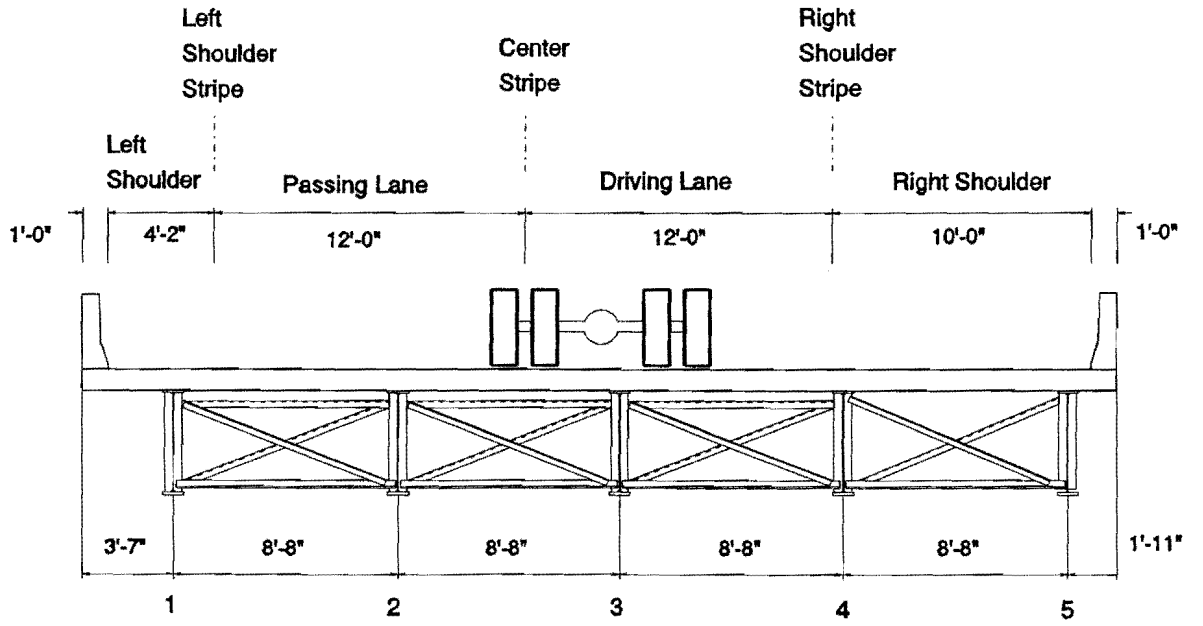

Figure B-7: Location for test truck positioned with left wheel on center stripe.

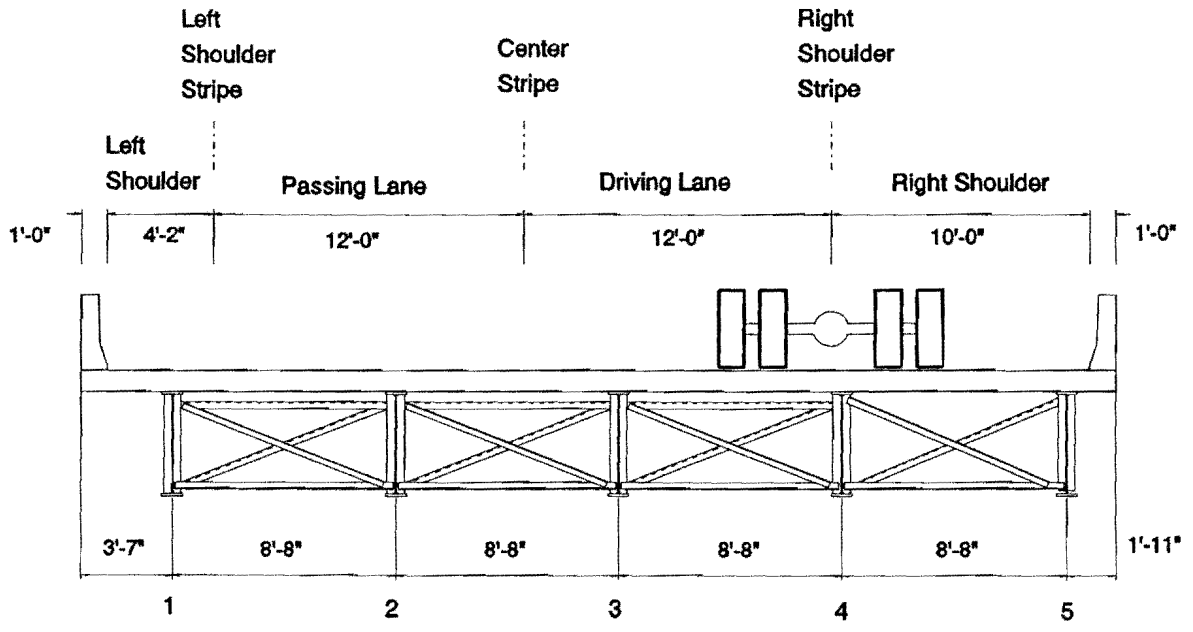

Figure B-8: Location for test truck positioned straddling right shoulder stripe.

(this page intentionally left blank)

Gage Group No. 1

Type C' Diaphragm, D-40
Positive Moment Region

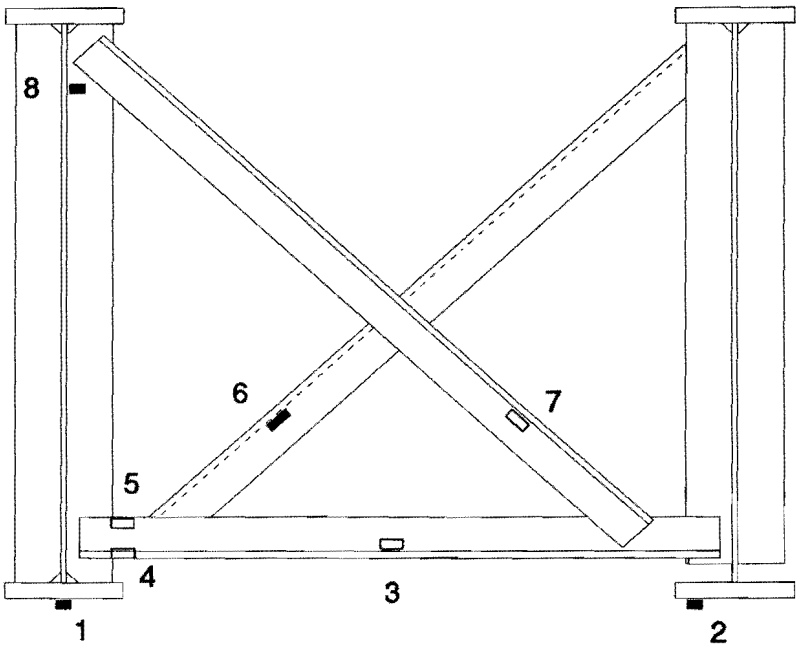

Gage No.	Position
1	bottom flange, centerline of web plate
2	bottom flange, 2" from flange edge
3	neutral axis
4	back of leg, bottom
5	back of leg, top
6	neutral axis
7	neutral axis
8	web plate, longitudinal direction (5-1/2" below flange)

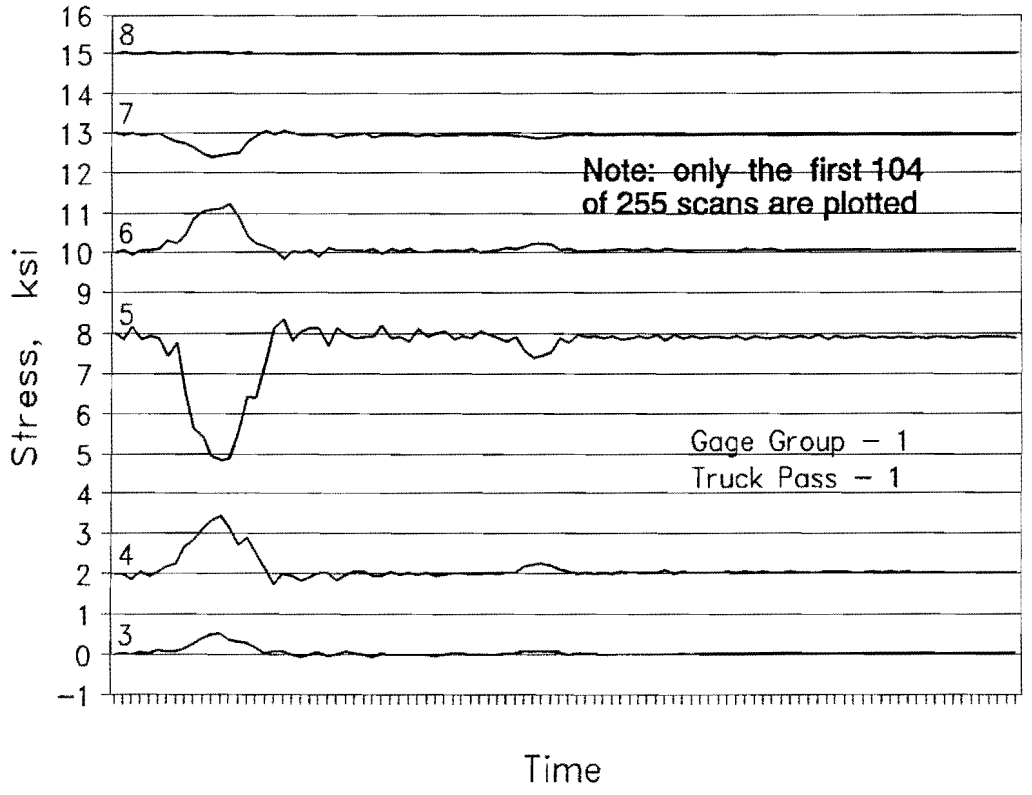

Figure B-9: Diaphragm D-40 member stress histories for Gage Group 1, Truck Pass 1 (test truck straddled center stripe).

Gage Number	Location	Max. Stress Range, ksi	Tension or Compression
1	Bottom flange, Girder No. 4	1.3	Tens.
2	Bottom flange, Girder No. 5	0.9	Tens.
3	Lower strut, Type C' Diaphragm	0.6	Tens.
4	Lower strut, at bottom	1.7	Tens.
5	Lower strut, at top	3.5	Comp.
6	Diagonal, Type C' Diaphragm	1.4	Tens.
7	Diagonal, Type C' Diaphragm	0.7	Comp.
8	Web plate, longitudinal bending stress	0.1	-----

Table B-2: Maximum measured stress ranges and direction for Gage Group 1, Truck Pass 1 (test truck straddled center stripe).

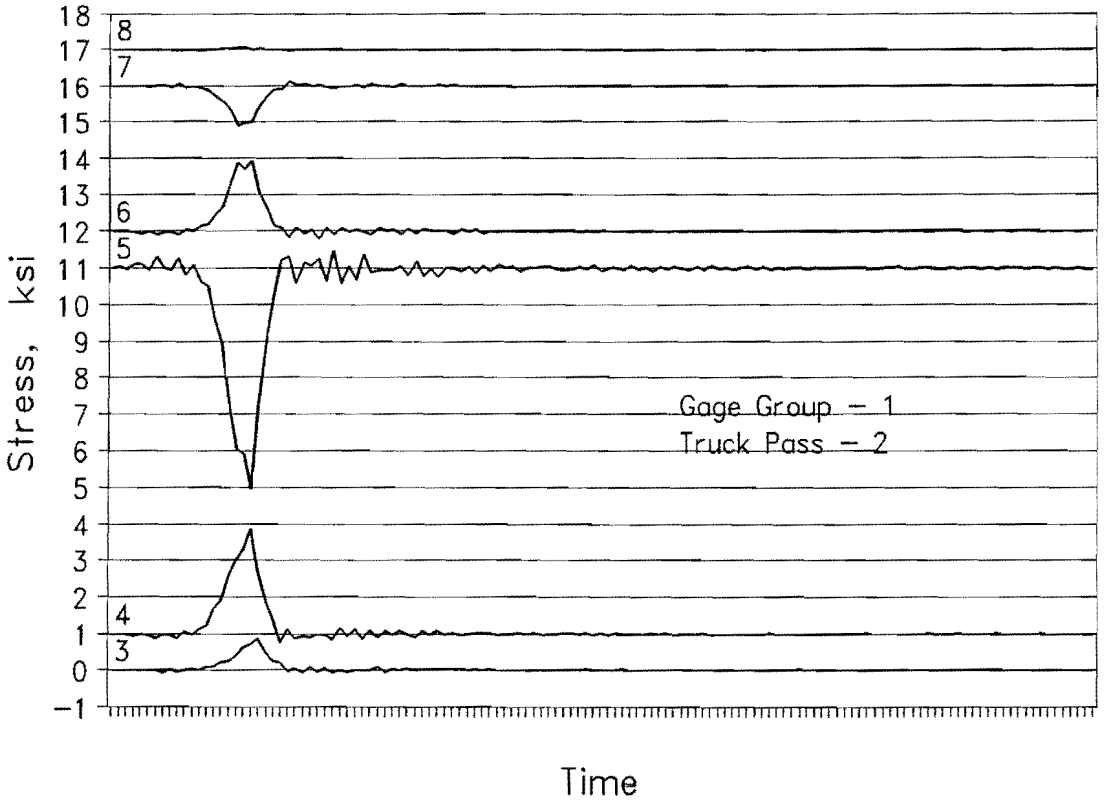

Figure B-10: Diaphragm D-40 member stress histories for Gage Group 1, Truck Pass 2 (test truck centered in driving lane).

Gage Number	Location	Max. Stress Range, ksi	Tension or Compression
1	Bottom flange, Girder No. 4	1.8	Tens.
2	Bottom flange, Girder No. 5	1.1	Tens.
3	Lower strut, Type C' Diaphragm	0.9	Tens.
4	Lower strut, at bottom	3.1	Tens.
5	Lower strut, at top	6.6	Comp.
6	Diagonal, Type C' Diaphragm	2.1	Tens.
7	Diagonal, Type C' Diaphragm	1.2	Comp.
8	Web plate, longitudinal bending stress	0.1	-----

Table B-3: Maximum measured stress ranges and direction for Gage Group 1, Truck Pass 2 (test truck centered in driving lane).

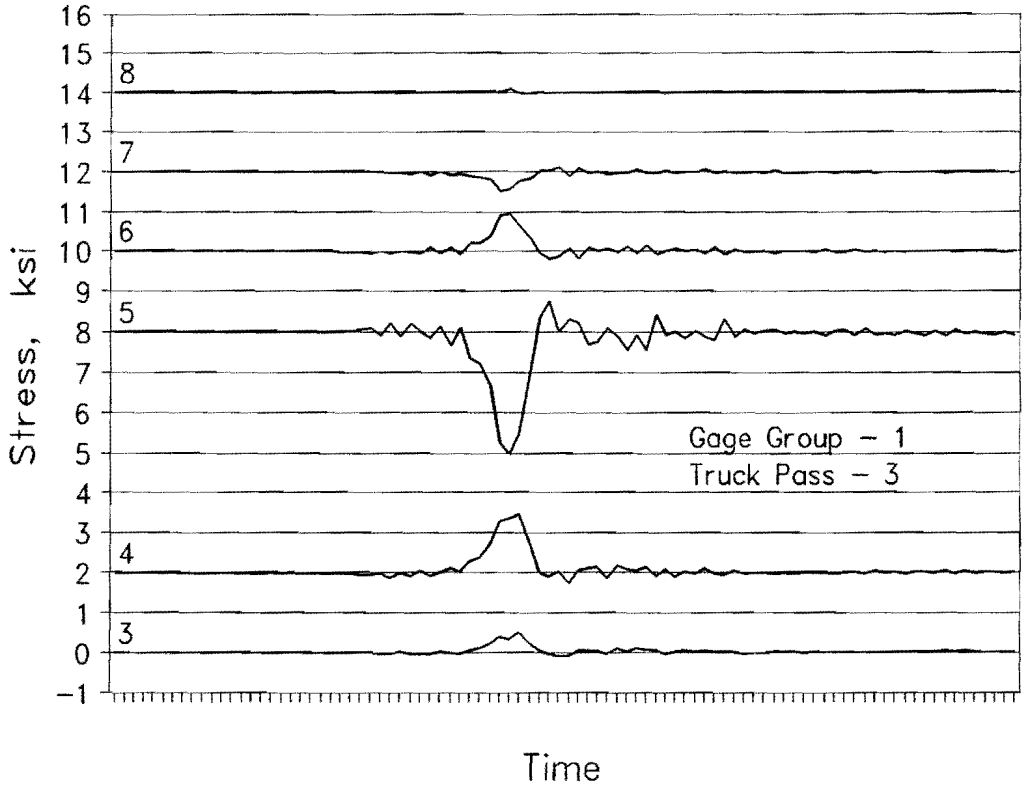

Figure B-11: Diaphragm D-40 member stress histories for Gage Group 1, Truck Pass 3 (test truck centered in right shoulder).

Gage Number	Location	Max. Stress Range, ksi	Tension or Compression
1	Bottom flange, Girder No. 4	2.2	Tens.
2	Bottom flange, Girder No. 5	2.1	Tens.
3	Lower strut, Type C' Diaphragm	0.6	Tens.
4	Lower strut, at bottom	1.7	Tens.
5	Lower strut, at top	3.8	Comp.
6	Diagonal, Type C' Diaphragm	1.1	Tens.
7	Diagonal, Type C' Diaphragm	0.6	Comp.
8	Web plate, longitudinal bending stress	0.1	-----

Table B-4: Maximum measured stress ranges and direction for Gage Group 1, Truck Pass 3 (test truck centered in right shoulder).

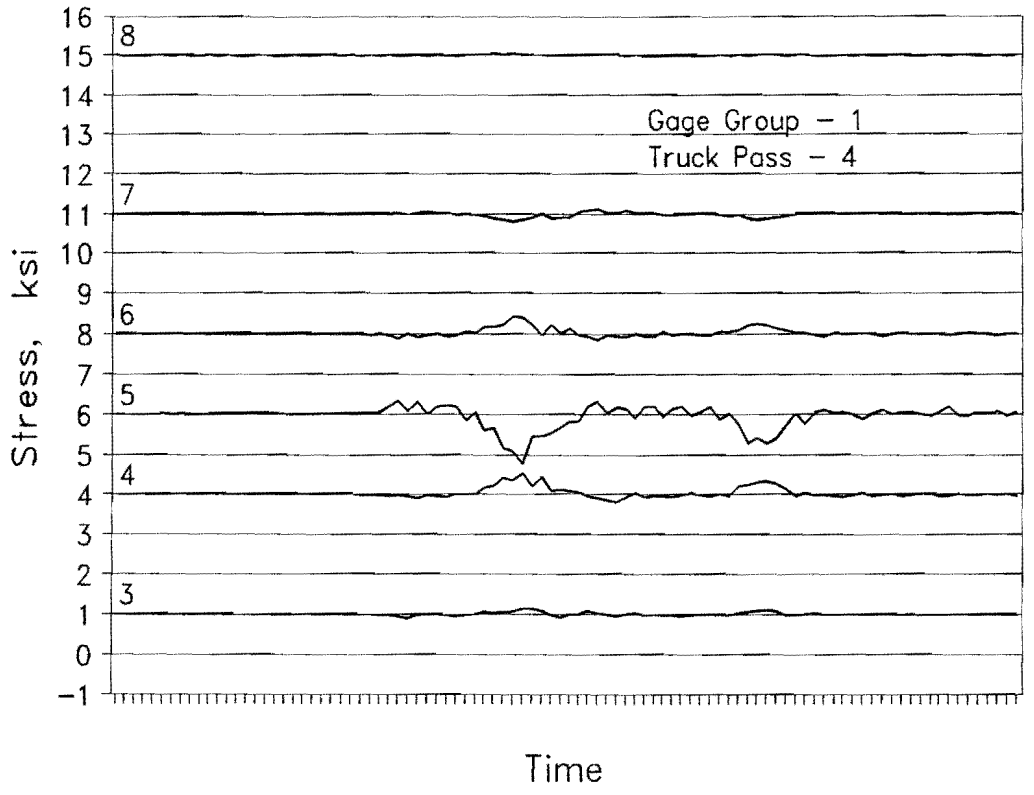

Figure B-12: Diaphragm D-40 member stress histories for Gage Group 1, Truck Pass 4 (test truck centered in passing lane).

Gage Number	Location	Max. Stress Range, ksi	Tension or Compression
1	Bottom flange, Girder No. 4	0.9	Tens.
2	Bottom flange, Girder No. 5	0.6	Tens.
3	Lower strut, Type C' Diaphragm	0.3	-----
4	Lower strut, at bottom	0.7	Tens.
5	Lower strut, at top	1.6	Comp.
6	Diagonal, Type C' Diaphragm	0.6	Tens.
7	Diagonal, Type C' Diaphragm	0.3	-----
8	Web plate, longitudinal bending stress	0.1	-----

Table B-5: Maximum measured stress ranges and direction for Gage Group 1, Truck Pass 4 (test truck centered in passing lane).

(this page intentionally left blank)

Gage Group No. 2

Type B Diaphragm, C-40
Positive Moment Region

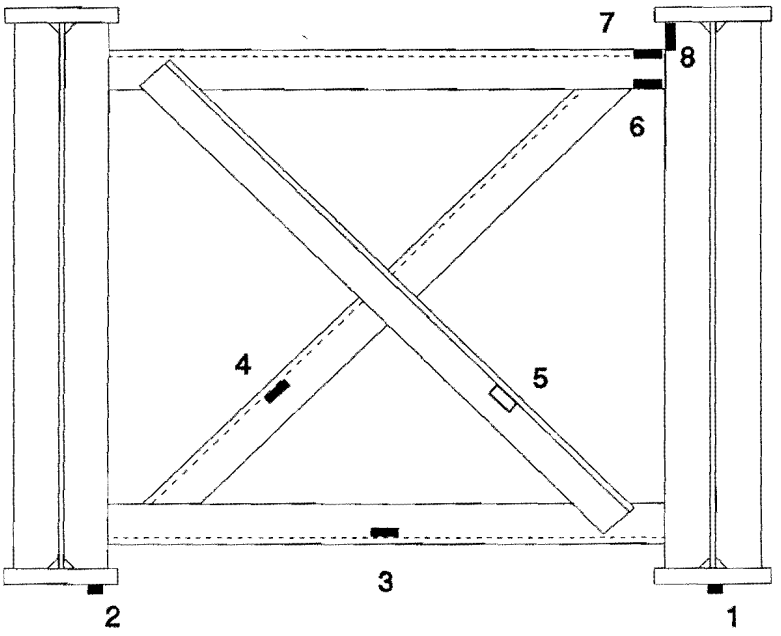

Girder 3 Girder 4

Gage No.	Position
1	bottom flange, centerline of web plate
2	bottom flange, 2" from edge
3	neutral axis
4	1" above neutral axis
5	1" above neutral axis
6	back of leg, bottom
7	back of leg, top
8	at plate edge, near fillet weld

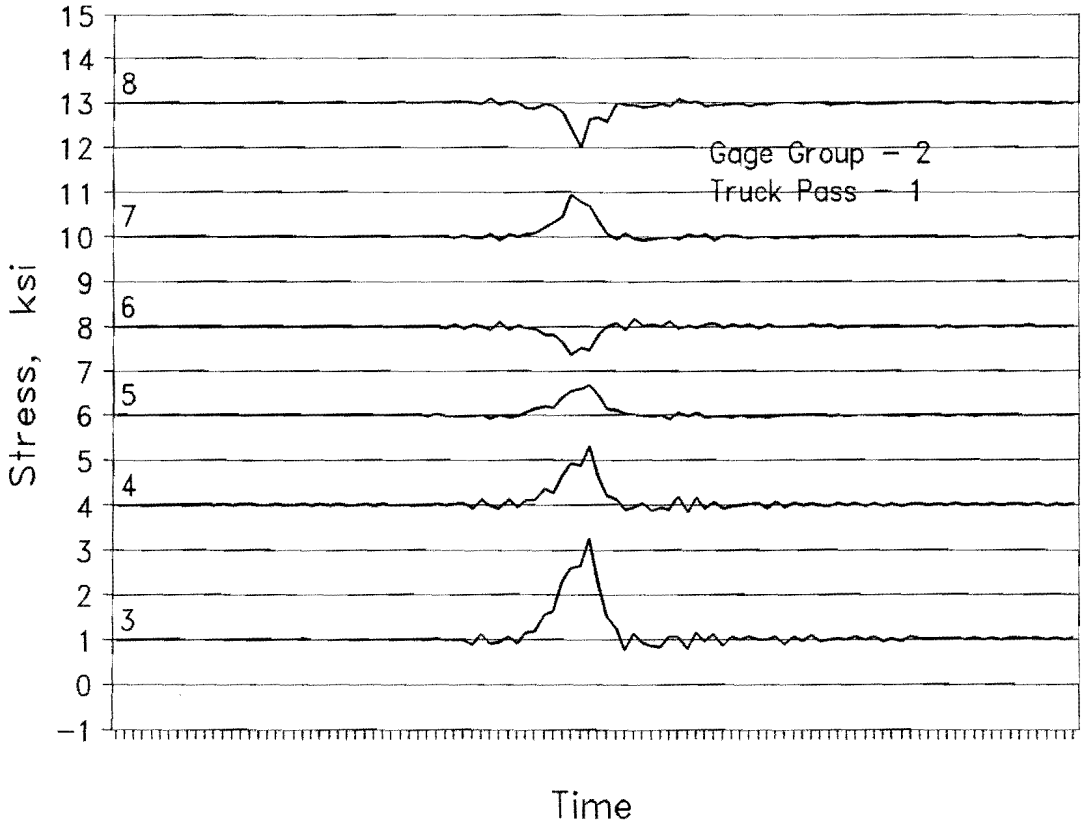

Figure B-13: Diaphragm C-40 member stress histories for Gage Group 2, Truck Pass 1 (test truck centered in driving lane).

Gage Number	Location	Max. Stress Range, ksi	Tension or Compression
1	Bottom flange, Girder No. 4	1.7	Tens.
2	Bottom flange, Girder No. 3	1.5	Tens.
3	Lower strut, Type C Diaphragm	2.5	Tens.
4	Diagonal, Type C Diaphragm	1.5	Tens.
5	Diagonal, Type C Diaphragm	0.8	Tens.
6	Upper strut, at bottom	0.8	Comp.
7	Upper strut, at top	1.0	Tens.
8	Top edge of connection plate	1.1	Comp.

Table B-6: Maximum measured stress ranges and direction for Gage Group 2, Truck Pass 1 (test truck centered in driving lane).

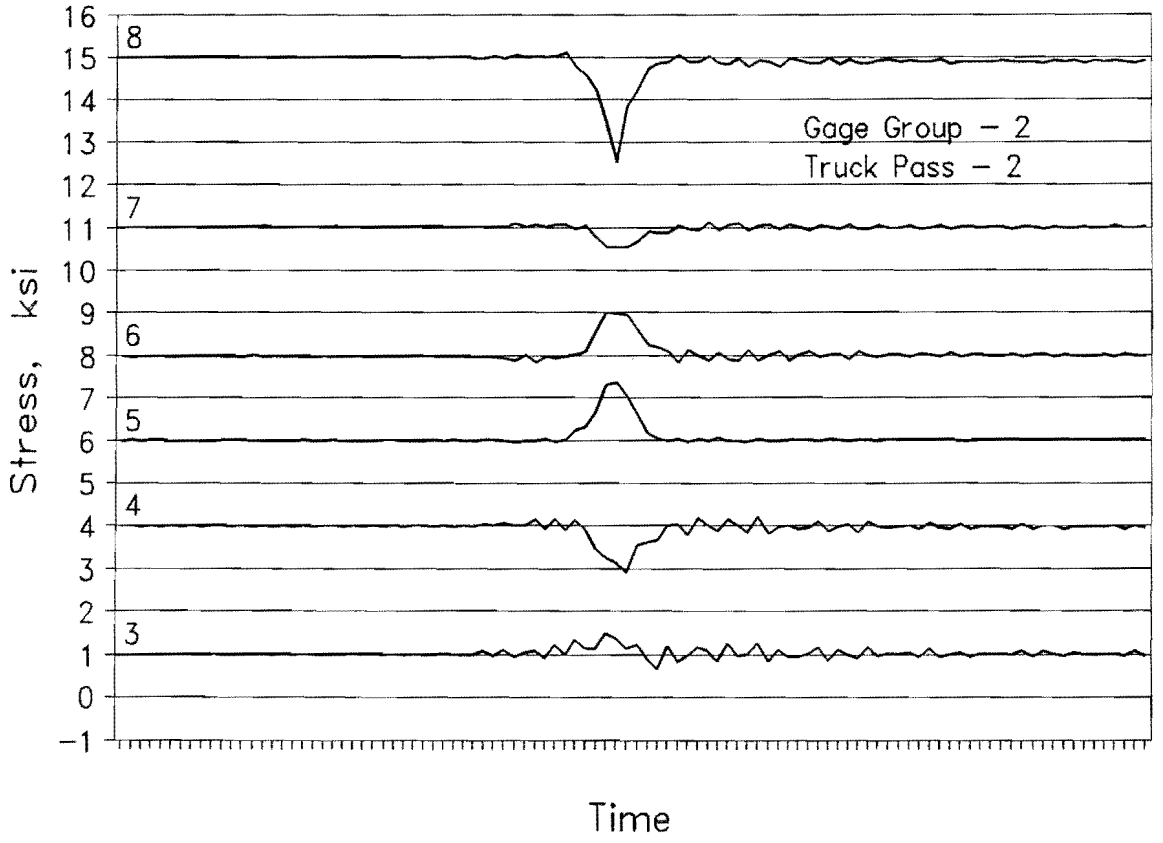

Figure B-14: Diaphragm C-40 member stress histories for Gage Group 2, Truck Pass 2 (test truck centered in right shoulder).

Gage Number	Location	Max. Stress Range, ksi	Tension or Compression
1	Bottom flange, Girder No. 4	2.3	Tens.
2	Bottom flange, Girder No. 3	0.9	Tens.
3	Lower strut, Type C Diaphragm	0.8	Tens.
4	Diagonal, Type C Diaphragm	1.3	Comp.
5	Diagonal, Type C Diaphragm	1.4	Tens.
6	Upper strut, at bottom	1.2	Tens.
7	Upper strut, at top	0.6	Comp.
8	Top edge of connection plate	2.6	Comp.

Table B-7: Maximum measured stress ranges and direction for Gage Group 2, Truck Pass 2 (test truck centered in right shoulder).

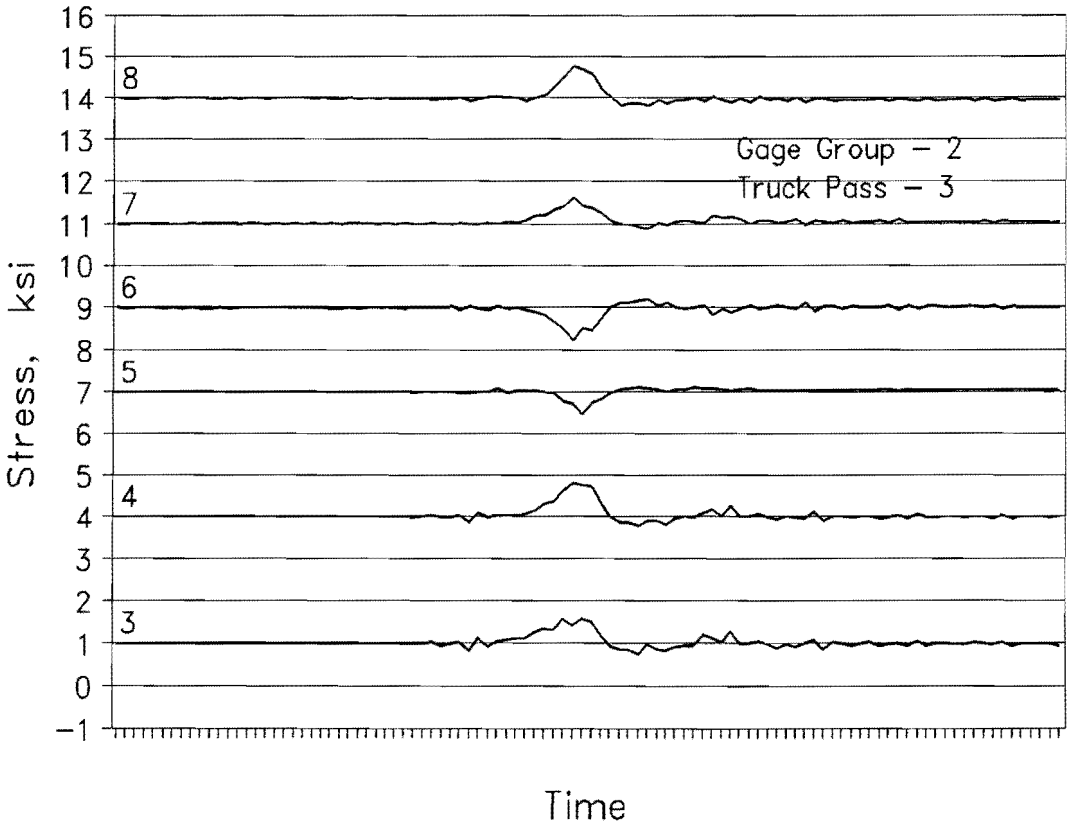

Figure B-15: Diaphragm C-40 member stress histories for Gage Group 2, Truck Pass 3 (test truck centered in passing lane).

Gage Number	Location	Max. Stress Range, ksi	Tension or Compression
1	Bottom flange, Girder No. 4	0.9	Tens.
2	Bottom flange, Girder No. 3	0.9	Tens.
3	Lower strut, Type C Diaphragm	0.8	Tens.
4	Diagonal, Type C Diaphragm	1.1	Tens.
5	Diagonal, Type C Diaphragm	0.7	Comp.
6	Upper strut, at bottom	1.0	Comp.
7	Upper strut, at top	0.7	Tens.
8	Top edge of connection plate	1.0	Tens.

Table B-8: Maximum measured stress ranges and direction for Gage Group 2, Truck Pass 3 (test truck centered in passing lane).

Gage Group No. 3

Type C Diaphragm, C-43
Negative Moment Region

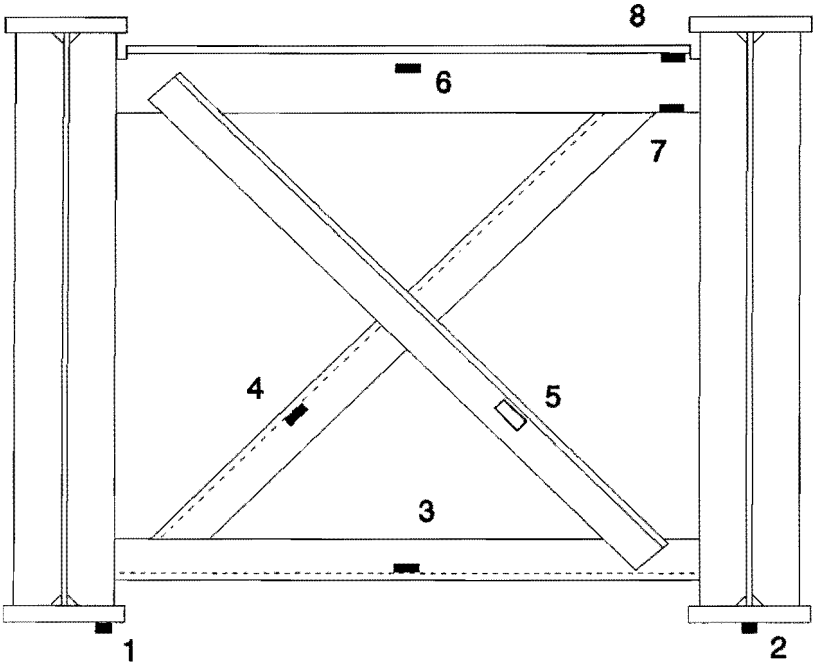

Gage No.	Position
1	bottom flange, 2" from flange edge
2	bottom flange, centerline of web plate
3	1-1/4" above neutral axis
4	3/4" above neutral axis
5	3/4" above neutral axis
6	neutral axis
7	bottom of stem
8	top of WT, below fillet radius

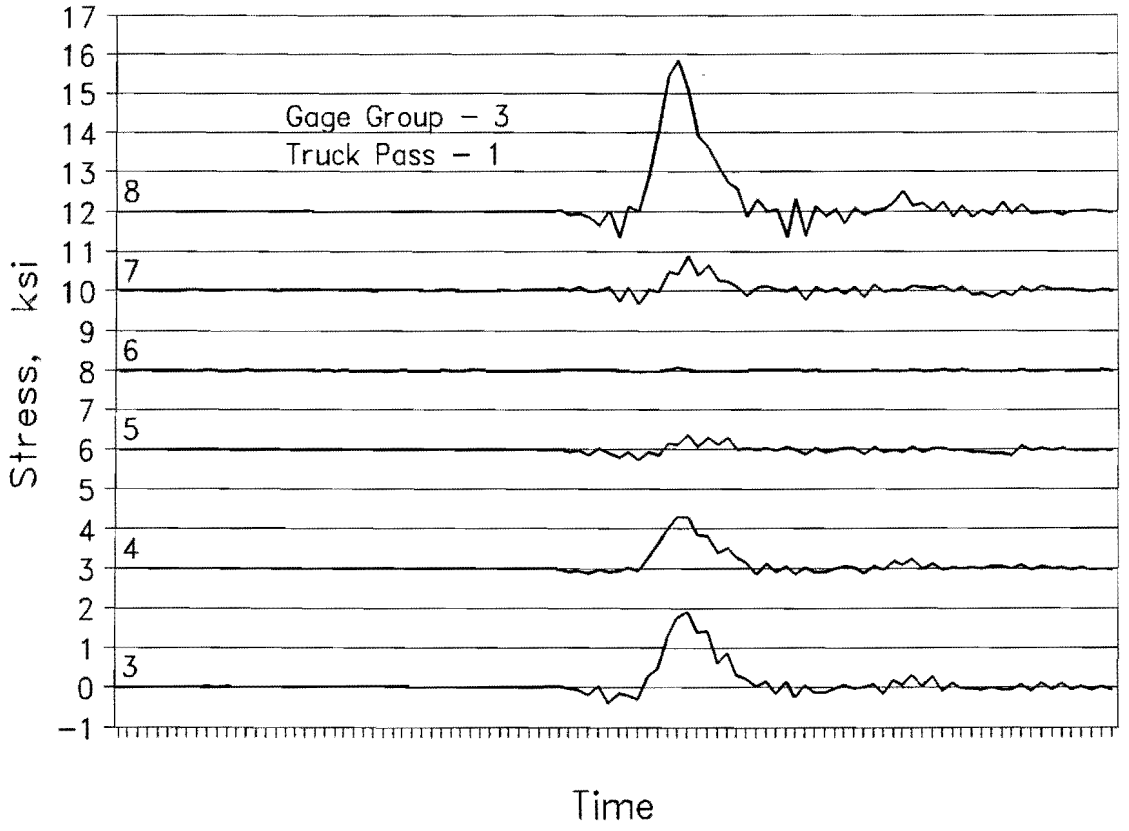

Figure B-16: Diaphragm C-43 member stress histories for Gage Group 3, Truck Pass 1 (test truck centered in driving lane).

Gage Number	Location	Max. Stress Range, ksi	Tension or Compression
1	Bottom flange, Girder No. 3	1.3	Tens.
2	Bottom flange, Girder No. 4	1.8	Tens.
3	Lower strut, Type C Diaphragm	2.3	Tens.
4	Diagonal, Type C Diaphragm	1.5	Tens.
5	Diagonal, Type C Diaphragm	0.7	Both
6	Upper strut, Type C Diaphragm	0.1	-----
7	Upper strut at bottom	1.2	Tens.
8	Upper strut near top cope	4.5	Tens.

Table B-9: Maximum measured stress ranges and direction for Gage Group 3, Truck Pass 1 (test truck centered in driving lane).

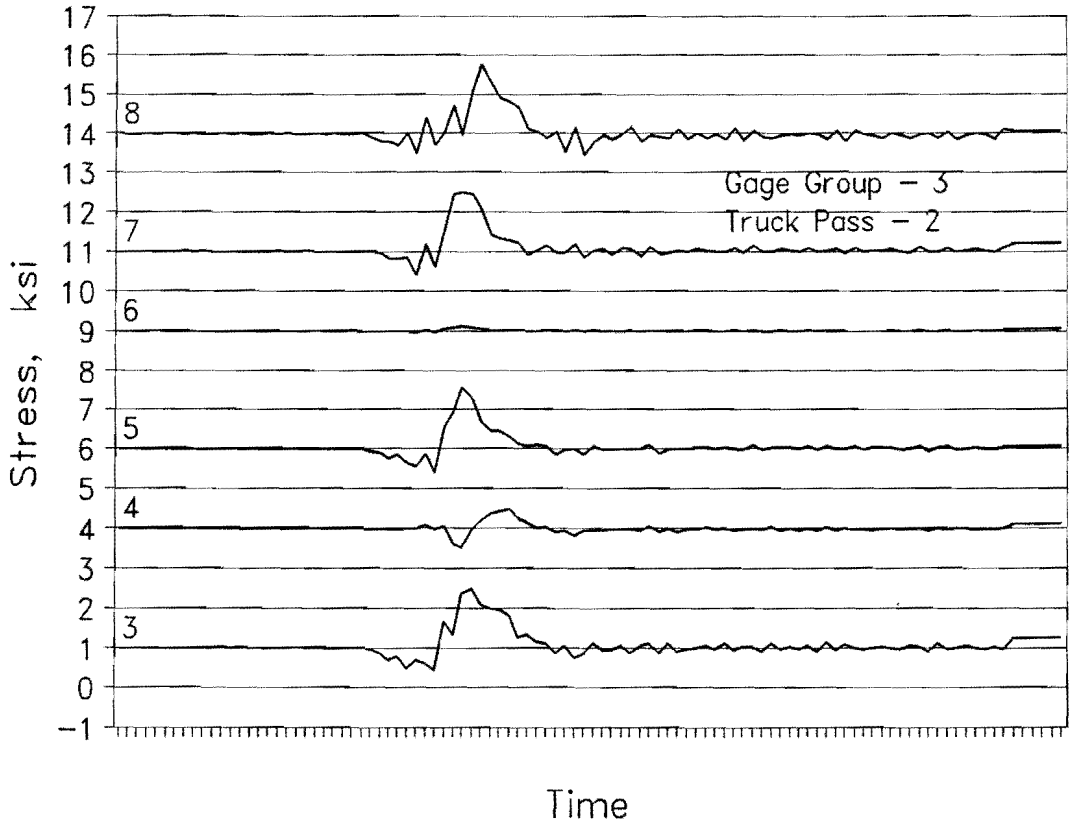

Figure B-17: Diaphragm C-43 member stress histories for Gage Group 3, Truck Pass 2 (test truck centered in right shoulder).

Gage Number	Location	Max. Stress Range, ksi	Tension or Compression
1	Bottom flange, Girder No. 3	0.8	Tens.
2	Bottom flange, Girder No. 4	1.3	Tens.
3	Lower strut, Type C Diaphragm	2.1	Tens.
4	Diagonal, Type C Diaphragm	1.0	Both
5	Diagonal, Type C Diaphragm	2.1	Tens.
6	Upper strut, Type C Diaphragm	0.1	-----
7	Upper strut at bottom	2.1	Tens.
8	Upper strut near top cope	2.4	Tens.

Table B-10: Maximum measured stress ranges and direction for Gage Group 3, Truck Pass 2 (test truck centered in right shoulder).

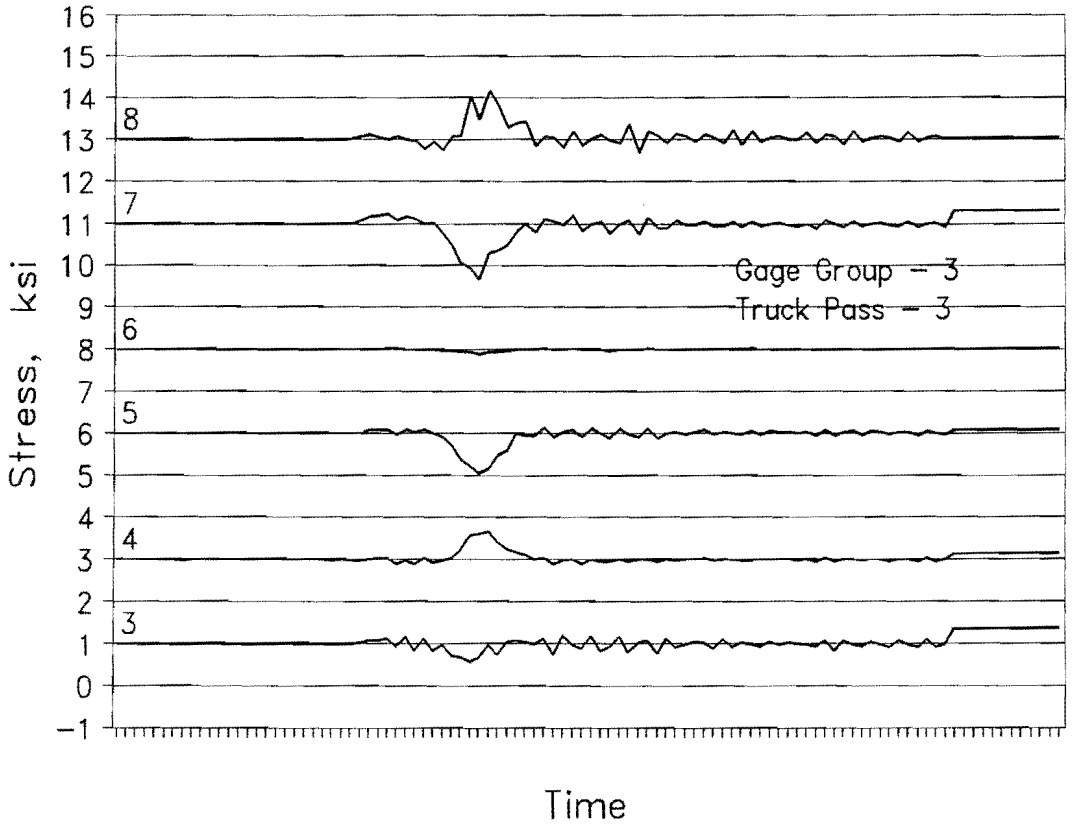

Figure B-18: Diaphragm C-43 member stress histories for Gage Group 3, Truck Pass 3 (test truck centered in passing lane).

Gage Number	Location	Max. Stress Range, ksi	Tension or Compression
1	Bottom flange, Girder No. 3	1.2	Tens.
2	Bottom flange, Girder No. 4	1.1	Tens.
3	Lower strut, Type C Diaphragm	0.8	Comp.
4	Diagonal, Type C Diaphragm	0.8	Tens.
5	Diagonal, Type C Diaphragm	1.1	Comp.
6	Upper strut, Type C Diaphragm	0.2	-----
7	Upper strut at bottom	1.6	Comp.
8	Upper strut near top cope	1.5	Tens.

Table B-11: Maximum measured stress ranges and direction for Gage Group 3, Truck Pass 3 (test truck centered in passing lane).

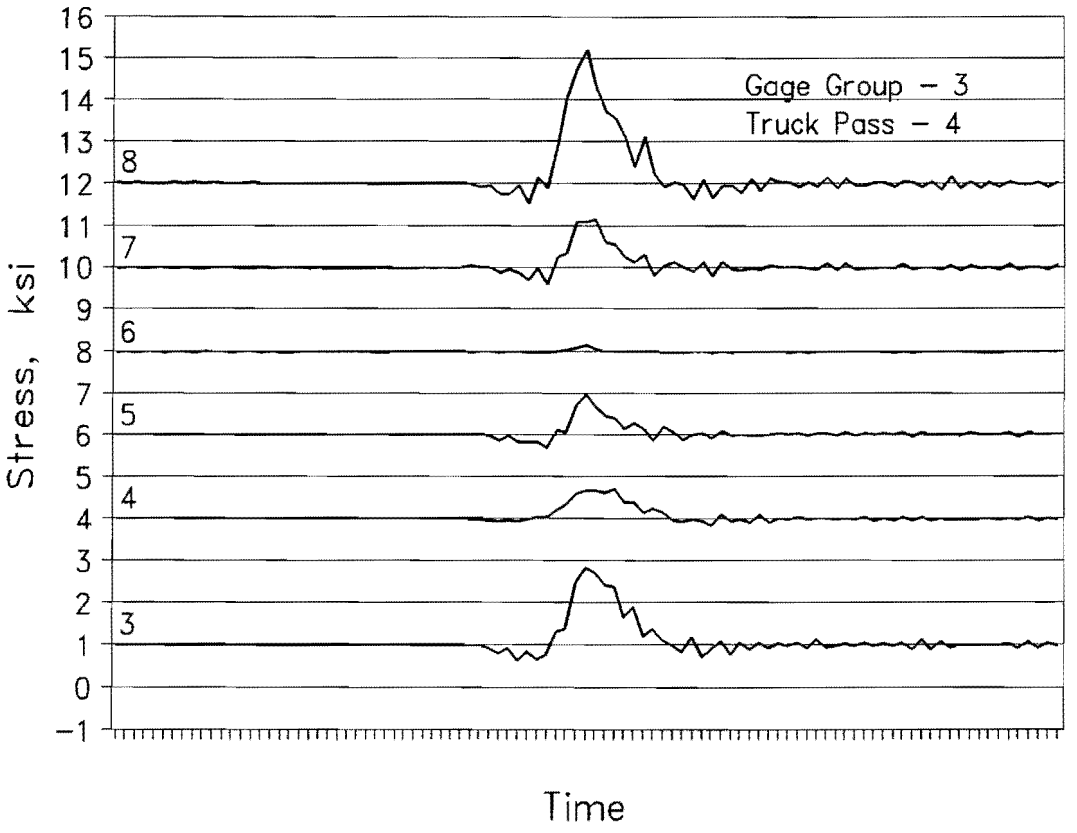

Figure B-19: Diaphragm C-43 member stress histories for Gage Group 3, Truck Pass 4 (test truck with right wheel on right shoulder stripe).

Gage Number	Location	Max. Stress Range, ksi	Tension or Compression
1	Bottom flange, Girder No. 3	1.3	Tens.
2	Bottom flange, Girder No. 4	1.8	Tens.
3	Lower strut, Type C Diaphragm	2.2	Tens.
4	Diagonal, Type C Diaphragm	0.9	Tens.
5	Diagonal, Type C Diaphragm	1.3	Tens.
6	Upper strut, Type C Diaphragm	0.2	-----
7	Upper strut at bottom	1.6	Tens.
8	Upper strut near top cope	3.7	Tens.

Table B-12: Maximum measured stress ranges and direction for Gage Group 3, Truck Pass 4 (test truck with right wheel on right shoulder stripe).

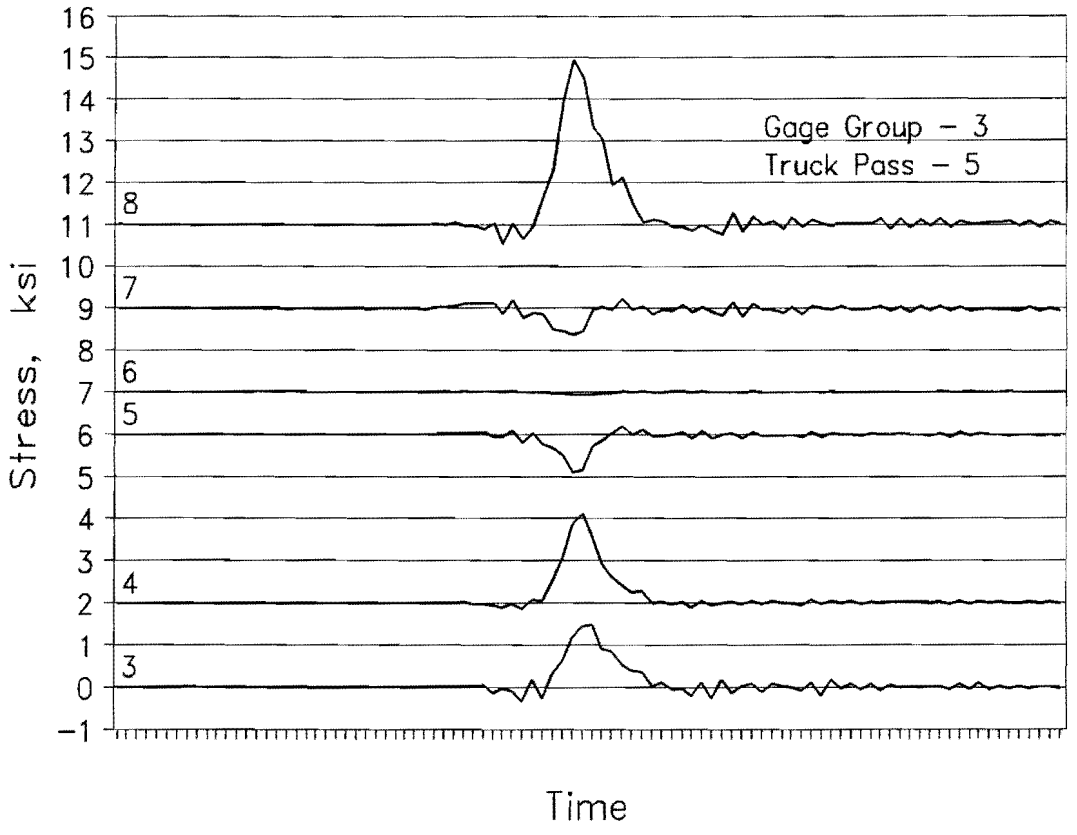

Figure B-20: Diaphragm C-43 member stress histories for Gage Group 3, Truck Pass 5 (test truck with left wheel on center stripe).

Gage Number	Location	Max. Stress Range, ksi	Tension or Compression
1	Bottom flange, Girder No. 3	1.6	Tens.
2	Bottom flange, Girder No. 4	1.3	Tens.
3	Lower strut, Type C Diaphragm	1.8	Tens.
4	Diagonal, Type C Diaphragm	2.3	Tens.
5	Diagonal, Type C Diaphragm	1.1	Comp.
6	Upper strut, Type C Diaphragm	0.1	-----
7	Upper strut at bottom	0.9	Comp.
8	Upper strut near top cope	4.4	Tens.

Table B-13: Maximum measured stress ranges and direction for Gage Group 3, Truck Pass 5 (test truck with left wheel on center stripe).

Gage Group No. 4

Type C' Diaphragm, D-43
Negative Moment Region

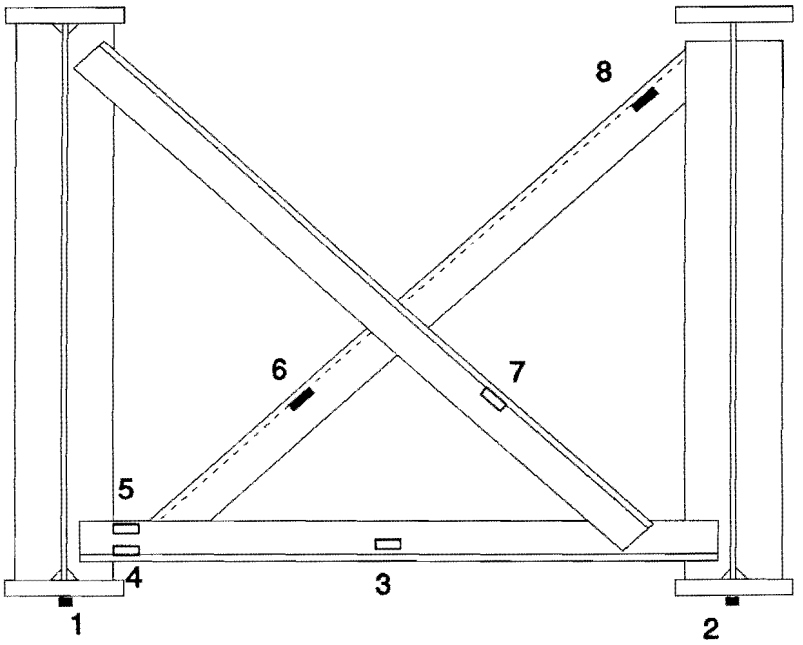

Gage No.	Position
1	bottom flange, centerline of web plate
2	bottom flange, centerline of web plate
3	1-1/4" above neutral axis
4	back of leg, bottom
5	back of leg, top
6	3/4" above neutral axis
7	3/4" above neutral axis
8	3/4" above neutral axis

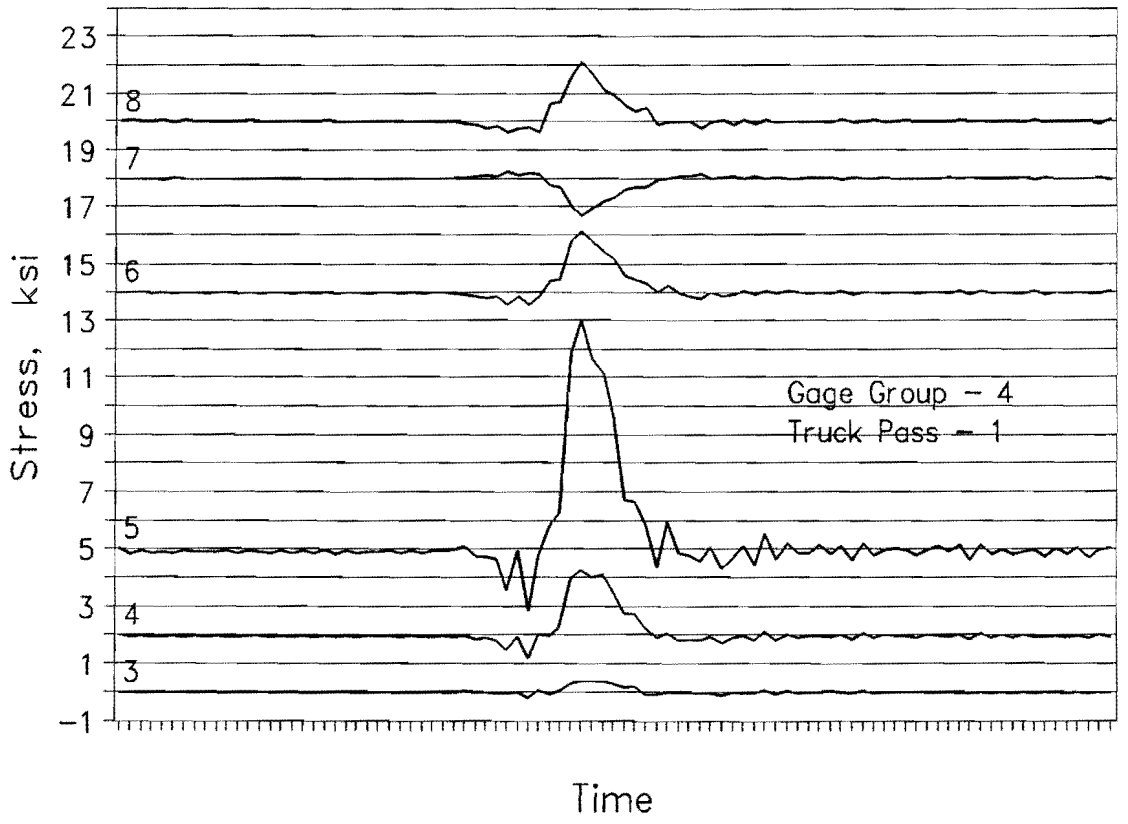

Figure B-21: Diaphragm D-43 member stress histories for Gage Group 4, Truck Pass 1 (test truck centered in driving lane).

Gage Number	Location	Max. Stress Range, ksi	Tension or Compression
1	Bottom flange, Girder No. 4	0.7	Tens.
2	Bottom flange, Girder No. 5	1.6	Tens.
3	Lower strut, Type C' Diaphragm	0.6	Tens.
4	Lower strut, at bottom	3.1	Tens.
5	Lower strut, at top	10.2	Tens.
6	Diagonal, Type C' Diaphragm	2.6	Tens.
7	Diagonal, Type C' Diaphragm	1.6	Comp.
8	Diagonal, Type C' Diaphragm	2.5	Tens.

Table B-14: Maximum measured stress ranges and direction for Gage Group 4, Truck Pass 1 (test truck centered in driving lane).

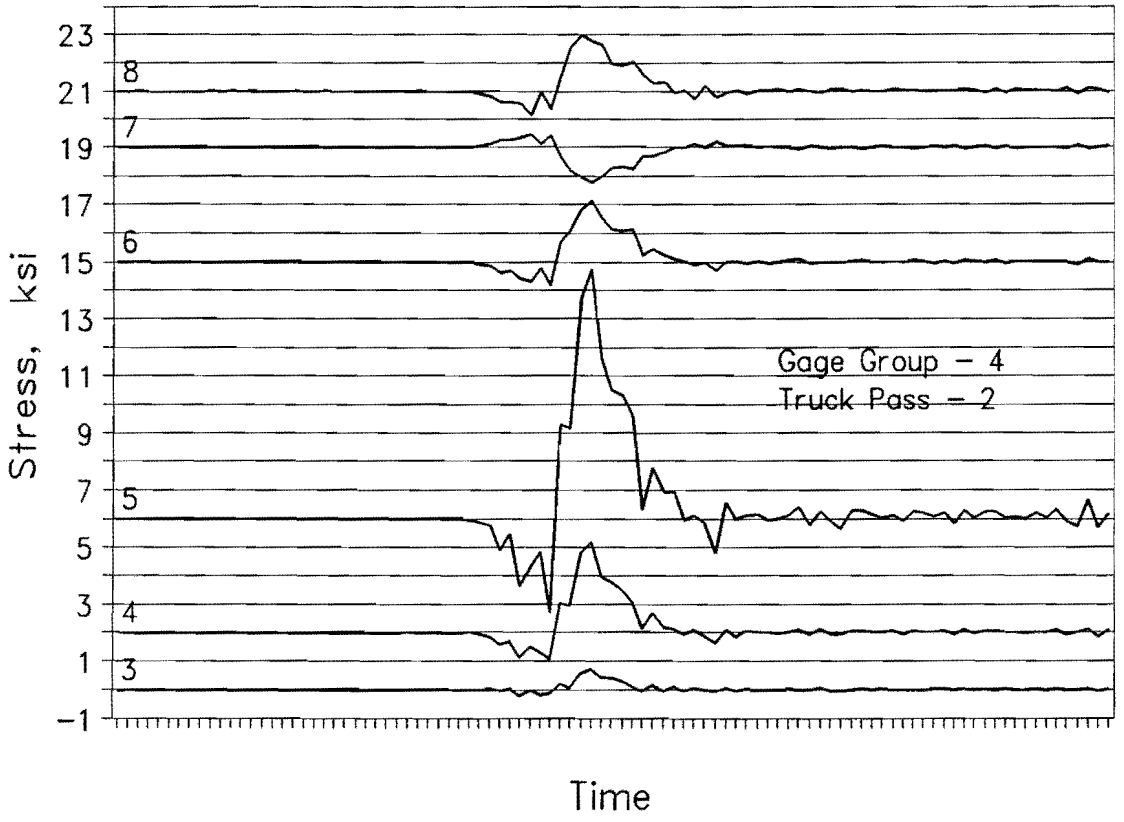

Figure B-22: Diaphragm D-43 member stress histories for Gage Group 4, Truck Pass 2 (test truck centered in right shoulder).

Gage Number	Location	Max. Stress Range, ksi	Tension or Compression
1	Bottom flange, Girder No. 4	1.0	Tens.
2	Bottom flange, Girder No. 5	1.4	Tens.
3	Lower strut, Type C' Diaphragm	0.9	Tens.
4	Lower strut, at bottom	4.1	Tens.
5	Lower strut, at top	12.0	Tens.
6	Diagonal, Type C' Diaphragm	2.9	Tens.
7	Diagonal, Type C' Diaphragm	1.7	Comp.
8	Diagonal, Type C' Diaphragm	2.8	Tens.

Table B-15: Maximum measured stress ranges and direction for Gage Group 4, Truck Pass 2 (test truck centered in right shoulder).

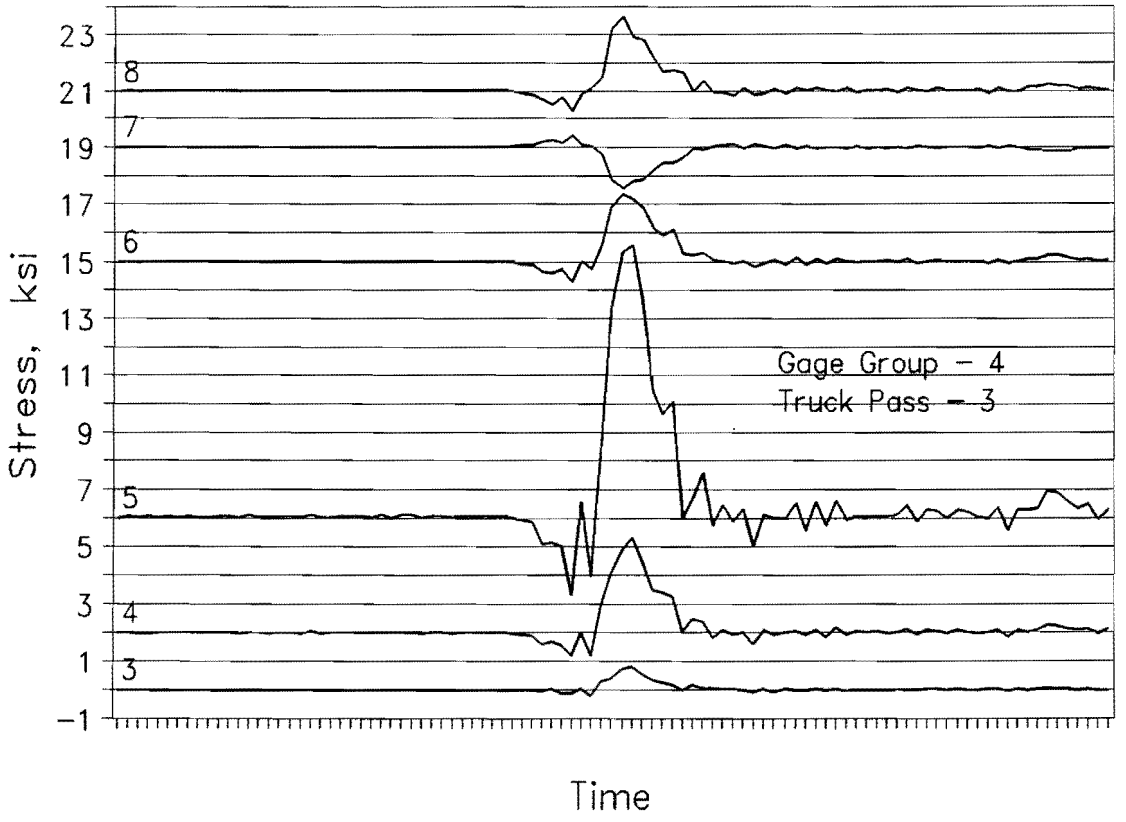

Figure B-23: Diaphragm D-43 member stress histories for Gage Group 4, Truck Pass 3 (test truck straddled right shoulder stripe).

Gage Number	Location	Max. Stress Range, ksi	Tension or Compression
1	Bottom flange, Girder No. 4	0.9	Tens.
2	Bottom flange, Girder No. 5	1.5	Tens.
3	Lower strut, Type C' Diaphragm	1.0	Tens.
4	Lower strut, at bottom	4.1	Tens.
5	Lower strut, at top	12.3	Tens.
6	Diagonal, Type C' Diaphragm	3.1	Tens.
7	Diagonal, Type C' Diaphragm	1.8	Comp.
8	Diagonal, Type C' Diaphragm	3.4	Tens.

Table B-16: Maximum measured stress ranges and direction for Gage Group 4, Truck Pass 3 (test truck straddled right shoulder stripe).

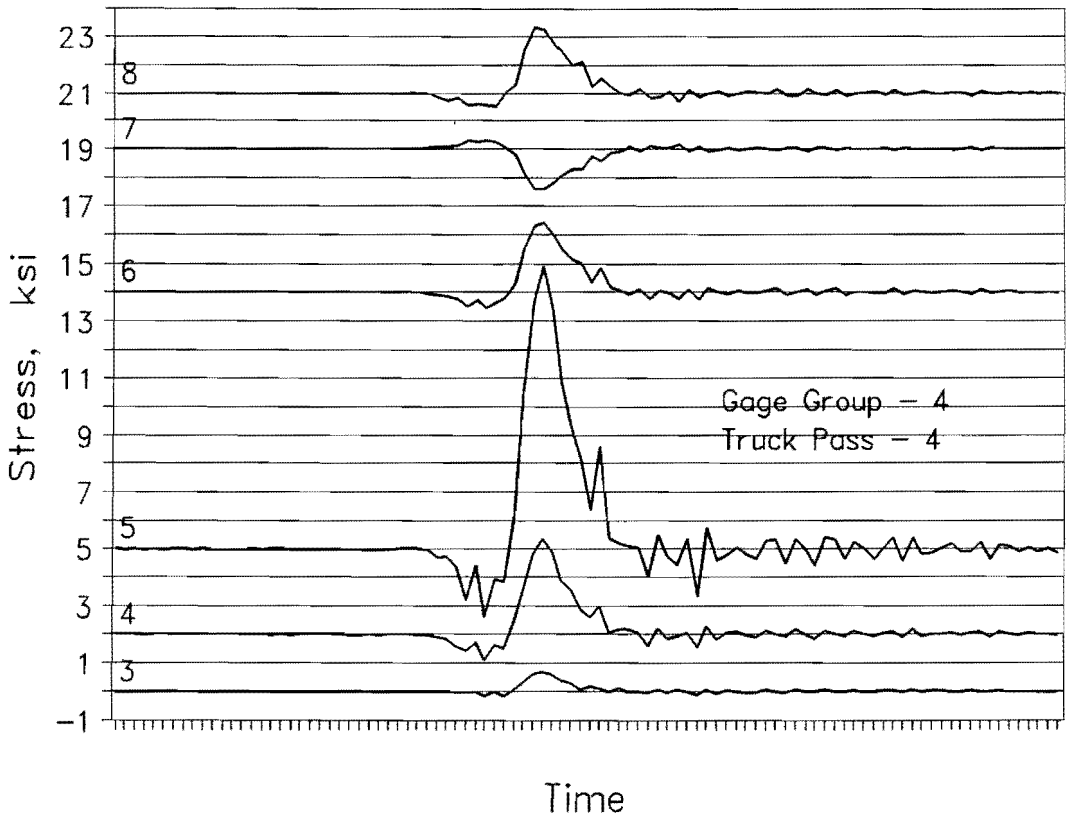

Figure B-24: Diaphragm D-43 member stress histories for Gage Group 4, Truck Pass 4 (test truck straddled right shoulder stripe, same as Pass 3).

Gage Number	Location	Max. Stress Range, ksi	Tension or Compression
1	Bottom flange, Girder No. 4	0.8	Tens.
2	Bottom flange, Girder No. 5	1.4	Tens.
3	Lower strut, Type C' Diaphragm	0.9	Tens.
4	Lower strut, at bottom	4.3	Tens.
5	Lower strut, at top	12.3	Tens.
6	Diagonal, Type C' Diaphragm	3.0	Tens.
7	Diagonal, Type C' Diaphragm	1.7	Comp.
8	Diagonal, Type C' Diaphragm	2.8	Tens.

Table B-17: Maximum measured stress ranges and direction for Gage Group 4, Truck Pass 4 (test truck straddled right shoulder stripe).

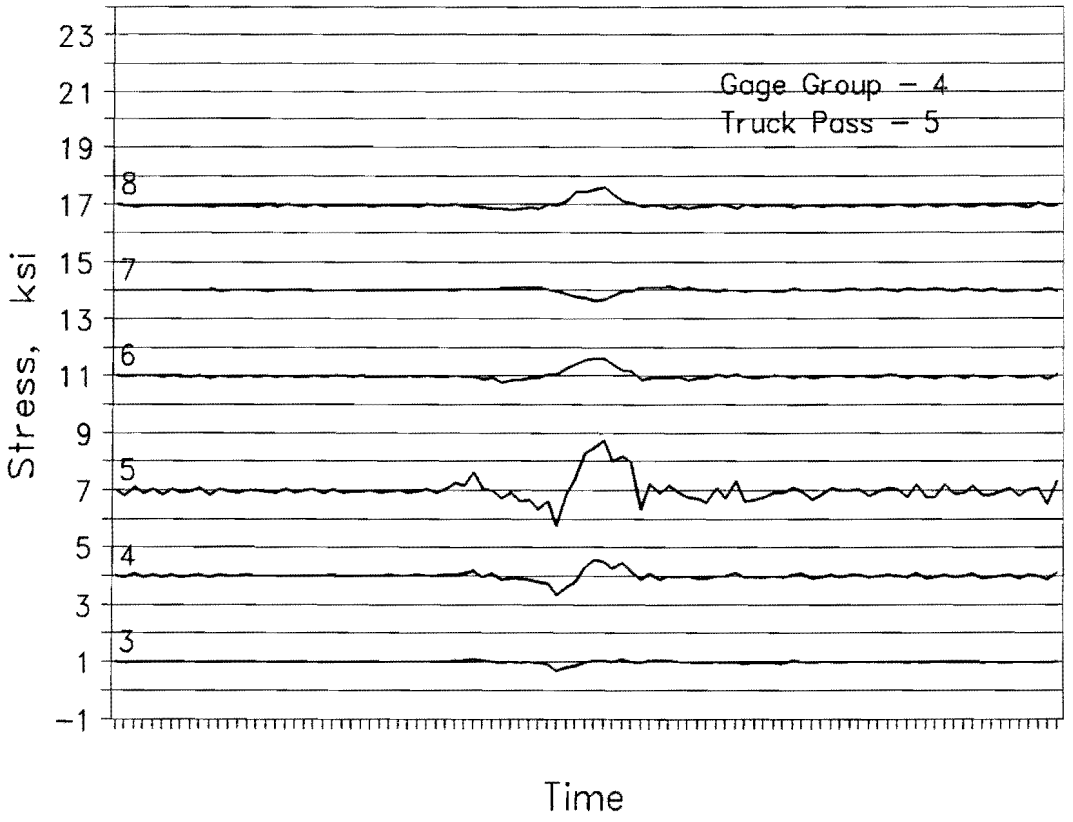

Figure B-25: Diaphragm D-43 member stress histories for Gage Group 4, Truck Pass 5 (test truck straddled center stripe).

Gage Number	Location	Max. Stress Range, ksi	Tension or Compression
1	Bottom flange, Girder No. 4	0.4	Tens.
2	Bottom flange, Girder No. 5	1.1	Tens.
3	Lower strut, Type C' Diaphragm	0.4	Comp.
4	Lower strut, at bottom	1.2	Both
5	Lower strut, at top	3.0	Tens.
6	Diagonal, Type C' Diaphragm	0.8	Tens.
7	Diagonal, Type C' Diaphragm	0.5	Comp.
8	Diagonal, Type C' Diaphragm	0.8	Tens.

Table B-18: Maximum measured stress ranges and direction for Gage Group 4, Truck Pass 5 (test truck straddled center stripe).

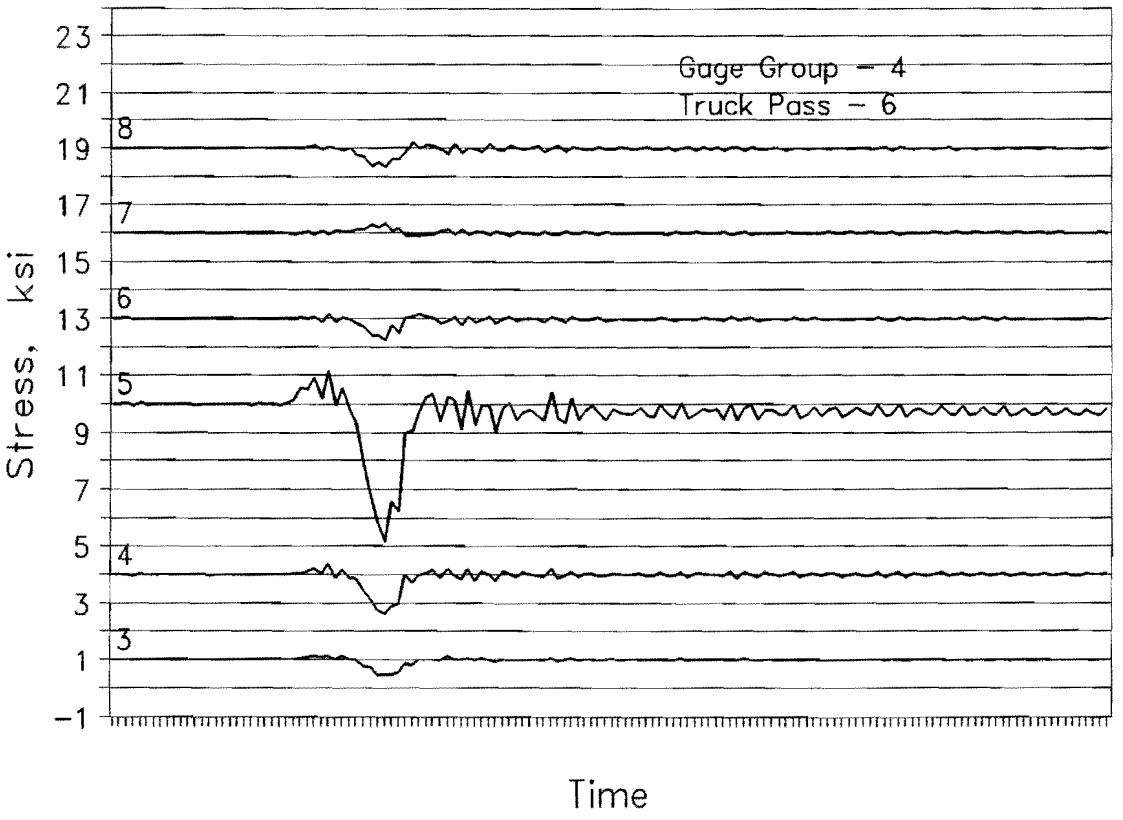

Figure B-26: Diaphragm D-43 member stress histories for Gage Group 4, Truck Pass 6 (test truck centered in passing lane).

Gage Number	Location	Max. Stress Range, ksi	Tension or Compression
1	Bottom flange, Girder No. 4	0.5	Tens.
2	Bottom flange, Girder No. 5	1.1	Tens.
3	Lower strut, Type C' Diaphragm	0.7	Comp.
4	Lower strut, at bottom	1.8	Comp.
5	Lower strut, at top	6.1	Comp.
6	Diagonal, Type C' Diaphragm	0.9	Comp.
7	Diagonal, Type C' Diaphragm	0.4	Tens.
8	Diagonal, Type C' Diaphragm	0.9	Comp.

Table B-19: Maximum measured stress ranges and direction for Gage Group 4, Truck Pass 6 (test truck centered in passing lane).

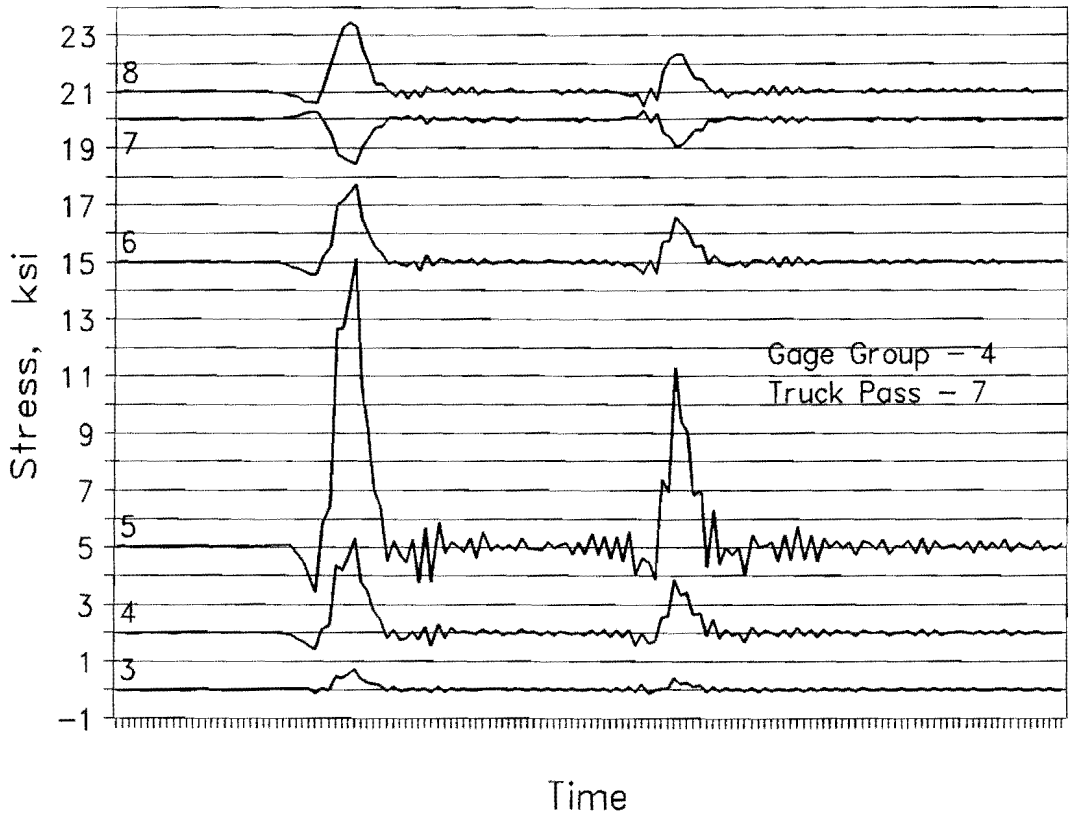

Figure B-27: Diaphragm D-43 member stress histories for Gage Group 4, Truck Pass 7 (18 wheeler centered in driving lane).

Gage Number	Location	Max. Stress Range, ksi	Tension or Compression
1	Bottom flange, Girder No. 4	0.7	Tens.
2	Bottom flange, Girder No. 5	1.5	Tens.
3	Lower strut, Type C' Diaphragm	0.9	Tens.
4	Lower strut, at bottom	3.9	Tens.
5	Lower strut, at top	11.7	Tens.
6	Diagonal, Type C' Diaphragm	3.2	Tens.
7	Diagonal, Type C' Diaphragm	1.9	Comp.
8	Diagonal, Type C' Diaphragm	3.0	Tens.

Table B-20: Maximum measured stress ranges and direction for Gage Group 4, Truck Pass 7 (18 wheeler centered in driving line).

Gage Group No. 5

Diaphragm Line 40
Positive Moment Region

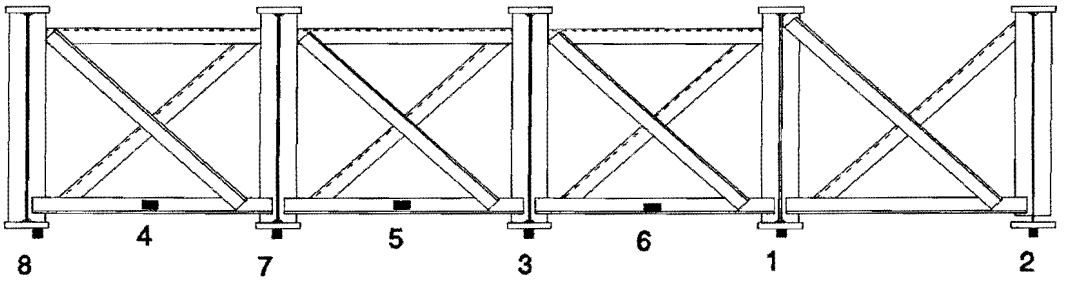

Gage No.	Position
1	bottom flange, centerline of web plate
2	bottom flange, centerline of web plate
3	bottom flange, centerline of web plate
4	1-1/4" above neutral axis
5	1-1/4" above neutral axis
6	1-1/4" above neutral axis
7	bottom flange, centerline of web plate
8	bottom flange, 2" from flange edge

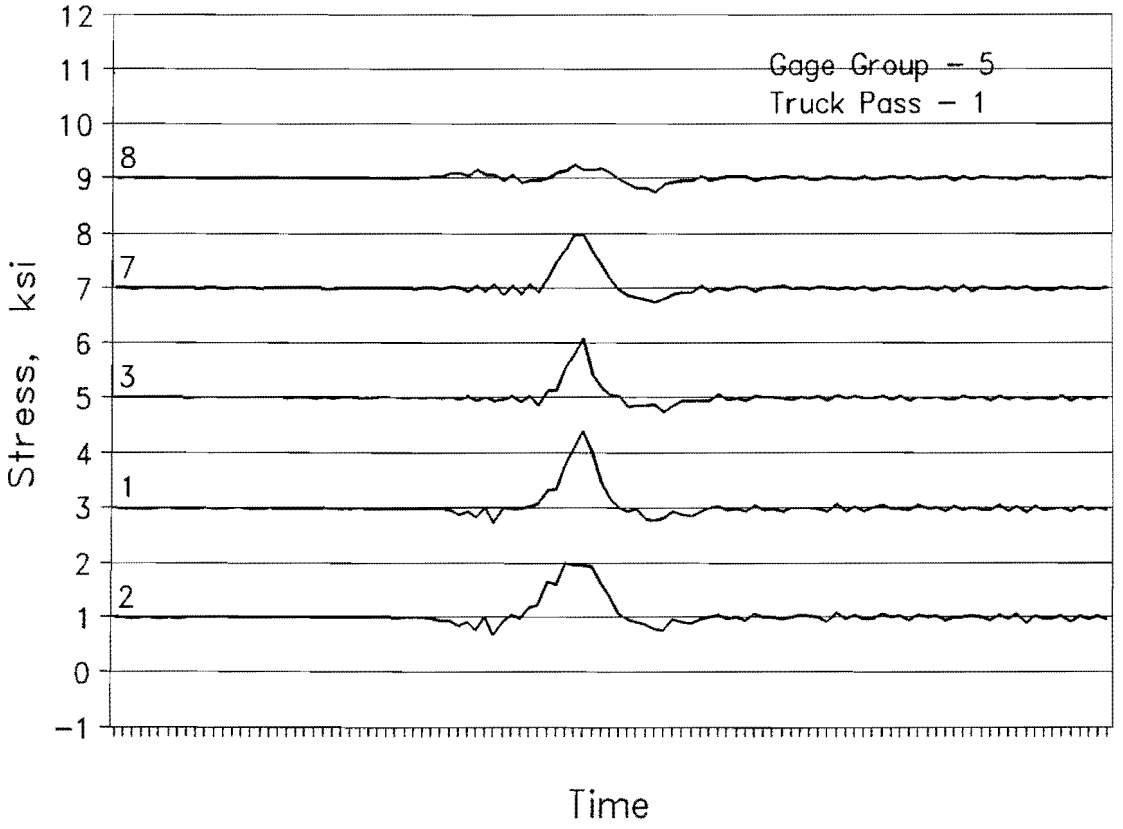

Figure B-28: Diaphragm Line 40 bottom flange stress histories for Gage Group 5, Truck Pass 1 (test truck centered in driving lane).

Gage Number	Location	Max. Stress Range, ksi	Tension or Compression
1	Bottom flange, Girder No. 4	1.7	Tens.
2	Bottom flange, Girder No. 5	1.3	Tens.
3	Bottom flange, Girder No. 3	1.4	Tens.
4	Diaphragm lower strut, Bay A	0.7	Tens.
5	Diaphragm lower strut, Bay B	1.9	Tens.
6	Diaphragm lower strut, Bay C	2.5	Tens.
7	Bottom flange, Girder No. 2	1.2	Tens.
8	Bottom flange, Girder No. 1	0.5	Both

Table B-21: Maximum measured stress ranges and direction for Gage Group 5, Truck Pass 1 (test truck centered in driving lane).

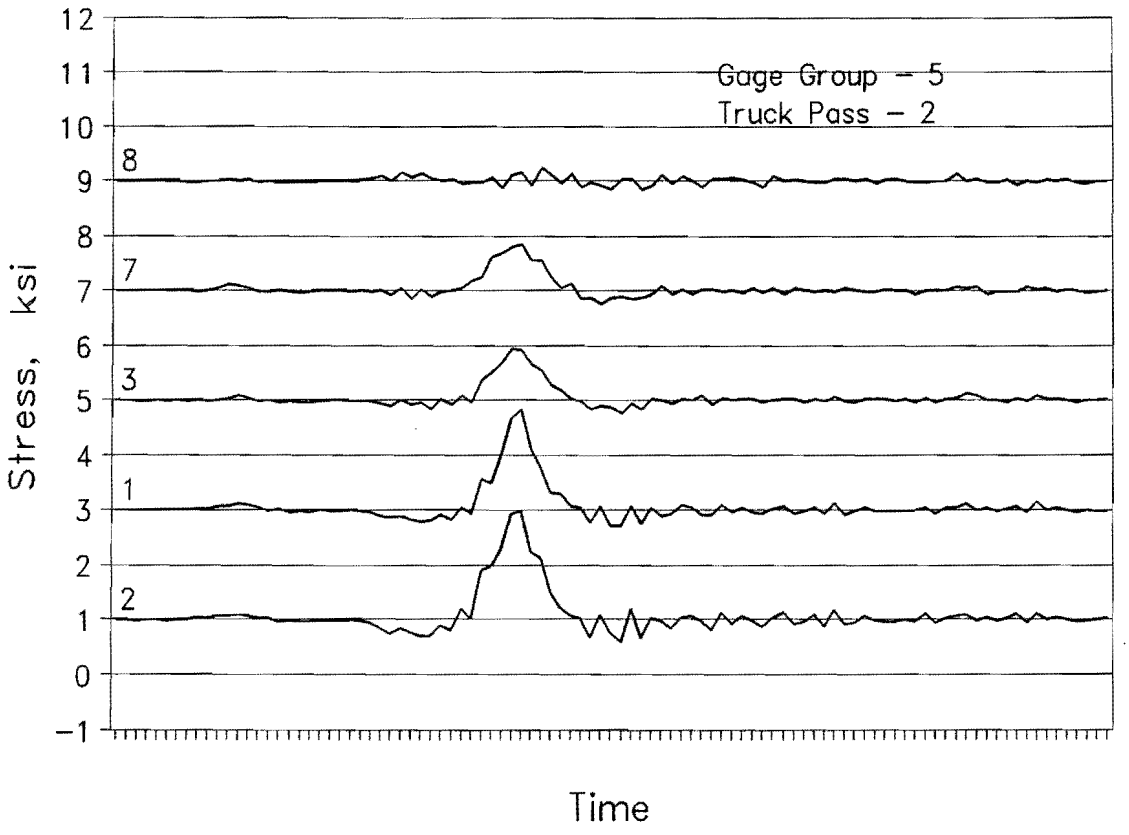

Figure B-29: Diaphragm Line 40 bottom flange stress histories for Gage Group 5, Truck Pass 2 (test truck centered in right shoulder).

Gage Number	Location	Max. Stress Range, ksi	Tension or Compression
1	Bottom flange, Girder No. 4	2.1	Tens.
2	Bottom flange, Girder No. 5	2.4	Tens.
3	Bottom flange, Girder No. 3	1.2	Tens.
4	Diaphragm lower strut, Bay A	0.7	Comp.
5	Diaphragm lower strut, Bay B	0.7	Comp.
6	Diaphragm lower strut, Bay C	0.8	Both
7	Bottom flange, Girder No. 2	1.1	Tens.
8	Bottom flange, Girder No. 1	0.4	Both

Table B-22: Maximum measured stress ranges and direction for Gage Group 5, Truck Pass 2 (test truck centered in right shoulder).

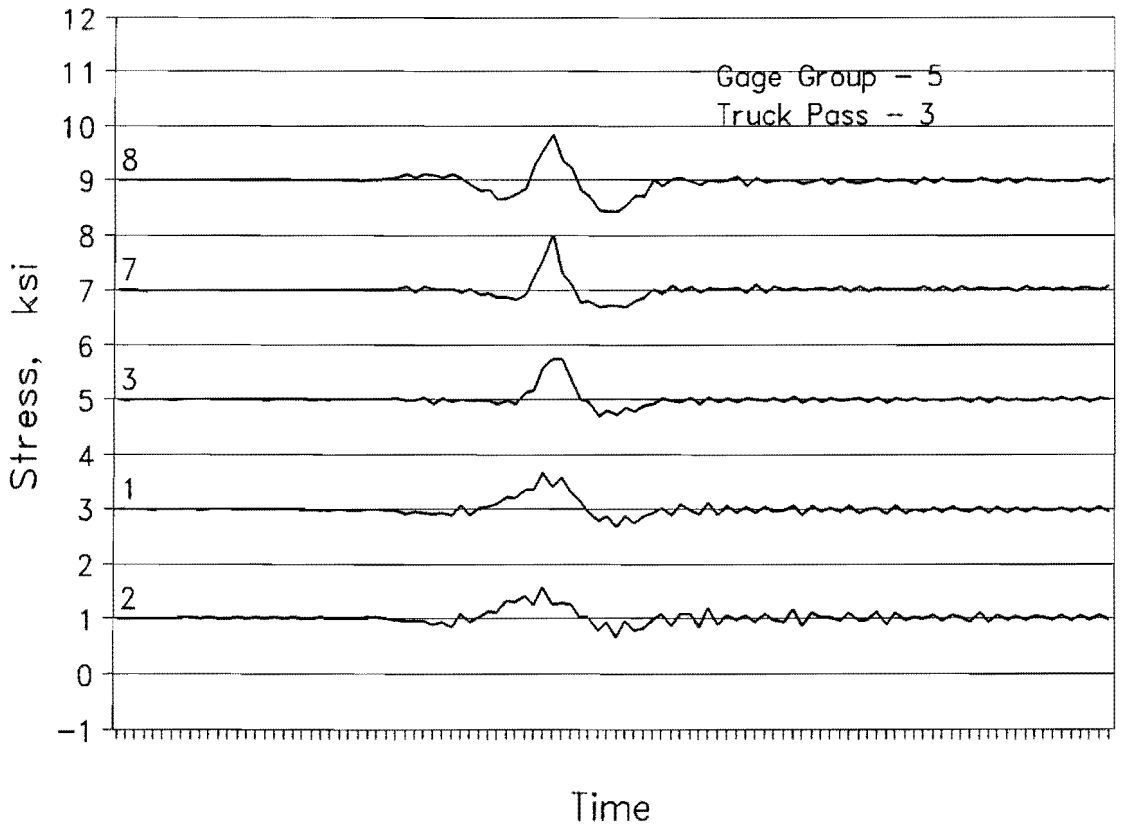

Figure B-30: Diaphragm Line 40 bottom flange stress histories for Gage Group 5 Truck Pass 3 (test truck centered in passing lane).

Gage Number	Location	Max. Stress Range, ksi	Tension or Compression
1	Bottom flange, Girder No. 4	1.0	Tens.
2	Bottom flange, Girder No. 5	0.9	Tens.
3	Bottom flange, Girder No. 3	1.1	Tens.
4	Diaphragm lower strut, Bay A	1.7	Tens.
5	Diaphragm lower strut, Bay B	1.6	Tens.
6	Diaphragm lower strut, Bay C	1.2	Tens.
7	Bottom flange, Girder No. 2	1.3	Comp.
8	Bottom flange, Girder No. 1	1.4	Both

Table B-23: Maximum measured stress ranges and direction for Gage Group 5, Truck Pass 3 (test truck centered in passing lane).

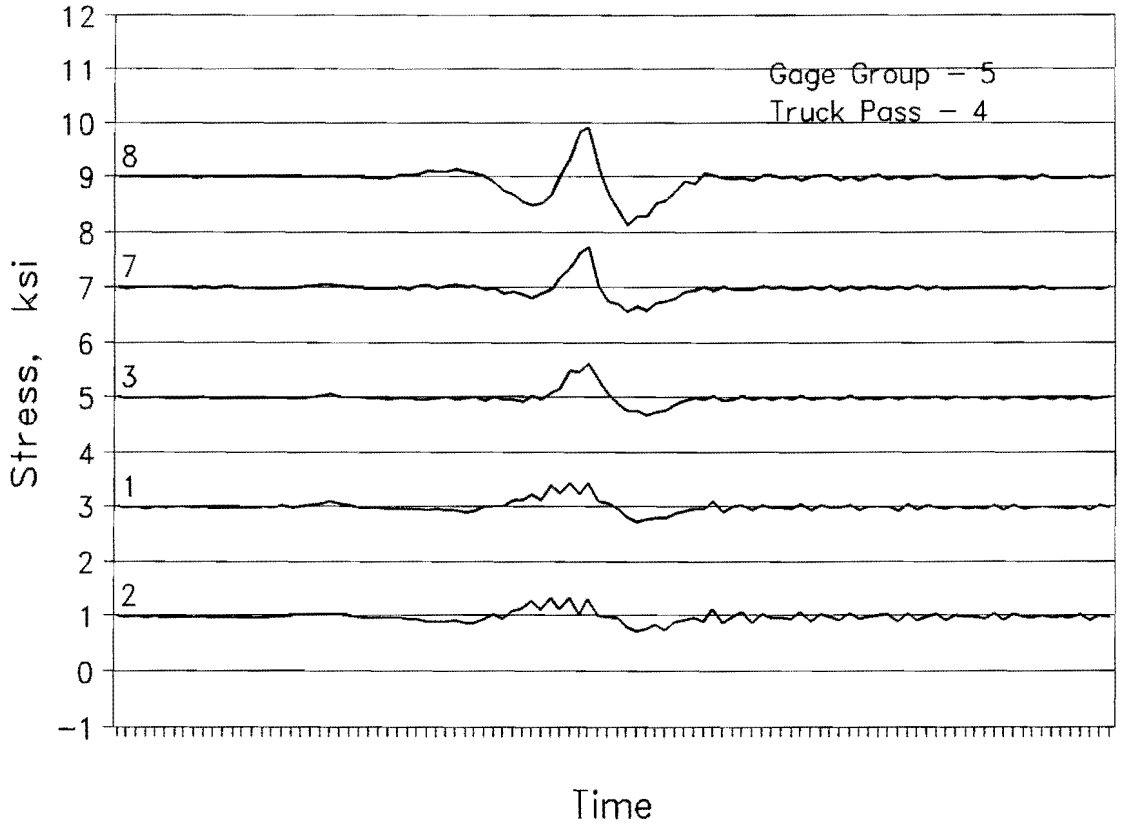

Figure B-31: Diaphragm Line 40 bottom flange stress histories for Gage Group 5, Truck Pass 4 (test truck in left shoulder).

Gage Number	Location	Max. Stress Range, ksi	Tension or Compression
1	Bottom flange, Girder No. 4	0.7	Tens.
2	Bottom flange, Girder No. 5	0.6	Both
3	Bottom flange, Girder No. 3	0.9	Tens.
4	Diaphragm lower strut, Bay A	1.0	Tens.
5	Diaphragm lower strut, Bay B	0.7	Tens.
6	Diaphragm lower strut, Bay C	0.7	Tens.
7	Bottom flange, Girder No. 2	1.2	Tens.
8	Bottom flange, Girder No. 1	1.8	Both

Table B-24: Maximum measured stress ranges and direction for Gage Group 5, Truck Pass 4 (test truck in left shoulder).

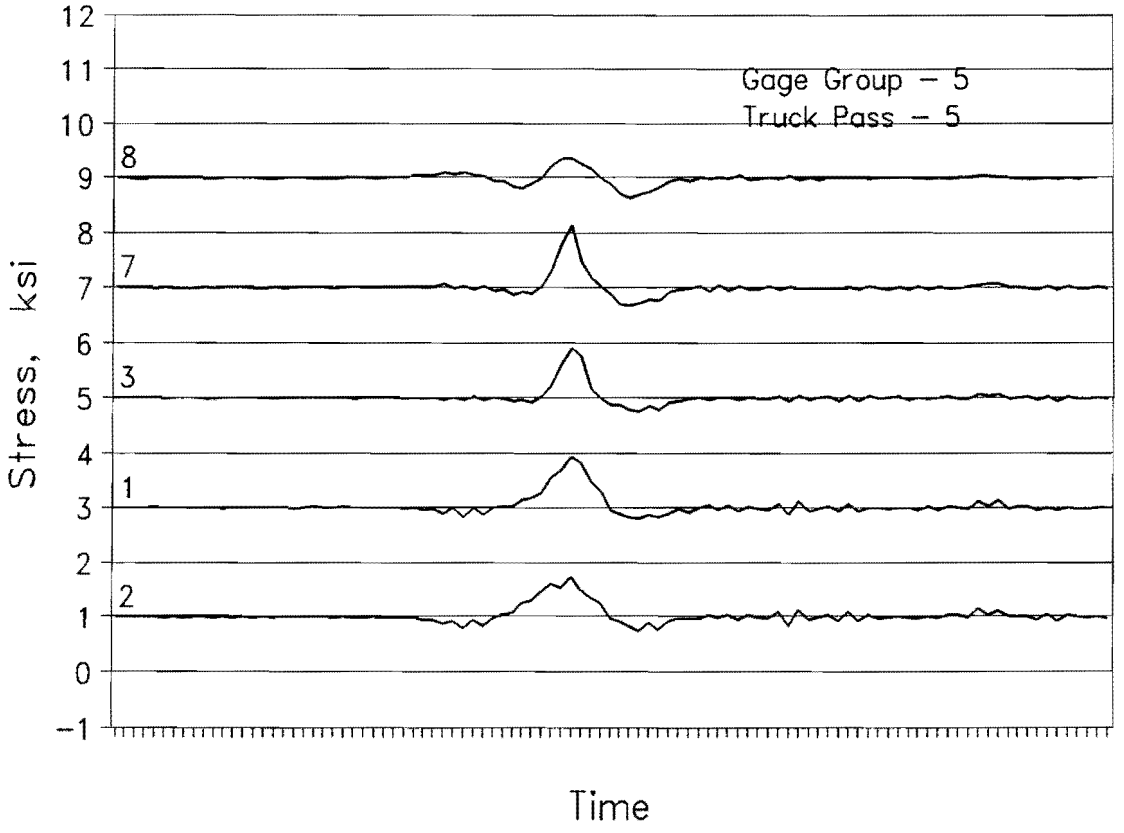

Figure B-32: Diaphragm Line 40 bottom flange stress histories for Gage Group 5, Truck Pass 5 (test truck straddled center stripe).

Gage Number	Location	Max. Stress Range, ksi	Tension or Compression
1	Bottom flange, Girder No. 4	1.1	Tens.
2	Bottom flange, Girder No. 5	1.0	Tens.
3	Bottom flange, Girder No. 3	1.2	Tens.
4	Diaphragm lower strut, Bay A	1.5	Tens.
5	Diaphragm lower strut, Bay B	2.0	Tens.
6	Diaphragm lower strut, Bay C	1.8	Tens.
7	Bottom flange, Girder No. 2	1.5	Comp.
8	Bottom flange, Girder No. 1	0.7	Both

Table B-25: Maximum measured stress ranges and direction for Gage Group 5, Truck Pass 5 (test truck straddled center stripe).

Gage Group No. 6

Type C Diaphragm, C-39
Positive Moment Region

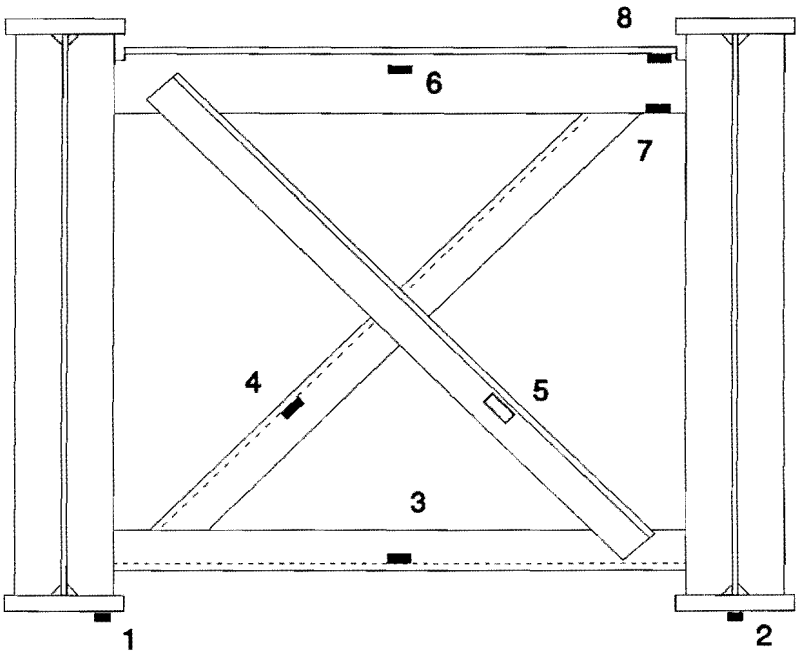

Girder 3

Girder 4

Gage No.	Position
1	bottom flange, 2" from flange edge
2	bottom flange, centerline of web plate
3	1-1/4" above neutral axis
4	3/4" above neutral axis
5	3/4" above neutral axis
6	neutral axis
7	bottom of stem
8	top of WT, below fillet radius

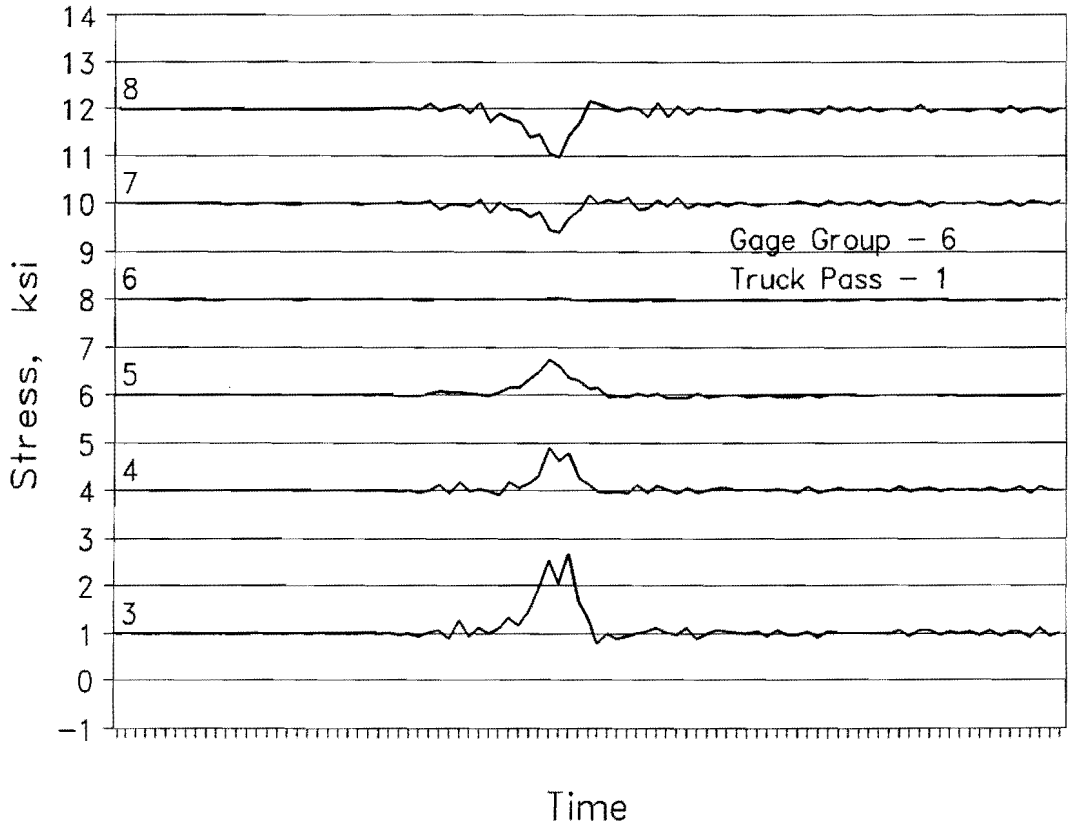

Figure B-33: Diaphragm C-39 member stress histories for Gage Group 6, Truck Pass 1 (test truck centered in driving lane).

Gage Number	Location	Max. Stress Range, ksi	Tension or Compression
1	Bottom flange, Girder No. 4	1.3	Tens.
2	Bottom flange, Girder No. 5	1.5	Tens.
3	Lower strut, Type C Diaphragm	1.9	Tens.
4	Diagonal, Type C Diaphragm	1.0	Tens.
5	Diagonal, Type C Diaphragm	0.8	Tens.
6	Upper strut, Type C Diaphragm	0.1	-----
7	Upper strut at bottom	0.8	Comp.
8	Upper strut near top cope	1.2	Comp.

Table B-26: Maximum measured stress ranges and direction for Gage Group 6, Truck Pass 1 (test truck centered in driving lane).

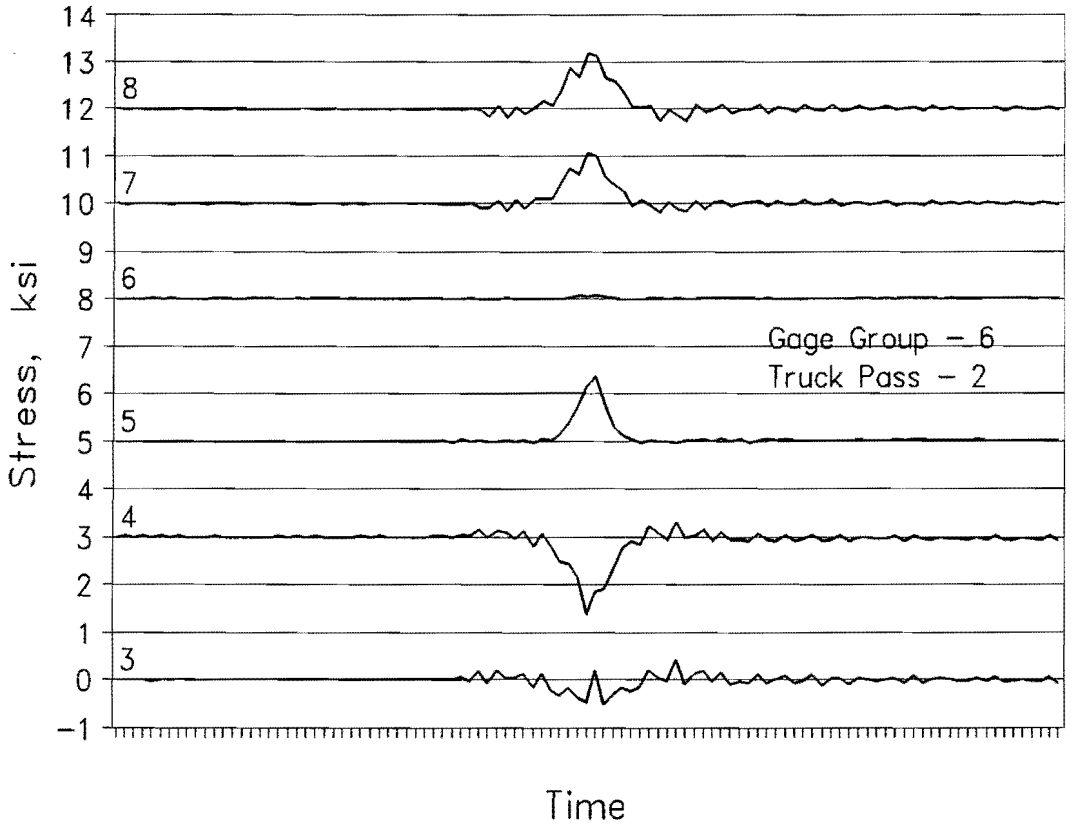

Figure B-34: Diaphragm C-39 member stress histories for Gage Group 6, Truck Pass 2 (test truck centered in right shoulder).

Gage Number	Location	Max. Stress Range, ksi	Tension or Compression
1	Bottom flange, Girder No. 4	0.9	Tens.
2	Bottom flange, Girder No. 5	1.9	Tens.
3	Lower strut, Type C Diaphragm	1.0	Comp.
4	Diagonal, Type C Diaphragm	1.9	Comp.
5	Diagonal, Type C Diaphragm	1.4	Tens.
6	Upper strut, Type C Diaphragm	0.1	-----
7	Upper strut at bottom	1.3	Tens.
8	Upper strut near top cope	1.5	Tens.

Table B-27: Maximum measured stress ranges and direction for Gage Group 6, Truck Pass 2 (test truck centered in right shoulder).

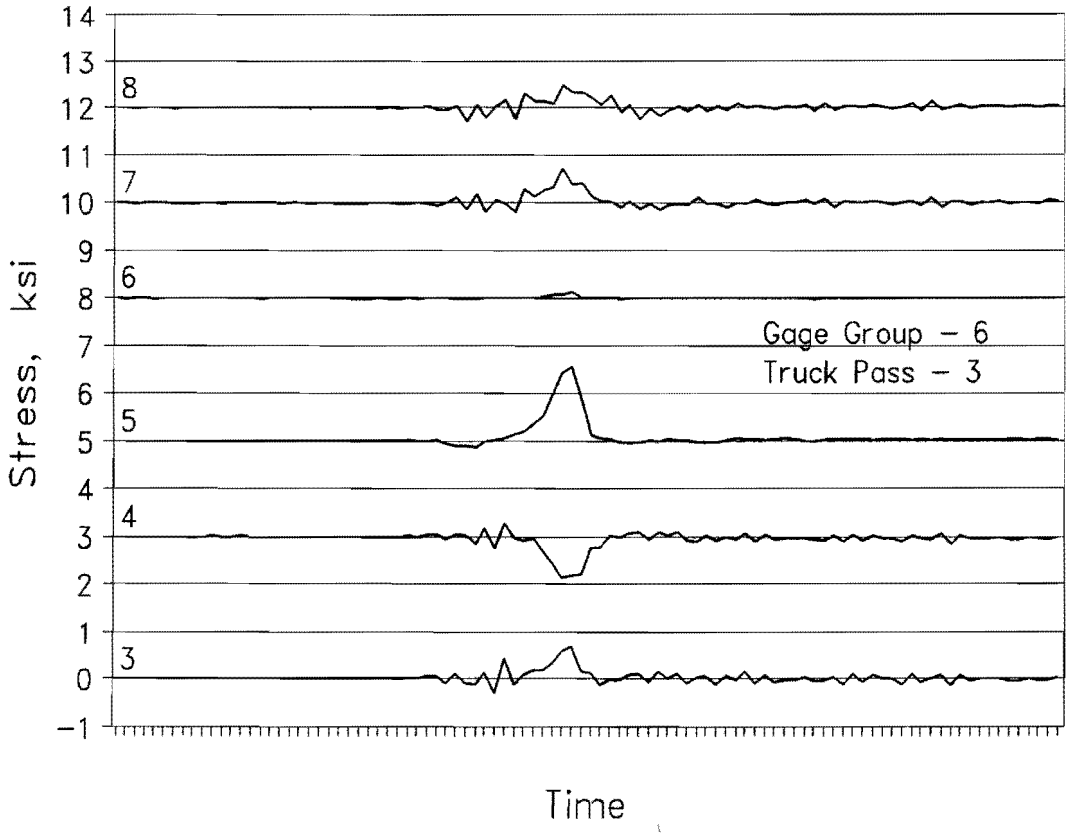

Figure B-35: Diaphragm C-39 member stress histories for Gage Group 6, Truck Pass 3 (test truck straddled right shoulder stripe).

Gage Number	Location	Max. Stress Range, ksi	Tension or Compression
1	Bottom flange, Girder No. 4	1.1	Tens.
2	Bottom flange, Girder No. 5	1.8	Tens.
3	Lower strut, Type C Diaphragm	1.0	Tens.
4	Diagonal, Type C Diaphragm	1.2	Comp.
5	Diagonal, Type C Diaphragm	1.7	Tens.
6	Upper strut, Type C Diaphragm	0.1	-----
7	Upper strut at bottom	0.9	Tens.
8	Upper strut near top cope	0.8	Tens.

Table B-28: Maximum measured stress ranges and direction for Gage Group 6, Truck Pass 3 (test truck straddled right shoulder stripe).

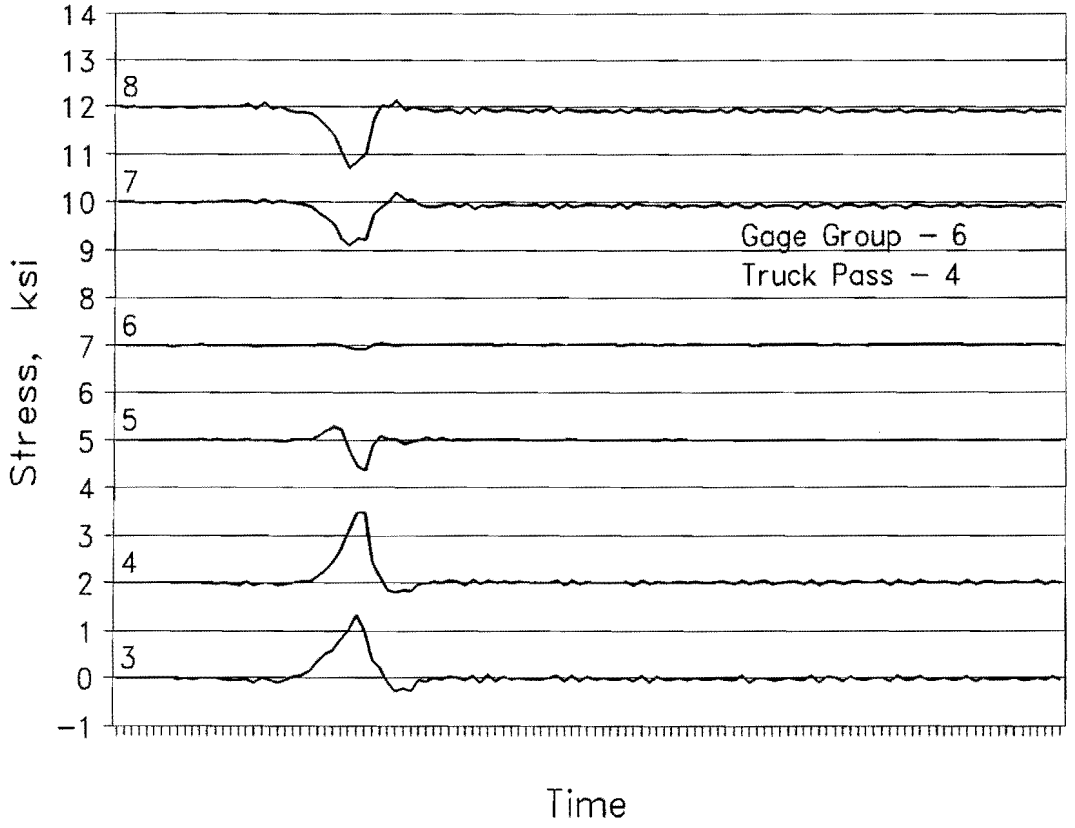

Figure B-36: Diaphragm C-39 member stress histories for Gage Group 6, Truck Pass 4 (test truck straddled center stripe).

Gage Number	Location	Max. Stress Range, ksi	Tension or Compression
1	Bottom flange, Girder No. 4	1.2	Tens.
2	Bottom flange, Girder No. 5	0.9	Tens.
3	Lower strut, Type C Diaphragm	1.6	Tens.
4	Diagonal, Type C Diaphragm	1.7	Tens.
5	Diagonal, Type C Diaphragm	0.9	Comp.
6	Upper strut, Type C Diaphragm	0.1	-----
7	Upper strut at bottom	1.1	Comp.
8	Upper strut near top cope	1.4	Comp.

Table B-29: Maximum measured stress ranges and direction for Gage Group 6, Truck Pass 4 (test truck straddled center stripe).

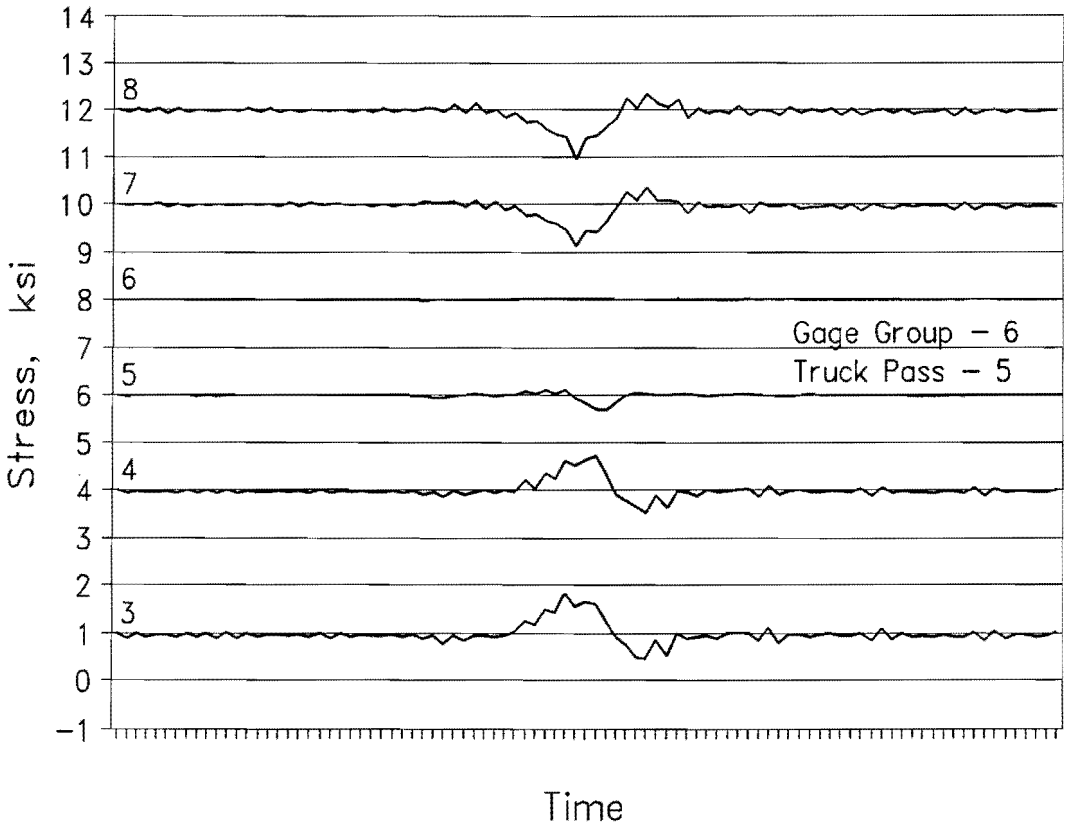

Figure B-37: Diaphragm C-39 member stress histories for Gage Group 6, Truck Pass 5 (test truck centered in passing lane).

Gage Number	Location	Max. Stress Range, ksi	Tension or Compression
1	Bottom flange, Girder No. 4	0.9	Tens.
2	Bottom flange, Girder No. 5	0.8	Tens.
3	Lower strut, Type C Diaphragm	1.4	Tens.
4	Diagonal, Type C Diaphragm	1.2	Tens.
5	Diagonal, Type C Diaphragm	0.4	Comp.
6	Upper strut, Type C Diaphragm	0.0	-----
7	Upper strut at bottom	1.2	Comp.
8	Upper strut near top cope	1.4	Comp.

Table B-30: Maximum measured stress ranges and direction for Gage Group 6, Truck Pass 5 (test truck centered in passing lane).

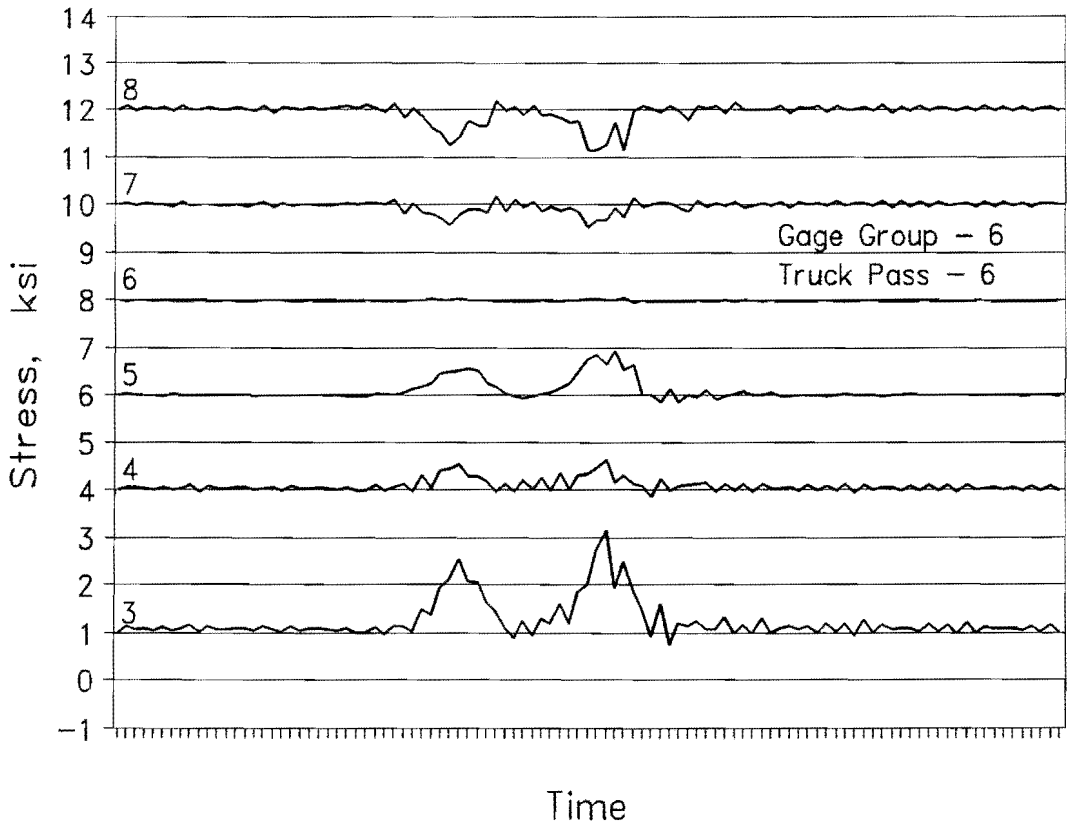

Figure B-38: Diaphragm C-39 member stress histories for Gage Group 6, Truck Pass 6 (two 18 wheelers in driving lane).

Gage Number	Location	Max. Stress Range, ksi	Tension or Compression
1	Bottom flange, Girder No. 4	1.6	Tens.
2	Bottom flange, Girder No. 5	1.9	Tens.
3	Lower strut, Type C Diaphragm	2.4	Tens.
4	Diagonal, Type C Diaphragm	0.8	Tens.
5	Diagonal, Type C Diaphragm	1.1	Tens.
6	Upper strut, Type C Diaphragm	0.1	-----
7	Upper strut at bottom	0.7	Comp.
8	Upper strut near top cope	1.0	Comp.

Table B-31: Maximum measured stress ranges and direction for Gage Group 6, Truck Pass 6 (two 18 wheelers in driving lane).

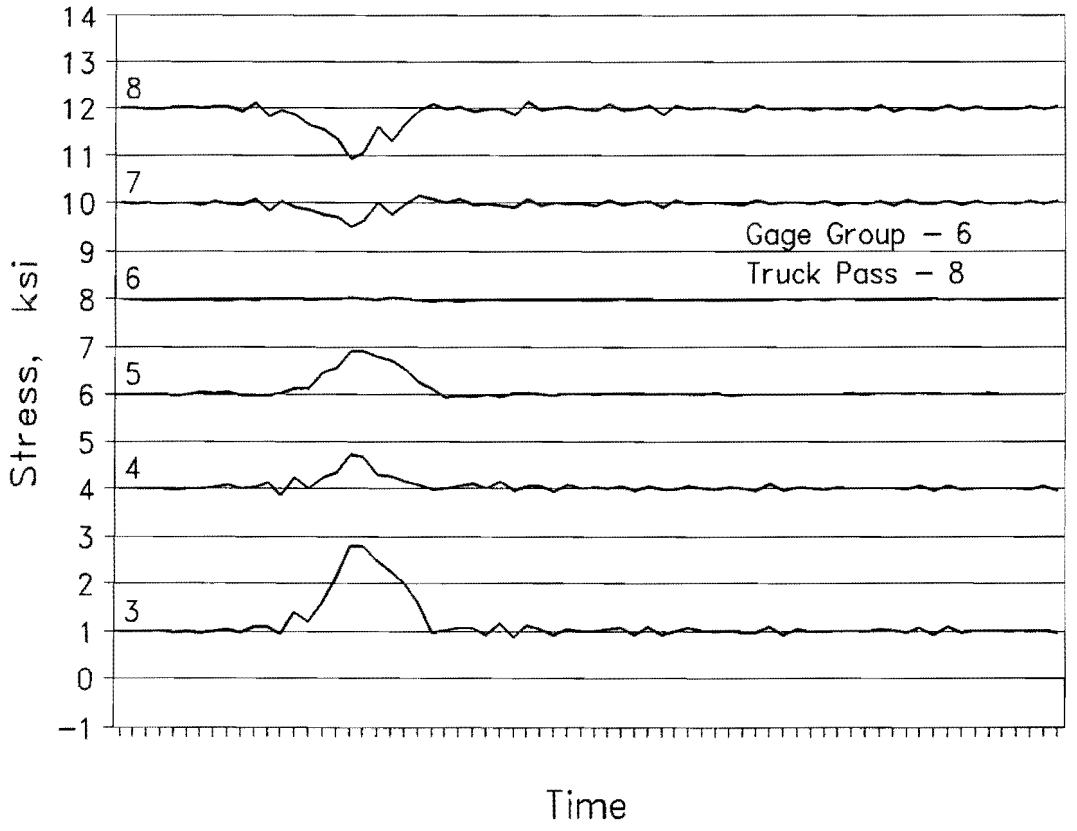

Figure B-39: Diaphragm C-39 member stress histories for Gage Group 6, Truck Pass 8 (tandem in driving lane).

Gage Number	Location	Max. Stress Range, ksi	Tension or Compression
1	Bottom flange, Girder No. 4	1.7	Tens.
2	Bottom flange, Girder No. 5	1.9	Tens.
3	Lower strut, Type C Diaphragm	2.0	Tens.
4	Diagonal, Type C Diaphragm	0.9	Tens.
5	Diagonal, Type C Diaphragm	1.0	Tens.
6	Upper strut, Type C Diaphragm	0.1	-----
7	Upper strut at bottom	0.7	Comp.
8	Upper strut near top cope	1.2	Comp.

Table B-32: Maximum measured stress ranges and direction for Gage Group 6, Truck Pass 8 (tandem in driving lane).

Appendix C

Finite Element Analysis Results

FEM Location	Diaphragm Number				
	Girder 1	Girder 2	Girder 3	Girder 4	Girder 5
0	Bent 8	Bent 8	Bent 8	Bent 8	Bent 8
1	-	53	52	51	50
2	-	-	-	-	-
3	53	52	51	50	49
4	-	-	-	-	-
5	52	51	50	49	48
6	-	-	-	-	-
7	51	50	49	48	47
8	-	-	-	-	-
9	50	49	48	47	46
10	-	-	-	-	-
11	49	48	47	46	45
12	-	-	-	-	-
13	48	47	46	45	44
14	Bent 7	Bent 7	Bent 7	Bent 7	Bent 7
15	47	46	45	44	43
16	-	-	-	-	-
17	46	45	44	43	42
18	-	-	-	-	-
19	45	44	43	42	41
20	-	-	-	-	-
21	44	43	42	41	40
22	-	-	-	-	-
23	43	42	41	40	39
24	-	-	-	-	-
25	42	41	40	39	38
26	-	-	-	-	-
27	41	40	39	38	37
28	-	-	-	-	-
29	40	39	38	37	36
30	-	-	-	-	-
31	Bent 6	Bent 6	Bent 6	Bent 6	Bent 6
32	-	-	-	-	-
33	38	37	36	35	34
34	-	-	-	-	-
35	37	36	35	34	33
36	-	-	-	-	-
37	36	35	34	33	32
38	-	-	-	-	-
39	35	34	33	32	31
40	-	-	-	-	-
41	34	33	32	31	30
42	-	-	-	-	-
43	33	32	31	30	-
44	Bent 5	Bent 5	Bent 5	Bent 5	Bent 5

Table C-1: Finite element model node locations with corresponding diaphragm or bent number.

Girder Flange Stresses (KSI)
All Diaframs

Location	Girder 1 Stresses		Girder 2 Stresses		Girder 3 Stresses		Girder 4 Stresses		Girder 5 Stresses	
	Top Flange	Bottom Flange	Top Flange	Bottom Flange	Top Flange	Bottom Flange	Top Flange	Bottom Flange	Top Flange	Bottom Flange
1	0.0031	0.0854	0.0104	0.0639	0.0182	-0.0715	0.0155	-0.0701	0.0158	-0.1765
2	0.0048	0.1029	0.0031	0.0744	-0.0027	0.0572	-0.0186	0.1378	-0.0249	0.0943
3	-0.0028	0.1196	-0.0041	0.0879	-0.0127	0.2215	-0.0156	0.2195	-0.0321	0.1396
4	-0.0074	0.1276	-0.0110	0.1245	-0.0161	0.2901	-0.0203	0.2431	-0.0375	0.1776
5	-0.0130	0.1455	-0.0151	0.1541	-0.0176	0.2859	-0.0232	0.2495	-0.0376	0.1932
6	-0.0176	0.1626	-0.0186	0.1971	-0.0209	0.3202	-0.0259	0.2622	-0.0350	0.2054
7	-0.0205	0.1849	-0.0189	0.2064	-0.0211	0.3018	-0.0270	0.2663	-0.0286	0.1942
8	-0.0218	0.2036	-0.0167	0.2345	-0.0196	0.3283	-0.0240	0.2776	-0.0197	0.1871
9	-0.0260	0.1854	-0.0172	0.2254	-0.0215	0.3074	-0.0234	0.2787	-0.0073	0.1597
10	-0.0966	0.1556	-0.0182	0.2189	-0.0266	0.2906	-0.0180	0.2313	0.0060	0.1087
11	-0.0460	0.0761	-0.1057	0.1886	-0.1643	0.2511	-0.0679	0.1717	0.0101	-0.1610
12	-0.0175	0.0307	-0.0562	0.1201	-0.0477	0.1622	-0.0370	-0.1026	0.0161	-0.1340
13	3.7040	-0.0674	-0.0257	0.0570	-0.0607	0.0855	0.0415	-0.0920	0.0206	-0.1198
14	0.0587	-0.1142	0.0322	-0.0574	0.0697	-0.0956	0.0729	-0.1042	0.0257	-0.1327
15	0.0324	-0.0663	0.0446	-0.0779	0.0527	-0.1077	0.0774	-0.1110	0.0192	-0.1236
16	0.0255	-0.0524	0.0333	-0.0973	0.0857	0.1281	-0.0708	0.1127	-0.0088	0.0547
17	0.0075	-0.0278	0.0150	-0.0656	0.0630	0.1831	-0.0970	0.1860	-0.0157	0.1310
18	0.0102	0.0433	-0.0375	0.0345	-0.0985	0.2595	-0.0995	0.2230	-0.0181	0.2027
19	-0.0304	0.0726	-0.0790	0.0779	-0.1139	0.2768	-0.1305	0.2398	-0.0236	0.2332
20	-0.0066	0.1094	-0.0171	0.1256	-0.1595	0.3025	-0.0296	0.2558	-0.0245	0.2287
21	-0.0124	0.1387	-0.0217	0.1588	-0.0255	0.3097	-0.0277	0.2820	-0.0218	0.2181
22	-0.0178	0.1599	-0.0225	0.1965	-0.0223	0.3363	-0.0233	0.2925	-0.0168	0.2619
23	-0.0252	0.1833	-0.0258	0.2219	-0.0223	0.3226	-0.0231	0.3096	-0.0087	0.2408
24	-0.0301	0.2013	-0.0242	0.2218	-0.0251	0.3524	-0.0235	0.3230	0.0128	0.2267
25	-0.0325	0.1862	-0.0280	0.2084	-0.0252	0.3526	-0.0137	0.3235	0.0226	0.1986
26	-0.0387	0.1614	-0.0316	0.2389	-0.0267	0.3251	-0.0150	0.2724	0.0315	0.1414
27	-0.1141	0.0826	-0.1245	0.2332	-0.0314	0.2921	-0.0128	0.2171	0.0371	0.0813
28	-0.0658	0.0366	-0.0737	0.2108	-0.1818	0.1852	-0.1139	0.1084	0.0367	0.0243
29	-0.0661	0.0176	-0.0506	0.1388	-0.1039	0.1179	-0.0457	0.0533	0.0348	-0.0349
30	-0.0399	-0.0649	-0.0321	0.0839	-0.0761	-0.0801	-0.0254	-0.0694	0.0337	-0.0507
31	-0.0296	-0.0891	0.0376	-0.0535	-0.0530	-0.0971	0.0422	-0.0874	0.0319	-0.0588
32	-0.0237	-0.1658	0.0435	-0.0796	0.0627	-0.1064	0.0545	-0.0866	-0.0176	-0.0610
33	0.0271	-0.1560	0.0429	-0.0944	0.0677	-0.1567	0.0380	-0.1309	-0.0303	-0.0786
34	0.0259	-0.1359	0.0210	-0.1580	0.0705	0.1335	-0.0694	0.1565	-0.0349	0.0990
35	0.0096	-0.1194	-0.0254	-0.1510	-0.0888	0.2100	-0.0882	0.1721	-0.0419	0.1375
36	0.0177	0.0910	0.0084	0.0821	-0.1345	0.2342	-0.1183	0.1866	-0.0430	0.1564
37	0.0144	0.1119	-0.0073	0.1151	-0.0200	0.2436	-0.0312	0.2136	-0.0423	0.1685
38	0.0099	0.1266	-0.0068	0.1458	-0.0181	0.2716	-0.0311	0.2297	-0.0401	0.1664
39	0.0061	0.1306	-0.0089	0.1670	-0.0180	0.2613	-0.0313	0.2259	-0.0367	0.1532
40	-0.0046	0.1245	-0.0095	0.1722	-0.0206	0.2710	-0.0317	0.2232	-0.0287	0.1303
41	0.0039	0.1276	-0.0104	0.1822	-0.0213	0.2483	-0.0282	0.1870	-0.0210	0.0999
42	0.0053	0.0790	-0.0072	0.1722	-0.0199	0.2904	-0.0238	0.1340	-0.0115	0.0752
43	0.0290	0.0267	-0.0057	0.2056	-0.0158	0.2045	-0.0183	0.0580	0.0018	0.0315

Table C-2: Girder flange stresses for as-built (Model 0), 10 kip unit axle load.

Girder Flange Stresses (KSI)
All Diaframs

Location	Girder 1 Stresses		Girder 2 Stresses		Girder 3 Stresses		Girder 4 Stresses		Girder 5 Stresses	
	Top Flange	Bottom Flange	Top Flange	Bottom Flange	Top Flange	Bottom Flange	Top Flange	Bottom Flange	Top Flange	Bottom Flange
1	0.0040	0.0966	0.0108	0.0798	0.0194	-0.0810	0.0141	-0.0924	0.0127	-0.1455
2	0.0050	0.1171	0.0039	0.0793	-0.0143	0.0504	-0.0242	0.1369	-0.0279	0.1009
3	-0.0019	0.1339	-0.0039	0.0864	-0.0114	0.2164	-0.0172	0.2416	-0.0396	0.1553
4	-0.0073	0.1407	-0.0060	0.1243	-0.0166	0.2988	-0.0255	0.2720	-0.0445	0.1851
5	-0.0131	0.1566	-0.0138	0.1536	-0.0234	0.3359	-0.0261	0.2720	-0.0395	0.1769
6	-0.0174	0.1692	-0.0183	0.1999	-0.0249	0.3665	-0.0280	0.2825	-0.0363	0.1833
7	-0.0191	0.1823	-0.0205	0.2049	-0.0220	0.3259	-0.0315	0.2938	-0.0337	0.1900
8	-0.0183	0.1827	-0.0183	0.2452	-0.0200	0.3520	-0.0285	0.3068	-0.0268	0.1906
9	-0.0224	0.1715	-0.0172	0.2483	-0.0248	0.3799	-0.0249	0.2900	-0.0191	-0.1297
10	-0.0933	0.1573	-0.0195	0.2417	-0.0296	0.3525	-0.0194	0.2381	0.0148	-0.1455
11	-0.0456	0.0786	-0.1142	0.2060	-0.1795	0.2601	-0.1177	0.1677	0.0174	-0.1627
12	-0.0116	0.0281	-0.0601	0.1321	-0.0980	0.1627	-0.0472	-0.1124	0.0217	-0.1336
13	0.0333	-0.0571	-0.0292	0.0671	-0.0681	-0.1057	0.0453	-0.1000	0.0252	-0.1174
14	0.0489	-0.0949	0.0382	-0.0649	0.0806	-0.1234	0.0789	-0.1128	0.0264	-0.1205
15	0.0364	-0.0614	0.0435	-0.0742	0.0960	-0.1135	0.0872	-0.1211	0.0163	-0.1003
16	0.0134	-0.0381	0.0361	-0.0957	-0.0793	0.1360	-0.0690	0.1136	-0.0102	0.0650
17	-0.0131	-0.0304	0.0139	-0.0766	-0.1140	0.2308	-0.1005	0.1996	-0.0135	0.1142
18	-0.0323	0.0465	-0.0404	-0.0407	-0.1314	0.2968	-0.1066	0.2453	-0.0156	0.1822
19	-0.0086	0.0662	-0.0846	0.0802	-0.1625	0.2896	-0.1504	0.2779	-0.0271	0.2311
20	-0.0140	0.0948	-0.0193	0.1251	-0.0248	0.3219	-0.0340	0.2842	-0.0289	0.2483
21	-0.0210	0.1239	-0.0219	0.1657	-0.0258	0.3659	-0.0274	0.2993	-0.0230	0.2442
22	-0.0292	0.1528	-0.0235	0.2045	-0.0256	0.3852	-0.0231	0.3164	-0.0175	0.2393
23	-0.0328	0.1722	-0.0284	0.2259	-0.0243	0.3421	-0.0262	0.3288	-0.0137	0.2362
24	-0.0329	0.1725	-0.0269	0.2186	-0.0245	0.3669	-0.0209	0.3467	-0.0068	0.2297
25	-0.0385	0.1633	-0.0278	0.2501	-0.0288	0.4046	-0.0163	0.3338	0.0161	0.1968
26	-0.1119	0.1592	-0.0326	0.2559	-0.0334	0.3826	-0.0150	0.2814	0.0260	0.1372
27	-0.0663	0.0827	-0.1308	0.2466	-0.1932	0.3026	-0.1292	0.2393	0.0333	0.0800
28	-0.0335	0.0292	-0.0769	0.2192	-0.1093	0.1952	-0.0532	0.1213	0.0336	0.0291
29	-0.0249	-0.0168	-0.0524	0.1453	-0.0902	0.1348	-0.0266	0.0537	0.0319	-0.0261
30	-0.0212	-0.0559	-0.0314	0.0892	-0.0635	0.0860	0.0473	-0.0774	0.0326	-0.0441
31	0.0221	-0.0797	0.0448	0.0459	0.0649	-0.1081	0.0574	-0.0956	-0.0165	-0.1067
32	0.0298	-0.1623	0.0512	-0.0860	0.0751	-0.1208	0.0492	-0.0685	-0.0199	-0.0869
33	0.0197	-0.1608	0.0477	-0.1040	0.0839	-0.1839	-0.0707	0.1103	-0.0299	-0.0738
34	0.0162	-0.1373	0.0210	-0.1689	-0.1071	-0.1553	-0.0944	0.1719	-0.0328	0.0796
35	-0.0042	-0.1165	-0.0276	-0.1585	-0.1393	0.2204	-0.1400	0.2074	-0.0433	0.1397
36	0.0143	-0.1075	0.0074	-0.1188	-0.0196	0.2522	-0.0375	0.2150	-0.0462	0.1670
37	0.0108	0.1016	-0.0068	0.1217	-0.0218	0.3009	-0.0322	0.2287	-0.0445	0.1799
38	0.0070	0.1171	-0.0070	0.1540	-0.0218	0.3187	-0.0313	0.2379	-0.0417	0.1777
39	-0.0050	0.1144	-0.0114	0.1737	-0.0214	0.2836	-0.0321	0.2392	-0.0376	0.1609
40	-0.0034	0.0956	-0.0121	0.1753	-0.0205	0.2775	-0.0287	0.2261	-0.0294	0.1365
41	-0.0031	0.0978	-0.0116	0.1912	-0.0192	0.2514	-0.0242	0.1889	-0.0214	0.1047
42	0.0042	0.0749	-0.0073	0.1849	-0.0156	0.2910	-0.0187	0.1359	-0.0117	0.0814
43	0.0295	0.0318	-0.0063	0.2167	-0.0163	0.2051	-0.0054	0.0596	0.0017	0.0337

Table C-3: Girder flange stresses for no Type B diaphragms (Model 1) 10 kip unit axle load.

Girder Flange Stresses (KSI)

No Diaframs

Location	Girder 1 Stresses		Girder 2 Stresses		Girder 3 Stresses		Girder 4 Stresses		Girder 5 Stresses	
	Top Flange	Bottom Flange	Top Flange	Bottom Flange	Top Flange	Bottom Flange	Top Flange	Bottom Flange	Top Flange	Bottom Flange
1	0.0104	0.1413	0.0140	0.0773	0.0188	-0.1373	0.0110	-0.1307	-0.0408	0.1650
2	0.0068	0.1622	0.0070	0.0839	-0.0195	-0.0338	-0.0361	0.1481	-0.0468	0.1735
3	-0.0012	0.1675	0.0024	0.1065	-0.0144	0.2606	-0.0299	0.2808	-0.0556	0.1889
4	-0.0043	0.1615	-0.0088	0.1440	-0.0211	0.3542	-0.0378	0.3394	-0.0594	0.1878
5	-0.0097	0.1653	-0.0139	0.1759	-0.0276	0.3956	-0.0398	0.3547	-0.0601	0.1826
6	-0.0143	0.1640	-0.0194	0.2174	-0.0295	0.4386	-0.0422	0.3731	-0.0590	0.1834
7	-0.0168	0.1699	-0.0214	0.2402	-0.0294	0.4487	-0.0415	0.3683	-0.0531	0.1757
8	-0.0175	0.1726	-0.0206	0.2746	-0.0269	0.4855	-0.0367	0.3728	-0.0439	0.1716
9	-0.0190	0.1526	-0.0208	0.2904	-0.0275	0.4889	-0.0358	0.3581	0.0330	0.1563
10	-0.0590	0.1282	-0.0252	0.2776	-0.0331	0.4390	-0.0313	0.2868	0.0352	-0.1647
11	-0.0250	0.0696	-0.1413	0.2459	-0.2158	0.3649	-0.1395	0.2078	0.0365	-0.1790
12	-0.0095	0.0375	-0.0755	0.1461	-0.1156	0.2684	-0.0533	-0.1480	0.0346	-0.1351
13	0.0167	0.0243	-0.0370	0.0639	-0.0725	-0.1229	0.0648	-0.1369	0.0301	-0.1028
14	0.0303	-0.0491	0.0498	-0.0853	0.0869	-0.1401	0.1075	-0.1558	0.0240	-0.0908
15	0.0422	-0.0811	0.0842	-0.1261	0.1060	-0.1666	0.1178	-0.1639	0.0125	-0.0714
16	0.0488	-0.0957	0.0626	-0.1489	-0.0899	-0.1670	-0.0733	0.1288	-0.0133	-0.0646
17	-0.0239	-0.0979	0.0159	-0.0726	-0.1157	0.2376	-0.1203	0.2456	-0.0259	0.1603
18	-0.0411	-0.0943	-0.0452	0.0897	-0.1434	0.3242	-0.1407	0.3165	-0.0318	0.1856
19	-0.0175	0.0704	-0.0913	0.1410	-0.2086	0.3777	-0.1750	0.3397	-0.0426	0.1973
20	-0.0231	0.0897	-0.0210	0.1755	-0.0307	0.4039	-0.0411	0.3449	-0.0473	0.2132
21	-0.0264	0.1035	-0.0253	0.2156	-0.0273	0.4476	-0.0372	0.3698	-0.0493	0.2167
22	-0.0306	0.1131	-0.0248	0.2406	-0.0259	0.4688	-0.0378	0.3815	-0.0484	0.2073
23	-0.0332	0.1281	-0.0280	0.2536	-0.0297	0.4702	-0.0263	0.3801	-0.0438	0.2054
24	-0.0326	0.1391	-0.0277	0.2804	-0.0282	0.5025	-0.0325	0.3929	-0.0364	0.1910
25	-0.0337	0.1328	-0.0270	0.3001	-0.0299	0.5091	-0.0329	0.3891	-0.0321	0.1476
26	-0.0691	0.1192	-0.0325	0.2925	-0.0373	0.4627	-0.0304	0.3280	-0.0194	0.0962
27	-0.0379	0.0661	-0.1454	0.2789	-0.2322	0.4104	-0.1593	0.2623	-0.0118	0.0310
28	-0.0208	0.0360	-0.0875	0.1755	-0.1284	0.2483	-0.0678	0.1329	0.0221	-0.0721
29	-0.0140	0.0242	-0.0548	0.0995	-0.0957	0.1460	0.0140	0.0673	0.0200	-0.0702
30	-0.0137	0.0161	-0.0290	0.0510	-0.0625	-0.1180	0.0375	-0.0949	0.0170	-0.0648
31	0.0131	-0.0375	0.0629	-0.0960	0.0816	-0.1435	0.0904	-0.1181	0.0137	-0.0438
32	0.0394	-0.1063	0.0732	-0.1227	0.0865	-0.1573	0.0716	-0.0877	0.0078	0.0714
33	0.0499	-0.1309	0.0805	-0.0625	0.0959	-0.2523	0.0267	0.1383	-0.0223	0.1175
34	0.0490	-0.1242	0.0489	0.0293	-0.1160	0.2507	-0.1229	0.2498	-0.0296	0.1404
35	0.0269	-0.1107	-0.0667	0.0860	-0.1861	0.3077	-0.1650	0.2842	-0.0399	0.1511
36	0.0224	-0.1050	-0.0147	0.1304	-0.0270	0.3411	-0.0389	0.2897	-0.0442	0.1640
37	-0.0201	0.0811	-0.0200	0.1753	-0.0258	0.3902	-0.0354	0.3124	-0.0457	0.1677
38	-0.0249	0.0862	-0.0203	0.2099	-0.0246	0.4166	-0.0352	0.3223	-0.0443	0.1603
39	-0.0281	0.0869	-0.0245	0.2307	-0.0273	0.4185	-0.0343	0.3120	-0.0395	0.1447
40	-0.0279	0.0831	-0.0260	0.2426	-0.0283	0.4102	-0.0299	0.2806	-0.0305	0.1233
41	-0.0278	0.0954	-0.0265	0.2313	-0.0230	0.3620	-0.0233	0.2249	-0.0228	0.1147
42	-0.0216	0.0846	-0.0178	0.2657	-0.0150	0.3652	-0.0166	0.1620	-0.0139	0.0614
43	0.0163	0.0503	0.0190	0.1807	0.0204	0.2258	0.0044	0.0645	0.0080	0.0199

Table C-3: Girder flange stresses for no diaphragms (Model 2) 10 kip unit axle load.

Girder Flange Stresses (KSI)
Staggered Diafragms

Location	Girder 1 Stresses		Girder 2 Stresses		Girder 3 Stresses		Girder 4 Stresses		Girder 5 Stresses	
	Top Flange	Bottom Flange	Top Flange	Bottom Flange	Top Flange	Bottom Flange	Top Flange	Bottom Flange	Top Flange	Bottom Flange
1	0.0065	0.1016	0.0129	0.0655	0.0203	-0.1172	0.0143	-0.0864	-0.0140	-0.1054
2	0.0040	0.1248	0.0045	0.0716	-0.0181	0.0428	-0.0279	0.1473	-0.0335	0.1222
3	-0.0020	0.1380	-0.0032	0.0887	-0.0140	0.2463	-0.0249	0.2604	-0.0467	0.1810
4	-0.0063	0.1400	-0.0104	0.1432	-0.0206	0.3431	-0.0290	0.2905	-0.0524	0.2047
5	-0.0118	0.1518	-0.0146	0.1606	-0.0261	0.3599	-0.0293	0.2880	-0.0486	0.1874
6	-0.0163	0.1639	-0.0198	0.2095	-0.0272	0.3730	-0.0317	0.2984	-0.0463	0.1839
7	-0.0179	0.1816	-0.0216	0.2224	-0.0233	0.3234	-0.0361	0.3124	-0.0442	0.1800
8	-0.0179	0.1955	-0.0182	0.2663	-0.0215	0.3389	-0.0340	0.3300	-0.0381	0.1780
9	-0.0231	0.1945	-0.0163	0.2774	-0.0261	0.4037	-0.0325	0.3108	0.0255	-0.1473
10	-0.0964	0.1889	-0.0183	0.2623	-0.0324	0.3942	-0.0278	0.2531	0.0276	-0.1684
11	-0.0501	0.1032	-0.1152	0.2352	-0.2067	0.3661	-0.0893	0.1780	0.0297	-0.1906
12	-0.0111	0.0391	-0.0662	0.1333	-0.1156	0.2216	-0.0541	-0.1283	0.0309	-0.1526
13	0.0295	-0.0412	-0.0335	0.0633	-0.0724	-0.1122	0.0591	-0.1149	0.0305	-0.1279
14	0.0530	-0.0858	0.0381	-0.0654	0.0848	-0.1250	0.0930	-0.1249	0.0299	-0.1274
15	0.0561	-0.1249	0.0385	-0.0929	0.0994	-0.1369	0.0935	-0.1224	0.0208	-0.1115
16	0.0185	-0.0314	0.0302	-0.0853	-0.0890	0.1446	-0.0736	0.1320	-0.0083	-0.0646
17	-0.0227	-0.0288	0.0138	-0.0442	-0.1190	0.2407	-0.1156	0.2315	-0.0240	0.1530
18	-0.0409	0.0473	-0.0453	0.0922	-0.1444	0.3319	-0.1219	0.2797	-0.0293	0.2228
19	-0.0171	0.0662	-0.0849	0.1427	-0.1879	0.3620	-0.1353	0.2722	-0.0325	0.2258
20	-0.0217	0.0898	-0.0219	0.1669	-0.0292	0.3562	-0.0319	0.2821	-0.0364	0.2364
21	-0.0242	0.1097	-0.0266	0.2021	-0.0219	0.3350	-0.0338	0.3209	-0.0421	0.2663
22	-0.0283	0.1302	-0.0250	0.2334	-0.0220	0.3626	-0.0346	0.3361	-0.0418	0.2682
23	-0.0325	0.1665	-0.0252	0.2416	-0.0304	0.3783	-0.0326	0.3300	-0.0340	0.2347
24	-0.0341	0.2059	-0.0235	0.2702	-0.0303	0.4176	-0.0278	0.3449	-0.0261	0.2175
25	-0.0365	0.2002	-0.0267	0.2618	-0.0296	0.3764	-0.0304	0.3627	-0.0249	0.1990
26	-0.0905	0.1646	-0.0282	0.2717	-0.0362	0.3404	-0.0282	0.3146	-0.0144	0.1508
27	-0.0506	0.0908	-0.1201	0.2611	-0.2095	0.3775	-0.1421	0.2386	0.0105	0.0951
28	-0.0335	0.0525	-0.0737	0.1655	-0.1305	0.2424	-0.0568	0.1174	0.0146	0.0319
29	-0.0203	0.0288	-0.0476	0.0972	-0.0937	0.1565	-0.0376	0.0661	0.0164	-0.0852
30	0.0201	-0.0421	-0.0272	0.0454	-0.0630	-0.0757	0.0318	-0.0760	0.0170	-0.0929
31	0.0335	-0.0723	0.0474	-0.0818	0.0703	-0.1043	0.0719	-0.0891	0.0162	-0.0923
32	0.0534	-0.1535	0.0563	-0.1077	0.0830	-0.1273	0.0555	-0.0663	0.0091	-0.0625
33	0.0439	-0.1555	0.0638	-0.1860	-0.0720	0.1446	-0.0716	0.1338	-0.0219	0.0838
34	0.0356	-0.1331	0.0384	-0.1732	-0.1186	0.2507	-0.1071	0.2157	-0.0318	0.1552
35	0.0169	-0.1121	-0.0571	0.0874	-0.1696	0.2876	-0.1257	0.2213	-0.0375	0.1596
36	-0.0136	0.0783	-0.0144	0.1222	-0.0251	0.2903	-0.0293	0.2316	-0.0415	0.1640
37	-0.0162	0.0936	-0.0198	0.1581	-0.0189	0.2761	-0.0334	0.2695	-0.0472	0.1837
38	-0.0200	0.1077	-0.0182	0.1929	-0.0193	0.3079	-0.0363	0.2849	-0.0472	0.1840
39	-0.0244	0.1206	-0.0183	0.2079	-0.0254	0.3501	-0.0345	0.2724	-0.0413	0.1626
40	-0.0260	0.1294	-0.0187	0.2167	-0.0273	0.3637	-0.0304	0.2495	-0.0319	0.1369
41	-0.0229	0.1419	-0.0203	0.2012	-0.0226	0.3442	-0.0264	0.2138	-0.0235	0.1093
42	-0.0145	0.0851	-0.0149	0.2230	-0.0157	0.3394	-0.0189	0.1598	-0.0141	0.0916
43	0.0229	0.0299	-0.0081	0.1483	-0.0202	0.2128	-0.0056	0.0647	0.0045	0.0396

Table C-5: Girder flange stresses for staggered diaphragm pattern (Model 3) 10 kip unit axle load.

Diaphragm #	Diagonal	Diagonal	Lower Strut
51	.512 (.457)	-.338 (-.305)	.311 (.278)
50	.72	-.467	.422
49	.685 (1.2)	-.630 (-1.07)	.59 (.979)
48	.856	-.450	.38
47	.464	-.281	.25
46	-.413	.252	-.233
45	-.270	.100	-.091
44	.563 (.278)	-.372 (-.208)	.336 (.191)
43	.630	-.413	.377
42	.663 (1.16)	-.441 (-.737)	.401 (.671)
41	.574	-.541	.494
40	.747 (1.16)	-.360 (-.58)	.343 (.538)
39	.648	-.965	-.8303
38	.39	.194	-.179
37	-.25	.141	-.129
36	.34 (.339)	-.230 (-.227)	.210 (.208)
35	.574	-.378	.345
34	.777 (1.25)	-.512 (-.79)	.471 (.723)
33	.774	-.500	.441

Values in parenthesis are for Model 3
Forces are in kips

Table C-6: Diaphragm member forces for as-built (Model 0) and staggered diaphragms (Model 3), Bay A, 10 kip unit axle load.

Diaphragm #	Diagonal	Diagonal	Lower Strut
51	1.05 (-.235)	-.41 (.506)	.89 (.203)
50	1.55	-.44	1.33
49	1.66 (2.26)	-.67 (-.872)	1.43 (1.98)
48	1.22	-.69	1.35
47	1.44	-.98	.35
46	.513	-1.37	.358
45	-.252	-.56	.616
44	1.1 (-.425)	.500 (.568)	1.02 (.361)
43	1.56	-.542	1.255
42	1.61 (2.195)	-.718 (-.75)	1.33 (2.09)
41	1.24	-.73	1.24
40	1.153 (1.52)	-.705 (-1.3)	1.205 (1.54)
39	1.323	-.986	.36
38	1.07	-1.39	-.71
37	-.160	-1.34	-.37
36	-.381 (-.386)	-.148 (-.528)	.624 (.345)
35	1.19	-.303	.986
34	1.643 (2.22)	-.541 (-.776)	1.445 (2.08)
33	1.514	-.672	1.205
32	1.6	-.725	.64

Values in parenthesis are for Model 3
Forces are in kips

Table C-7: Diaphragm member forces for as-built (Model 0) and staggered diaphragms (Model 3), Bay B, 10 kip unit axle load.

Diaphragm #	Diagonal	Diagonal	Lower Strut
51	-.752	-1.26	.718
50	.20	1.18	1.66
49	.133 (.272)	1.23 (1.67)	1.60 (2.514)
48	.17	.984	1.55
47	-.095 (-0.82)	.416 (-.68)	1.232 (.375)
46	.381	-.427	.341
45	-.410	.582	-.3055
44	-.870	1.135	.939
43	-.210	.870	1.723
42	.175 (.271)	1.112 (1.647)	1.794 (2.61)
41	.0695	1.107	1.622
40	.128 (.28)	.911 (1.132)	1.411 (1.06)
39	-.107	.343	1.186
38	.184 (.67)	-.402 (-.652)	.648 (2.345)
37	.507	-.761	-.566
36	-1.367	1.116	-.155
35	-.828	.832	1.293
34	.175 (.30)	1.193 (1.67)	1.864 (2.6)
33	.152	1.058	1.613
32	.317 (.735)	.376 (0.956)	.906 (.792)

Values in parenthesis are for Model 3
Forces are in kips

Table C-8: Diaphragm member forces for as-built (Model 0) and staggered diaphragms (Model 3), Bay C, 10 kip unit axle load.

Diaphragm #	Diagonal	Diagonal	Lower Strut
51	-	-	-
50	-.697	1.154	.627
49	-.757 (-1.09)	1.216 (1.743)	.707 (.995)
48	-.684	1.06	.625
47	-.488 (-.463)	.764 (.754)	.445 (.424)
46	-.2768	.361	.253
45	.212	.279	-.1877
44	.198	.486	-.2096
43	-.485	1.369	.421
42	-.788 (-1.156)	1.248 (1.862)	.724 (1.058)
41	-.682	1.05	.622
40	-.618 (-.863)	.936 (1.356)	.5655 (.788)
39	-.471	.708	.430
38	-.306 (-.379)	.452 (.524)	.280 (.348)
37	-.195	-.332	.179
36	-.372	.938	.355
35	-1.255	1.521	-.773
34	-.802 (-1.14)	1.285 (1.83)	.740 (1.04)
33	-.692	1.087	.630
32	-.472 (-.60)	.721 (.982)	.431 (.547)

Values in parenthesis are for Model 3
Forces are in kips

Table C-9: Diaphragm member forces for as-built (Model 0) and staggered diaphragms (Model 3), Bay D, 10 kip unit axle load.

Location	As-built	No Diaphragms	Staggered
0	-0.009	-0.009	-0.009
1	-0.0422	-0.08724	-0.0573
2	-0.0739	-0.11807	-0.1004
3	-0.0916	-0.18836	-0.1347
4	-0.0985	-0.2006	-0.1445
5	-0.1033	-0.22388	-0.1446
6	-0.1014	-0.23848	-0.1524
7	-0.0983	-0.2381	-0.163
8	-0.0964	-0.2316	-0.1695
9	-0.0982	-0.20067	-0.1763
10	-0.0934	-0.158	-0.1637
11	-0.0564	-0.0596	-0.1147
12	0.02348	0.03553	0.02658
13	0.02338	0.02759	0.03146
14	0.0263	-0.0583	-0.058
15	-0.0382	-0.1317	-0.1212
16	-0.0833	-0.2019	-0.1648
17	-0.1146	-0.2443	-0.1694
18	-0.1238	-0.2639	-0.1571
19	-0.1113	-0.2706	-0.1431
20	-0.1026	-0.27	-0.1385
21	-0.0986	-0.2665	-0.1294
22	-0.0945	-0.2585	-0.1304
23	-0.0928	-0.2493	-0.1304
24	-0.0936	-0.2411	-0.143
25	-0.1011	-0.2191	-0.15
26	-0.104	-0.174	-0.1268
27	-0.0928	-0.1304	-0.0804
28	-0.061	-0.1101	-0.0238
29	-0.018	0.01352	0.03329
30	0.02689	0.04438	0.0561
31	0.03952	0.05829	-0.0719
32	-0.0518	-0.0736	-0.1272
33	-0.0896	-0.1429	-0.1521
34	-0.1122	-0.1946	-0.1499
35	-0.1097	-0.2203	-0.1531
36	-0.1067	-0.228	-0.1545
37	-0.1009	-0.2296	-0.1537
38	-0.0938	-0.2233	-0.1537
39	-0.0902	-0.2051	-0.146
40	-0.0884	-0.1808	-0.1373
41	-0.0642	-0.1387	-0.103
42	-0.0286	-0.0751	-0.0509
43	-0.009	-0.009	-0.009

Table C-10: Summary of maximum transverse slab bending stresses in Bay C for three diaphragm conditions: as-built, no diaphragms, and staggered.

(this page intentionally left blank)

Appendix D

1983 SPECIAL REPORT

(this page intentionally left blank)

SPECIAL REPORT

ON

REPAIR AND RETROFIT OF CRACKED STEEL BRIDGE GIRDERS

IN

MIDLAND, TEXAS

DONALD E. HARLEY
FEDERAL HIGHWAY ADMINISTRATION
TEXAS DIVISION
AUGUST 1983

TABLE OF CONTENTS

I. Project History and Scope

A contract to widen the dual bridges carrying IH 20 over US Highway 80 and the Missouri Pacific Railroad in Midland County, Texas, was let in May 1982. The widening required the addition of a line of continous steel plate girders to each structure. The angle of the crossing required that the supporting concrete bents be set at a 60° skew to the girder lines. Continuous girder units with spans of 90'-125'-125'-105' and 90'-125'-105' had been used on the structure.

The details for the widening called for additional transverse stiffeners to be welded to the existing exterior girder lines so that diaframs could join the new girder line. While welding these stiffeners into place, a crack was noted in the 5/16" thick web just below the web to flange fillet welds. A visual examination of the bridges disclosed a total of at least 28 similar cracks, all located in the web above transverse stiffeners which also served as connection plates for the diaframs. The cracked areas seemed to be limited to 20' on either side of the skewed bents. Diaframs were placed normal to girder lines.

The concentration of the cracking problem adjacent to the skewed bents, the rigid diafram design, welding details for stiffeners, and crack location above the stiffeners all suggested that out of plane bending was the major cause of the cracking.

Interstate 20 at this location serves some 10,000 vehicles per day. Approximately 40% of the vehicles are trucks with interstate cargos as well as trucks with loads which support the petroleum and other industries in the area.

II. Repair and Retrofit Procedure Selection

A number of repair/retrofit procedures were presented and discussed by engineers for DHT and FHWA. Two factors seemed essential to any procedure.

A. Stop further propagation of the cracks.

B. Strengthen the diafram connection detail to reduce local bending in the thin web.

Based on these two factors, a three step procedure was adopted.

A. Drill a 3/4" diameter hole at the extremities of the crack.

B. Back gouge the crack between the holes and replace with weld metal.

C. Attach stiffeners to the top flange with a fillet weld.

The contractor for the bridge widening project, Clearwater Contractors, Inc., was asked to prepare an estimate for two types of repairs/retrofits based on these procedures. The first type would be for those stiffeners within 20' of a bent that had not yet developed a crack adjacent to the top of the stiffener along the web to flange weld. The retrofit procedure in these cases would be to place a fillet weld to connect the stiffeners to the top flange. The second type would be for those stiffeners within 20' of a bent that had developed a crack. The retrofit procedure in these cases would be to drill holes to intercept the tips of the cracks, repair cracked area between holes, and weld stiffener to flange. The contractor estimated $250 and $375 for the two types of procedures. A $43,000 field change authorized the contractor to do the work.

III. Contractor Operations

A team of welders and a welder's helper/equipment operator performed the work. Access to the work area was supplied by a platform mounted on a light-duty, rubber-tired crane with an extendable boom. From the platform, access to both sides of the girder line was possible.

When a crack in the web was evident or suspected, dye penetrant was sprayed on one side of the web. After allowing time for penetration, the opposite side of the web was examined. The dye made location of the crack tips more assured. With the crack tip located, holes were drilled to intercept the crack. A total of 43 cracks were located during the retrofit operation.

After trying several pieces of drilling equipment, the crew selected a right angle drill and bit extension as the best combination to allow proper placement of the bit. Drilling pressure was supplied by a wooden lever system blocked off of the diafram. Finished holes were given a close visual inspection to assure that the crack tip was removed.

With the crack stopped and bounded by holes, the repair and retrofit could begin. Next, corners from the top horizontal member of the diafram were flame cut to improve working room, the crack was back gouged, the groove welded between holes, stiffeners were welded to the top flange, and, finally, the area was cleaned and painted.

IV. Summary

The problem and procedures to combat it are similar to those reported in other States. It is the first reported girder cracking caused by out of plane bending in Texas. The attached sketches and photographs should provide additional clarity to the problem and adopted solutions.

SKETCH OF TYPICAL STIFFENER AND DIAFRAM CONNECTION

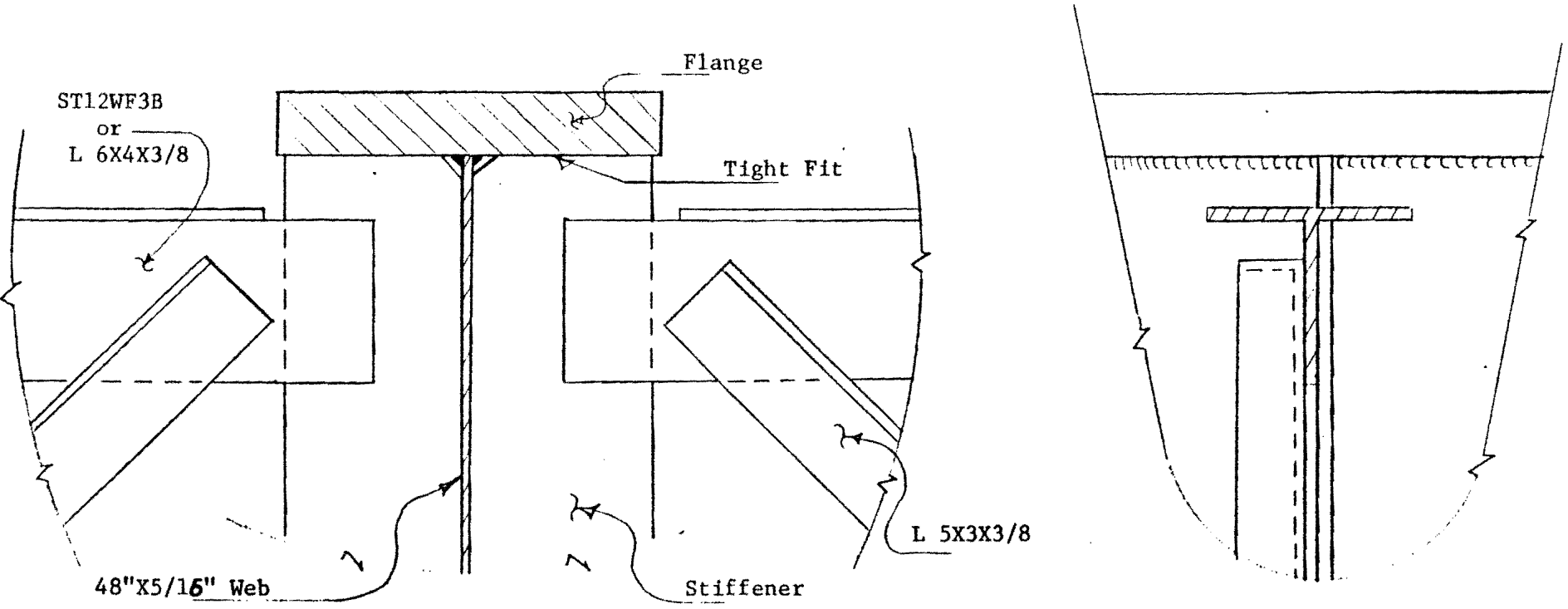

SECTION

ELEVATION

REPAIR PROCEDURES:

1. Drill 3/4" diameter holes through web and fillet weld beyond end of crack.
2. Gouge out crack in one side of web and fill with low hydrogen filler metal and grind smooth.
3. Weld web stiffener to top flange.
4. Repeat Steps 2 and 3 on opposite side.
5. If no crack is noted, weld web stiffeners to top flange of diaframs that are within 20' of the interior bearings.
6. Preheat to above 70°F and maintain while welding.
7. Paint steel at repair areas with System I-Aluminum.

Attachment A

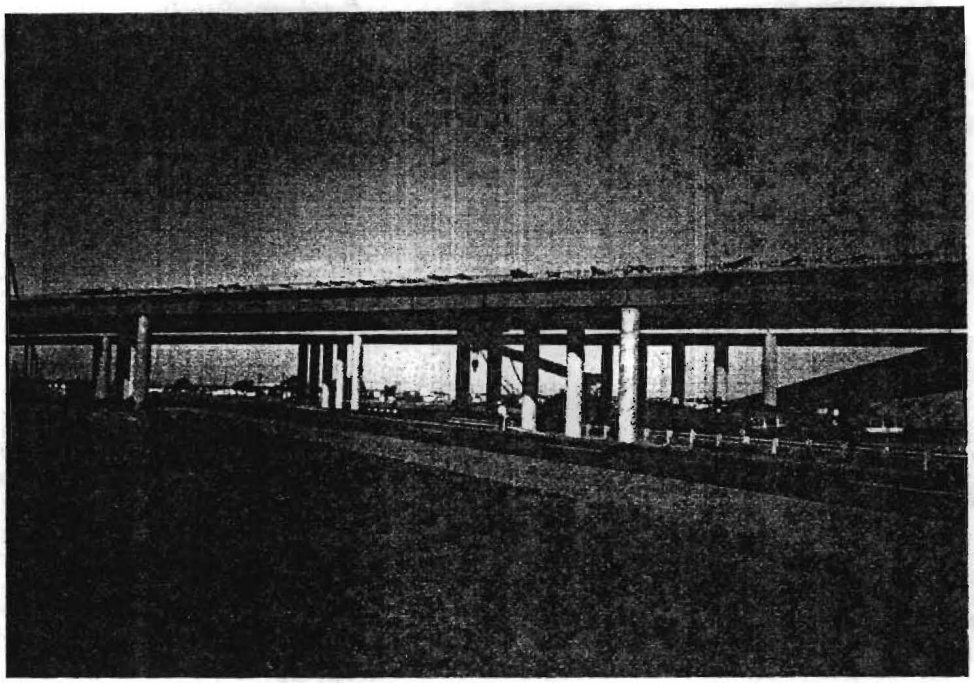

ELEVATION OF I 20 TWIN STRUCTURES

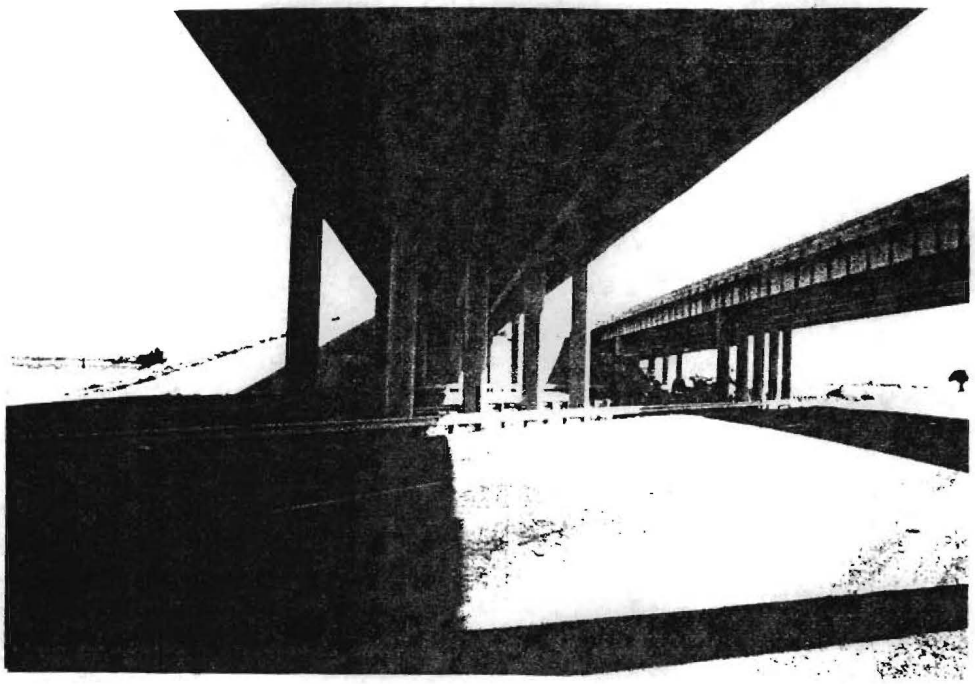

GIRDER LINES, DIAFRAMS & SKEWED BENTS

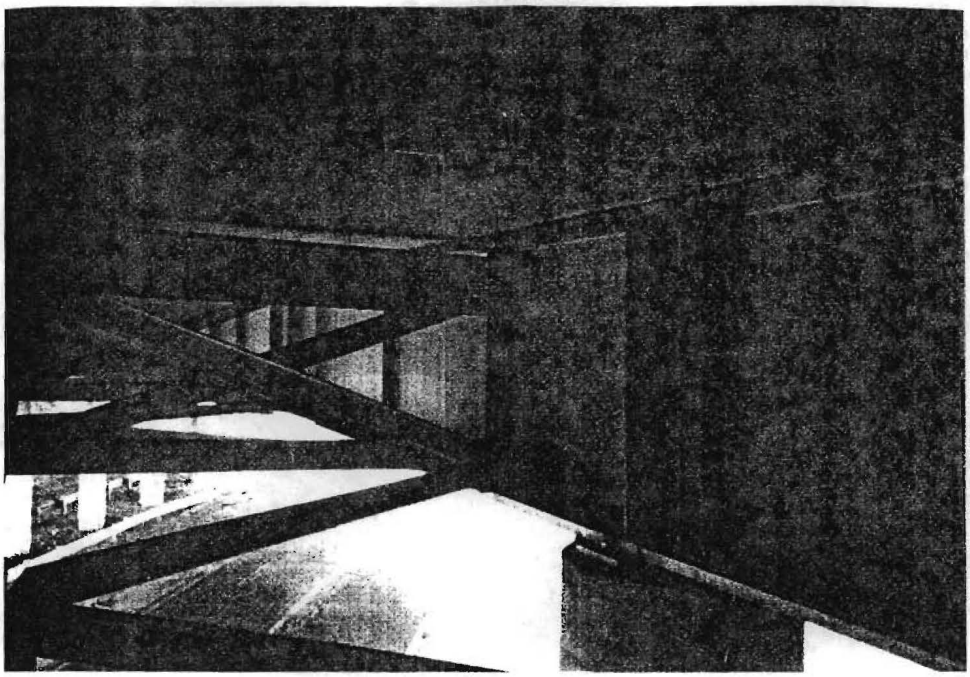

TYPICAL DIAFRAMS AND STIFFENERS

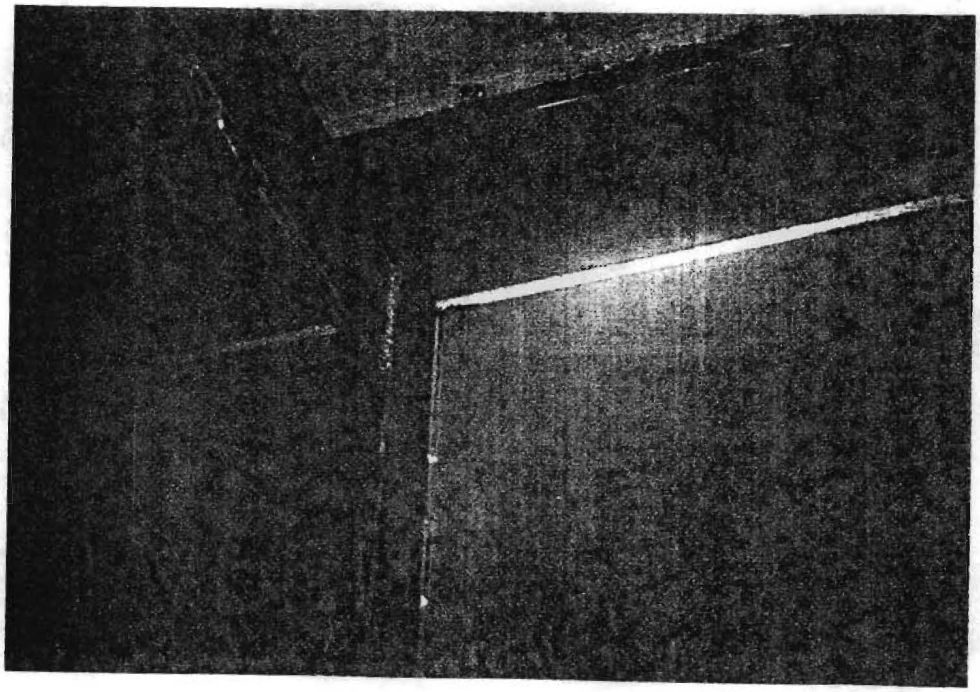

CRACK OVER STIFFENER

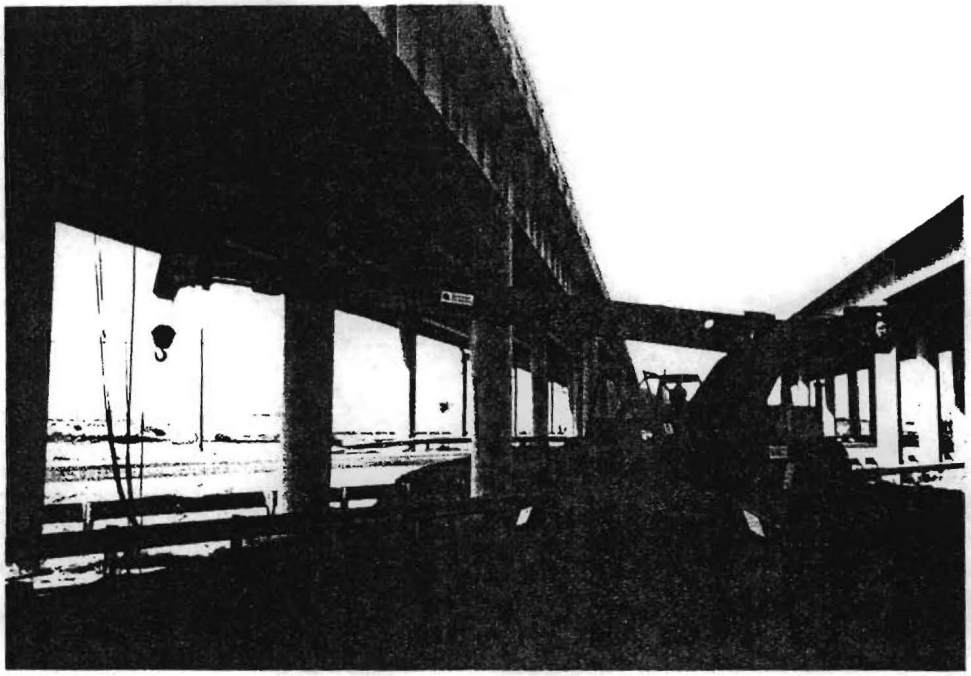

LIFTING EQUIPMENT

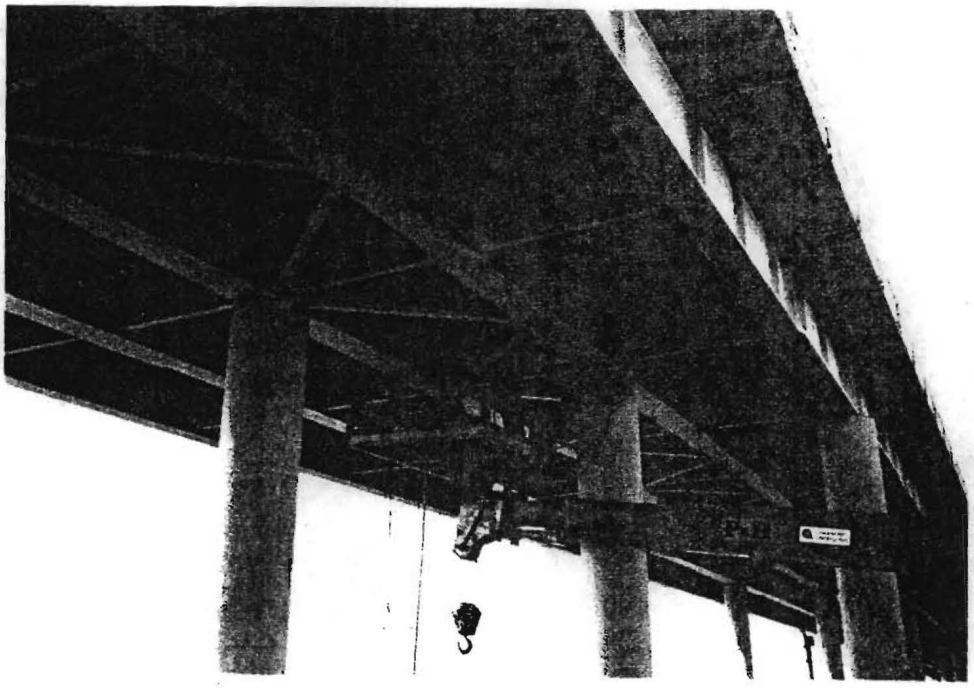

WELDING PLATFORM

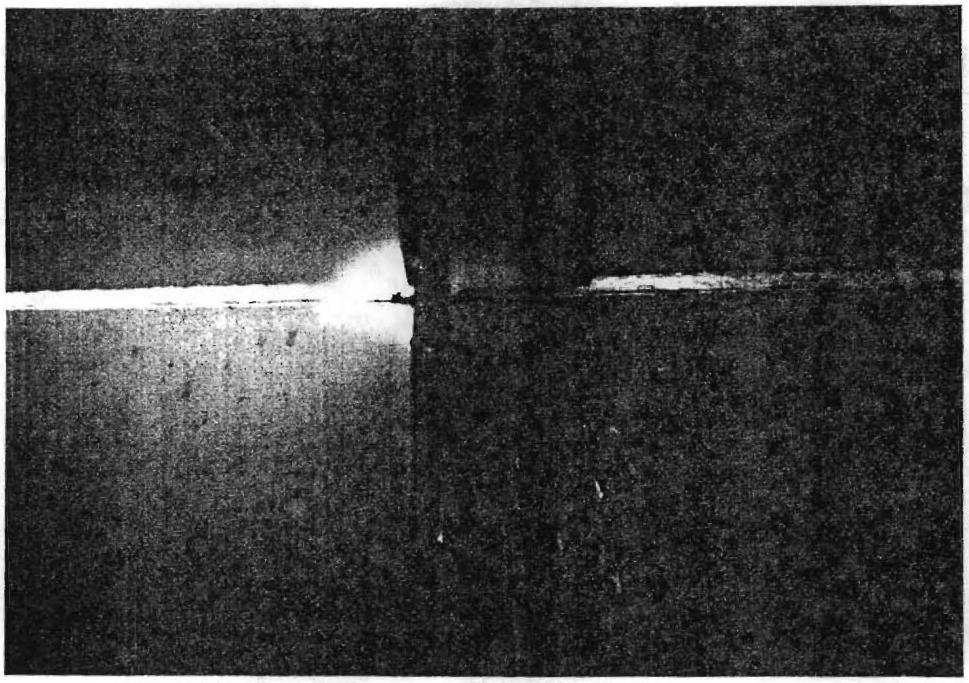

CRACK FURTHER DEFINED WITH DYE PENETRANT

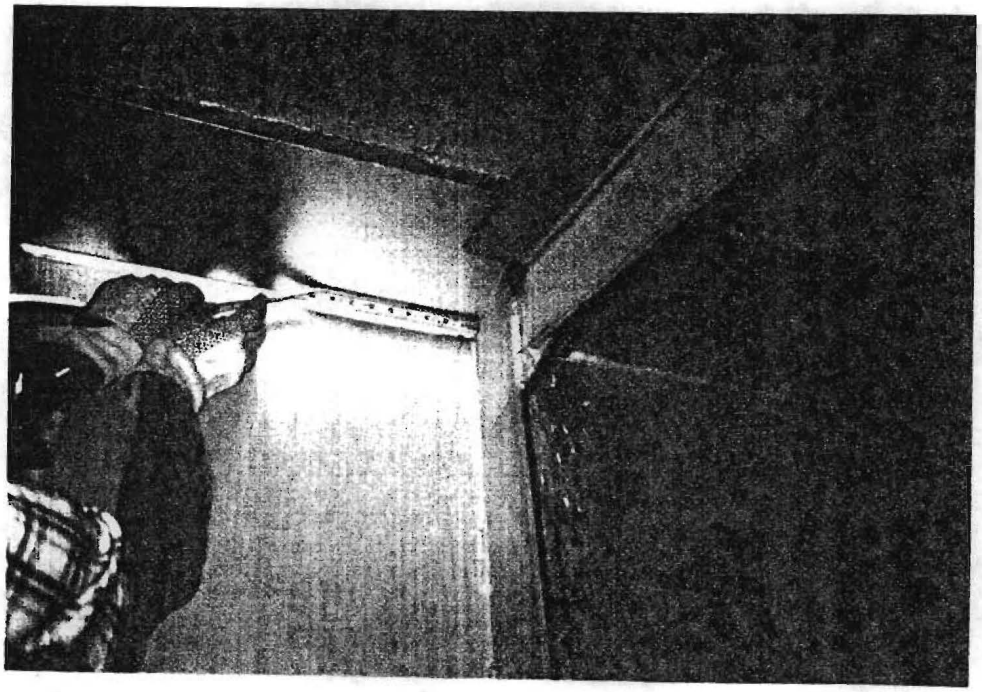

TYPICAL CRACK LENGTH 2-4" ON EITHER
SIDE OF STIFFENER

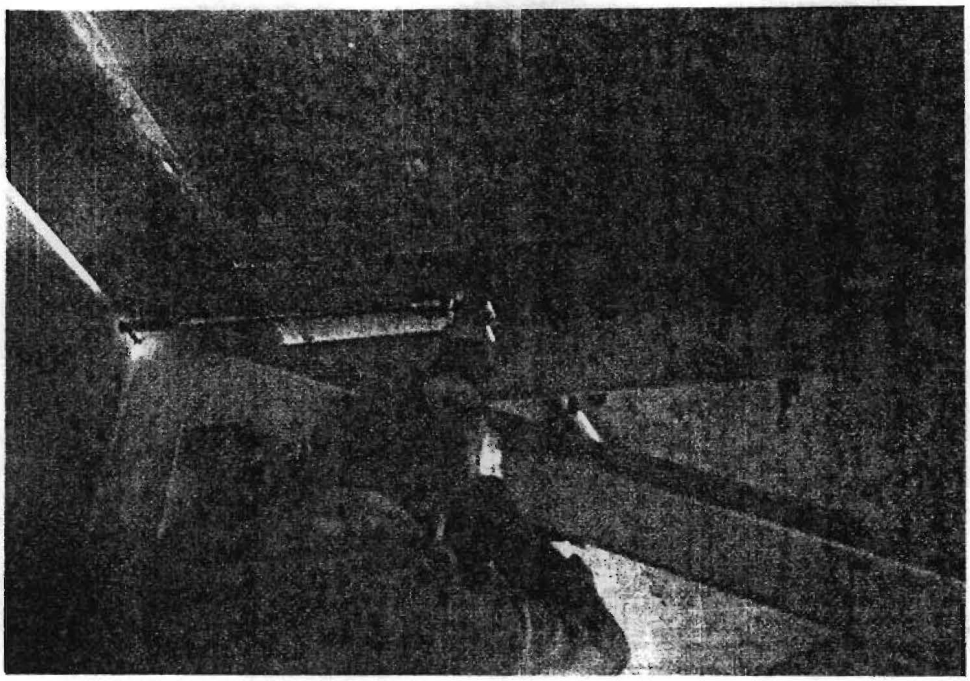

DRILL OPERATION USING RIGHT ANGLE DRILL

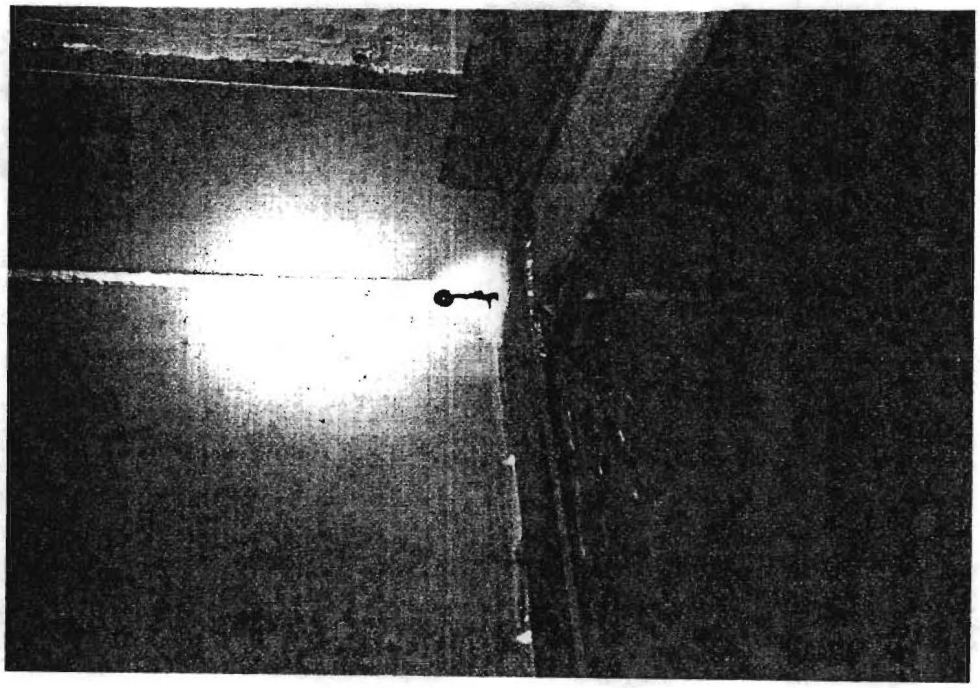

COMPLETED 3/4" HOLE

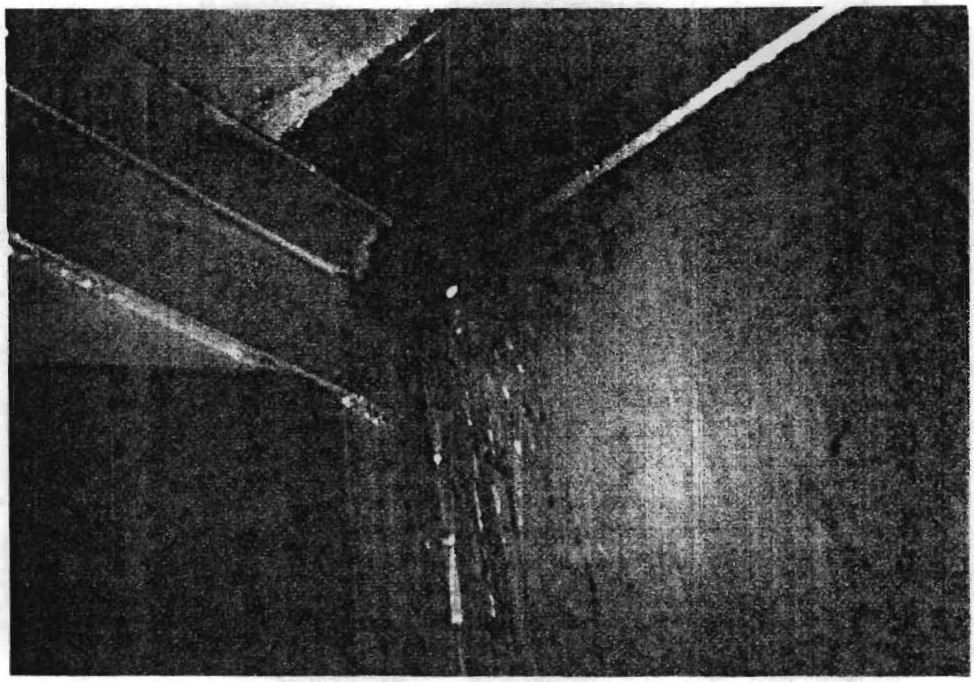

CLIPPED CORNER OF DIAFRAM ANGLE TO
ALLOW ACCESS FOR WELDING

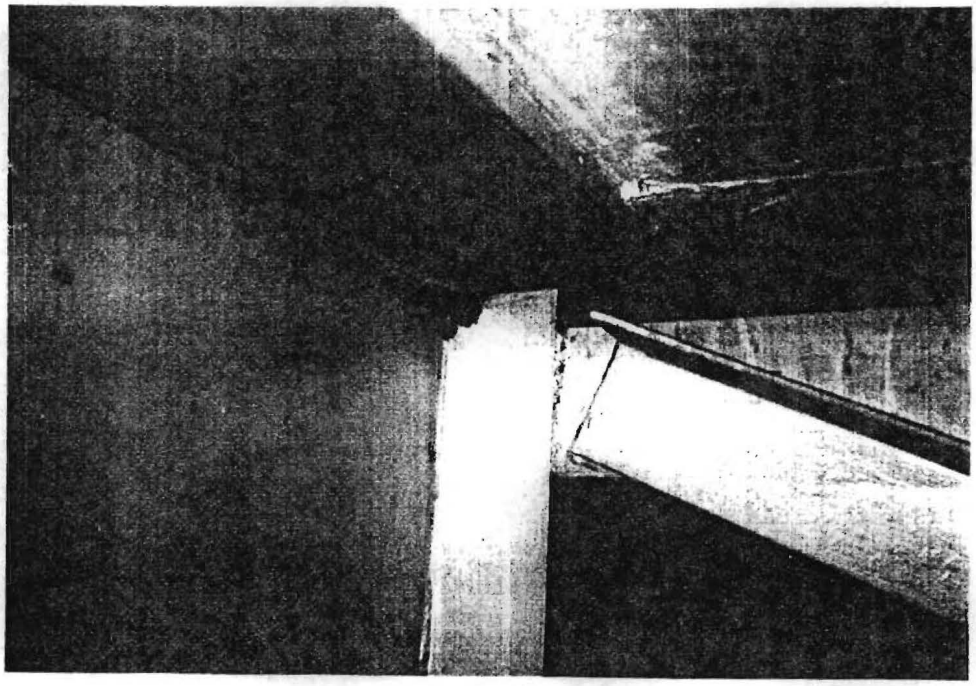

BACK GOUGED CRACK READY FOR REPAIR

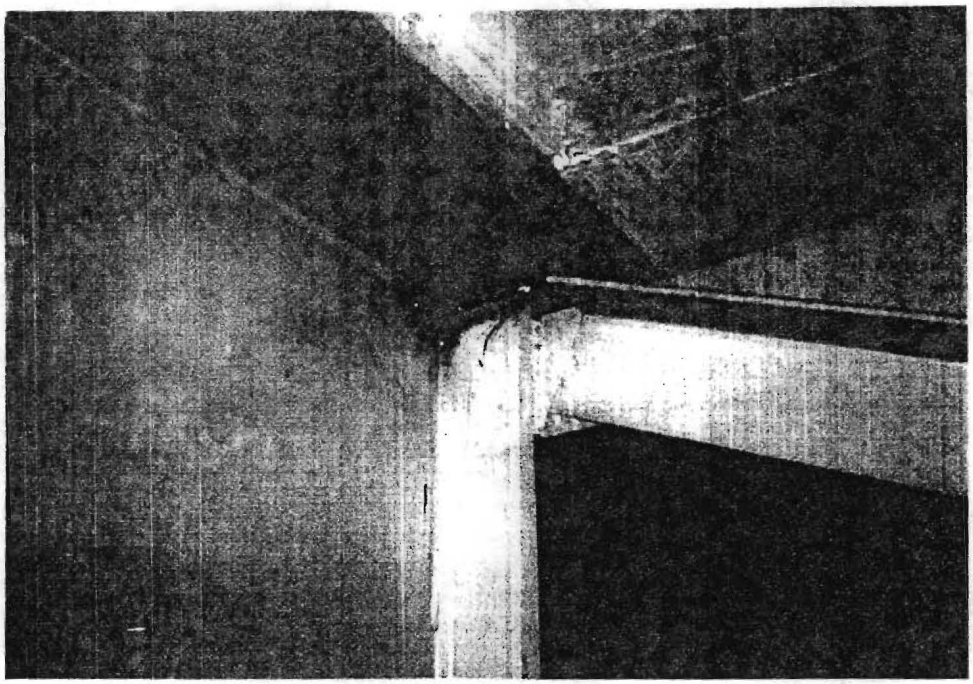

COMPLETED REPAIR AND RETROFIT AT DIAFRAM

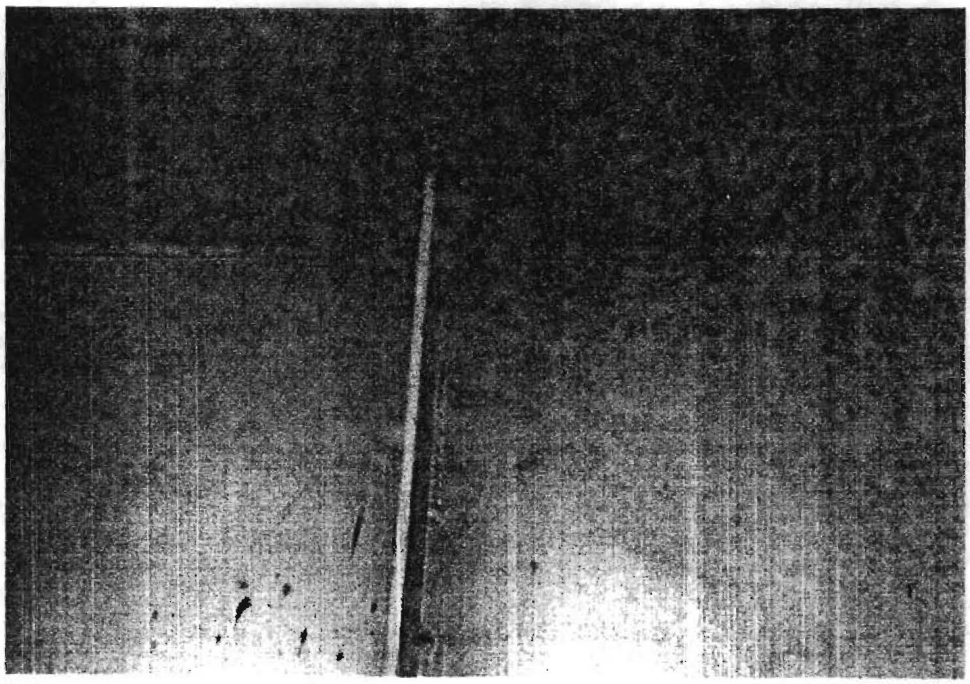

COMPLETED REPAIR AND RETROFIT ON
BACKSIDE OF DIAFRAM CONNECTION